AN OPTIMAL CONTROL PROBLEM FOR A TIMOSHENKO BEAM

by

Mohsen Tadi

Dissertation submitted to the Faculty of the

Virginia Polytechnic Institute and State University

in partial fulfillment of the requirements for the degree of

DOCTOR OF PHILOSOPHY

in

Engineering Mechanics

APPROVED:

John A. Burns, Chairman

Eugene M. Cliff

Dean T. Mook

Ali H. Nayfeh

Scott Hendricks

August, 1991

Blacksburg, Virginia

AN OPTIMAL CONTROL PROBLEM FOR A TIMOSHENKO BEAM

by

Mohsen Tadi

Committe Chairman: John A. Burns
Mathematics

Abstract

In this paper we consider computational algorithms for constructing design models for LQR control of a Timoshenko structure. We consider two finite element schemes and compare their robustness property. The functional gains are also compared against their counterpart when an Euler-Bernoulli model is used to describe the dynamics of the beam. Results indicates that the choice of finite element scheme has a direct bearing on the convergence of the functional gains.

ACKNOWLEDGMENTS

I wish to thank Professor John A. Burns for his constant support and guidance throughout this work. I am grateful to Dr. Eugene Cliff for many helpful discussions and for serving on my committe. Also, I wish to thank Professors D. Mook, A. Nayfeh and S. Hendricks for serving on my committee. Special thanks are due to Dr. Terry Herdman, Director of the Interdisciplineary Center for Applied Mathematics.

I wish to thank Mr. Jim Brown, Director of the Student Accounts, for his understanding and Dr. Von Kerzcek of UMBC for his optimistic recommendation on my behalf.

In general, I wish to thank the ICAM group. Just the thought of being associated with them gives me pride and joy.

The research that led to the results in this thesis was supported in part by the Air Force Office of Scientific Research under grant AFOSR 89-0001 and the Defense Advanced Research Projects Agency under contracts FA9620-87-C-0116 and N00014-88-K-0721.

TABLE OF CONTENTS

Chapter I

Introduction

1.1 Problem Statement and History.

In this paper, we consider various approximation schemes for control of an elastic system that consists of a slewing beam attached to a rigid hub at one end and a tip mass at the other end. Our interest is to suppress the lateral vibrations of the beam and thereby that of the tip mass around the rigid body location, by applying a controlling torque at the hub.

Although several authors have considered similar problems, almost all of the existing results assume an Euler-Bernoulli model for the beam. Assuming such a model, Gibson [1] used cubic B-splines to obtain convergent finite-dimensional approximations to the functional gains. Banks and Crowley [2] considered a parameter estimation problem using Timoshenko beam theory. They used cubic B-splines for both rotation and displacement of the beam. In [3] Burns, Cliff and et. al., studied the problem of controlling a Timoshenko beam with a tip mass. They used the same cubic B-splines as in [2] to construct finite-dimensional spaces for the beam displacement and shear. Although convergence was obtained for certain problems, the methods in [3] failed when the beam parameters were such that Timoshenko theory was needed. In this paper, in addition to cubic B-splines we apply a set of

conforming finite element schemes to obtain finite dimensional approximations to the problem of controlling a Timoshenko beam with a tip mass. These schemes require certain smoothness on the shear across each element which results in a coupling between finite element spaces for displacements and rotation.

Consider the beam-hub-mass structure as shown in Figure 1. Let $\theta(t)$ denote the rigid body rotation of the hub, $u(t,x)$ be the lateral elastic displacement of the beam and $\psi(t,x)$ be the elastic rotation of the the beam. The parameter I_h is the moment of inertia of the hub, E is the Young's modulus and G is the shear modulus of elasticity of the beam. The beam cross-sectional area is denoted by A and I is the moment of inertia of the beam cross-section. Also, m_c and I_c are the mass and mass moment of inertia of the tip mass and M_a is the applied torque. Subscripts t and x represent differentiations with respect to time and to the spatial variable along the beam. We consider the Timoshenko model governed by the linear system

$$I_h\ddot{\theta}(t) = EI\psi_x(t,0) + M_a(t) \tag{1.1.1}$$

$$\rho A(u_{tt}(t,x) + x\ddot{\theta}(t)) = KGA(u_x(t,x) - \psi(t,x))_x \tag{1.1.2}$$

$$\rho I(\psi_{tt}(t,x) + \ddot{\theta}(t)) = EI\psi_{xx}(t,x) + KGA(u_x(t,x) - \psi(t,x)) \tag{1.1.3}$$

$$m_c(u_{tt}(t,l) + l\ddot{\theta}(t)) = -KGA(u_x(t,l) - \psi(t,l)) \tag{1.1.4}$$

$$I_c(\psi_{tt}(t,l) + \ddot{\theta}(t)) = -EI\psi_x(t,l). \tag{1.1.5}$$

Boundary conditions for this model follow from the geometry of the structure which requires that the tip mass has the same displacement and rotation as the beam at its right end which are stated in equations (1.1.4) and (1.1.5), and also the beam is cantileavered to the hub at its left end. That is

$$u(t,0) = 0$$

$$\psi(t,0) = 0.$$

This model does not take into account any loss of energy. However, all structures have some inherent damping and as shown by Gibson [1], it is necessary to have some damping in the structure for the control problem to have a solution. Here we concentrate on external damping. We use a viscous model for external damping and we discuss a Kelvin-Voigt model for internal damping.

Kelvin-Voigt damping is obtained by using the stress-strain laws of the form

$$\sigma_{xx} = E\varepsilon_{xx} + \kappa E\varepsilon_{xxt}$$

$$\sigma_{xz} = G\varepsilon_{xz} + \kappa G\varepsilon_{xzt},$$

where κ is a "damping ratio". This gives rise to the model where the damping operator is proportional to the stiffness operator. Using this model, the internally

damped equations of motion are:

$$I_h\ddot{\theta}(t) = \kappa EI\psi_{xt}(t,0) + EI\psi_x(t,0) + M_a(t) \tag{1.1.6}$$

$$\begin{aligned}\rho A(u_{tt}(t,x) + x\ddot{\theta}(t)) = &+ \kappa KGA(u_x(t,x) - \psi(t,x))_{xt} \\ &+ KGA(u_x(t,x) - \psi(t,x))_x\end{aligned} \tag{1.1.7}$$

$$\begin{aligned}\rho I(\psi_{tt}(t,x) + \ddot{\theta}(t)) = &\kappa EI\psi_{xxt}(t,x) + \kappa KGA(u_x(t,x) - \psi(t,x))_t \\ &+ EI\psi_{xx}(t,x) + KGA(u_x(t,x) - \psi(t,x))\end{aligned} \tag{1.1.8}$$

$$\begin{aligned}m_c(u_{tt}(t,l) + l\ddot{\theta}(t)) = &- \kappa KGA(u_x(t,l) - \psi(t,l))_t \\ &- KGA(u_x(t,l) - \psi(t,l))\end{aligned} \tag{1.1.9}$$

$$I_c(\psi_{tt}(t,l) + \ddot{\theta}(t)) = - \kappa EI\psi_x(t,l) - EI\psi_x(t,l), \tag{1.1.10}$$

with boundary conditions

$$u(t,0) = 0$$

$$\psi(t,0) = 0.$$

A standard external damping is the "viscous" damping model. We assume that viscous damping is proportional to the velocity of beam. If one assumes that there is no damping on the displacement of the hub, the viscously damped equations of

motion are

$$I_h\ddot{\theta}(t) = EI\psi_x(t,0) + M_a(t) \tag{1.1.11}$$

$$\begin{aligned}\rho A(u_{tt}(t,x) + x\ddot{\theta}(t)) = &- \kappa\rho A(u_t(t,x) + x\dot{\theta}(t)) \\ &+ KGA(u_x(t,x) - \psi(t,x))_x\end{aligned} \tag{1.1.12}$$

$$\begin{aligned}\rho I(\psi_{tt}(t,x) + \ddot{\theta}(t)) = &- \kappa\rho I(\psi_t(t,x) + \dot{\theta}(t)) + EI\psi_{xx}(t,x) \\ &+ KGA(u_x(t,x) - \psi(t,x))\end{aligned} \tag{1.1.13}$$

$$\begin{aligned}m_c(u_{tt}(t,l) + l\ddot{\theta}(t)) = &- \kappa m_c(u_t(t,l) + l\dot{\theta}(t)) \\ &- KGA(u_x(t,l) - \psi(t,l))\end{aligned} \tag{1.1.14}$$

$$I_c(\psi_{tt}(t,l) + \ddot{\theta}(t)) = - \kappa I_c(\psi_t(t,l) + \dot{\theta}(t)) - EI\psi_x(t,l). \tag{1.1.15}$$

We shall formulate the control problem by using the theory of semigroups. In the next two sections we review some of the basic definitions and results on linear dynamical systems and linear quadratic regulator problems (LQR). In Chapter 2, we summarize the general theory for structural vibration problems and use standard techniques from semigroup theory to prove well-posedness. In Chapter 3 we specialize to the Timoshenko model and discuss the conditions under which this problem can be placed within the general framework given in Chapter 2. Chapter 4 deals with approximation schemes, and numerical experiments are presented in Chapter 5. We shall use two types of finite element schemes to approximate the LQR problem. The first scheme uses standard cubic B-splines and the second scheme is based

on a special conforming finite element algorithm for Timoshenko beams which was first introduced by Tessler [4].

We shall use standard notation throughout the paper. If $\mathbf{Y}$ is a Hilbert space with inner-product $< .,. >_Y$, then the norm of an element $y \in \mathbf{Y}$ is given by $||y||_Y = (< y, y >_Y)^{1/2}$. The space of integers will be denoted by $\mathbf{N}$. When there is no chance of confusion the subscripts will be omitted. It will be essential to distinguish between linear operators and their (matrix) representations. Bold script capital letters will always denote operators. If $\mathcal{A} : \mathbf{X} \rightarrow \mathbf{Y}$ is a linear operator from the finite dimensional Hilbert space $\mathbf{X}$ into $\mathbf{Y}$, then A will denote a particular matrix representation of $\mathcal{A}$. If $\mathbf{Z}$ is a Hilbert space, then the set of all square integrable functions defined on $[a, b]$ with values in $\mathbf{Z}$ will be denoted by $\mathbf{L}_2(a, b; \mathbf{Z})$. The space of all strongly absolutely continuous functions $f \in \mathbf{L}_2(a, b; \mathbf{Z})$ with jth derivative $f^{(j)}$ strongly absolutely continuous for $j = 1, 2, ..., k-1$ and $f^{(k)} \in \mathbf{L}_2(a, b; \mathbf{Z})$ is denoted by $\mathbf{W}^{k,2}(a, b; \mathbf{Z})$. It is useful to denote by $\mathbf{W}_L^{1,2}(a, b; \mathbf{Z})$ the set of all $\mathbf{W}^{1,2}$ functions that vanish at the left end of the interval. We use the superscript T to denote the transpose of a matrix (A^T), and $*$ will be used to denote the adjoint of an operator ($\mathcal{A}^*$).

1.2 Review of Basic Mathematical Definitions and Results.

Vibrating systems with infinitely many degrees of freedom, such as a continuous deformable media, can be studied as dynamical systems in infinite dimensional Hilbert spaces. We first recall some of the definitions and properties of these spaces. These definitions can be found in standard books on semigroup theory and dynamical systems and the precise definitions given below can be found in [5,6,7,10].

Let $\mathbf{H}$ denote a real inner-product space with inner-product $< .,. >: \mathbf{H} \times \mathbf{H} \rightarrow \mathbf{R}$. If $u, v \in \mathbf{H}$, and $\lambda, \mu \in \mathbf{R}$, then

$$< u, v > =< v, u >,$$

$$< u, v + w > =< u, v > + < u, w >,$$

$$< \lambda u, \mu v > = \lambda\mu < u, v >,$$

and $< u, u >= 0$ if and only if $u = 0$. The inner product space $\mathbf{H}$ is a normed linear space with norm defined by

$$||u|| =< u, u >^{1/2} .$$

A sequence $\{u^m\} \in \mathbf{H}, m \in \mathbf{N}$ is a Cauchy sequence if, for every $\epsilon > 0$, there exists an integer N_ϵ such that for $k, l \geq N_\epsilon$

$$||u^k - u^l|| < \epsilon.$$

A sequence $\{u^m\} \in \mathbf{H}, m \in \mathbf{N}$ is said to converge in norm (or strongly in $\mathbf{H}$) to an element $u \in \mathbf{H}$ if and only if

$$||u^m - u|| \rightarrow 0 \qquad as \qquad m \rightarrow \infty.$$

If $\{u^n\}$ converges strongly to u^0 in $\mathbf{H}$, then we use the notation $u^n \to u^0$. A point $u^0 \in \mathbf{H}$ is a limit point of the set $\mathbf{S} \subset \mathbf{H}$, if there is a sequence $\{u^n\} \in \mathbf{S}$ such that $u^n \to u^0$. A set $\mathbf{S}$ is said to be closed if it contains all of its limit points. The set of all limit points of $\mathbf{S}$ is called the closure of $\mathbf{S}$, and is denoted by $\overline{\mathbf{S}}$. A set $\mathbf{S}$ is said to be closed if and only if $\mathbf{S} = \overline{\mathbf{S}}$. A set $\mathbf{S}$ is said to be dense in $\mathbf{H}$, if $\overline{\mathbf{S}} = \mathbf{H}$.

A set $\mathbf{S}$ is precompact if every sequence $\{u^n\} \in \mathbf{S}$ contains a Cauchy subsequence. A set $\mathbf{S}$ is compact if every sequence $\{u^n\} \in \mathbf{S}$ contains a subsequence converging to a point in $\mathbf{S}$. The inner product space $\mathbf{H}$ is said to be complete if every Cauchy sequence converges in norm to some element of $\mathbf{H}$.

An inner product space $\mathbf{H}$ is called a Hilbert space if it is complete. It is said to be separable, if there exists a countable subset $\mathbf{X}$ everywhere dense in $\mathbf{H}$. If $\mathbf{X}$ is dense in $\mathbf{H}$, then any $u \in \mathbf{H}$ is the limit (in norm) of a sequence belonging to $\mathbf{X}$.

Given two Hilbert spaces $\mathbf{X}, \mathbf{Y}$, an operator from a subset $D(\mathcal{F}) \subset \mathbf{X} \to \mathbf{Y}$ is a rule that assigns to each $x \in D(\mathcal{F})$ a unique $y \in \mathbf{Y}$. This is denoted by $\mathcal{F} : (D(\mathcal{F}) \subset \mathbf{X}) \to \mathbf{Y}$, where $D(\mathcal{F})$ is the domain of $\mathcal{F}$ and $\{y \in \mathbf{Y} | y = \mathcal{F}x; \quad x \in D(\mathcal{F})\}$ is the range of $\mathcal{F}$, $R(\mathcal{F}) \subset \mathbf{Y}$. If $R(\mathcal{F}) = \mathbf{Y}$ then $\mathcal{F}$ is onto. If $\mathcal{F}x = \mathcal{F}x'$ implies that $x = x'$, then $\mathcal{F}$ is one-to-one. In this case the inverse operator $\mathcal{F}^{-1}$ exists.

Let $\mathcal{F} : (D(\mathcal{F}) \subset \mathbf{X}) \to \mathbf{Y}$, with $\mathbf{X}, \mathbf{Y}$ Hilbert spaces. The operator $\mathcal{F}$ is continuous at $x_0 \in D(\mathcal{F})$ if for every $\epsilon > 0$, there exists $\delta(x_0, \epsilon)$ such that if $x \in D(\mathcal{F})$ and $||x - x_0|| < \delta$, then $||\mathcal{F}x - \mathcal{F}x_0|| < \epsilon$. If $\mathcal{F}$ is continuous at every $x_0 \in D(\mathcal{F})$,

then it is called a continuous operator. If δ is independent of x_0, then $\mathcal{F}$ is said to be uniformly continuous on $D(\mathcal{F})$. An operator $\mathcal{F} : (D(\mathcal{F}) \subset \mathbf{X}) \to \mathbf{Y}$ is bounded if $\mathcal{F}$ maps bounded sets in $D(\mathcal{F})$ into bounded sets in $\mathbf{Y}$, and it is compact if $\mathcal{F}$ maps bounded sets in $D(\mathcal{F})$ into precompact sets in $\mathbf{Y}$. An operator $\mathcal{F} : (D(\mathcal{F}) \subset \mathbf{X}) \to \mathbf{Y}$, is said to be closed if given any sequence $\{x^n\} \in D(\mathcal{F})$ such that $x^n \to x^0$ and $\mathcal{F}x^n \to v$, then $x^0 \in D(\mathcal{F})$ and $\mathcal{F}x^0 = v$. An operator $\mathcal{F} : (D(\mathcal{F}) \subset \mathbf{X}) \to \mathbf{Y}$ is said to be linear if $D(\mathcal{F})$ is a linear space and $\mathcal{F}(\alpha x + \beta x') = \alpha \mathcal{F}x + \beta \mathcal{F}x'$ for all $x, x' \in D(\mathcal{F})$ and $\alpha, \beta \in \mathbf{C}$. If $\mathcal{F} : (D(\mathcal{F}) \subset \mathbf{X}) \to \mathbf{Y}$ is a linear operator then $\mathcal{F}$ is bounded if and only if it is continuous [7, Theorem 6.1.1].

Let $\mathcal{T}(t)$, $t \geq 0$, be a family of continuous linear transformations mapping a Hilbert space $\mathbf{H}$ into itself. The family $\mathcal{T}(t)$ is said to be a strongly continuous semigroup on $\mathbf{H}$ if

$$\mathcal{T}(0) = I \qquad \text{(identity)}$$

$$\mathcal{T}(t_1 + t_2) = \mathcal{T}(t_1)\mathcal{T}(t_2) = \mathcal{T}(t_2)\mathcal{T}(t_1), \qquad t_1, t_2 \in \mathbf{R}^+$$

and in addition, if for each $x \in \mathbf{H}$

$$||T(t)x - x|| \to 0 \qquad as \qquad t \to 0^+.$$

A family of operators having all of these properties is called a C_0-semigroup.

Let $T(t), t \geq 0$ be a C_0-semigroup on $\mathbf{H}$ and let $\mathbf{D} \subseteq \mathbf{H}$ be the subspace of elements $x \in \mathbf{H}$ such that the limit of $(\mathcal{T}(\mu)x - x)/\mu$ converges as $\mu \to 0$. The

infinitesimal generator of the semigroup $\mathcal{T}(t)$ is the linear operator $\mathcal{A}$ defined on $\mathbf{D}$ by

$$\mathcal{A}x = \lim_{\mu \to 0} \frac{\mathcal{T}(\mu)x - x}{\mu}.$$

Formally, the semigroup property suggests that $\mathcal{T}(t) = e^{"\mathcal{A}t"}$, where $\mathcal{A} = (\frac{d}{dt})\mathcal{T}(t)|_{t=0}$.

In the study of systems governed by partial differential equations, the infinitesimal generators are never continuous. A C_0- semigroup $\mathcal{T}(t)$ is uniformly exponentially stable if there exist two positive real numbers M and ω such that for any $t > 0$

$$||\mathcal{T}(t)|| \leq Me^{-\omega t}.$$

A C_0-semigroup $\mathcal{T}(t)$, on $\mathbf{H}$, is said to be a contraction semigroup if,

$$||\mathcal{T}(t)|| \leq 1 \qquad \forall t \in \mathbf{R}^+.$$

If both $\mathcal{A}$ and $-\mathcal{A}$ are infinitesimal generators of C_0-semigroups on $\mathbf{H}$, then [6, Proposition 2.2] the C_0- semigroup $\{\mathcal{T}(t)\}_{t \geq 0}$ generated by $\mathcal{A}$ must be invertible, and $-\mathcal{A}$ generates $\{\mathcal{T}^{-1}(t)\}_{t \geq 0}$. In this case if one defines $\mathcal{T}(-t) \equiv \mathcal{T}^{-1}(t)$, $t \geq 0$, then $\mathcal{A}$ is said to generate the C_0-group $\{\mathcal{T}(t)\}_{t \in \mathbf{R}}$, and the direction of time is of no importance.

If $\mathbf{H}$ is a Hilbert space, then the set of all bounded linear functionals(ℓ : $\mathbf{H} \mapsto \mathbf{R}^1$) on $\mathbf{H}$ is called the dual space of $\mathbf{H}$ and is denoted by $\mathbf{H}'$. If $\ell \in \mathbf{H}'$ and the norm of ℓ is defined by

$$||\ell||_{H'} = \sup_{u \in H} \frac{\ell(u)}{||u||_H},$$

then $\mathbf{H}'$ becomes a Hilbert space. Moreover, $\mathbf{H}'$ may be identified with $\mathbf{H}$ through Riesz Representation Theorem [8].

Theorem 1.2.1. (Riesz Representation Theorem) If ℓ is a bounded linear functional on $\mathbf{H}$, then there exists a unique $v \in \mathbf{H}$ such that,

$$\ell(u) = < v, u > \qquad \forall u \in \mathbf{H}.$$

If $\mathbf{H}$ is a Hilbert space, then a sequence $\{v^n\} \in \mathbf{H}$ is said to converge weakly to $v \in \mathbf{H}$ if and only if

$$\ell(v^n) \rightarrow \ell(v).$$

for each $\ell \in \mathbf{H}'$. In view of the Riesz Representation Theorem it follows that $\{v^n\} \rightarrow v$ weakly if and only if for each $u \in \mathbf{H}$,

$$< v^n, u > \rightarrow < v, u >$$

as $n \rightarrow \infty$.

We now consider a very special class of linear operators that map $\mathbf{H}$ into itself. By $\mathbf{L}(\mathbf{H})$ we denote the space of continuous linear operators that map $\mathbf{H}$ into itself, and by $\mathbf{L}(\mathbf{H}, \mathbf{E})$ we denote the space of continuous linear operators that map $\mathbf{H}$ into $\mathbf{E}$.

If $\Gamma : (D(\Gamma) \subseteq \mathbf{H}) \mapsto \mathbf{H}$ is a linear operator on $\mathbf{H}$, then the (Hilbert) adjoint of Γ, Γ^* is defined on $\mathbf{H}$ by

$D(\Gamma^*) = \{g \in \mathbf{H}|$ there exists $f \in \mathbf{H}$ such that,

$$< \Gamma u, g > - < u, f >= 0, \qquad \forall u \in D(\Gamma)\},$$

and if $g \in D(\Gamma^*)$, then

$$\Gamma^* g = f.$$

In the case that $\mathbf{X}$ and $\mathbf{Y}$ are Hilbert spaces and $\Gamma \in \mathbf{L}(\mathbf{X}, \mathbf{Y})$, then the (Hilbert adjoint) $\Gamma^* \in \mathbf{L}(\mathbf{Y}, \mathbf{X})$ is defined by

$$< \Gamma x, y >_Y = < x, \Gamma^* y >_X,$$

for all $x \in \mathbf{X}$, $y \in \mathbf{Y}$. We note that this definition of adjoint makes use of the equivalence between $\mathbf{X}$ and $\mathbf{X}'$ and $\mathbf{Y}$ and $\mathbf{Y}'$.

The operator Γ is said to be <u>self-adjoint</u> if $\Gamma = \Gamma^*$, and is said to be <u>skew-adjoint</u> if $\Gamma = -\Gamma^*$. Note that $\Gamma = \Gamma^*$ means that $D(\Gamma) = D(\Gamma^*)$ and $\Gamma x = \Gamma^* x$ for all $x \in D(\Gamma)$.

An operator $\Gamma : (D(\Gamma) \subseteq \mathbf{H}) \mapsto \mathbf{H}$ is said to be <u>H-coercive</u> if there exists a constant $\rho > 0$ such that

$$< \Gamma x, x >_H \geq \rho ||x||_H^2, \qquad \forall x \in D(\Gamma).$$

An operator $\Gamma : (D(\Gamma) \subseteq \mathbf{H}) \mapsto \mathbf{H}$ is said to be <u>dissipative</u> in $\mathbf{H}$ if

$$< \Gamma x, x >_H \leq 0 \qquad \forall x \in D(\Gamma).$$

A dissipative operator $\Gamma : (D(\Gamma) \subseteq \mathbf{H}) \mapsto \mathbf{H}$ is said to be maximal dissipative if it is not a proper restriction of another dissipative operator.

The following lemma is used to determine if a dissipative operator is maximal dissipative. [12, corollary to Theorem 1.1.1]

Lemma 1.2.1. Let $\lambda > 0$ and suppose that Γ is a dissipative operator on $\mathbf{H}$ with dense domain. Then Γ is maximal dissipative if and only if

$$R(\lambda I - \Gamma) = \mathbf{H}, \qquad \forall \lambda > 0.$$

We now have the following theorem for well-posedness [6, Page 26].

Theorem 1.2.1. The operator $\mathcal{A}$ generates a C_0 contraction semigroup on $\mathbf{H}$ if and only if $\mathcal{A}$ is densely defined and maximal dissipative.

1.3 Review of Basic Results on Linear Regulator Problems.

In this section, we review some of the basic definitions and results , which can be found in [6,14], on the control of a linear time invariant dynamical system given by

$$\dot{z}(t) = \mathcal{A}z(t) + \mathcal{B}u(t), \quad z(0) = z_0 \tag{1.3.1}$$

$$y(t) = \mathcal{C}z(t), \tag{1.3.2}$$

where, $z \in \mathbf{Z}$, $\mathcal{A} : (D(\mathcal{A}) \subseteq \mathbf{Z}) \mapsto \mathbf{Z}$, $\mathcal{B} \in \mathbf{L}(\mathbf{R}^m, \mathbf{Z})$ and $\mathcal{C} \in \mathbf{L}(\mathbf{Z}, \mathbf{R}^n)$. We shall always assume that $\mathcal{A}$ generates a C_0-semigroup, $T(t)$, on the real Hilbert space

$\mathbf{Z}$. The standard LQR problem on $\mathbf{Z}$ is to choose a control $u \in \mathbf{L}_2(0,\infty;\mathbf{R}^m)$ to minimize the cost functional

$$J(z(0),u) = \int_0^\infty (< y(t), y(t) >_{R^n} + < \mathcal{R}u(t), u(t) >_{R^m})\, dt \tag{1.3.3}$$

subject to (1.3.1) and (1.3.2). Here, $\mathcal{R} = \mathcal{R}^* \in \mathbf{L}(\mathbf{R}^m)$ is assumed to be positive definite. If $\mathcal{Q} = \mathcal{Q}^* \in \mathbf{L}(\mathbf{Z})$ is given by

$$\mathcal{Q} = \mathcal{C}^*\mathcal{C}, \tag{1.3.4}$$

then (1.3.3) becomes

$$J(z(0),u) = \int_0^\infty (< \mathcal{Q}z(t), z(t) >_Z + < \mathcal{R}u(t), u(t) >_{R^m})\, dt. \tag{1.3.3'}$$

Mild solutions to (1.3.1) are given by the variation of parameters formula

$$z(t) = T(t)z(0) + \int_0^t T(t-\eta)\mathcal{B}u(\eta)\, d\eta, \quad t \geq 0, \tag{1.3.5}$$

where $T(t)$ is the C_0-semigroup generated by $\mathcal{A}$.

A function $u \in \mathbf{L}_2(0,\infty;\mathbf{R}^m)$ is said to be an admissible control for z_0 if $J(z_0,u)$ is finite, i.e., if the state $z(t)$ given by (1.3.5) is in $\mathbf{L}_2(0,\infty;\mathbf{Z})$.

Next, we introduce the definitions of stabilizability and detectability. The following definitions are taken from [14].

Definition 1.3.1. Consider the system given by (1.3.1). The system is said to be stabilizable if there exists a bounded linear operator $\mathcal{K} : \mathbf{Z} \mapsto \mathbf{R}^m$ such that $(\mathcal{A} - \mathcal{B}\mathcal{K})$ generates a strongly continuous semigroup which is exponentially stable.

Definition 1.3.2. Consider the system given by (1.3.1) and (1.3.2) with $\mathcal{C} \in \mathbf{L}(\mathbf{Z}, \mathbf{R}^n)$. The system is said to be detectable if there exists a continuous linear operator

$$\mathcal{F} : \mathbf{R}^n \to \mathbf{Z}$$

such that $(\mathcal{A} - \mathcal{F}\mathcal{C})$ generates a strongly continuous semigroup which is exponentially stable.

It is known [1], that if the system (1.3.1)-(1.3.2) is stabilizable and detectable then there exist a unique control $u_{opt} \in \mathbf{L}_2(0, \infty; \mathbf{R}^m)$ such that

$$J(z, u_{opt}) = \min_{u \in L_2(0,\infty;U)} J(z, u)$$

and this control can be written in a feedback form

$$u_{opt}(t) = -R^{-1}\mathcal{B}^*\Pi z(t) \tag{1.3.6}$$

where $\Pi \in \mathbf{L}(\mathbf{Z})$ is the nonnegative self-adjoint solution of the algebriac Riccati equation

$$\mathcal{A}^*\Pi + \Pi\mathcal{A} - \Pi\mathcal{B}R^{-1}\mathcal{B}^*\Pi + \mathcal{Q} = 0 \tag{1.3.7}$$

To assure the existence of an optimal solution, we have the following result which may be found in [1].

Theorem 1.3.1. Let the operators $\mathcal{A}, \mathcal{B}, \mathcal{Q}$, and $\mathcal{R}$ be as previously defined. The algebriac Riccati equation (1.3.7) has a unique nonnegative self-adjoint solution, if

and only if for each $z \in \mathbf{Z}$ there is an admissible control for the initial state z_0. The unique control which minimizes $J(z,.)$ is given by (1.3.6), and the corresponding optimal trajectory $z(t)$ is given by $z(t) = S(t)z_0$, where $S(t)$ is the strongly continuous semigroup generated by $\mathcal{A} - \mathcal{B}R^{-1}\mathcal{B}^*\Pi$ which is uniformly exponentially stable. Furthermore,

$$J(z, u_{opt}) = \min_{u \in \mathbf{L}_2(0,\infty;\mathbf{U})} J(z,u) =< \Pi z, z >_{\mathbf{Z}} . \tag{1.3.8}$$

In general, equation (1.3.7) is a nonlinear partial (functional) differential equation. A direct analytical solution of such a system is usually impossible. Therefore, it has become a standard practice to approximate the entire control problem, thereby leading to an indirect approximation of (1.3.7).

The basic requirement of an approximation scheme is to produce suboptimal controls, $u^N_{opt}(t)$, such that if $u^N_{opt}(t)$ is applied to the infinite dimensional system (1.3.1)-(1.3.2), the closed- loop system response is "close" to optimal for any initial condition and such that $u^N_{opt}(t)$ converges to $u_{opt}(t)$ in an appropriate sense.

In essence, we need to construct a series of finite dimensional control problems that converges to the infinite dimensional control problem. One way of achieving this is to project the infinite dimensional control problem defined on $\mathbf{Z}$ onto series of finite dimensional subspaces $\mathbf{Z}^N, N = 1, 2, \ldots$.

Let $\mathcal{P}^N$, for $N = 1, 2, \ldots$. denote a sequence of orthogonal projections $\mathcal{P}^N : \mathbf{Z} \mapsto \mathbf{Z}^N \subset \mathbf{Z}$. To assure that the finite dimensional approximations of the open loop

problems converge in some sense to the infinite dimensional problem, the projections $\mathcal{P}^N$ must converge to the identity operator as $N \to \infty$ and $||\mathcal{P}^N|| \leq 1$ for all N. In addition, we will require the following convergence

$$\mathcal{P}^N \mathcal{B}u = \mathcal{B}^N u \to \mathcal{B}u, \mathcal{B}^{N*} z \to \mathcal{B}^* z, \mathcal{Q}^N \mathcal{P}^N z \to \mathcal{Q}z,$$

$$as \quad N \to \infty \quad \forall z \in Z, \quad u \in \mathbf{U}.$$

To assure convergence of the finite dimensional closed-loop problems, one also needs to have $\mathcal{T}^N(t)$ and $\mathcal{T}^{N*}(t)$ converge strongly and uniformly in t (for t in compact intervals) to $\mathcal{T}(t)$ and $\mathcal{T}^*(t)$, respectively. Moreover, the approximating systems must preserve stabilizability and detectability uniformly in N [5].

For $N = 1, 2, ...$, let $\mathcal{A}^N$ be the generator of C_0- semigroup $T^N(t)$ on $\mathbf{Z}^N$. Assume that $\mathcal{B}^N \in \mathbf{L}(\mathbf{R}^m, \mathbf{Z}^N)$, and $\mathcal{Q}^N \in \mathbf{L}(\mathbf{Z}^N)$ are uniformly bounded in N. The N-th order approximation to the problem is to minimize

$$J^N(z^N, u) = \int_0^\infty (< \mathcal{Q}^N z^N(s), z^N(s) >_Z + < Ru(s), u(s) >_{R^m}) \, ds \tag{1.3.9}$$

subject to

$$\dot{z}^N(t) = \mathcal{A}^N z^N(t) + \mathcal{B}^N u(t), \qquad z^N(0) = \mathcal{P}^N z_0 \tag{1.3.10}$$

$$y^N(t) = \mathcal{C}^N z^N(t). \tag{1.3.11}$$

Similarly, under the assumption that (1.3.9)-(1.3.10) is stabilizable and detectable, there is a unique optimal control $u^N_{opt} \in \mathbf{L}_2(0, \infty; \mathbf{U})$ of the form

$$u^N_{opt}(t) = -R^{-1} \mathcal{B}^{N*} \Pi^N z^N(t), \tag{1.3.12}$$

where $\Pi^N \in \mathbf{L}(\mathbf{Z}^N)$ is the unique solution of the algebraic (operator) Riccati equation

$$\mathcal{A}^{N*}\Pi^N + \Pi^N\mathcal{A}^N - \Pi^N\mathcal{B}^N R^{-1}\mathcal{B}^{N*}\Pi^N + \mathcal{Q}^N = 0. \tag{1.3.13}$$

In Chapter 2, we discuss the application of these general results on the approximation theory to a second order distributed parameter system.

Chapter II

A Review of General Theory of LQR for Second Order DPS

In this chapter, we summarize the theory of LQR problems for a class of structural vibration problems, and prove well-posedness and stability under a general set of conditions. The basic theoretical results may be found in [1].

2.1. Abstract Conservative System.

The second order dynamical system that we consider here is given by

$$\ddot{x}(t) + \mathcal{A}_0 x(t) = \mathcal{B}_0 u(t), \quad x(0) = x_0, \quad \dot{x}(0) = v_0, \tag{2.1.1}$$

where $x(t)$ is in a real Hilbert space $\mathbf{H}$ and $u(t) \in \mathbf{R}^m$. We assume that the linear stiffness operator $\mathcal{A}_0$ is densely defined and self-adjoint with compact resolvent and has at most a finite number of negative eigenvalues. The input operator $\mathcal{B}_0$ is assumed to be a bounded linear operator from $\mathbf{R}^m$ to $\mathbf{H}$. Thus we are restricting our efforts to compact input operators. Equation (2.1.1) includes the case where the mass operator is explicitly present, that is

$$\mathcal{M}_0 \ddot{x}(t) + \mathcal{A}_0' x(t) = \mathcal{B}_0' u(t) \qquad t > 0. \tag{2.1.1'}$$

The mass operator $\mathcal{M}_0$ is a continuous, self-adjoint, linear operator with continuous inverse $\mathcal{M}_0^{-1}$. Equation (2.1.1) is obtained after multiplying (2.1.1') on the left by $\mathcal{M}_0^{-1}$.

In order to write the system in a first order form, we define the "elastic energy space" $\mathbf{V}$ and the "total energy space" $\mathbf{E}$. We choose a bounded self-adjoint linear operator $\mathcal{A}_1$ on $\mathbf{H}$ such that $\tilde{\mathcal{A}}_0 = \mathcal{A}_0 + \mathcal{A}_1$ is $\mathbf{H}$- coercive, that is, there exists a $\rho > 0$ for which

$$< \tilde{\mathcal{A}}_0 x, x >_H \geq \rho ||x||_H^2 \qquad x \in D(\tilde{\mathcal{A}}_0) = D(\mathcal{A}_0).$$

Such an operator is not unique and since $\mathcal{A}_0$ is bounded from below, there are infinitely many choices for $\mathcal{A}_1$.

Once the operator $\tilde{\mathcal{A}}_0$ is fixed it follows that [10, Page 187] the eigenvalues of $\tilde{\mathcal{A}}_0$ are strictly positive, countable, isolated with finite multiplicities and no finite limit points. In addition, the eigenvectors $\{\phi_k\}$ of $\tilde{\mathcal{A}}_0$ are orthogonal and form a basis of $\mathbf{H}$. In this case one can define an operator $\tilde{\mathcal{A}}_0^{1/2}$, the square root of $\tilde{\mathcal{A}}_0$, using the eigenvalues $\{\omega_k^2\}$, and the eigenvectors $\{\phi_k\}$ of $\tilde{\mathcal{A}}_0$ by

$$\tilde{\mathcal{A}}_0^{1/2} w = \sum_{k=1}^{\infty} \omega_k < \phi_k, w > \phi_k.$$

It follows from this definition that $\tilde{\mathcal{A}}_0^{1/2}$ is linear, unbounded, non-negative, and self-adjoint. The domain, $D(\tilde{\mathcal{A}}_0^{1/2})$ can be identified with an inner product space with inner product $< ., . >_V$ defined by

$$< v_1, v_2 >_V = < \tilde{\mathcal{A}}_0^{1/2} v_1, \tilde{\mathcal{A}}_0^{1/2} v_2 >_H .$$

The completion of $D(\tilde{\mathcal{A}}^{1/2})$ with this inner product is a Hilbert space which we denote by $\mathbf{V}$. Since every element of $\mathbf{V}$ is also an element of $\mathbf{H}$, and we can use the

algebraic imbedding

$$\mathbf{V} \subset \mathbf{H} = \mathbf{H}' \subset \mathbf{V}'.$$

where the injections from $\mathbf{V}$ into $\mathbf{H}$ and from $\mathbf{H}$ into $\mathbf{V}'$ are continuous with dense ranges. If Λ_V denotes the Riesz map from $\mathbf{V}$ onto its dual $\mathbf{V}'$ [1] defined by

$$(\Lambda_V v_1)(v) =< v, v_1 >_V \qquad v, v_1 \in \mathbf{V},$$

then it follows that $\tilde{\mathcal{A}}_0$ is the restriction of Λ_V to $D(\mathcal{A}_0)$ in the sense that if $v_1 \in D(\tilde{\mathcal{A}}_0)$, then

$$(\Lambda_V v_1)(v) =< v, \tilde{\mathcal{A}}_0 v_1 >_H =< v, v_1 >_V, \quad v \in \mathbf{V}.$$

If $v \in \mathbf{V}$, then (2.1.1) implies that

$$< \tilde{x}, v >_H + < \mathcal{A}_0 x, v >_H - < \mathcal{B}_0 x, v >_H = 0.$$

Consequently, it follows that

$$0 =< \tilde{x}, v >_H + < \tilde{\mathcal{A}}_0 x, v >_H - < \mathcal{A}_1 x, v >_H - < \mathcal{B}_0 x, v >$$

or equivalently,

$$0 =< \tilde{x}, v >_H + < x, v >_V - < \mathcal{A}_1 x, v >_H - < \mathcal{B}_0 x, v > \qquad (2.1.2)$$

for all $v \in \mathbf{V}$. We shall use this variational formulation of (2.1.1) to construct approximating systems.

In the case where there is no rigid body mode, the third term in equation (2.1.2) vanishes and the equation reduces to the virtual work relation associated

with (2.1.1). Therefore, the inner products in $\mathbf{H}$ and $\mathbf{V}$ represent the virtual work due to 'inertial' and 'elastic' forces, respectively.

With the strain energy space $\mathbf{V}$ defined as above, the total energy space $\mathbf{E}$ is defined to be the Hilbert space $\mathbf{E} = \mathbf{V} \times \mathbf{H}$ with the energy inner product

$$< (v_1, h_1), (v_2, h_2) >_E = < v_1, v_2 >_V + < h_1, h_2 >_H .$$

If $\mathcal{A}_0$ is coercive and $x(t)$ is the solution of (2.1.1), then $||x(t), \dot{x}(t)||_E^2$ is twice the total energy (Kinetic and Potential) in the system. We may consider the system (2.1.1) in first order state space form on $\mathbf{E}$ by defining $z(t) = \begin{pmatrix} x(t) \\ \dot{x}(t) \end{pmatrix}$ and

$$\dot{z}(t) = \mathcal{A}z(t) + \mathcal{B}u(t), \qquad z(0) = \begin{pmatrix} x_0 \\ v_0 \end{pmatrix}, \tag{2.1.3}$$

where $\mathcal{A}$ given by

$$\mathcal{A} = \begin{pmatrix} 0 & I \\ -\mathcal{A}_0 & 0 \end{pmatrix}, \qquad D(\mathcal{A}) = D(\mathcal{A}_0) \times \mathbf{V}, \tag{2.1.4}$$

and

$$\mathcal{B} = \begin{pmatrix} 0 \\ \mathcal{B}_0 \end{pmatrix}. \tag{2.1.5}$$

The system (2.1.3) has a unique solution if and only if the operator $\mathcal{A}$ generates a C_0-group on the Hilbert space $\mathbf{E}$ [6, page 87]. In this case the problem (2.1.1) is said to be well-posed. It is easy to show that the operator $\mathcal{A}$, given by (2.1.4) is skew-adjoint. Therefore, one can use the following version of Stone's Theorem [6,page 32].

Theorem 2.1.2. (Stone's Theorem) The linear operator $\mathcal{A}$ is the generator of a C_0-unitary group on $\mathbf{E}$ if and only if $\mathcal{A}$ is skew-adjoint.

In the remaining sections of this chapter, we consider the problems of well-posedness and stability for the damped versions of (2.1.1). Once the damping is introduced into the model the $\mathcal{A}$ operator for the first order system will no longer be skew-adjoint and Stone's Theorem cannot be used for well-posedness.

2.2 Damped System of Equations.

In this section, we introduce damping into the elastic system by means of a "damping operator". This general formulation allows one to consider both internal and external damping in one formulation. Upon adding damping to the system, equation (2.1.1) becomes

$$\ddot{x}(t) + \mathcal{D}_0\dot{x}(t) + \mathcal{A}_0x(t) = \mathcal{B}_0u(t), \tag{2.2.1}$$

and, in first order form

$$\dot{z}(t) = \mathcal{A}z(t) + \mathcal{B}u(t), \tag{2.2.2}$$

where $\mathcal{A}$ is given by

$$\mathcal{A} = \begin{pmatrix} 0 & I \\ -\mathcal{A}_0 & -D_0 \end{pmatrix}, \quad D(\mathcal{A}) = D(\mathcal{A}_0) \times \mathbf{V}. \tag{2.2.3}$$

In [11], Chen and Russell presented a mathematical theory for general internal damping operators that exhibits empirically observed damping rates in many elastic systems. They considered the damping operator, $\mathcal{D}_0$ to be proportional to the

positive square root $\mathcal{A}_0^{1/2}$ of $\mathcal{A}_0$. Also in [13], Hanson studied this "square root damping" for the case of an Euler-Bernoulli beam. However, given a self- adjoint positive definite operator $\mathcal{A}_0$, it is not always possible to obtain an explicit representation of $\mathcal{A}_0^{1/2}$.

We shall follow Gibson's approach [1] and use a variational formulation and assume that there exists a damping "functional"

$$d_0(v_1, v_2) : \mathbf{V} \times \mathbf{V} \mapsto \mathbf{R}$$

such that d_0 is bilinear, symmetric, continuous on $\mathbf{V} \times \mathbf{V}$ and nonnegative.

If $\mathcal{D}_0$ is a symmetric nonnegative "damping operator" defined on $D(\mathcal{A}_0)$ such that $\mathcal{D}_0$ is bounded relative to $\mathcal{A}_0$, i.e.,

$$||\mathcal{D}_0 x|| \leq \lambda^2 ||\mathcal{A}_0 x|| \qquad \forall x \in D(\mathcal{D}_0),$$

then $< \mathcal{D}_0 v_1, v_2 >_H$ defines a bilinear, symmetric, bounded, nonnegative functional on a dense subset of $\mathbf{V} \times \mathbf{V}$. In this case the unique extension of this functional to $\mathbf{V} \times \mathbf{V}$ is d_0 [1]. Both damping models considered in this paper satisfy the conditions given above. External damping is modeled by viscous damping which is provided by an operator proportional to the mass operator, and internal damping is modeled by Kelvin-Voigt damping which is represented by an operator proportional to the stiffness operator. In particular, $\mathcal{D}_0 = c\mathcal{M}_0$ represents "viscous damping" and $\mathcal{D}_0 = c\mathcal{A}_0$ provides a model of "Kelvin-Voigt" damping.

Under these hypotheses on d_0, there exists a unique bounded linear operator Λ_D from $\mathbf{V}$ into $\mathbf{V}'$ such that

$$d_0(v, v_1) = (\Lambda_D v_1)(v) \qquad v, v_1 \in \mathbf{V}.$$

The operator $(\Lambda_V^{-1}\Lambda_D)$ is then a bounded linear operator from $\mathbf{V}$ to $\mathbf{V}$ and $(\Lambda_V^{-1}\Lambda_D)$ is self-adjoint (on $\mathbf{V}$) since d_0 is symmetric. Moreover, if $v, v_1 \in \mathbf{V}$, then

$$d_0(v, v_1) =< v, \Lambda_V^{-1}\Lambda_D v_1 >_V =< \Lambda_V^{-1}\Lambda_D v, v_1 >_V .$$

The operator $(\Lambda_V^{-1}\Lambda_D)$ defines the damping operator, $\mathcal{D}_0$ that we consider in this paper.

To prove well-posedness for the system given by (2.2.1) or (2.2.2)-(2.2.3), we need the following result.

Lemma 2.2.1. The operator $\mathcal{A}$ given by (2.2.4) is dissipative in $\mathbf{E}$.

Proof:. Calculating the inner-product $< \mathcal{A}u, u >_E$ we find that for $u \in D(\mathcal{A})$

$$\begin{aligned} < \mathcal{A}u, u >_E &=< \begin{pmatrix} u_2 \\ -\mathcal{A}_0 u_1 - \mathcal{D}_0 u_2 \end{pmatrix}, \begin{pmatrix} u_1 \\ u_2 \end{pmatrix} >_E \\ &=< \mathcal{A}_0 u_2, u_1 >_H - < \mathcal{A}_0 u_1, u_2 >_H - < \mathcal{D}_0 u_2, u_2 >_H \\ &= - < \mathcal{D}_0 u_2, u_2 >_H \\ &= -d_0(u_2, u_2) \leq 0, \end{aligned}$$

which implies that $\mathcal{A}$ is dissipative.

In order to derive the semigroup generator, we need to invert the $\mathcal{A}_0$ operator. But $\mathcal{A}_0$ may be singular due to the existance of rigid-body modes. The operator $\mathcal{A}_1$ was added to assure coercivity of $\tilde{\mathcal{A}}_0$. Next, following the steps in [1], we define $\mathcal{A}^{-1} \in \mathbf{L}(\mathbf{E}, \mathbf{E})$ by

$$\mathcal{A}^{-1} = \begin{bmatrix} -\tilde{\mathcal{A}}_0^{-1}\mathcal{D}_0 & -\tilde{\mathcal{A}}_0^{-1} \\ I & 0 \end{bmatrix}.$$

This operator is clearly one-to-one and its range is dense since $\mathbf{V}$ is dense in $\mathbf{H}$ and $\overline{D(\mathcal{A}_0)} = \mathbf{V}$. Now, we take

$$\mathcal{A} = (\mathcal{A}^{-1})^{-1}.$$

The operator $\mathcal{A}$ is dissipative with dense domain (Lemma 2.2.1), and since $D(\mathcal{A}^{-1}) = \mathbf{E}$, $\mathcal{A}$ is maximal dissipative. Well-posedness will then follow from Theorem (1.2.1). The open-loop semigroup generator for the elastic system is given by

$$\tilde{\mathcal{A}} = \mathcal{A} + \begin{bmatrix} 0 & 0 \\ \mathcal{A}_1 & 0 \end{bmatrix}, \qquad D(\tilde{\mathcal{A}}) = D(\mathcal{A}).$$

The optimal control problem was sketched in Section (1.3) and results were given to insure the existence of a unique solution to the optimal control problem. Here, we specialize to the case where $\mathbf{E} = \mathbf{V} \times \mathbf{H}$, is the energy space and, $T(t)$, $S(t)$ are the open-loop and closed-loop semigroups, respectively. We need the following theorem [1, Page 24]

Theorem 2.2.2. Suppose that the open-loop semigroup $T(t)$ satisfies

$$||T(t)|| \leq M_1 e^{\alpha_1 t}, \qquad t \geq 0,$$

for positive constants M_1 and α_1, that $\Pi \in \mathbf{L}(\mathbf{E})$ is the minimal nonnegative self-adjoint solution to the algebraic Riccati equation (1.3.7), and that $S(t)$ is the optimal closed-loop semigroup given by $\mathcal{A} - \mathcal{B}R^{-1}\mathcal{B}^*\Pi$. If there exists a constant M_0 such that

$$\int_0^\infty ||S(t)z||^2 dt \leq M_0(< \Pi z, z >_E + ||z||^2) \qquad \forall z \in \mathbf{E},$$

and a constant M_0' such that

$$||\Pi|| \leq M_0',$$

then there exist positive constants M_2 and α_2, which are functions of M_0, M_0', M_1, and α_1 only, such that

$$||S(t)|| \leq M_2 e^{-\alpha_2 t}, \qquad t \geq 0.$$

The next theorem is for the case where all of the elastic components of the structure have some damping and the actuator is acting on the rigid-body mode. This is the case in most aerospace structures and in the problem considered here [1].

Theorem 2.2.3. i) Suppose that $\mathcal{A}_1 = \mathcal{B}_0\mathcal{B}_0^*$ and that $\tilde{\mathcal{A}}_0 = \mathcal{A}_0 + \mathcal{A}_1$ and $\tilde{d}_0 = d_0 + \mathcal{A}_1$ are $\mathbf{H}$-coercive, so that there exist positive constants ρ, γ, β such that for all $v \in \mathbf{V}$

$$||v||_V^2 \geq \rho ||v||_H^2 \tag{2.2.4}$$

$$\tilde{d}_0(v, v) \geq \rho ||v||_H^2 \tag{2.2.5}$$

and with $\mathcal{D}_0$ being bounded with respect to $\mathcal{A}_0$,ie., ($||\mathcal{D}_0 z|| \leq \tau^2 ||\mathcal{A}_0 z||$),

$$\tilde{d}_0(v, v) \leq \gamma ||v||_V^2 \tag{2.2.6}$$

and

$$max\{||\mathcal{B}_0||, ||\mathcal{Q}||, ||R||\} \leq \beta, \tag{2.2.7}$$

then (1.3.7) has a minimal nonnegative self-adjoint solution Π which satisfies

$$||\Pi|| \leq M_0'(\rho, \gamma, \beta)$$

ii) Suppose also that

$$< \mathcal{Q}z, z >_E \geq \rho||z||_E^2 \quad z \in \mathbf{E},$$

then the optimal closed-loop semigroup satisfies

$$||S(t)|| \leq M_2 e^{-\alpha_2 t} \qquad t \geq 0,$$

where M_2 and α_2 are positive constants depending on ρ, γ, β only.

Proof. i) The sub-optimal control

$$u(t) = -\mathcal{B}_0^*[x(t) + \dot{x}(t)]$$

presents an admissible control, and from theorem (1.3.1), there is a minimal nonnegative solution to the algebraic Riccati equation (1.3.7). To get the required upper bound, from (1.3.3) and (1.3.8), we get

$$< \Pi z, z > \leq \int_0^\infty [< \mathcal{Q}z, z >_E + < Ru, u >_{R^m}]dt,$$

or

$$| < \Pi z, z > | \leq | \int_0^\infty [< \mathcal{Q}z, z >_E + < Ru, u >_{R^m}]dt|.$$

Since both $\mathcal{Q}$ and $\mathcal{R}$ are bounded from above by (2.2.7), the left hand side is also bounded from above for every $z \in \mathbf{E}$. Then, using Uniform Boundedness Principle (Banach Steinhaus Theorem) [8,Page 74], we obtain the bound

$$||\Pi|| \leq M_1.$$

ii) In this case, the M_0 in the previous theorem is ρ, and the theorem yields the result.

Note that in this theorem $\mathcal{A}_1$, which is associated with the rigid body part of $\tilde{\mathcal{A}}_0$, is directly related to $\mathcal{B}_0$. This is the case with the problem considered in this paper where, the only control is a torque acting at the hub.

With $\Pi \in \mathbf{L}(\mathbf{E})$ and $\mathbf{E} = \mathbf{V} \times \mathbf{H}$, we can write

$$\Pi = \begin{bmatrix} \Pi_0 & \Pi_1 \\ \Pi_1^* & \Pi_2 \end{bmatrix},$$

where $\Pi_0 \in \mathbf{L}(\mathbf{V})$, $\Pi_1 \in \mathbf{L}(\mathbf{H}, \mathbf{V})$, $\Pi_2 \in \mathbf{L}(\mathbf{H})$ and Π_0 and Π_2 are nonnegative and self-adjoint. Since $z = (x, \dot{x})^T$, equation (1.3.6) becomes

$$u(t) = -R^{-1}\mathcal{B}_0^*[\Pi_1^* x(t) + \Pi_2 \dot{x}(t)]. \tag{2.2.8}$$

Since $\mathcal{B}_0 \in \mathbf{L}(\mathbf{R}^m, \mathbf{H})$, we must have vectors $b_i \in \mathbf{H}, \quad 1 \leq i \leq m$ such that

$$\mathcal{B}_0 u = \sum_{i=1}^{m} b_i u_i$$

for

$$u = [u_1, u_2, ..., u_m]^T \in \mathbf{R}^m$$

Also for $h \in \mathbf{H}$

$$\mathcal{B}_0^* h = [< b_1, h >_H, ..., < b_m, h >_H]^T. \tag{2.2.9}$$

Now $\Pi_1^* x(t)$ and $\Pi_2 \dot{x}(t)$ are elements of $\mathbf{H}$, and using (2.2.8) and (2.2.9), we can write the components of the optimal control in the feedback form

$$u_i(t) = - < f_i, x(t) >_V - < g_i, \dot{x}(t) >_H \qquad i = 1, ..., m. \tag{2.2.10}$$

Where $f_i \in \mathbf{V}$ and $g_i \in \mathbf{H}$ are given by

$$f_i = \sum_{j=1}^{m} (R_{ij})^{-1} \Pi_1 b_j$$

$$g_i = \sum_{j=1}^{m} (R_{ij})^{-1} \Pi_2 b_j, \qquad i = 1, m.$$

The elements f_i and g_i define the gain operator.

2.3. The Approximating Open Loop System.

We now introduce a general approximation scheme. We follow the framework given by Banks and Kunisch in [2] and Gibson in [1]. For each $N = 1, 2, ...$, let $\mathbf{V}^N$ be a finite-dimensional subspace of $\mathbf{V}$ with dimensions N and $\mathcal{P}_{V_N}$ be the orthogonal projection of $\mathbf{V}$ onto $\mathbf{V}^N$. We assume that the sequence of orthogonal projections $\mathcal{P}_{V_N}$ converges $\mathbf{V}$-strongly to the identity. Since $\mathbf{V}^N$ is finite dimensional it is the span of N linearly independent vectors e_i^N, $i = 1, 2, ..., N$.

For $N \geq 1$ if one assumes a general Galerkin approximation of the form

$$x^N(t) = \sum_{j=1}^{N} \xi_j(t) e_j^N, \tag{2.3.1}$$

then $\xi(t) = [\xi_1(t), \xi_2(t), ..., \xi_N(t)]^T$ will satisfy a system of the form

$$M^N\ddot{\xi}(t) + D^N\dot{\xi}(t) + K^N\xi(t) = B_0^N u(t), \tag{2.3.2}$$

where the mass matrix M^N, damping matrix D^N, stiffness matrix K^N, and actuator influence matrix B_0^N are given by

$$\begin{aligned}
M_{ij}^N &= [< e_i^N, e_j^N >_H], \\
D_{ij}^N &= [d_0(e_i^N, e_j^N)], \\
K_{ij}^N &= [< \mathcal{A}_0^{1/2} e_i^N, \mathcal{A}_0^{1/2} e_j^N >_H] = [< e_i^N, e_j^N >_V] - [< \mathcal{A}_1 e_i^N, e_j^N >_H], \\
B_{0_{ij}}^N &= [< e_i^N, b_j >_H].
\end{aligned} \tag{2.3.3}$$

There are several ways to write (2.3.2) in first order form. One way of representing (2.3.2) in a first order form would be to use the states $\eta = \begin{pmatrix} \xi \\ \dot{\xi} \end{pmatrix}$ and (2.3.2) becomes

$$\dot{\eta} = A^N\eta + B^N u, \tag{2.3.4}$$

where

$$A^N = \begin{bmatrix} 0 & I \\ -[M^N]^{-1}K^N & -[M^N]^{-1}D^N \end{bmatrix}, \qquad B^N = \begin{bmatrix} 0 \\ -[M^N]^{-1}B_0^N \end{bmatrix}.$$

It is useful to note that (2.3.2),(2.3.4) are matrix representation of the following ODE in $\mathbf{E}^N$,

$$\dot{z}^N(t) = \mathcal{A}^N z^N(t) + \mathcal{B}^N u(t) \tag{2.3.5}$$

where $z^N = (x^N, \dot{x}^N)^T \in \mathbf{E}^N$, and $\mathcal{A}^N \in L(\mathbf{E}^N), \mathcal{B}^N = L(\mathbf{R}^m, \mathbf{E}^N)$ are the operators whose matrix representations are given by (2.3.4).

The resolvent equation

$$(\lambda - \mathcal{A}^N)\begin{pmatrix} v_1^N \\ v_2^N \end{pmatrix} = \begin{pmatrix} h_1^N \\ h_2^N \end{pmatrix}, \tag{2.3.6}$$

can be represented in terms of the finite element system if one expands v_j^N and h_j^N, $j = 1, 2$ by

$$v_j^N = \sum_{i=1}^{N} \alpha_j^i e_i^N \quad h_j^N = \sum_{i=1}^{N} \beta_j^i e_i^N \tag{2.3.7}$$

and uses the definitions above. In particular (2.3.6) becomes

$$(\lambda^2 M^N + \lambda D^N + K^N)\vec{\alpha}_1 = (\lambda M^N + D^N)\vec{\beta}_1 + M^N \vec{\beta}_2, \tag{2.3.8}$$

and

$$\vec{\alpha}_2 = \lambda \vec{\alpha}_1 - \vec{\beta}_1, \tag{2.3.9}$$

where $\vec{\alpha}_j = [\alpha_j^1, \alpha_j^2, ..., \alpha_j^N]^T$ and $\vec{\beta}_j = [\beta_j^1, \beta_j^2, ..., \beta_j^N]^T$, for $j = 1, 2$.

These relations hint to a particular norm on $\mathbf{V}$, where convergence of the approximation scheme is studied.

To study the approximation scheme we use the Trotter-Kato theorem which is the infinite dimensional version of the Lax equivalence theorem. There are several version of this theorem. The following theorem may be found in the paper by Banks, Burns and Cliff [15] and Theorem 2.3.2 can be found in [Kato, Page 504].

Let $\mathbf{Z}$, and $\mathbf{Z}^N, N = 1, 2, ..$ be Hlibert spaces with norms $||.||_Z$ and $||.||_{Z^N}$. Let $\mathbf{X}^N$ be a closed subspaces of $\mathbf{Z}^N$ and $\pi^N : \mathbf{Z}^N \mapsto \mathbf{X}^N$ be the orthogonal projection

of $\mathbf{Z}^N$ onto $\mathbf{X}^N$. Suppose $\Im^N : \mathbf{Z} \mapsto \mathbf{Z}^N$ is a mapping satisfying $R(\Im^N) = \mathbf{Z}^N$ and $||\Im^N z||_{Z^N} \leq ||z||_Z$ for $z \in \mathbf{Z}$. Finally define $\mathcal{P}^N : \mathbf{Z} \mapsto \mathbf{X}^N$ by $\mathcal{P}^N = \pi^N \Im^N$. Also, for a Hilbert space $\mathbf{X}$, we write $\mathcal{A} \in \mathbf{G}(M, \beta)$ to mean $\mathcal{A} : (D(\mathcal{A}) \subset \mathbf{X}) \mapsto \mathbf{X}$ is the infinitesimal generator of a C_0-semigroup $T(t)$ satisfying $||T(t)|| \leq Me^{\beta}t$.

Theorem 2.3.1. (Trotter-Kato) Let $\mathbf{Z}, \mathbf{Z}^N, \mathbf{X}^N$ and $\mathcal{P}^N$ be given as above. Suppose for some M, β we have $\mathcal{A}^N \in \mathbf{G}(M, \beta)$ on $\mathbf{Z}$. Further suppose there exists $\hat{D} \subset D(\mathcal{A})$, D dense in $\mathbf{Z}$ such that

i) $(\lambda \mathcal{I} - \mathcal{A})^{-1} \hat{D} \subset D$ for $Re\lambda > \beta$,

ii) for every $z \in \hat{D}$, $||\mathcal{A}^N \mathcal{P}^N z - \mathcal{P}^N \mathcal{A} z||_{Z^N} \to 0 \quad as \quad N \to \infty$.

Then, for every $z \in \mathbf{Z}$

$$||S^N(t)\mathcal{P}^N z - \mathcal{P}^N S(t) z||_{Z^N} \to 0 \quad as \quad N \to \infty,$$

and the convergence is uniform in t on compact intervals. Here $\mathcal{A}^N$ is the infinitesimal generator for $S^N(t)$ and $\mathcal{A}$ is the infinitesimal generator for $S(t)$.

Theorem 2.3.2. Let $\mathcal{A}$ and $\mathcal{A}^N$, $N = 1, 2, ..$ belong to $\mathbf{G}(M, \beta)$. If

$$(\xi - \mathcal{A}^N)^{-1} z \to (\xi - \mathcal{A})^{-1} z$$

for all $z \in \mathbf{Z}$ and some ξ with $\mathrm{Re}\xi > \beta$, then for each $z \in \mathbf{Z}$

$$e^{t\mathcal{A}^N} z \to e^{t\mathcal{A}} z$$

uniformly in any finite interval of $t \geq 0$.

We first treat the case in which $\mathcal{A}_0$ is coercive (no rigid- body modes). The general case is a straight forward extension. The main idea is to project $(\lambda - \mathcal{A})^{-1}$ onto $\mathbf{E}^N$ in a certain inner product and observe that the result is exactly $(\lambda - \mathcal{A}^N)^{-1}$ where $\mathcal{A}^N$ is the operator on $\mathbf{E}^N$ in (2.3.5) and (2.3.6).

For real $\lambda > 0$, define an inner product on $\mathbf{V}$ by

$$< .,. >_\lambda = \lambda^2 < .,. >_H + \lambda d_0(.,.) + < .,. >_V . \tag{2.3.10}$$

Let $\mathcal{P}^N(\lambda)$ be the projection operator of $\mathbf{V}$ onto $\mathbf{V}^N$ in the inner product $< .,. >_\lambda$, now let $h_1, h_2 \in \mathbf{H}$ and note that

$$(\lambda - \mathcal{A}) \begin{pmatrix} v_1 \\ v_2 \end{pmatrix} = \begin{pmatrix} h_1 \\ h_2 \end{pmatrix} \tag{2.3.11}$$

is equivalent to

$$\begin{pmatrix} v_1 \\ v_2 \end{pmatrix} = \mathcal{A}^{-1} \left[\lambda \begin{pmatrix} v_1 \\ v_2 \end{pmatrix} - \begin{pmatrix} h_1 \\ h_2 \end{pmatrix} \right]. \tag{2.3.12}$$

After substituting $\mathcal{A}^{-1}$ into equation (2.3.12), one obtains

$$(I + \lambda \Lambda_V^{-1} \Lambda_D + \lambda^2 \mathcal{A}_0^{-1}) v_1 = (\lambda \mathcal{A}_0^{-1} + \Lambda_V^{-1} \Lambda_D) h_1 + \mathcal{A}_0^{-1} h_2 \tag{2.3.13}$$

and

$$v_2 = \lambda v_1 - h_1. \tag{2.3.14}$$

If $v_1^N = \mathcal{P}^N(\lambda) v_1$ and $v_2^N = \mathcal{P}^N(\lambda) v_2$, then

$$< e_i^N, v_1^N >_\lambda = < e_i^N, v_1 >_\lambda,$$

$$< e_i^N, v_2^N >_\lambda = < e_i^N, v_2 >_\lambda .$$

Using (2.3.10), the λ-inner product $< e_i^N, v_1^N >_\lambda$ gives

$$\begin{aligned} < e_i^N, v_1^N >_\lambda &=< e_i^N, v_1 >_\lambda \qquad (2.3.15) \\ &=< e_i^N, \mathcal{A}_0\mathcal{A}_0^{-1}v_1 >_H + \lambda < e_i^N, \Lambda_V^{-1}\Lambda_D v_1 >_V + < e_i^N, v_1 >_V \\ &=< e_i^N, (\lambda^2\mathcal{A}_0^{-1} + \lambda\Lambda_V^{-1}\Lambda_D + I)v_1 >_V \\ &=< e_i^N, (\lambda\mathcal{A}_0^{-1} + \Lambda_V^{-1}\Lambda_D)h_1 + \mathcal{A}_0^{-1}h_2 >_V \end{aligned}$$

and from (2.3.14), $< e_i^N, v_2^N >_\lambda$ becomes

$$< e_i^N, v_2^N >_\lambda =< e_i^N, v_2 >_\lambda = \lambda < e_i^N, v_1 >_\lambda - < e_i^N, h_1 >_\lambda . \qquad (2.3.16)$$

If $h_1 = h_1^N \in \mathbf{V}^N$ and $h_2 = h_2^N \in \mathbf{V}^N$, we use the representations (2.3.7) for $v_1^N, v_2^N, h_1^N, h_2^N$ in (2.3.15) and carry out the inner products. For each $i = 1, 2, ..., N$ the left hand side of (2.3.15) simplifies to

$$\begin{aligned} < e_i^N, v_1^N >_\lambda &= \lambda^2 < e_i^N, v_1^N >_H + \lambda d_0(e_i^N, v_1^N) + < e_i^N, v_1^N >_V \\ &= \sum_{j=1}^{N} (\lambda^2 < e_i^N, e_j^N >_H \alpha_j + \lambda d_0(e_i^N, e_j^N)\alpha_j + < e_i^N, e_j^N >_V \alpha_j). \end{aligned}$$

Consequently, $[< e_1^N, v_1^N >_\lambda, < e_2^N, v_2^N >_\lambda, ..., < e_N^N, v_1^N >_\lambda]^T \equiv [< e_i^N, v_1^N >_\lambda]$ is given by

$$[< e_i^N, v_1^N >_\lambda] = (\lambda^2 M^N + \lambda D^N + K^N)\overrightarrow{\alpha}_1.$$

Likewise, (2.3.15) yields

$$[< e_i^N, v_1^N >_\lambda] = \lambda M^N \overrightarrow{\beta}_1 + D^N \overrightarrow{\beta}_1 + M^N \overrightarrow{\beta}_2.$$

Comparing the above results, it follows that

$$(\lambda^2 M^N + \lambda D^N + K^N)\vec{\alpha}_1 = (\lambda M^N + D^N)\vec{\beta}_1 + M^N \vec{\beta}_2,$$

which is identical to (2.3.8). Similar calculation yields

$$\begin{bmatrix} \mathcal{P}^N(\lambda) & 0 \\ 0 & \mathcal{P}^N(\lambda) \end{bmatrix} (\lambda - \mathcal{A})^{-1}|_{\mathbf{E}^N} = (\lambda - \mathcal{A}^N)^{-1},$$

and

$$\begin{bmatrix} \mathcal{P}^N(\lambda) & 0 \\ 0 & \mathcal{P}^N(\lambda) \end{bmatrix} (\lambda - \mathcal{A})^{-1}\mathcal{P}_{E^N} = (\lambda - \mathcal{A}^N)^{-1}\mathcal{P}_{E^N},$$

where $\mathcal{P}_{E^N}$ is the orthogonal projection onto $\mathbf{E}^N$. Therefore, $\mathcal{P}_{E^N}$ can be written in the form

$$\mathcal{P}_{E^N} = \begin{bmatrix} \mathcal{P}_{V^N} & 0 \\ 0 & \mathcal{P}_{H^N} \end{bmatrix},$$

where $\mathcal{P}_{H^N}$ is the orthogonal projection of $\mathbf{H}$ onto $\mathbf{H}^N$. Since the $\mathbf{V}$ norm is stronger than the $\mathbf{H}$ norm (convergence in $\mathbf{V}$ implies convergence in $\mathbf{H}$), the norm induced by the λ-inner product is equivalent to the $\mathbf{V}$ norm. Thus, it follows that $(\lambda - \mathcal{A}^N)^{-1}\mathcal{P}_{E^N}$ converges strongly in $\mathbf{E}$ to $(\lambda - \mathcal{A})^{-1}$ as $N \to \infty$. Also, with $\mathcal{A}^N$ extended to $\mathbf{E}^{N^\perp}$ (the orthogonal complement of $\mathbf{E}^N$), as say, $N(\mathcal{P}_{E^N} - I)$, Theorem 2.3.2 yields the following result.

Theorem 2.3.3. Assume that $\mathcal{A}_0$ is coercive and $T^N(.)$ is the semigroup generated on $\mathbf{E}^N$ by $\mathcal{A}^N$. Then for each $t > 0$, $T^N(t)\mathcal{P}_{E^N}$ converges strongly to $T(t)$, uniformly in t for t in bounded intervals.

In the general case, when $\mathcal{A}_0$ is not coercive, the open loop generator $\mathcal{A}$ is obtained from the dissipative $\mathcal{A}$ by the bounded perturbation in (2.1.3) and the following generalization of the theorem holds (see [1], Corollary 4.3)

Lemma 2.3.1. Let $T^N(.)$ be the semigroup generated on $\mathbf{E}^N$ by $\mathbf{A}^N$. Then for each $t \geq 0$, $T^N(t)\mathcal{P}_{E^N}$ converges strongly to $T(t)$, uniformly in t for t in bounded intervals.

Entirely similar arguments are used to show that the adjoint semigroups also converge strongly. In particular we have the following result ([1],Theorem 4.5)

Theorem 2.3.4. Let $T^N(.)$ be the sequence of semigroups in Lemma 2.3.1. Then, for each $t \geq 0$, $T^{N^*}(t)\mathcal{P}_{E^N}$ converge strongly to $T^*(t)$, uniformly in t for t in bounded intervals.

The approximation to the actuator influence operator $\mathcal{B} \in \mathbf{L}(\mathbf{R}^m, \mathbf{E})$ is $\mathcal{B}^N \in \mathbf{L}(\mathbf{R}^m, \mathbf{E}^N)$ whose matrix representation is B^N given in equation (2.3.4). From equations (2.3.3), it follows that

$$\mathcal{B}^N = \mathcal{P}_{E^N}\mathcal{B}.$$

Since $\mathcal{B}$ has finite rank m, $\mathcal{B}^N$ and $\mathcal{B}^{N^*}$ converge strongly to $\mathcal{B}$ and $\mathcal{B}^*$, respectively.

2.4. The Approximating Optimal Control Problem.

In this section, we study the approximate optimal control problem, which is

the projection of the infinite-dimensional optimal control problem on $\mathbf{E}$ onto the subspace $\mathbf{E}^N$.

The N-th Optimal Control Problem is to choose $u^N \in L_2(0,\infty,\mathbf{R}^m)$ to minimize

$$J^N(z^N(0),u^N) = \int_0^\infty (< \mathcal{Q}^N z^N(t), z^N(t) >_E + < Ru(t), u(t) >_R)\, dt, \qquad (2.4.1)$$

subject to

$$\dot{z}^N(t) = \mathcal{A}^N z(t) + \mathcal{B}^N u^N$$

$$y^N(t) = \mathcal{C}^N z(t),$$

given an initial condition $z^N(0) = (x^N(0), \dot{x}^N(0))^T \in \mathbf{E}^N$, where

$$\mathcal{Q}^N = \mathcal{C}^{N*}\mathcal{C}^N = \mathcal{P}_{E^N}\mathcal{Q}|_{E^N}.$$

To assure existence of an admissible sub-optimal control, it is sufficient to assume that for each N, $(\mathcal{A}^N, \mathcal{B}^N, \mathcal{C}^N)$ is stabilizable and detectable, then the optimal control $u^N(t)$ has the feedback form

$$u^N(t) = -R^{-1}\mathcal{B}^{N*}\Pi^N z^N(t), \qquad (2.4.2)$$

where Π^N is a linear positive definite self-adjoint operator on $\mathbf{E}^N$, and satisfies the Riccati equation

$$\mathcal{A}^{N*}\Pi^N + \Pi^N\mathcal{A}^N - \Pi^N\mathcal{B}^N R^{-1}\mathcal{B}^{N*}\Pi^N + \mathcal{Q}^N = 0. \qquad (2.4.3)$$

If $(\mathcal{A}^N, \mathcal{Q}^N)$ is observable, then Π^N is the unique positive definite self-adjoint solution of (2.4.3). We partition Π^N as

$$\Pi^N = \begin{bmatrix} \Pi_0^N & \Pi_1^N \\ \Pi_1^{N*} & \Pi_2^N \end{bmatrix}, \qquad (2.4.4)$$

then (2.4.2) can be written as

$$u^N(t) = - < f^N, x^N(t) >_V - < g^N, \dot{x}^N(t) >_H, \tag{2.4.5}$$

with,

$$f^N = R^{-1}\Pi_1^N \mathcal{P}_{H^N} b$$

$$g^N = R^{-1}\Pi_2^N \mathcal{P}_{H^N} b,$$

where $b \in \mathbf{H}$ and f^N, g^N are the N-th approximation to the gain operators.

For the numerical solution of the N-th problem, the matrix representations of these equations are used. We will need the following matrices

$$\begin{aligned} \tilde{K}^N &= [< e_i^N, e_j^N >_V] \\ &= K^N + [< \mathcal{A}_1 e_i^N, e_j^N >_H] \\ W^N &= \begin{bmatrix} \tilde{K}^N & 0 \\ 0 & M^N \end{bmatrix}. \end{aligned} \tag{2.4.6}$$

Since $\mathcal{Q} = \mathcal{Q}^* \in L(\mathbf{E})$ and $\mathbf{E} = \mathbf{V} \times \mathbf{H}$, we can write

$$\mathcal{Q} = \begin{bmatrix} \mathcal{Q}_0 & \mathcal{Q}_1 \\ \mathcal{Q}_1^* & \mathcal{Q}_2 \end{bmatrix},$$

with $\mathcal{Q}_0 = \mathcal{Q}_0^* \in L(\mathbf{V})$, $\mathcal{Q}_1 \in L(\mathbf{H}, \mathbf{V})$, $\mathcal{Q}_2 = \mathcal{Q}_2^* \in L(\mathbf{H})$.

For the matrix representation of $\mathcal{Q}_0^N \in L(\mathbf{V})$, let

$$u^N = \mathcal{Q}_0 v^N, \qquad u^N, v^N \in \mathbf{V^N}.$$

Since u^N and v^N are elements of $\mathbf{V}^N$, they have the representations

$$u^N = \sum_{j=1}^{N} \alpha_j^N e_j^N, \qquad v^N = \sum_{j=1}^{N} \beta_j^N e_j^N.$$

Substituting into the above equation and taking the inner-product with e_i^N, it yields

$$[< e_i^N, e_j^N >]\vec{\alpha} = [< e_i^N, \mathcal{Q}_0 e_j^N >]\vec{\beta},$$

therefore, the matrix representation of $\mathcal{Q}_0^N$ is $[< e_i^N, e_j^N >_V]^{-1}[< e_i^N, \mathcal{Q}_0 e_j^N >_V]$.

Following the same procedure for the rest of $\mathcal{Q}$'s, one gets

$$Q^N = [W^N]^{-1}\tilde{Q}^N. \tag{2.4.7}$$

Where Q^N is the matrix representation of $\mathcal{Q}^N$ and $\tilde{Q}_N$ is the nonnegative, symmetric matrix

$$\tilde{Q}^N = \begin{bmatrix} \tilde{Q}_0^N & \tilde{Q}_1^N \\ \tilde{Q}_1^{N^T} & \tilde{Q}_2^N \end{bmatrix} \tag{2.4.8}$$

with

$$\tilde{Q}_0^N = [< e_i^N, \mathcal{Q}_0 e_j^N >_V]$$

$$\tilde{Q}_1^N = [< e_i^N, \mathcal{Q}_1 e_j^N >_V]$$

$$\tilde{Q}_2^N = [< e_i^N, \mathcal{Q}_2 e_j^N >_H].$$

Also, the matrix representations of $\mathcal{A}^{N^*}, \mathcal{B}^{N^*}$ are given by

$$[W^N]^{-1}[A^N]^T W^N, \qquad \textit{and} \qquad [B^N]^T W^N,$$

respectively.

Denoting the matrix representation of Π^N by Π^N, the Riccati operator equation is equivalent to Riccati matrix equation

$$[W^N]^{-1}[A^N]^T W^N \Pi^N + \Pi^N A^N - \Pi^N B^N R^{-1}[B^N]^T W^N \Pi^N + Q^N = 0.$$

Premultiplying by W^N, and letting $\tilde{\Pi}^N = W^N \Pi^N$, we obtain

$$[A^N]^T \tilde{\Pi}^N + \tilde{\Pi}^N A^N - \tilde{\Pi}^N B^N R^{-1}[B^N]^T \tilde{\Pi}^N + \tilde{Q}^N = 0, \tag{2.4.9}$$

which is the Riccati matrix equation to be solved numerically.

Since the gains are elements of $\mathbf{V}^N$ and $\mathbf{H}^N$ they can be written as

$$f^N = \sum_{j=1}^{N} \beta_j^f e_j^N \qquad g^N = \sum_{j=1}^{N} \beta_j^g e_j^N, \tag{2.4.10}$$

where $\vec{\beta}^f = [\beta_1^f, \beta_2^f, ..., \beta_N^f]^T$ and $\vec{\beta}^g = [\beta_1^g, \beta_2^g, ..., \beta_N^g]^T$. The equations relating $\vec{\beta}^f$ and $\vec{\beta}^g$ to $\tilde{\Pi}^N$ are given by [1],

$$\begin{pmatrix} \vec{\beta}^f \\ \vec{\beta}^g \end{pmatrix} = [W^N]^{-1} \tilde{\Pi}^N B^N R^{-1}. \tag{2.4.11}$$

The goal is to compute the gains, which then, can be used to obtain the control input, using (2.4.5). The complete solution to the N-th optimal control problem is then, to solve the Riccati matrix equation (2.4.9) for $\tilde{\Pi}^N$, then the optimal control is given by (2.4.5), with the gains given by (2.4.10) and (2.4.11).

Chapter III

The Timoshenko Beam Control Problem

In Chapter 2, we apply the general theory of LQR to a particular class of structural vibration problems. We prove well-posedness and stability under a general set of conditions for a dynamical system given by an abstract second-order equation. In this chapter, we specialize to a slewing beam problem sketched in Chapter 1. The results in [1] were applied to an Euler-Bernoulli model and until now the Timoshenko model has not been fully investigated. The main contribution of this dissertation is then to obtain convergent results for an LQR problem on a hub-beam-tip structure governed by Timoshenko model, and to study the effect of system parameters, as well as different finite element spaces on the convergence of the gain operators. We write equations (1.1.1) in a standard second order form, and proceed to show that the control problem for the Timoshenko beam governed by (1.1.1) can be put in the general framework given in Chapter 2. Well-posedness for this particular problem will then follow from the results in Chapter 2.

3.1. The Timoshenko System.

The equations of motion for the structure in Figure 1 were given in Chapter 1.

With the parameters defined as before, they are

$$\begin{aligned}
I_h\ddot{\theta}(t) &= EI\psi_x(t,0) + M_a(t) \\
\rho A(u_{tt}(t,x) + x\ddot{\theta}(t)) &= KGA(u_x(t,x) - \psi(t,x))_x \\
\rho I(\psi_{tt}(t,x) + \ddot{\theta}(t)) &= EI\psi_{xx}(t,x) + KGA(u_x(t,x) - \psi(t,x)) \\
m_c(u_{tt}(t,l) + l\ddot{\theta}(t)) &= -KGA(u_x(t,l) - \psi(t,l)) \\
I_c(\psi_{tt}(t,l) + \ddot{\theta}(t)) &= -EI\psi_x(t,l),
\end{aligned} \tag{1.1.1}$$

along with the boundary conditions

$$u(t,0) = \psi(t,0) = 0.$$

Define the vector z to be

$$z = \begin{pmatrix} \theta(t) \\ u(t,x) + x\theta(t) \\ \psi(t,x) + \theta(t) \\ u(t,l) + l\theta(t) \\ \psi(t,l) + \theta(t) \end{pmatrix},$$

then equations (1.1.1) can be put in a standard second order form

$$\ddot{z}(t) + \mathcal{A}_0 z(t) = \mathcal{B}_0 u(t), \tag{3.1.1}$$

where z is in a real Hilbert space $\mathbf{H} = \mathbf{R}^1 \times \mathbf{L}_2 \times \mathbf{L}_2 \times \mathbf{R}^1 \times \mathbf{R}^1$, $u(t)$ is in $\mathbf{R}^1$, $\mathcal{B}_0 : \mathbf{R}^1 \mapsto \mathbf{H}$ and $\mathcal{A}_0 : D(\mathcal{A}_0) \mapsto \mathbf{H}$, with $\mathcal{A}_0$ given by:

$$\mathcal{A}_0 = -\begin{bmatrix} 0 & 0 & \frac{EI}{I_h}\delta_0 D & 0 & 0 \\ 0 & \frac{KGA}{\rho A}D^2 & -\frac{KGA}{\rho A}D & 0 & 0 \\ 0 & \frac{KGA}{\rho I}D & \frac{EI}{\rho I}D^2 - \frac{KGA}{\rho I} & 0 & 0 \\ 0 & -\frac{KGA}{m_c}\delta_l D & \frac{KGA}{m_c}\delta_l & 0 & 0 \\ 0 & 0 & -\frac{EI}{I_c}\delta_l D & 0 & 0 \end{bmatrix}. \tag{3.1.2}$$

Here D denotes differentiation with respect to x. The notation δ_x is the standard notation for the delta function with the property that if $\phi \in \mathbf{C}[0,\ell]$

$$\delta_x \phi(.) = \phi(x).$$

The domain of $\mathcal{A}_0$ is given by, $D(\mathcal{A}_0) =$

$$\{z \in \mathbf{H}/z_2, z_3 \in \mathbf{W}^{2,2}, z_2(0) = 0., z_2(l) = z_4, z_3(0) = z_1, z_3(l) = z_5\}. \qquad (3.1.3)$$

The Hilbert space $\mathbf{H}$ is equipped with the inner product

$$< z, \hat{z} >_H = I_h z_1 \hat{z}_1 + \rho A \int_0^l z_2 \hat{z}_2 \, dx + \rho I \int_0^l z_3 \hat{z}_3 \, dx + m_c z_4 \hat{z}_4 + I_c z_5 \hat{z}_5. \qquad (3.1.4)$$

In order to apply the results presented in Chapter 2, we first need to prove that the operator $\mathcal{A}_0$ is self-adjoint with dense domain, and one can find an operator $\mathcal{A}_1$ so that $\tilde{\mathcal{A}}_0 = \mathcal{A}_0 + \mathcal{A}_1$ is coercive.

Lemma 3.1.1. Domain of $\mathcal{A}_0$ is dense in $\mathbf{H} = (\mathbf{R}^1 \times \mathbf{L}_2 \times \mathbf{L}_2 \times \mathbf{R}^1 \times \mathbf{R}^1)$.

Proof:. Let $\epsilon > 0$ and assume that $h = (r_1, \phi_2(.), \phi_3(.), r_4, r_5) \in \mathbf{H}$. Let $\psi_2(.) \in \mathbf{W}^{2,2}$ be such that $\psi_2(0) = 0, \psi_2(l) = r_4$ and

$$\rho A \int_0^l ||\psi_2(s) - \phi_2(s)||^2, ds < \frac{\epsilon}{3}.$$

Likewise, pick $\psi_3(.) \in \mathbf{W}^{2,2}$ such that $\psi_3(0) = r_1, \psi_3(l) = r_5$ and

$$\rho I \int_0^l ||\psi_3(s) - \phi_3(s)||^2, ds < \frac{\epsilon}{3}.$$

It follows that $h_\epsilon = (r_1, \psi_2(.), \psi_3(.), r_4, r_5)^T \in D(\mathcal{A}_0)$ and

$$\begin{aligned} ||h - h_\epsilon||_H^2 &\leq \rho A \int_0^l ||\psi_2(s) - \phi_2(s)||^2, ds + \rho I \int_0^l ||\psi_3(s) - \phi_3(s)||^2, ds \\ &< \frac{\epsilon}{3} + \frac{\epsilon}{3} < \epsilon. \end{aligned}$$

Hence $D(\mathcal{A}_0)$ is dense in $\mathbf{H}$.

Theorm 3.1.1. The operator $\mathcal{A}_0$ is self-adjoint with respect to the Hilbert space $\mathbf{H}$.

Proof. We proceed to find the adjoint of $\mathcal{A}_0$. Let $u \in \mathbf{H}$ and assume that there exists $\tilde{u}$ such that

$$0 = < \mathcal{A}_0 v, u >_H - < v, \tilde{u} >_H \qquad \forall v \in D(\mathcal{A}_0).$$

The definition of $\mathcal{A}_0$ yields that for all $v \in D(\mathcal{A}_0)$

$$\left\langle \begin{pmatrix} \frac{EI}{I_h}\delta_0 v_3' \\ \frac{KGA}{\rho A}(v_2'' - v_3') \\ \frac{KGA}{\rho I}(v_2' - v_3) + \frac{EI}{\rho I}v_3'' \\ -\frac{KGA}{m_c}\delta_l(v_2' - v_3) \\ -\frac{EI}{I_c}\delta_l v_3' \end{pmatrix}, \begin{pmatrix} u_1 \\ u_2 \\ u_3 \\ u_4 \\ u_5 \end{pmatrix} \right\rangle + \left\langle \begin{pmatrix} v_1 \\ v_2 \\ v_3 \\ v_4 \\ v_5 \end{pmatrix}, \begin{pmatrix} \tilde{u}_1 \\ \tilde{u}_2 \\ \tilde{u}_3 \\ \tilde{u}_4 \\ \tilde{u}_5 \end{pmatrix} \right\rangle = 0.$$

Expanding this expression and using (3.1.4), it follows that for $v \in D(\mathcal{A}_0)$,

$$\begin{aligned} &EIu_1 v_3'(0) + KGA \int_0^l u_2(x)(v_2''(x) - v_3'(x))\, dx + KGA \int_0^l u_3(x)(v_2'(x) - v_3(x))\, dx \\ &+ EI \int_0^l u_3(x) v_3''(x)\, dx - KGAu_4(v_2'(l) - v_3(l)) - EIu_5 v_3'(l) + I_h v_1 \tilde{u}_1 + \\ &\rho A \int_0^l v_2(x)\tilde{u}_2(x)\, dx + \rho I \int_0^l v_3(x)\tilde{u}_3(x)\, dx + m_c v_4 \tilde{u}_4 + I_c v_5 \tilde{u}_5 = 0. \end{aligned} \tag{3.1.3}$$

After integrating by parts and grouping terms, we obtain

$$EIu_1v_3'(0) - KGAv_3'(x)(\int_0^x u_2(\mu)\,d\mu)|_0^l + KGAv_2'(x)(\int_0^x u_3(\mu)\,d\mu)|_0^l -$$

$$KGAv_3(x)(\int_0^x u_3(\mu)\,d\mu)|_0^l + KGAv_3'(x)(\int_0^x \int_0^\nu u_3(\mu)\,d\mu\,d\nu)|_0^l -$$

$$KGAu_4\delta_l(v_2' - v_3) - EIu_5v_3'(l) + I_hv_1\tilde{u}_1 + m_cv_4\tilde{u}_4 + I_cv_5\tilde{u}_5 +$$

$$KGA\int_0^l v_2''(x)(u_2(x) - \int_0^x u_3(\mu)\,d\mu + \frac{\rho A}{KGA}\int_0^x \int_0^\nu \tilde{u}_2(\mu)\,d\mu\,d\nu)\,dx +$$

$$KGA\int_0^l v_3''(x)(\int_0^x u_2(\mu)\,d\mu - \int_0^x \int_0^\nu u_3(\mu)\,d\mu\,d\nu + \frac{EI}{KGA}u_3(x) +$$

$$\frac{\rho I}{KGA}\int_0^x \int_0^\nu \tilde{u}_3(\mu)\,d\mu\,d\nu)\,dx + \rho Av_2(x)(\int_0^x \tilde{u}_2(\mu)\,d\mu)|_0^l -$$

$$\rho Av_2'(x)(\int_0^x \int_0^\nu \tilde{u}_2(\mu)\,d\mu\,d\nu)|_0^l + \rho Iv_3(x)(\int_0^x \tilde{u}_3(\mu)\,d\mu)|_0^l -$$

$$\rho Iv_3'(x)(\int_0^x \int_0^\nu \tilde{u}_3(\mu)\,d\mu\,d\nu)|_0^l = 0. \tag{3.1.5}$$

Now the domain of $\mathcal{A}_0$ includes

$$D_1 = \{z \in \mathbf{H} | z_1 = z_3 = z_4 = z_5 = 0, \quad z_2 \in \mathbf{W}_0^{2,2}\}.$$

Therefore, it follows that (3.1.5) holds for all $v \in D_1$ and hence

$$\int_0^l v_2''(x)(u_2(x) - \int_0^x u_3(\mu)\,d\mu + \frac{\rho A}{KGA}\int_0^x \int_0^\nu \tilde{u}_2(\mu)\,d\mu\,d\nu)\,dx = 0,$$

for all $v_2 \in \mathbf{H}_0^2$. Applying the Fundamental Lemma of Calculus of Variations [5], we obtain

$$u_2(x) - \int_0^x u_3(\mu)\,d\mu + \frac{\rho A}{KGA}\int_0^x \int_0^\nu \tilde{u}_2(\mu)\,d\mu\,d\nu = ax + b$$

for some constants a and b. Therefore, we have that

$$u_2(x) = \int_0^x u_3(\mu)\,d\mu - \frac{\rho A}{KGA}\int_0^x \int_0^\nu \tilde{u}_2(\mu)\,d\mu\,d\nu + ax + b$$

which proves that u_2 belongs to $\mathbf{W}^{1,2}$. Consequently, $u_2(x)$ can be differentiated once to give

$$u_2'(x) - u_3(x) - \frac{\rho A}{KGA}\int_0^x \tilde{u}_2(\nu)\,d\nu = a. \tag{3.1.6}$$

Note that, it is not a priori obvious that u_3 can be differentiated. Returning to (3.1.5) and noting that $D(\mathcal{A}_0)$ also contains

$$D_2 = \{z \in \mathbf{H} | z_1 = z_2 = z_4 = z_5 = 0, z_3 \in \mathbf{W}_0^{2,2}\},$$

it follows that for each $v \in \mathbf{W}_0^{2,2}$,

$$\int_0^l v_3''(x)(\int_0^x u_2(\mu)\,d\mu - \int_0^x \int_0^\nu u_3(\mu)\,d\mu\,d\nu + \frac{EI}{KGA}u_3(x) +$$
$$\frac{\rho I}{KGA}\int_0^x \int_0^\nu \tilde{u}_3(\mu)\,d\mu, d\nu)\,dx = 0.$$

Again, an application of the Fundamental Lemma of Calculus of Variations yields

$$\int_0^x u_2(\mu)\,d\mu - \int_0^x \int_0^\nu u_3(\mu)\,d\mu\,d\nu + \frac{EI}{KGA}u_3(x) +$$
$$\frac{\rho I}{KGA}\int_0^x \int_0^\nu \tilde{u}_3(\mu)\,d\mu\,d\nu = ax + b.$$

It follows from this equation that $u_3(x)$ belongs to $\mathbf{W}^{1,2}$, and hence it follows that

$$u_2(x) - \int_0^x u_3(\nu)\,d\nu + \frac{EI}{KGA}u_3'(x) + \frac{\rho I}{KGA}\int_0^x \tilde{u}_3(\nu)\,d\nu = a. \tag{3.1.7}$$

Since $u_2(x)$ belongs to $\mathbf{W}^{1,2}$ it now follows that $u_3'(x) \in \mathbf{W}^{1,2}$. Therefore, differentiating (3.1.7) once more yields

$$\tilde{u}_3(x) = -\frac{EI}{\rho I}u_3''(x) - \frac{KGA}{\rho I}(u_2'(x) - u_3(x)). \tag{3.1.8}$$

Returning to (3.1.6), we note that $u_3(x) \in \mathbf{W}^{2,2}$ now implies that $u_2' \in \mathbf{W}^{1,2}$. Consequently, (3.1.6) can be differentiated once again to yield

$$\tilde{u}_2(x) = -\frac{KGA}{\rho A}(u_2''(x) - u_3'(x)). \tag{3.1.9}$$

Since $u_2(x), u_3(x)$ belong to $\mathbf{W}^{2,2}$, equation (3.1.3) can be again integrated by parts. After carrying out these integrations and introducing the expressions for u_2 and u_3 and grouping terms, one arrives at

$$\begin{aligned}
&-(KGA\delta_l(u_2'(x) - u_3(x)) - m_c\tilde{u}_4)v_2(x) + EI\delta_0(u_1 - u_3(x))v_3'(0) \\
&+ EI\delta_l(u_3(x) - u_5)v_3'(l) + KGA\delta_l(u_2(x) - u_4)v_2'(l) - KGAu_2(0)v_2'(0) \\
&- KGA\delta_l(u_2(x) - u_4)v_3(l) + KGAu_2(0)v_3(0) - \delta_l(EIu_3'(x) - I_c\tilde{u}_5)v_3(l) \\
&+ \delta_0(EIu_3'(x) + I_h\tilde{u}_1)v_1(0) = 0,
\end{aligned}$$

which must hold for all $v \in D(\mathcal{A}_0)$. Selecting different domains for v which are included in $D(\mathcal{A}_0)$, corresponds to the vanishing of these terms independently and in turn determines the domain for the adjoint operator

$$\begin{aligned}
u_3(0) &= u_1 \\
u_3(l) &= u_5 \\
u_2(l) &= u_4 \\
u_2(0) &= 0.
\end{aligned} \tag{3.1.10}$$

Moreover, it follows that

$$\tilde{u}_4 = \frac{KGA}{m_c}(u_2'(l) - u_3(l))$$
$$\tilde{u}_5 = \frac{EI}{I_c}u_3'(l) \tag{3.1.11}$$

and

$$\tilde{u}_1 = -\frac{EI}{I_h}u_3'(0).$$

Combining these results with (3.1.8) and (3.1.9), we find that

$$\tilde{u}_2(x) = -\frac{KGA}{\rho A}(u_2''(x) - u_3'(x))$$
$$\tilde{u}_3(x) = -\frac{EI}{\rho I}u_3''(x) - \frac{KGA}{\rho I}(u_2'(x) - u_3(x)). \tag{3.1.12}$$

Comparing the adjoint operator $\mathcal{A}_0^*$ and the operator $\mathcal{A}_0$ and noting that $D(\mathcal{A}_0^*) = D(\mathcal{A}_0)$ completes the proof.

In the next lemma, we deal with the non-coercivity of $-\mathcal{A}_0$, which is due to the presence of the rigid-body motion. This will amount to simply shifting the zero eigenvalue to the left by adding an operator $-\mathcal{A}_1$.

Lemma 3.1.2. If $-\mathcal{A}_0$ is given as above, then there exists an operator $-\mathcal{A}_1$ such that $-\tilde{\mathcal{A}}_0 = -\mathcal{A}_0 - \mathcal{A}_1$ is coercive. In particular, there exits a constant $\rho > 0$ such that

$$< -\tilde{\mathcal{A}}_0 v, v >_H \quad \geq \quad \rho^2 ||v||_H^2 \qquad \forall v \in D(\mathcal{A}_0) \tag{3.1.13}$$

Proof. Expanding the left hand side of (3.1.13), it becomes

$$< -\tilde{\mathcal{A}}_0 v, v >_H = < -(\mathcal{A}_0 + \mathcal{A}_1)v, v >_H = < -\mathcal{A}_0 v, v >_H - < \mathcal{A}_1 v, v >_H .$$

The first **H**-inner product on the right hand side of the above relation yields

$$< -\mathcal{A}_0 v, v >_H = \left\langle - \begin{pmatrix} \frac{EI}{I_0} v_3'(0) \\ \frac{KGA}{\rho I}(v_2'' - v_3') \\ \frac{KGA}{\rho I}(v_2' - v_3) + \frac{EI}{\rho I} v_3'' \\ -\frac{KGA}{m_c}\delta_l(v_2' - v_3) \\ -\frac{EI}{I_c} v_3'(l) \end{pmatrix}, \begin{pmatrix} v_1 \\ v_2 \\ v_3 \\ v_4 \\ v_5 \end{pmatrix} \right\rangle .$$

After integrating terms by parts the left hand side of (3.1.13) simplifies to

$$< -\tilde{\mathcal{A}}_0 v, v >_H = KGA \int_0^l (v_2' - v_3)^2 \, dx + EI \int_0^l v_3' v_3' \, dx - < \mathcal{A}_1 v, v >_H .$$

Looking at the above equation, it is clear that the operator $\mathcal{A}_0$ does not impose any constraint on v_1, where as the norm on the right hand side of (3.1.13) certainly includes v_1. Choosing $\mathcal{A}_1$ such that

$$< \mathcal{A}_1 v, v >_H = -v_1^2,$$

would make the above inner product positive definite for every $v \in D(\mathcal{A}_0)$ and (3.1.13) follows.

In this section, we proved that the stiffness operator $-\mathcal{A}_0$ for the Timoshenko beam is self-adjoint with dense domain, and there exists a bounded self-adjoint operator $-\mathcal{A}_1$ such that $-\tilde{\mathcal{A}}_0 = -\mathcal{A}_0 - \mathcal{A}_1$ is coercive. The existance and uniqueness

of the solution to the system given in equations (1.1.1)- (1.1.5) follows from the general framework sketched in Chapter 2, in the sense that, with $\tilde{\mathcal{A}}_0$ self-adjoint, then $\mathcal{A}$ in equation (2.1.2) becomes skew-adjoint and well-posedness for the conservative case follows from Stone's Theorem (Theorem 2.1.2). Also, for the damped system, with $\tilde{\mathcal{A}}_0$ coercive, well-posedness follows from Theorem (2.2.1), provided that the damping operator satisfies the conditions given in section 2.2.

It is important to note that $D(\mathcal{A}_0) \subset \mathbf{V}$. thus, any space $\mathbf{V}^N \subset D(\mathcal{A}_0)$ will automatically belong to $\mathbf{V}$. This will be the case in the finite element method used in the next section.

Chapter 4

Finite Element Approximations for Control

In this chapter, we use the general approximation theory from above to generate finite dimensional approximation to the optimal control problem for the Timoshenko beam. As was noted in Section 1.1, very few other authors have considered this particular problem. In [2], Banks and Crowley considered a parameter estimation problem for a simply supported Timoshenko beam. They used cubic B-splines to approximate both rotation and displacement of the beam. They did not consider the control problem. In [3], Burns, Cliff and et. al., studied the problem of controlling a slewing Timoshenko beam. They used the same finite element space that Banks and Crowley used in [2]. However, they were able to obtain satisfactory convergence only for a small range of beam specifications. In other cases the sub-optimal gains diverged.

The choice of a finite element space to be used in finite dimensional approximation of the optimal control problems clearly plays an important part in the convergence of the sub-optimal feedback gains. In this paper, we investigate two different schemes. One is the standard cubic B-splines which was used in [2] and [3], and another is a set of conforming finite element schemes for Timoshenko beam that was first introduced by A. Tessler [4]. In the next chapter, numerical experiments

will show that the new scheme has much better convergence properties than the standard cubic B-spline. We shall modify a particular set of these elements to apply to the Timoshenko beam slewing problem.

4.1 Finite Dimensional Approximations.

In this sections, we discuss the application of a particular conforming finite-element scheme to the problem of computing sub-optimal feedback gains for the system (1.1.1). A series of comforming finite element schemes for Timoshenko beams were introduced by A.Tessler [4]. Here we employ a particular set of these elements (T2CL6) to compute LQR functional gains.

The idea behind these schemes is to relax the smoothness requirement on the shear $(\frac{\partial u(t,x)}{\partial x} - \psi(t,x))$. This will result in a coupling between the finite-element spaces for the displacement and rotation. The scheme (T2CL6) that we shall employ proved useful in various simulations (see [4]). In this notation T stands for Timoshenko, 2 is the order of polynomial for rotation, C corresponds to having a constraint on the elements, L corresponds to requiring the shear to be linear across each element, and 6 is the number of degrees of freedom in each element. Therefore, this scheme uses a cubic polynomial for displacement $u(t,x)$ and a quadratic polynomial for rotation $\psi(t,x)$ and requires that the shear $(\frac{\partial u(t,x)}{\partial x} - \psi(t,x))$ vary linearly across each element.

Recall that

$$z(t) = \begin{pmatrix} z_1 \\ z_2 \\ z_3 \\ z_4 \\ z_5 \end{pmatrix} = \begin{pmatrix} \theta(t) \\ u(t,x) + x\theta(t) \\ \psi(t,x) + \theta(t) \\ u(t,l) + l\theta(t) \\ \psi(t,l) + \theta(t) \end{pmatrix} \tag{4.1.1}$$

with $z \in \mathbf{H} = \mathbf{R}^1 \times \mathbf{L}_2 \times \mathbf{L}_2 \times \mathbf{R}^1 \times \mathbf{R}^1$. If one employs a Ritz-Galerkin approximation, then the vector $z(t)$ may be approximated by

$$z^N(t) = \sum_{j=1}^{N} w_j(t) e_j^N(x).$$

Since $e_j^N(x) \in \mathbf{V}^N$, it has five components. For simplicity, we use $\alpha_j(x), \beta_j(x), \gamma_j(x), \sigma_j(x), \tau_j(x)$ to denote them. That is, for every j,

$$e_j^N(x) = (\alpha_j(x), \beta_j(x), \gamma_j(x), \sigma_j(x), \tau_j(x))^T.$$

If one is to approximate z_2 by

$$z_2^N(t,x) = u^N(t,x) + x\theta(t) = \sum_{j=1}^{N} w_j(t)\beta_j(x) \tag{4.1.2}$$

then, compatibility suggests using $\beta_j(l)$ to represent z_4. In particular,

$$z_2^N(t,l) = z_4^N(t) = u^N(t,l) + l\theta(t) = \sum_{j=1}^{N} w_j(t)\sigma_j, \qquad \sigma_j = \beta_j(l), \tag{4.1.3}$$

likewise, approximating z_3 by

$$z_3^N(t,x) = \psi^N(t,x) + \theta(t) = \sum_{j=1}^{N} w_j(t)\gamma_j(x) \tag{4.1.4}$$

would suggest that z_5 be approximated by

$$z_5^N(t) = \psi^N(t,l) + \theta(t) = \sum_{j=1}^{N} w_j(t)\tau_j, \qquad \tau_j = \gamma_j(l). \tag{4.1.5}$$

The splines used to construct bases for (z_2, z_3) are taken from [4] and are plotted in Figure 3. We refer the reader to [4] for a complete discussion. However, we shall give a basic outline of this method. The method makes use of three quadratic polynomials on $[-1,1]$ of the form

$$q_1(\zeta) = \frac{1}{2}\zeta(\zeta - 1)$$

$$q_2(\zeta) = 1 - \zeta^2$$

$$q_3(\zeta) = \frac{1}{2}\zeta(\zeta + 1),$$

and three cubic polynomials on $[-1,1]$ defined by

$$c_1(\zeta) = \frac{h}{6}(\zeta^3 - \zeta)$$

$$c_2(\zeta) = -\frac{h}{3}(\zeta^3 - \zeta)$$

$$c_3(\zeta) = \frac{h}{6}(\zeta^3 - \zeta).$$

Here ζ is a nondimensional variable that varies between -1 and $+1$ and h is the half the length of the element.

With these notes in mind, we divide the beam $(0,l)$ into n elements with equal length. This will give rise to $(2n)$ nodal points along the beam. With each node having a displacement and a rotation, one then approximates z by the $2(2n) = N$

Ritz-Galerkin approximation

$$z \approx z^N = \sum_{j=0}^{2(2n)} w_j^N(t) e_j^N(x), \tag{4.1.6}$$

where the basis functions are chosen as

$$e_0^N(x) = \begin{pmatrix} 1 \\ x \\ 1 \\ l \\ 1 \end{pmatrix}$$

$$e_j^N(x) = \begin{pmatrix} 0 \\ q_j(x) \\ 0 \\ q_j(l) \\ 0 \end{pmatrix} \quad for \quad 1 \le j \le 2n$$

$$e_j^N(x) = \begin{pmatrix} 0 \\ c_i(x) \\ q_i(x) \\ c_i(l) \\ q_i(l) \end{pmatrix} \quad 2n+1 \le j \le 2(2n), \quad i = j - (2n)$$

and where $q_i(x)$ and $c_i(x)$ are the quadratic and cubic polynomials given above. These polynomials will be modified to satisfy the physical boundary conditions at the left. In terms of a nondimensional local variable $\xi = \frac{x}{h}$ with h being half the length of an element, and ξ varying from $0 \rightarrow 1$ across each subinterval, the cubic interpolating functions are given by

$$c_i(\xi) = \begin{cases} 0, & \text{for } x < (i-2)h \\ -\frac{h}{3}\xi^3 + \xi^2 - \frac{2}{3}\xi, & \text{for } (i-2)h \le x \le (i-1)h \\ -\frac{h}{3}\xi^3 + \frac{h}{3}\xi, & \text{for } (i-1)h \le x \le ih \\ 0, & \text{for } ih \le x. \end{cases}$$

for odd i's, and

$$c_i(\xi) = \begin{cases} 0, & \text{for } x < (i-3)h \\ \frac{h}{6}\xi^3 - \frac{h}{2}\xi^2 + \frac{h}{3}\xi, & \text{for } (i-3)h \le x \le (i-2)h \\ \frac{h}{6}\xi^3 - \frac{h}{6}\xi, & \text{for } (i-2)h \le x \le (i-1)h \\ \frac{h}{6}\xi^3 - \frac{h}{2}\xi^2 + \frac{h}{3}\xi, & \text{for } (i-1)h \le x \le ih \\ \frac{h}{6}\xi^3 - \frac{h}{6}\xi, & \text{for } ih \le x \le (i+1)h \\ 0, & \text{for } (i+1)h < x. \end{cases}$$

for even i's. Likewise the quadratic functions are defined by

$$q_i(\xi) = \begin{cases} 0, & \text{for } x < (i-2)h \\ -\xi^2 + 2\xi, & \text{for } (i-2)h \le x \le (i-1)h \\ -\xi^2 + 1, & \text{for } (i-1)h \le x \le ih \\ 0, & \text{for } ih < x. \end{cases}$$

for odd i's, and

$$q_i(\xi) = \begin{cases} 0, & \text{for } x < (i-3)h \\ \frac{1}{2}(\xi^2 - \xi), & \text{for } (i-3)h \le x \le (i-2)h \\ \frac{1}{2}(\xi^2 + \xi), & \text{for } (i-2)h \le x \le (i-1)h \\ \frac{1}{2}\xi^2 - \frac{3}{2}\xi + 1, & \text{for } (i-1)h \le x \le ih \\ \frac{1}{2}(\xi^2 - \xi), & \text{for } ih \le x \le (i+1)h \\ 0, & \text{for } (i+1)h < x. \end{cases}$$

for even i's.

The basis functions are required to satisfy the physical boundary conditions on the left, namely no displacement and no rotation at the hub. T2CL6 is a conforming finite element scheme and satisfying the required boundary condition is done by simply dropping the first global basis element.

Once the basis elements are chosen, we can proceed to construct the system

matrices, given by (2.3.3), (2.3.4), (3.1.2), (2.4.6). The mass matrix is given by

$$[M^N]_{ij} = [< e_i^N, e_j^N >_H], \qquad i,j = 1,N, \qquad N = 2(2n), \tag{4.1.7}$$

$$= I_0[< \alpha_i, \alpha_j >_{R^1}] + \rho A[< \beta_i, \beta_j >_{L_2}] + \rho I[< \gamma_i, \gamma_j >_{L_2}]$$

$$+ m_c[< \sigma_i, \sigma_j >_{R^1}] + I_c[< \tau_i, \tau_j >_{R^1}].$$

Using the above expression, the symmetric mass matrix has the form

$$M^N = \begin{bmatrix} M_{11}^N & M_{12}^N & M_{13}^N \\ . & M_{22}^N & M_{23}^N \\ . & . & M_{33}^N \end{bmatrix}, \tag{4.1.8}$$

where M_{11}^N is a (1×1) matrix, M_{12}^N is a $(1 \times (2n))$ row matrix, M_{13}^N is a $(1 \times (2n))$ row matrix, M_{22}^N, M_{23}^N, and M_{33}^N are $((2n) \times (2n))$ square matrices with values given by

$$M_{11}^N = I_0 + \rho A < x, x >_{L_2} + \rho I < 1, 1 >_{L_2} + m_c l^2 + I_c$$

$$[M_{12}^N]_j = \rho A[< x, q_j(x) >_{L_2}] + m_c[< l, q_j(l) >_{L_2}]$$

$$[M_{13}^N]_j = \rho A[< x, c_j(x) >_{L_2}] + \rho I[< 1, q_j(x) >_{L_2}] + m_c[< l, c_j(l) >_{R^1}]$$

$$+ I_c[< 1, q_j(l) >_{R^1}]$$

$$[M_{22}^N]_{ij} = \rho A[< q_i(x), q_j(x) >_{L_2}] + m_c[< q_i(l), q_j(l) >_{L_2}]$$

$$[M_{23}^N]_{ij} = \rho A[< q_i(x), c_j(x) >_{L_2}] + m_c[< q_i(l), c_j(l) >_{R^1}]$$

$$[M_{33}^N]_{ij} = \rho A[< c_i(x), c_j(x) >_{L_2}] + \rho I[< q_i(x), q_j(x) >_{L_2}] + m_c[< c_i(l), c_j(l) >_{R^1}]$$

$$+ I_c[< q_i(l), q_j(l) >_{R^1}], \qquad for \quad i,j = 1,N.$$

The stiffness matrix is given by

$$[K^N]_{ij} = [< e_i^N, e_j^N >_V] - [< \mathcal{A}_1 e_i^N, e_j^N >_H] \tag{4.1.9}$$

$$= [< -\mathcal{A}_0 e_i^N, e_j^N >_H].$$

Also, after expanding the inner-products and following the steps taken in the proof of Lemma (3.1.1), equation (4.1.9) simplifies to

$$[K^N]_{ij} = KGA[< (\beta_i' - \gamma_i), (\beta_j' - \gamma_j) >_{L^2}] + EI[< \gamma_i', \gamma_j' >_{L^2}].$$

As is noted $[K^N]_{ij}$ is symmetric and after substituting for the basis functions and expanding the norms, it simplifies to

$$K^N = \begin{bmatrix} 0 & 0 & 0 \\ 0 & K_{11}^N & K_{12}^N \\ 0 & . & K_{22}^N \end{bmatrix} \tag{4.1.10}$$

where for $i, j = 1, N$,

$$[K_{11}^N]_{ij} = -KGA[< q_i'(x), q_j'(x) >_{L_2}]$$

$$[K_{12}^N]_{ij} = -KGA[< q_i'(x), c_j'(x) >_{L_2}] + KGA[< q_i'(x), q_j(x) >_{L_2}]$$

$$[K_{22}^N]_{ij} = -KGA[< c_i'(x), c_j'(x) >_{L_2}] + KGA[< c_i'(x), q_j(x) >_{L_2}] -$$

$$KGA[< q_i(x), q_j(x) >_{L_2}] - EI[< q_i'(x), q_j'(x) >_{L_2}] + KGA[< q_i(x), c_j'(x) >_{L_2}].$$

The stiffness matrix K^N has one zero row and column, this produces the zero eigenvalue due to the rigid body motion. The grammian $\tilde{W}^N$ is given by (2.4.6) where $\tilde{K}^N$ is K^N with a one added to the (1,1) element (a consequence of adding the $\mathcal{A}_1$ operator). Recall that this operator was added to assure coercivity of $\tilde{\mathcal{A}}_0$.

As was mentioned in Section 1.1, we need to introduce some damping into the system. The external damping used for numerical experiments in this paper is viscous damping. The viscously damped equations of motion are given in Section 1.1. Writing equations (1.1.11) -(1.1.16) in a standard second order form they become

$$\mathcal{M}\ddot{z} + \kappa\mathcal{D}_0\dot{z} + \mathcal{K}z = \tilde{\mathcal{B}}_0 u.$$

This falls under the general damped system of equations given in Section 2.2 (see equation 2.2.1) where $\mathcal{A}_0$ and $\mathcal{B}_0$ in equation (2.2.1) are given as

$$\mathcal{A}_0 = \mathcal{M}^{-1}\mathcal{K}, \qquad \mathcal{B}_0 = \mathcal{M}^{-1}\tilde{\mathcal{B}}_0$$

with $D(\mathcal{K}) = D(\mathcal{A}_0)$, and

$$d_0(z, \hat{z}) =< \mathcal{D}_0 z, \hat{z} >= \mathcal{M} - I_0 < z_1, \hat{z}_1 >_{R^1} .$$

Following the steps in Section 2.3 the damping functional simplifies to

$$\begin{aligned}[D^N]_{ij} = [d_0(e_i^N, e_j^N)] &= M^N - I_0[< \alpha_i, \alpha_j >_{R^1}] \\ &= [< e_i^N, e_j^N >_H] - I_0[< \alpha_i, \alpha_j >], \quad i, j = 1, N.\end{aligned}$$

After expanding the **H**-inner product in the above relation, the expression for $[D^N]_{ij}$ simplifies to

$$\begin{aligned}[D^N]_{ij} =& \rho A[< \beta_i, \beta_j >_{L_2}] + \rho I[< \gamma_i, \gamma_j >_{L_2}] + m_c[< \sigma_i, \sigma_j >_{R^1}] + \\ & I_c[< \tau_i, \tau_j >_{R^1}],\end{aligned}$$

for $i, j = 1, N$. Comparing the above expression for D^N to the expression for M^N in equation (4.1.7), it becomes clear that, after substituting for the basis functions, the elements in the symmetric damping matrix D^N, are identical to M^N in equation (4.1.8), except for the (1,1) element where D_{11}^N is given by

$$D_{11}^N = \rho A < x, x >_{L_2} + \rho I < 1, 1 >_{L_2} + m_c l^2 + I_c.$$

For internal damping we use a Kelvin-Voigt damping model. The equation of motion for the damped structure is again

$$\mathcal{M}\ddot{z} + \kappa \mathcal{D}_0 \dot{z} + \mathcal{K} z = \tilde{\mathcal{B}}_0 u,$$

where again, $\mathcal{A}_0$ and $\mathcal{B}_0$ in equation (3.1.1) are given as

$$\mathcal{A}_0 = \mathcal{M}^{-1}\mathcal{K}, \qquad \mathcal{B}_0 = \mathcal{M}^{-1}\tilde{\mathcal{B}}_0,$$

and $\mathcal{D}_0 = \mathcal{K}$, with $D(\mathcal{D}_0) = D(\mathcal{K}) = D(\mathcal{A}_0)$.

In this case the damping functional is given by

$$d_0(z, \hat{z}) = (< z, \hat{z} >_V - < \mathcal{A}_1 z, \hat{z} >_H).$$

Following the steps in Section 2.3 it follows that

$$[D^N]_{ij} = [d_0(e_i^N, e_j^N)] = [< e_i^N, e_j^N >_V - < \mathcal{A}_1 e_i^N, e_j^N >_H], \quad i, j = 1, N.$$

In this case D^N simplifies to the symmetric matrix K^N given in equation (4.1.10).

Taking $\mathcal{Q} = I$ in the performance index (1.2.1) corresponds to the state weighting term $< \mathcal{Q} z, z >_E$ being twice the total energy in the structure plus the square

of the rigid-body rotation. The Grammian matrix $\tilde{W}^N$ is the matrix representation of $\mathcal{Q}$. Since there is only one input, the control weighting R is a scalar.

Once the system matrices are generated, the matrix Riccati equation (2.4.9) is solved for Π^N, using Potter's method. According to (2.2.10) the optimal control has the feedback form

$$u(t) = - < f, z(t) >_V - < g, \dot{z}(t) >_H \tag{4.1.11}$$

where $z(t)$ has the form (4.1.1), and

$$\begin{aligned} f &= (\alpha_f, \psi_f(x), \phi_f(x), \mu_f, \nu_f)^T \in V \\ g &= (\alpha_g, \psi_g(x), \phi_g(x), \mu_g, \nu_g)^T \in H \end{aligned} \tag{4.1.12}$$

with f, g given by (2.4.5). Note that

$$\begin{aligned} \mu_f &= \psi_f(l) \qquad 0 = \psi_f(0) \\ \nu_f &= \phi_f(l) \qquad \alpha_f = \phi_f(0). \end{aligned} \tag{4.1.13}$$

Expanding the feedback control law yields

$$\begin{aligned} u(t) &= - < f, z >_V - < g, \dot{z} >_H \\ &= - < f, \mathcal{A}_0 z >_H - < f, \mathcal{A}_1 z >_H - < g, \dot{z} >_H . \end{aligned}$$

Expanding the first term in the above relation

$$< f, \mathcal{A}_0 z >_H = \left\langle \begin{pmatrix} f_1 \\ f_2 \\ f_3 \\ f_4 \\ f_5 \end{pmatrix}, \begin{pmatrix} \frac{EI}{I_h} z_3'|_0 \\ \frac{KGA}{\rho A}(z_2'' - z_3') \\ \frac{KGA}{\rho I}(z_2' - z_3) + \frac{EI}{\rho I} z_3'' \\ -\frac{KGA}{m_c}(z_2' - z_3)|_l \\ -\frac{EI}{I_c} z_3'|_l \end{pmatrix} \right\rangle,$$

$$= - EI f_1 z_3'|_0 - KGA \int_0^l f_2(z_2'' - z_3')dx - KGA \int_0^l f_3(z_2' - z_3)dx$$

$$- EI \int_0^l f_3 z_3'' dx + KGA f_4(z_2' - z_3)|_l + EI f_5 z_3'|_l.$$

After integrating by parts and using the properties of space, the above relation yields

$$< f, \mathcal{A}_0 z >_H = KGA \int_0^l (f_2' - f_3)(z_2' - z_3)dx + EI \int_0^l f_3' z_3' dx.$$

Note that the components f_4 and f_5 do not appear in the control law. Also, the term $< f, \mathcal{A}_1 z >_H$ yields $I_h f_1 z_1$. Grouping all the terms and writing the relation for the control law in our primitive variables yields

$$\begin{aligned} u(t) = & - I_h K_0 \theta - KGA \int_0^l K_1(x)(u'(t,x) - \psi(t,x))\, dx \\ & - EI \int_0^l K_2(x)\psi'(t,x)\, dx - I_0 K_3 \dot{\theta}(t) \\ & - \rho A \int_0^l K_4(x)(u_t(t,x) + x\dot{\theta}(t))\, dx \\ & - \rho I \int_0^l K_5(x)(\psi_t(t,x) + \dot{\theta}(t))\, dx \\ & - m_c K_6(u_t(t,l) + l\dot{\theta}(t)) - I_c K_7(\psi_t(t,l) + \dot{\theta}(t)) \end{aligned} \tag{4.1.14}$$

where

$$\begin{aligned} K_0 &= \alpha_f & K_4(x) &= \psi_g(x) + x\alpha_g \\ K_1(x) &= \psi_f'(x) - \phi_f(x) & K_5(x) &= \phi_g(x) + \alpha_g \\ K_2(x) &= \phi'(x) & K_6 &= \mu_g + l\alpha_g \\ K_3 &= \alpha_g & K_7 &= \nu_g + \alpha_g. \end{aligned} \tag{4.1.15}$$

The functions $K_1(x), K_2(x), K_4(x), K_5(x)$ are called the functional gains.

Chapter 5

Numerical Results

In this chapter, we develop computer algorithms to compute the gain operators for the optimal control of the structure in Figure 1. We study the effects of different parameters on the convergence of the functional gains.

Most of the numerical experiments were done on the CRAY-2 at the Air Force Super-Computing Center at Kirtland Air Force Base, New Mexico. In cases where memory requirments and speed were not a problem, the IBM-3090 at VPI was used.

To test the results, two different formulations of the problem were coded, both of which converged to the same gains. Also, as noted earlier two different finite element schemes were used. One is the Cubic B-splines [1,3], and the other is T2CL6 [4]. In addition, the open loop eigenvalues were compared against the natural frequencies, which are the solutions to the characteristic equation for the structure. Another code was developed to generate the gains for the optimal control of the same structure, assuming an Euler- Bernoulli model for the beam. In the limiting case, where the beam behaves like an Euler-Bernoulli model, the Timoshenko model generated very close results to the ones generated by the Euler-Bernoulli model. In this chapter, we discuss all of these findings.

The numerical procedure is to use equations (4.1.8), (4.1.10), and (2.4.6) to

generate the system matrices, and then solve the algebriac matrix Riccati equation (2.4.9) for Π^N. We use Potter's method to solve equation (2.4.9) for Π^N. Here we briefly outline the method.

The first step is to calculate eigenvalues and eigenvectors of the matrix

$$P^N = \begin{bmatrix} A^{NT} & \tilde{Q}^N \\ B^N R^{-1} B^{NT} & -A^N \end{bmatrix}.$$

Then form the matrix $X = \begin{bmatrix} X_1 \\ X_2 \end{bmatrix}$, where the columns of X are eigenvectors of P^N corresponding to the eigenvalues with positive real parts. When eigenvalues occure in complex conjugate pairs so do the eigenvectors. In this case, the real and imaginary parts of the eigenvector each forms a column in the matrix X. Then the solution to the Riccati equation is given by $\Pi^N = X_1 X_2^{-1}$. The sub-optimal control has the feedback form given by (4.1.11), which in turn, simplifies to (4.1.14).

In the figures below, the functional gains 1 and 2 correspond to $\psi_f(x)$ and $\phi_f(x)$, respectively. For the components of velocities, we plot $K_4(x)$ and $K_5(x)$.

Example 1..

To study the effect of the choice of basis functions on the open-loop eigenvalues,

we choose a structure with physical properties given by

$$\rho A = 5.744 \quad Kg/m \qquad \rho I = .0003088 \quad Kg - m \tag{5.1.1}$$

$$KGA = 19384. \quad N \qquad EI = 3.1883 \quad N - m^2 \tag{5.1.2}$$

$$I_0 = .9413 \quad Kg - m^2 \qquad I_c = .000001 \quad N - m^2 \tag{5.1.3}$$

$$m_c = 14.59 \quad Kg \qquad L = 2.794 \quad m. \tag{5.1.4}$$

Table 5.1 shows the open-loop eigenvalues for the above structure using Cubic-B splines. It is noted that the eigenvalues converge as the dimension of the system is increased. Table 5.2 shows the open-loop eigenvalues for the same structure using T2CL6. Again, it is noted that the eigenvalues converge. Next we use a modified version of T2CL6 which treats the left hand side boundary condition slightly differently. This scheme allows for the shear to be discontinuous across the first element. It also produces two more eigenvalues than T2CL6 for the same number of elements. Table 5.3 shows a comparison of these three schemes. As is noted all three schemes produce very close frequencies. Cubic B-splines predicts low frequencies more accurately where as for high frequencies T2CL6 seems to give a better account. It is noted that the modified T2CL6 is slightly better than T2CL6. However, this version did not significantly improve the results provided by T2CL6 so we devoted the remainder of our effort an investigation of T2CL6.

$ReN = 16$	$ImN = 16$	$ReN = 64$	$ImN = 64$
−0.049700	0.00000	−0.049700	0.00000
0.000000	0.00000	0.000000	0.00000
−0.021101	0.95115	−0.021101	0.95115
−0.012136	2.78169	−0.012136	2.78168
−0.019135	5.40925	−0.019135	5.40914
−0.023623	10.16414	−0.023623	10.16303
−0.024557	16.87419	−0.024557	16.86736
−0.024817	25.32452	−0.024817	25.29318
−0.024911	35.42307	−0.024911	35.30487
−0.024952	47.16884	−0.024952	46.78241
−0.024971	60.73528	−0.024972	59.60713
−0.024982	76.64301	−0.024983	73.66061
−0.024988	96.00536	−0.024989	88.82610
−0.024992	120.80812	−0.024993	104.99036
−0.024995	154.15933	−0.024995	122.04547
−0.024997	199.68848	−0.024996	139.89000
−0.024999	257.36719	−0.024997	158.42979
−0.025000	317.74805	−0.024998	177.57849
−0.024996	353.11133	−0.024999	197.25755
−0.025000	2497.86206	−0.024999	217.39626
−0.025000	2509.27637	−0.024999	237.93126
−0.025000	2519.57251	−0.024999	258.80640
−0.025000	2535.38135	−0.025000	279.97168
−0.025000	2556.40723	−0.025000	301.38403
−0.025000	2582.46851	−0.025000	323.00488
−0.025000	2613.40308	−0.025000	344.80176
−0.025000	2649.07520	−0.025000	366.74609
−0.025000	2689.43066	−0.025000	388.81421
−0.025000	2734.60938	−0.025000	410.98584
−0.025000	2785.09985	−0.025000	433.24438
−0.025000	2841.77344	−0.025000	455.57739
−0.025000	2905.15283	−0.025000	477.97437
−0.025000	2971.99243	−0.025000	500.42944
−0.025000	3024.48706	−0.025000	522.93848
−0.025000	3259.48267	−0.025000	545.50122
−0.025000	4239.11719	−0.025000	568.12061

TABLE 5.1 Open loop eigenvalues for Cubic, N=16,64

$ReNE = 8$	$ImNE = 8$	$ReNE = 32$	$ImNE = 32$
−0.049700	0.00000	−0.049700	0.00000
0.000000	0.00000	0.000000	0.00000
−0.021101	0.95116	−0.021101	0.95115
−0.012133	2.78186	−0.012136	2.78168
−0.019136	5.41128	−0.019135	5.40914
−0.023624	10.18072	−0.023623	10.16310
−0.024558	16.95059	−0.024557	16.86769
−0.024817	25.57068	−0.024817	25.29439
−0.024912	36.03041	−0.024911	35.30826
−0.024954	48.25481	−0.024952	46.79047
−0.024981	65.35107	−0.024972	59.62425
−0.024983	81.73528	−0.024983	73.69382
−0.024988	102.28844	−0.024989	88.88602
−0.024992	126.94066	−0.024993	105.09235
−0.024994	156.68860	−0.024995	122.21082
−0.024996	192.92651	−0.024996	140.14723
−0.024997	237.22504	−0.024997	158.81612
−0.024999	288.44995	−0.024998	178.14128
−0.024991	355.62427	−0.024999	198.05588
−0.024999	477.01685	−0.024999	218.50243
−0.024999	596.07837	−0.024999	239.43246
−0.024999	749.17871	−0.024999	260.80615
−0.025000	934.90161	−0.025000	282.59155
−0.025000	1139.83936	−0.025000	304.76489
−0.025000	1331.32104	−0.025000	327.30859
−0.025000	1466.41235	−0.025000	350.21216
−0.025000	2498.13086	−0.025000	373.47070
−0.025000	2509.34351	−0.025000	397.08423
−0.025000	2520.50977	−0.025000	421.05786
−0.025000	2539.68701	−0.025000	445.39917
−0.025000	2568.93994	−0.025000	470.11768
−0.025000	2609.56030	−0.025000	495.21729
−0.025000	2656.74292	−0.025000	520.67627
−0.025000	2693.54175	−0.025000	546.30957

TABLE 5.2 Open loop eigenvalues for T2CL6, NE=8,32

— — —	*Cubic*	*T2CL6*	*MT2CL6*
ω_{-1}	0.00000000	0.00000000	0.00000000
ω_0	0.00000000	0.00000000	0.00000000
ω_1	0.95178717	0.95178783	0.95178783
ω_2	2.78680992	2.78681087	2.78681087
ω_3	5.44417191	5.44418049	5.44418049
ω_4	10.29259872	10.29267120	10.29267120
ω_5	17.21237183	17.21272278	17.21272278
ω_6	26.04737854	26.04861450	26.04861450
ω_7	36.74490356	36.74841309	36.74841309
ω_8	49.27476501	49.28321838	49.28321838
ω_9	63.61157227	63.62979126	63.62977600
ω_{10}	79.73020935	79.76605225	79.76602173
ω_{15}	186.07723999	186.52949524	186.52810669
ω_{20}	332.43041992	334.96215820	334.94213867
ω_{25}	514.55395508	523.58593750	523.44702148
ω_{30}	728.98120117	751.80322266	751.24560547
ω_{35}	975.49023438	1039.36987305	1037.46972656
ω_{40}	1262.67797852	1369.32128906	1364.73095703
ω_{45}	1619.42114258	1773.86206055	1765.05273438
ω_{50}	2110.58959961	2273.39013672	2258.74780273
ω_{55}	2827.44042969	2898.47802734	2875.07592773
ω_{60}	3718.66333008	3675.79003906	3631.67871094
ω_{65}	4661.72656250	4569.97265625	4295.25781250
ω_{70}	7941.18359375	6073.73046875	5929.84375000
ω_{75}	8014.30468750	7359.99609375	7207.59765625
ω_{80}	8139.80078125	7927.46875000	7924.02734375
ω_{85}	8313.10937500	7980.64453125	7964.96093750
ω_{90}	8529.28515625	8070.65234375	8049.00781250

TABLE 5.3 Frequencies for Cubic, T2CL6, MT2CL6

NSYS = 262 for Cubic and MT2CL6

NSYS = 260 for T2CL6

Using these finite element schemes we compute finite dimensional approximations to the LQR problem and after following steps outlined earlier we obtain closed-loop eigenvalues. Table 5.4 show the eigenvalues using Cubic B-splines and Table 5.5 show the eigenvalues using T2CL6. As is noted closed-loop eigenvalues are in good agreement. Tables 5.6 and 5.7 give the constant gains using Cubic B-splines and T2CL6 respectively.

We note that this particular example is "marginal" for both schemes in that both schemes produced convergent functional gains but the convergence was slow. The cases where the convergence of functional gains was fast also yielded fast convergence of the constant gains.

Open – Real	*Open – Imag*	*Close – Real*	*Close – Imag*
−.049699	0.00000	−.064737	−.0409
0.000000	0.00000	−.064737	.04093
−.021089	.951787	−.289157	.96014
−.012138	2.78680	−.550004	2.7857
−.019168	5.44417	−.365778	5.4409
−.023623	10.2926	−.181731	10.292
−.024553	17.2123	−.106077	17.212
−.024813	26.0474	−.071228	26.047
−.024908	36.7449	−.052994	36.744
−.024950	49.2747	−.042671	49.274
−.024970	63.6115	−.036528	63.611
−.024981	79.7302	−.032742	79.730
−.024987	97.6043	−.030341	97.604
−.024991	117.617	−.028789	117.617
−.024993	139.295	−.027749	139.295
−.024995	162.934	−.027041	162.934
−.024996	188.696	−.026549	188.696
−.024997	216.851	−.026201	216.851
−.024997	247.826	−.025950	247.826
−.024998	282.269	−.025767	282.269
−.024998	321.130	−.025630	321.130
−.024998	365.743	−.025524	365.743
−.024999	417.930	−.025437	417.930
−.024999	480.085	−.025362	480.085
−.024999	555.258	−.025294	555.258
−.024999	647.136	−.025233	647.136
−.024999	759.835	−.025180	759.835
−.024999	897.301	−.025136	897.301
−.024999	1062.12	−.025101	1062.12
−.024999	1253.57	−.025074	1253.57
−.024999	1464.72	−.025054	1464.72
−.024999	1678.96	−.025037	1678.96
−.024999	1867.21	−.025021	1867.21
−.024999	1990.10	−.025005	1990.10
−.024999	2277.76	−.025239	2277.76
−.025000	7739.69	−.025000	7739.69
−.025000	7924.02	−.025000	7924.02
−.025000	7927.45	−.025000	7927.45

TABLE 5.4 Closed and Open Loop Eigenvalues for Cubic B-splines

Open – Real	*Open – Imag*	*Close – Real*	*Close – Imag*
−.049699	0.00000	−.06300	−.0398
0.000000	0.00000	−.06300	.03982
−.021089	.951787	−.31118	.98364
−.012138	2.78681	−.56226	2.7824
−.019168	5.44418	−.35952	5.4410
−.023623	10.2926	−.18145	10.292
−.024553	17.2127	−.10613	17.212
−.024813	26.0486	−.07122	26.048
−.024908	36.7484	−.05298	36.748
−.024950	49.2832	−.04267	49.283
−.024970	63.6297	−.03652	63.629
−.024981	79.7660	−.03274	79.766
−.024987	97.6700	−.03034	97.670
−.024991	117.319	−.02877	117.32
−.024993	141.139	−.02776	141.13
−.024995	165.463	−.02705	165.46
−.024996	191.725	−.02652	191.72
−.024997	218.928	−.02602	218.92
−.024999	263.058	−.02542	263.05
−.024998	292.674	−.02570	292.67
−.024998	329.511	−.02561	329.51
−.024998	370.416	−.02551	370.41
−.024999	415.289	−.02542	415.28
−.024999	464.425	−.02535	464.42
−.024999	518.252	−.02529	518.25
−.024999	577.270	−.02524	577.27
−.024999	641.998	−.02519	641.99
−.024999	712.885	−.02516	712.88
−.024999	790.134	−.02513	790.13
−.024999	873.351	−.02510	873.35
−.024999	960.850	−.02508	960.85
−.024999	1048.28	−.02506	1048.2
−.024999	1126.10	−.02503	1126.1
−.024999	1176.11	−.02500	1176.1
−.024999	1336.03	−.02566	1336.0
−.024999	2616.54	−.02501	2616.5
−.024999	2718.46	−.02503	2718.4
−.024999	2874.69	−.02502	2874.6

TABLE 5.5 Closed and Open Loop Eigenvlues for T2CL6

N	$NSYS$	K_0	K_3	K_6	K_7
8	38	−1.0	−2.8994	−8.101	−2.899
16	70	−1.0	−2.9531	−.1543	.0956
32	134	−1.0	−2.9669	−.1532	.1268
64	262	−1.0	−2.9472	−.1578	.1072

TABLE 5.6 Constant gains for Cubic B-splines

NE	$NSYS$	K_0	K_3	K_6	K_7
4	36	−1.0	−2.9492	−.15374	−.5549
8	68	−1.0	−2.9581	−.15484	.19975
16	132	−1.0	−2.9475	−.15523	.12772
32	260	−1.0	−2.9963	−.15049	.12367

TABLE 5.7 Constant Gains for T2CL6

Next we focus on the convergence of the functional gains and compare the results using Cubic B-splines and T2CL6. For the rest of the numerical experiments we do not present the constant gains or the eigenvalues. In all cases, convergence of the functional gains represents convergence of the constant gains as well as closed and open loop eigenvalues.

Example 2.

We choose a structure with physical properties given by (5.1.1)-(5.1.4), except for KGA which we reduce to $193.84N$. Figures 7-10 show the functional gains using Cubic B-splines and Figures 11-14 show the functional gains for the same structure using T2CL6. As is noted both schemes converge to the same functional gains. Looking at Figures 8 and 9 one notes that convergence of the Cubic B-splines is slower at the right end.

Next we increase KGA by a factor of 10 while keeping the rest of the parameters the same. Figures 15-18 and 19-22 show the functional gains using Cubic B-splines and T2CL6 respectively. Again both schemes produce convergent functional gains. We next increase KGA to $19384N$. Figures 23-26 and 27-30 show the functional gains using Cubic B-splines and T2CL6. Looking at Figure 28 one notes that the convergence is slow and one can expect that increasing KGA any further would cause the functional gains to diverge. We next reduce ρI by a factor of 10 while keeping

the rest of the parameters the same. Figures 31-34 and 35-38 show the functional gains using Cubic B-splines and T2CL6, respectively. As is noted neither of the two schemes can produce convergent functional gains. Some insight into this behavior can be obtained by rewriting the "fourth order" model for the Timoshenko beam. If one writes the basic equation in terms of the beam lateral displacement only, it becomes

$$EI\frac{\partial^4 u}{\partial x^4} + \rho A\frac{\partial^2 u}{\partial t^2} - (\rho I + \frac{EI\rho A}{KGA})\frac{\partial^4 u}{\partial x^2 \partial t^2} + \frac{\rho I \rho A}{KGA}\frac{\partial^4 u}{\partial t^4} = 0.$$

Increasing the G or reducing I makes the fourth term to be much smaller than the first two leading term. For small values of ρI, the same thing happens to the third term. In essence, for small values of ρI, as G is increased, the last two terms simply drop and the model simplifies to Euler-Bernoulli model for the beam. Although the Timoshenko model may be more accurate, the optimal control problem involves solving the Riccati operator equation. Its finite dimensional approximation is a highly nonlinear algebriac matrix equation. We speculate that having large differences in orders of magnitiude plays an important role in the divergence of the functional gains. Figures 39-40 are the functional gains for the same structure using Euler-Bernoulli model. Comparing Figure 29 to Figure 40, we see that the functional gains for velocity are similar.

Example 3.

To further study the effect of these parameters on the convergence of the optimal control law, we select another structure with physical properties given by

$$\rho A = 0.1 \quad Kg/m \qquad \rho I = 0.003 \quad Kg - m \tag{5.1.5}$$

$$KGA = 510.817 \quad N \qquad EI = 0.1 \quad N - m^2 \tag{5.1.6}$$

$$L = 2. \quad m, \qquad I_c = 1 \quad N - m^2 \tag{5.1.7}$$

$$H = .06 \quad m, \qquad m_c = 1 \quad Kg. \tag{5.1.8}$$

Figures 41-44 and 45-48 show the functional gains using Cubic B-splines and T2CL6, respectively. It is noted that for this particular structure Cubic B-spline fails to produce convergent functional gains where as T2CL6 produces convergent functional gains. Next we reduce KGA by a factor of 100 while keeping the rest of the parameters fixed as above. Figures 49-52 show the functional gains using Cubic B-splines. It is noted that Cubic B-splines still fails to obtain convergent functional gains. In order to investigate the roubustness of T2CL6 we return to the original data and increase KGA by a factor of 5. Figures 53-56 show the functional gains using T2CL6. It is noted that the scheme can still produce convergent functional gains. Next we increase KGA by a factor of 10 to 5108.17. Figures 57-60 show the functional gains using T2CL6. It is noted that the scheme fails to produce convergent functional gains as the beam starts to behave more like an Euler-Bernoulli beam. Figures 62-63 show the functional gains for the same structure when Euler-Bernoulli model

is used. To compare the results we differentiate the functional gain $\phi_f(x)$ given in Figure 58 (the component that acts on the bending of the beam in the control law). The differentiated form of $\phi_f(x)$ is given in Figure 61. If one compares Figure 61 to Figure 62 and Figure 59 to Figure 63, then one sees that T2CL6 applied to Timoshenko model generates functional gains that approach the gains computed using standard cubic splines for the Euler-Bernoulli model.

Example 4.

Next we return to the data given in (5.1.5)-(5.1.8) and study the effect of changing other system parameters on the convergence of the functional gains. Since T2CL6 is more roubust than the Cubic B-splines, it is used exclusively for the rest of the numerical experiments. Figures 64-67 show the functional gains when the beam length is increased to $6m$. Note that all the functional gains converge. Figures 68-71 show the functional gains when the tip mass and the tip moment of inertia are increased to 100. Observe that T2CL6 still produces convergent functional gains. Figures 72-75 contain the (convergent) functional gains when the hub moment of inertia is increased by a factor of 3, and in Figure 76-79 the the same is observed when the hub is increased by a factor of 100.

Chapter 6

Conclusions

6.1 Summary of Basic Results.

In this thesis we investigated the use of finite element schemes in the construction of design models for LQR control of a Timoshenko structure. Previous efforts had employed standard cubic finite element approximations and produced divergent functional gains. We applied a conforming finite element scheme that had been specifically designed for simulation of Timoshenko type models (T2CL6) to the problem of computing optimal functional gains. We made the following discoveries:

1. The choice of the local basis functions used to generate a finite dimensional design model has considerable impact on both the question of convergence and the rates of convergence of the control design. This feature is clearly illustrated by Example 3. The T2CL6 algorithm produced convergent gains for a problem where the standard cubic finite element failed to converge. Moreover, in Example 2 we observed a problem for which both schemes produced convergent gains, yet T2CL6 converged faster. Finally, Example 3 clearly demonstrates the superior roubustness of the T2CL6 algorithm.

2. The problems that cause both algorithms to diverge are constructed by selecting system parameters so that the structure is close to an Euler-Bernoulli beam.

In particular, both schemes fail when the beam is 'truely' an Euler-Bernoulli beam. This was observed previously for simulations based on the cubic spline scheme. However, T2CL6 was designed specifically as a simulation scheme to overcome this problem. Although T2CL6 did produce convergent functional gains for a larger set of parameter values, T2CL6 eventually failed.

3. Example 4 illustrates that variations in certain other parameters do not significantly alter the convergence of the gains.

4. Although the Euler-Bernoulli beam model may be viewed as a (singular) perturbation of the Timoshenko model, T2CL6 produced functional gains that are nearly the same as those gains computed by using the Euler-Bernoulli model and cubic finite element. This observation is rather interesting in that there is almost no theory to support the convergence of open-loop solutions and the theory that exists usually produces only weak convergence(see [16]).

5. Although theoretical issues and computational methods have been fully addressed for control problems governed by Euler-Bernoulli models, the development of computational methods for control of Timoshenko type structures remain incomplete. The numerical examples show that both T2CL6 and cubic splines can fail to produce finite dimensional models that preserve exponential stabalizability uniformly under approximation (POES) (see [17]). The interesting observation is

that for true Timoshenko beams (with the type of damping considered here) the functional gains still converge.

6.2 Future Research Plans.

The observations above have raised several research issues.

[A] If T2CL6 satisfied POES uniformly under approximation, then it would do so independently of the parameter values. Consequently, the convergence of the functional gains for certain parameter values imply that sufficient conditions for convergence of optimal functional gains might exist that fail for various parameters and work for others. Preservation of exponential stabilizability uniformly under approximation is a sufficient condition for convergence, but not necessary. An analysis of the T2CL6 algorithm might provide insight into a minimal sufficient condition for convergence of control designs based on finite element schemes.

[B] Damping greatly impacts POES and it would be interesting to conduct a battery of numerical experiments using viscoelastic damping since Kelvin-Voigt damping implies POES for the Euler-Bernoulli beam. We plan to investigate this issue by conducting various numerical experiment using Kelvin-Voigt damping with the Timoshenko model.

[C] It may happen that all of the 'theoretical' conditions for convergence of func-

tional gains are satisfied, yet because of numerical ill-conditioning, convergence is lost due to 'round off'. We propose to use the theory of "control system radii" (see [18,19]) to investigate the condition numbers of the LQR problems constructed via T2CL6 and cubic spline.

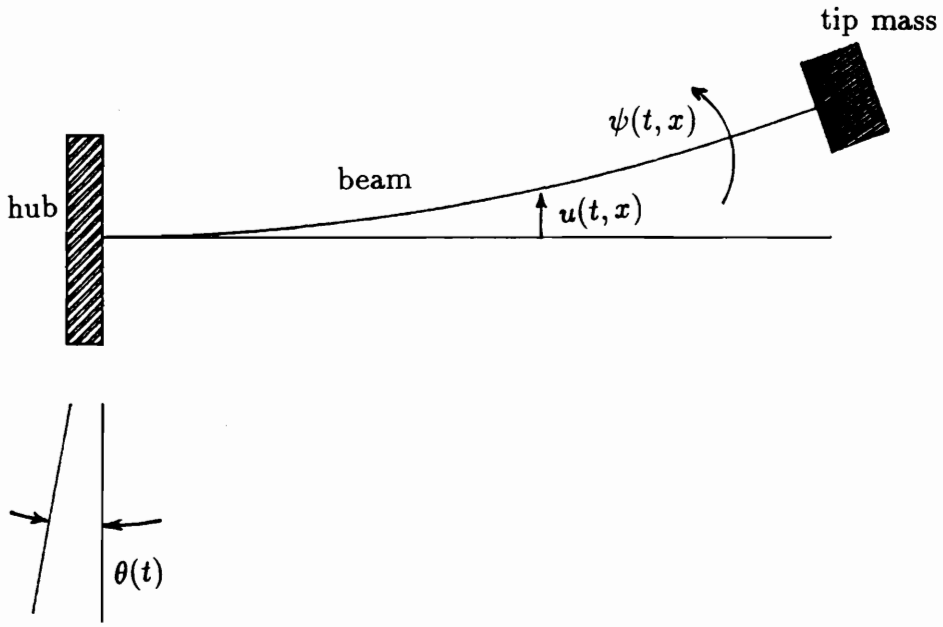

FIGURE 1. Hub-Beam-Tip Structure

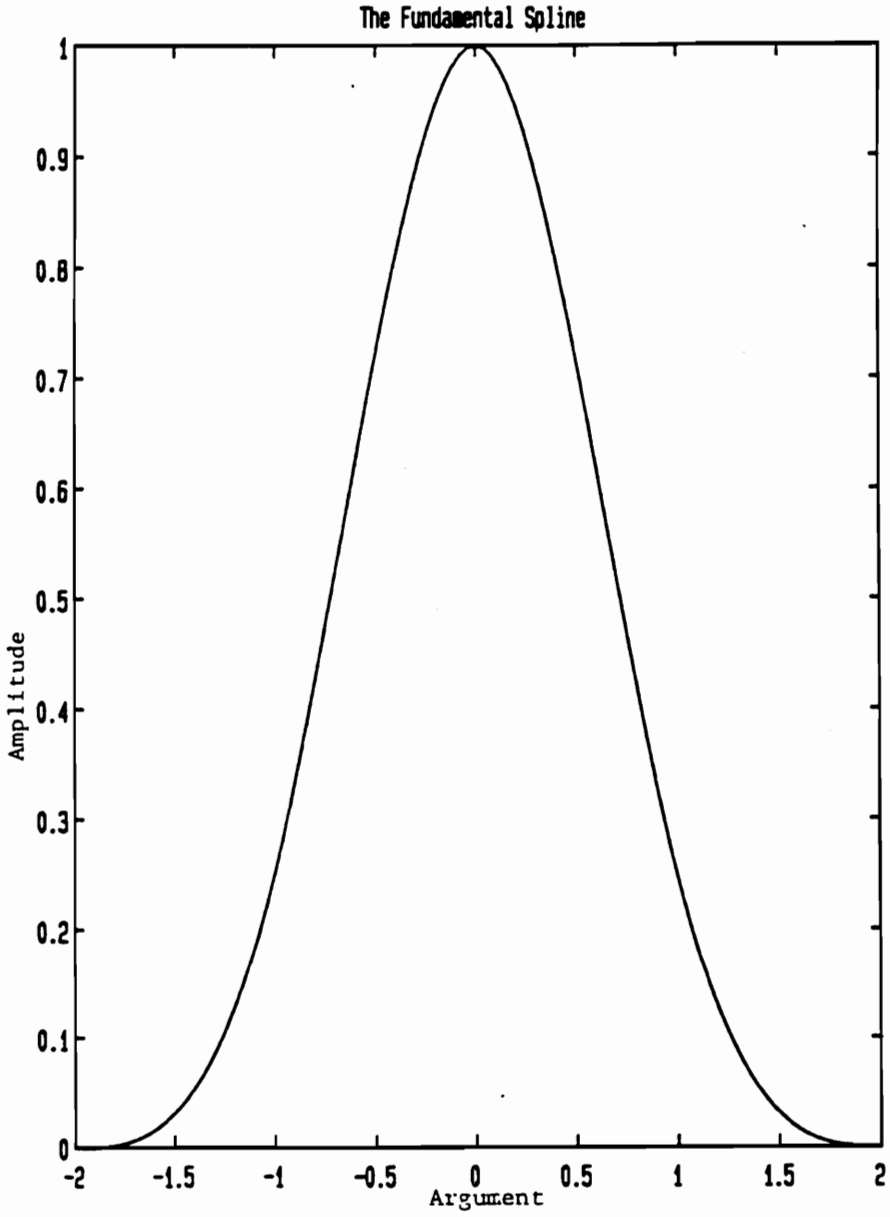

FIGURE 2. Cubic B-spline

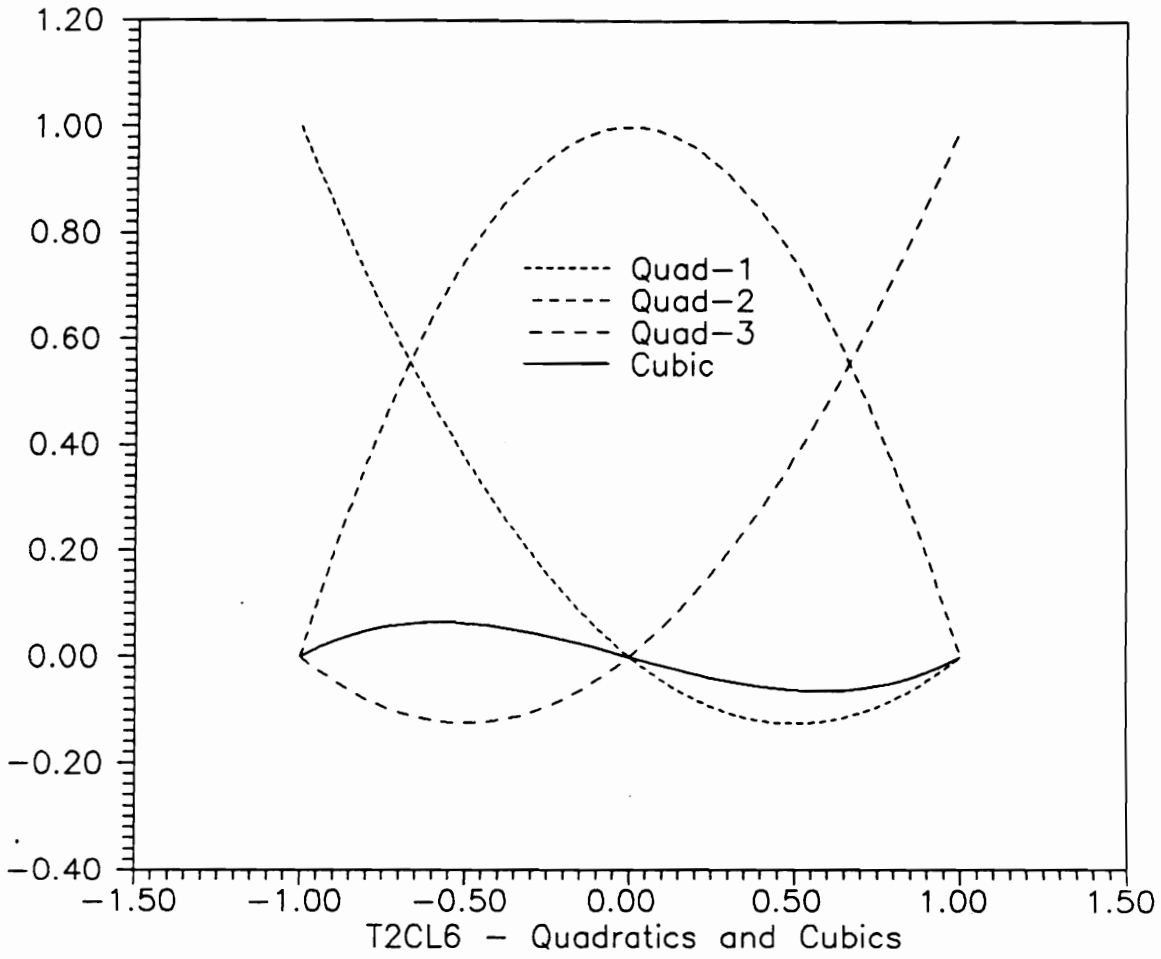

FIGURE 3. T2CL6 Quadratic and Cubic Polynomials

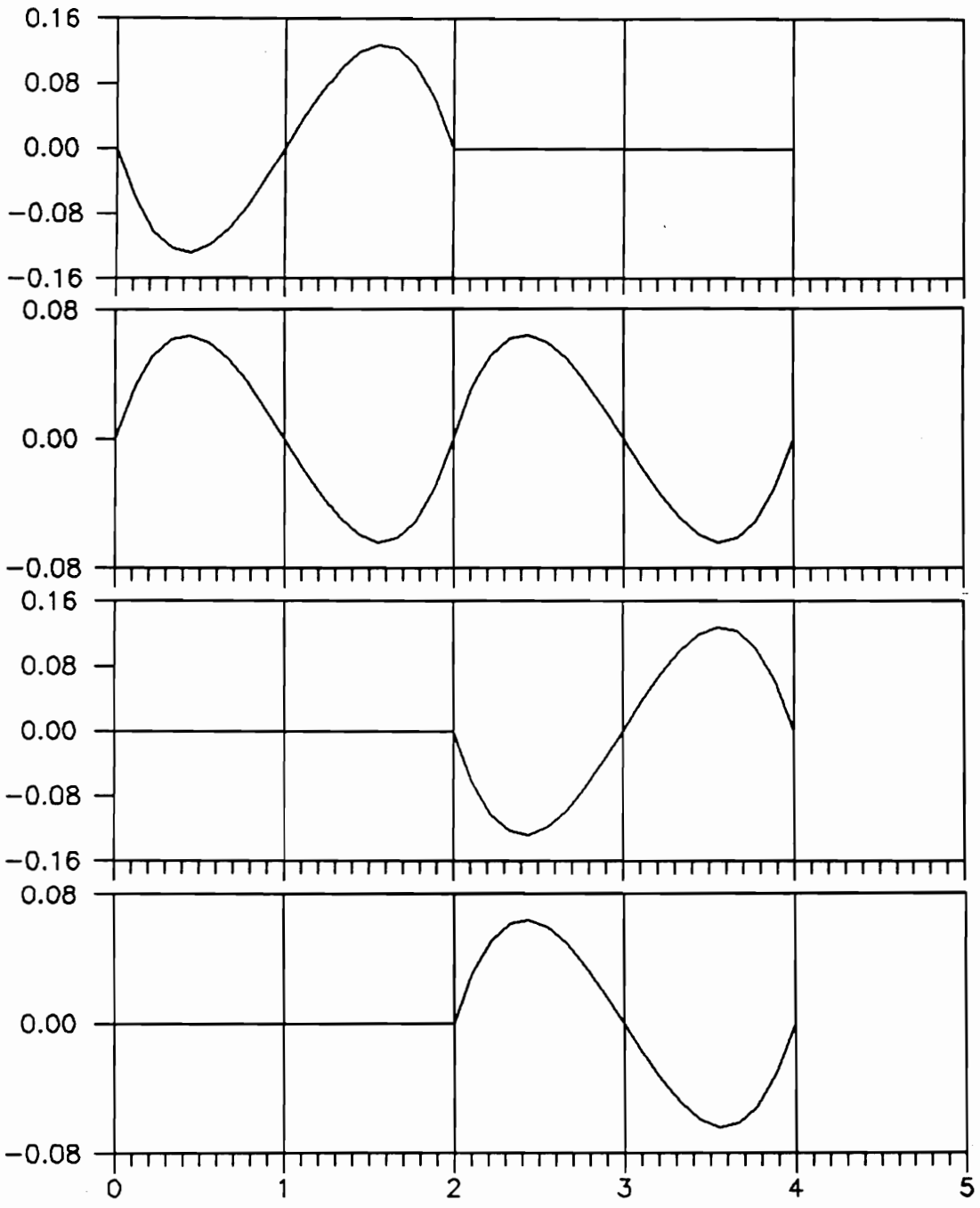

FIGURE 4. T2CL6 Global Basis functions, Cubics

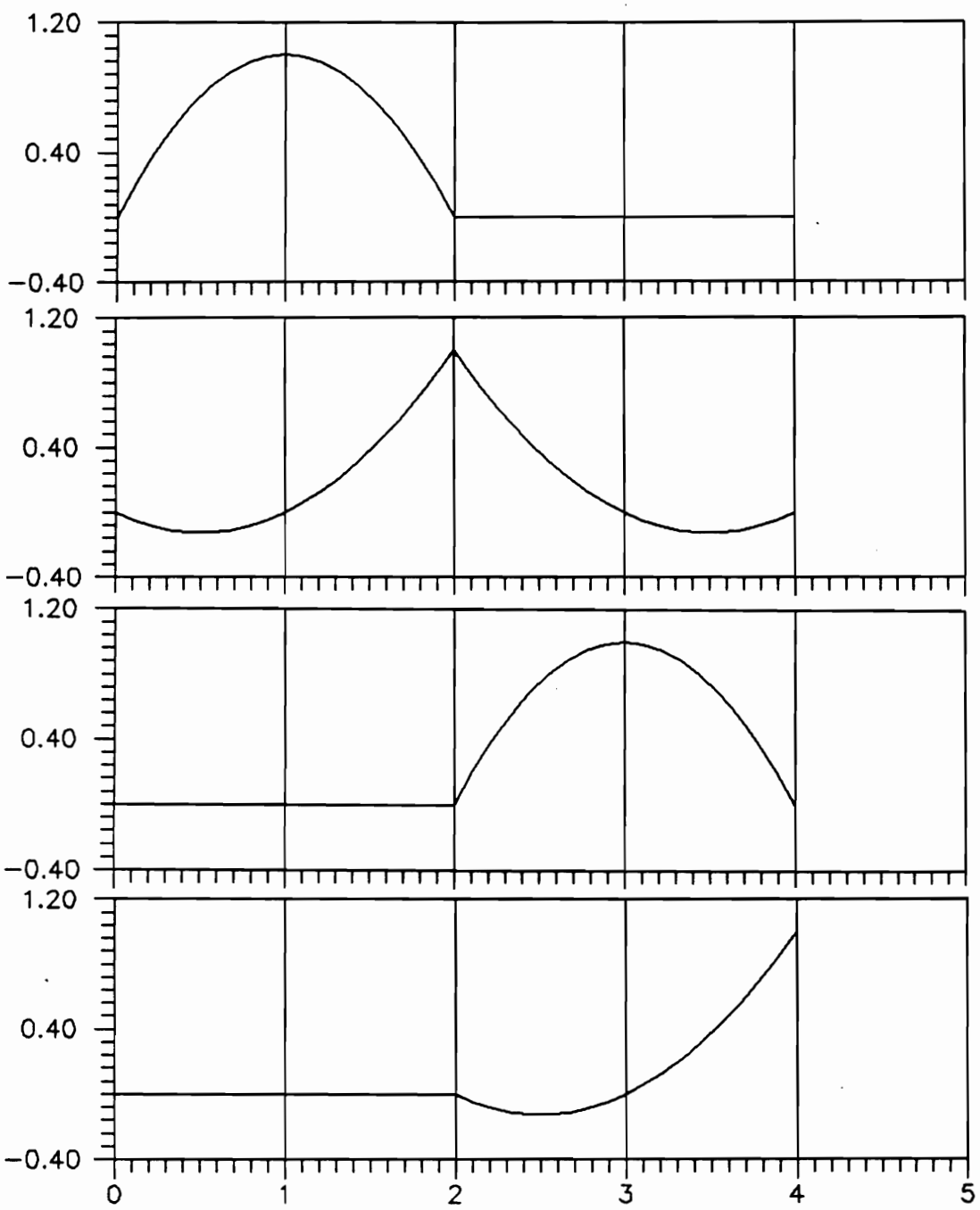

FIGURE 5. T2CL6 Global Basis functions, Quadratics

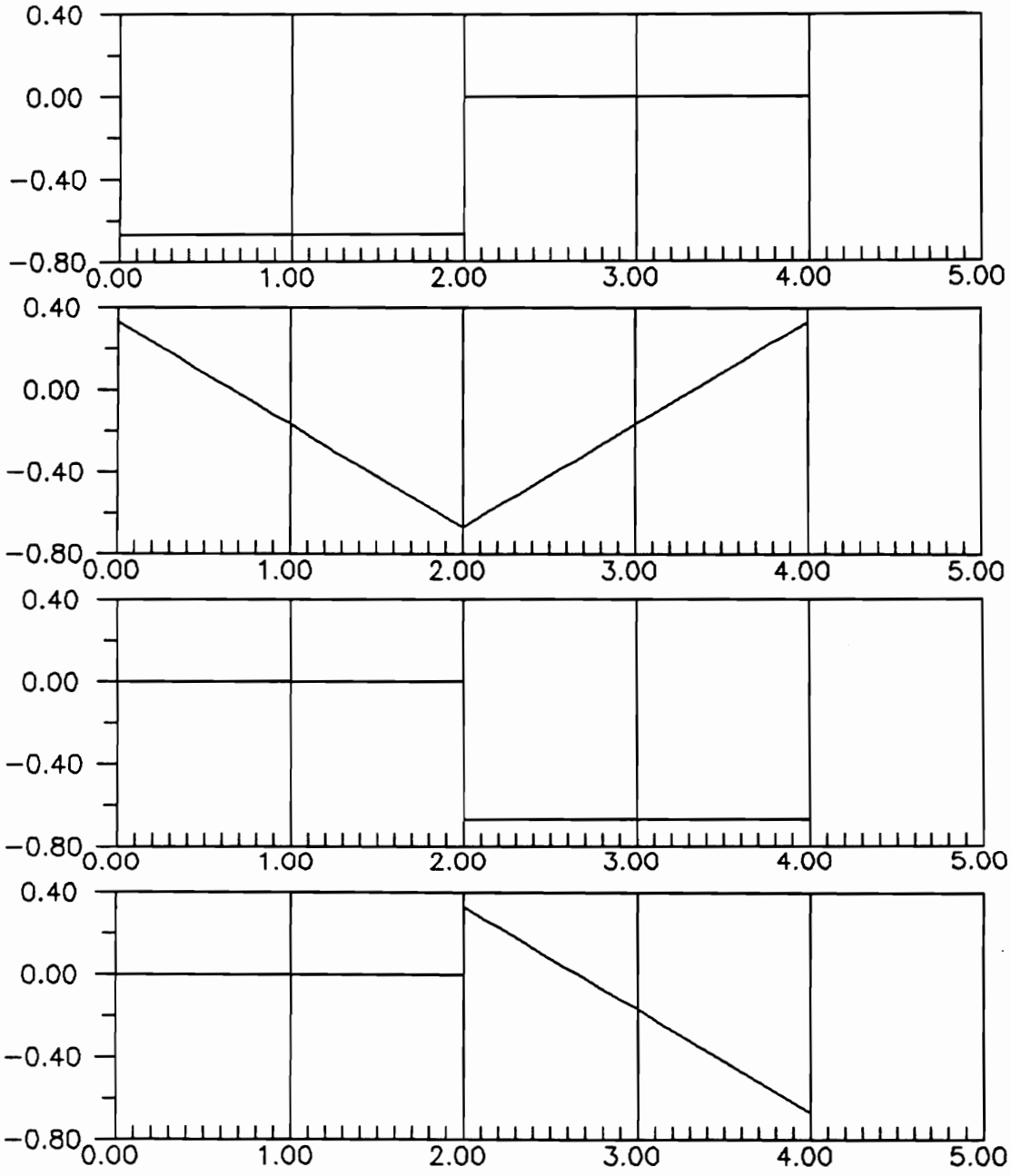

FIGURE 6. T2CL6 Global Basis functions for Shear

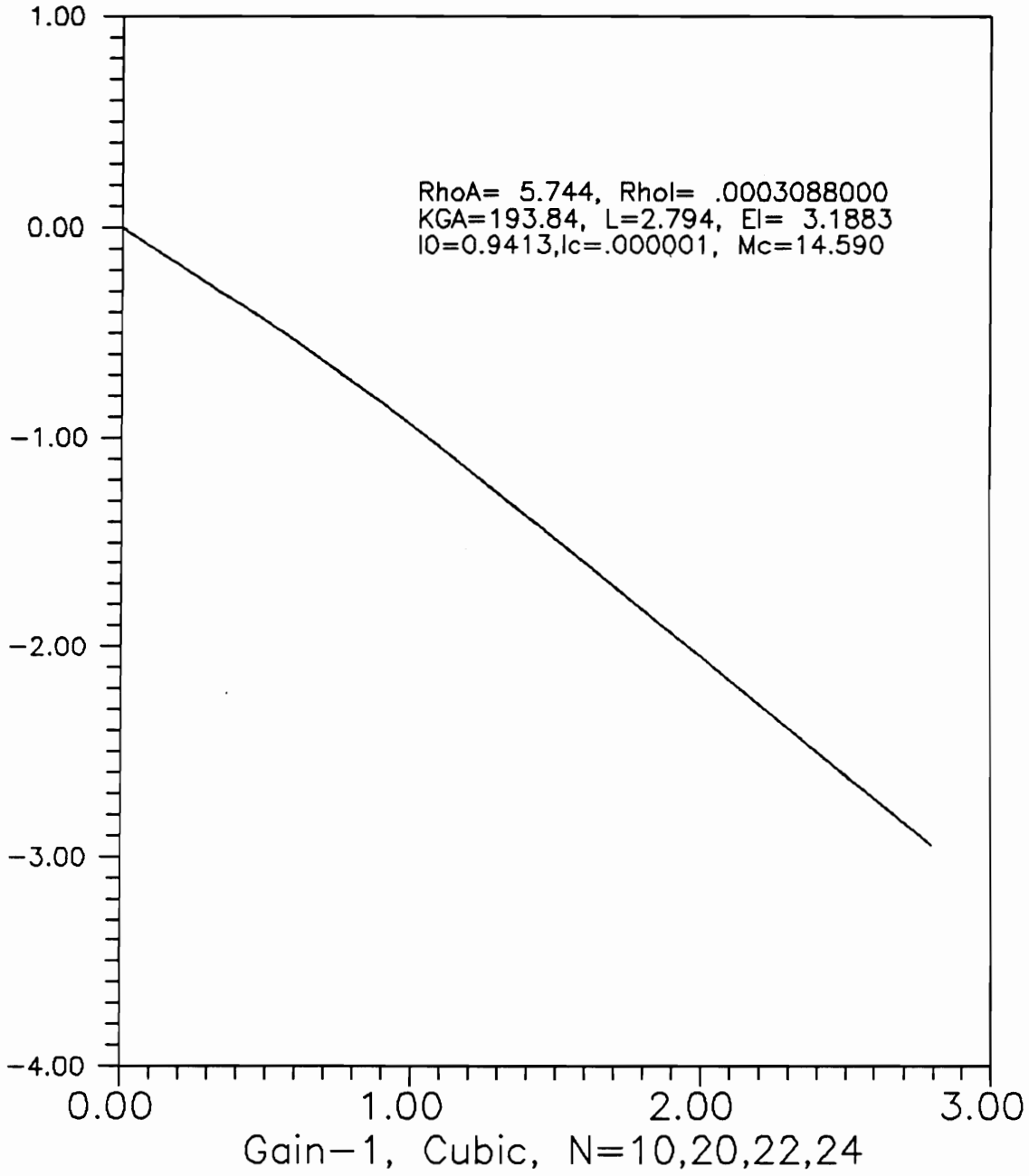

FIGURE 7. Functional Gain $\psi_f(x)$ vs x, Cubic

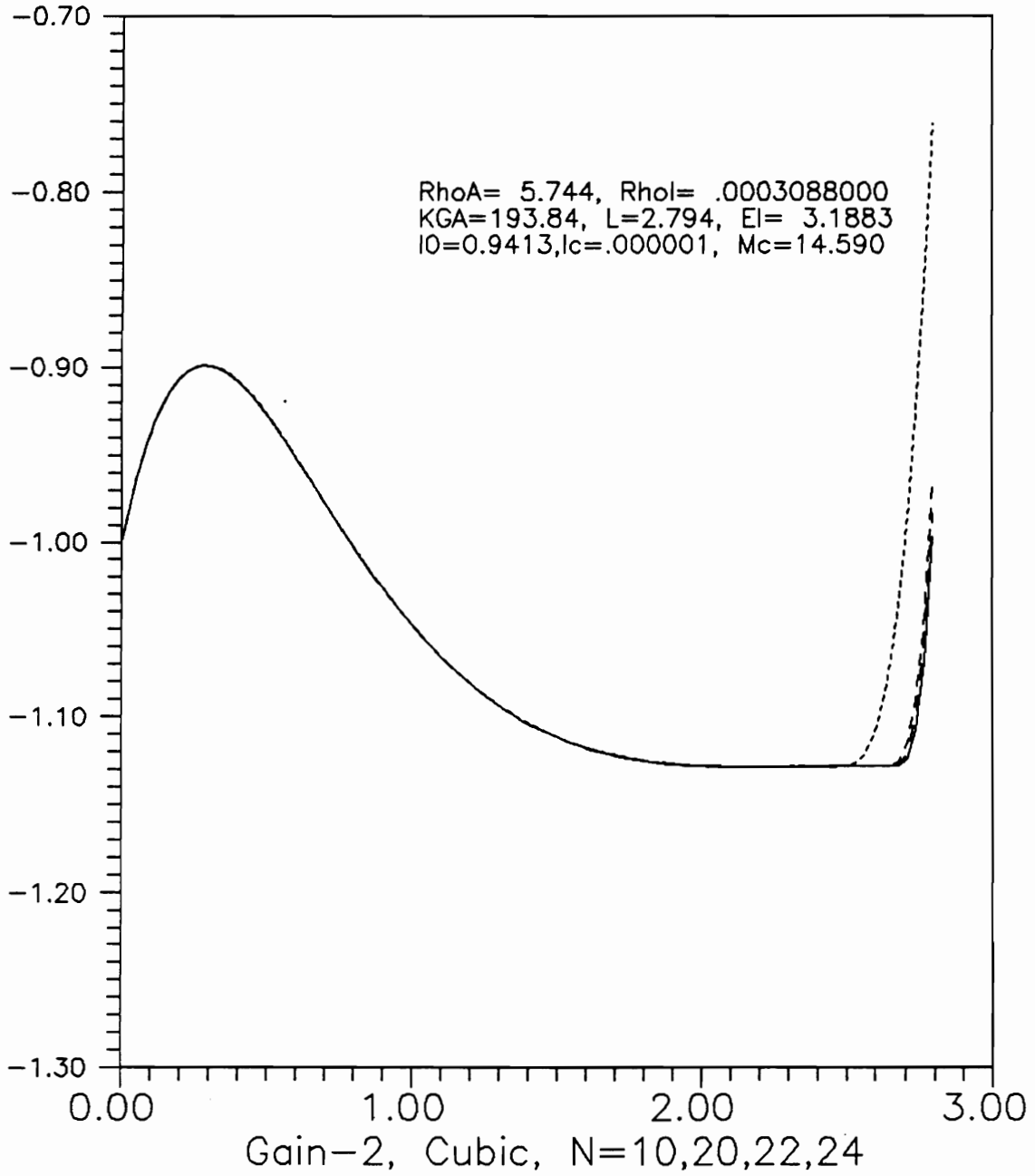

FIGURE 8. Functional Gain $\phi_f(x)$ vs x, Cubic

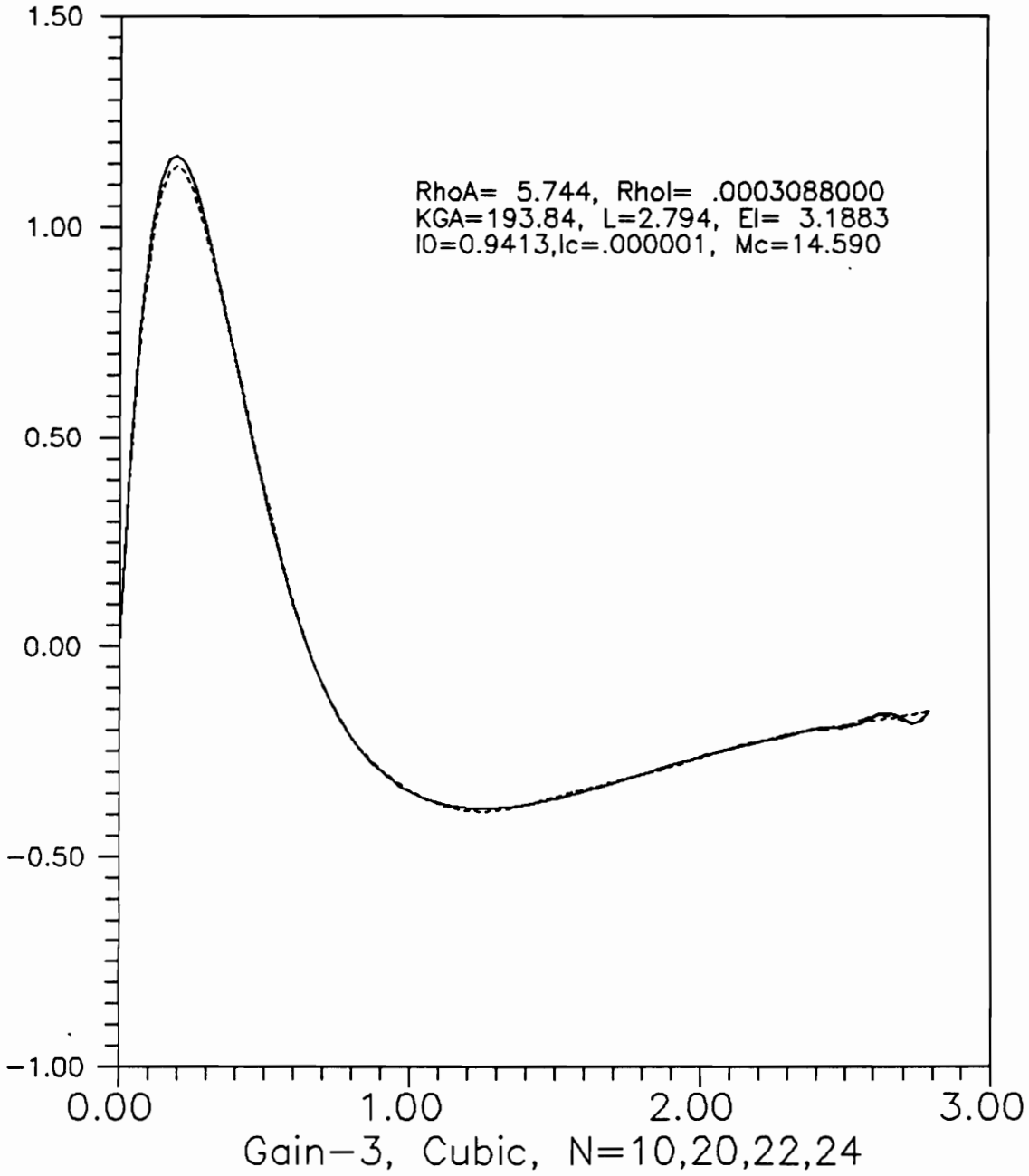

FIGURE 9. Functional Gain $K_4(x)$ vs x, Cubic

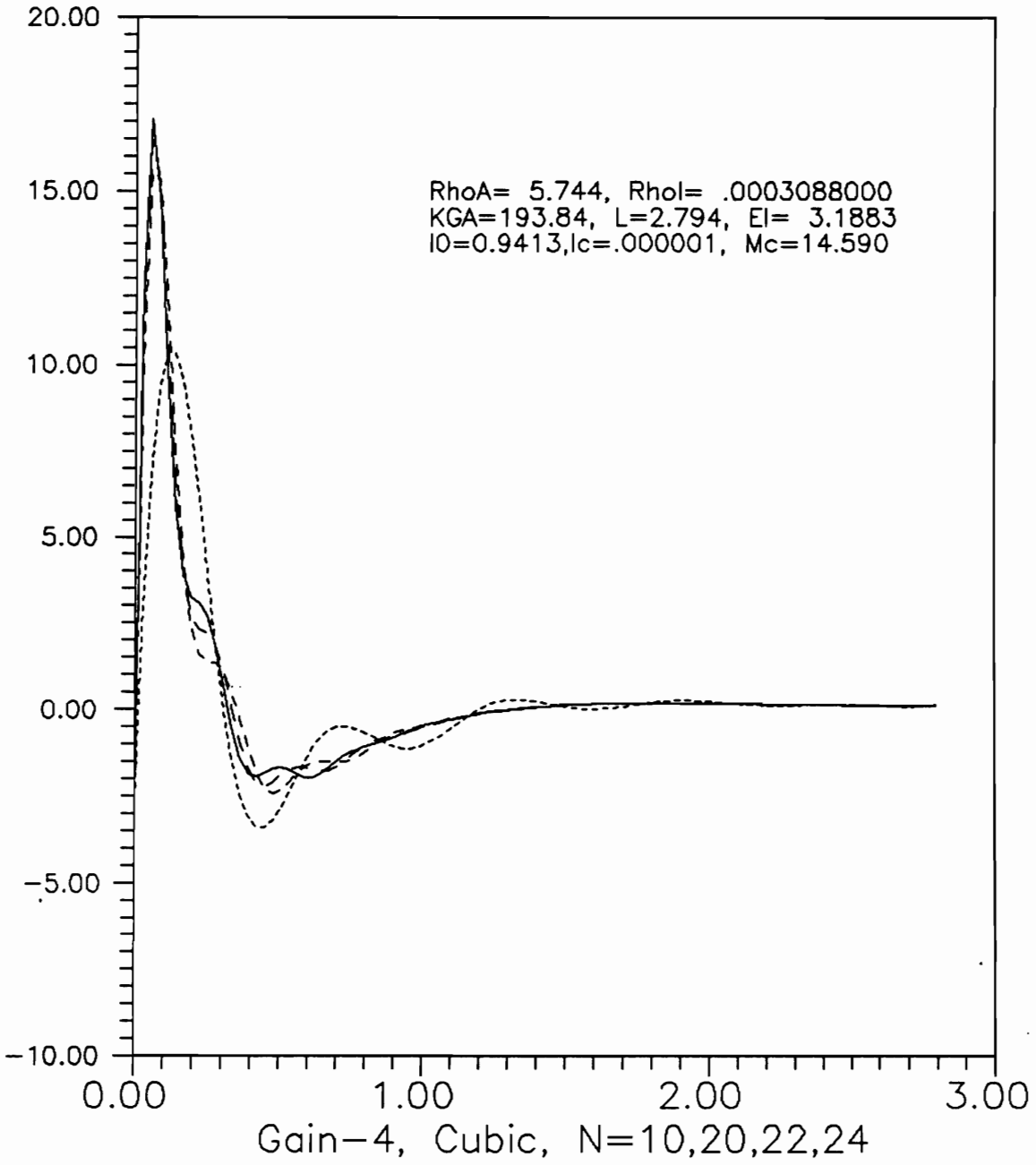

FIGURE 10. Functional Gain $K_5(x)$ vs x, Cubic

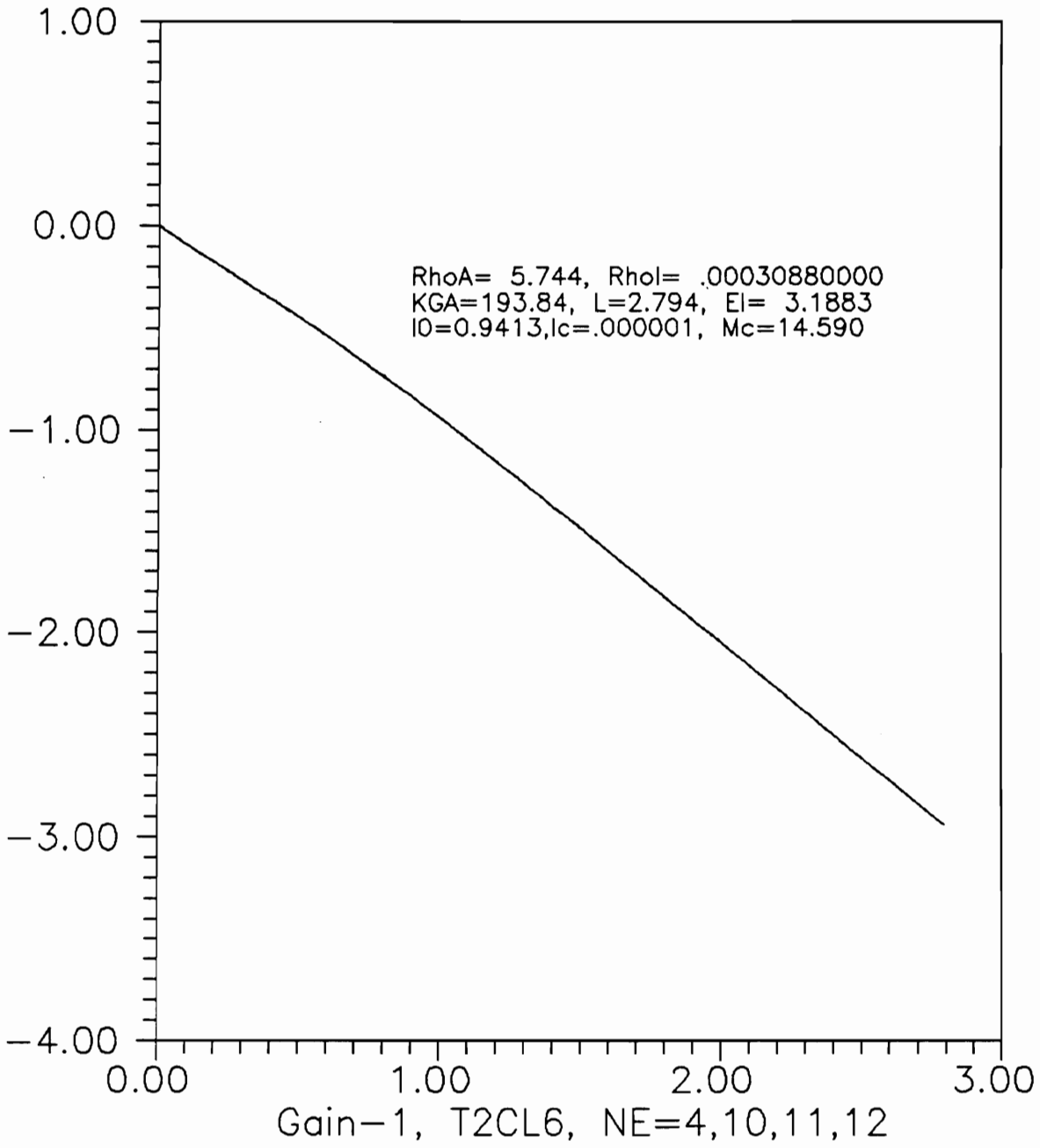

FIGURE 11. Functional Gain $\psi_f(x)$ vs x, T2CL6

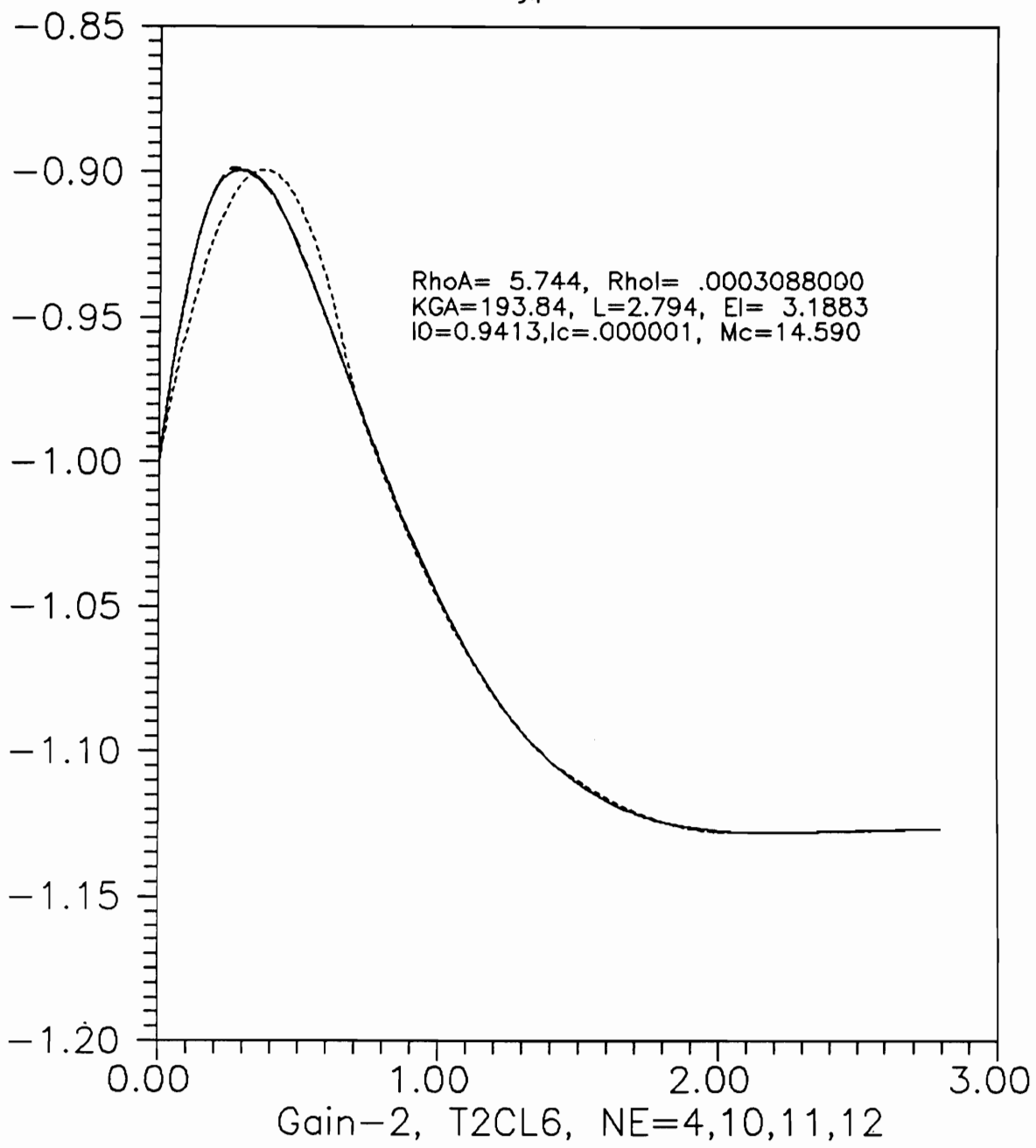

FIGURE 12. Functional Gain $\phi_f(x)$ vs x, T2CL6

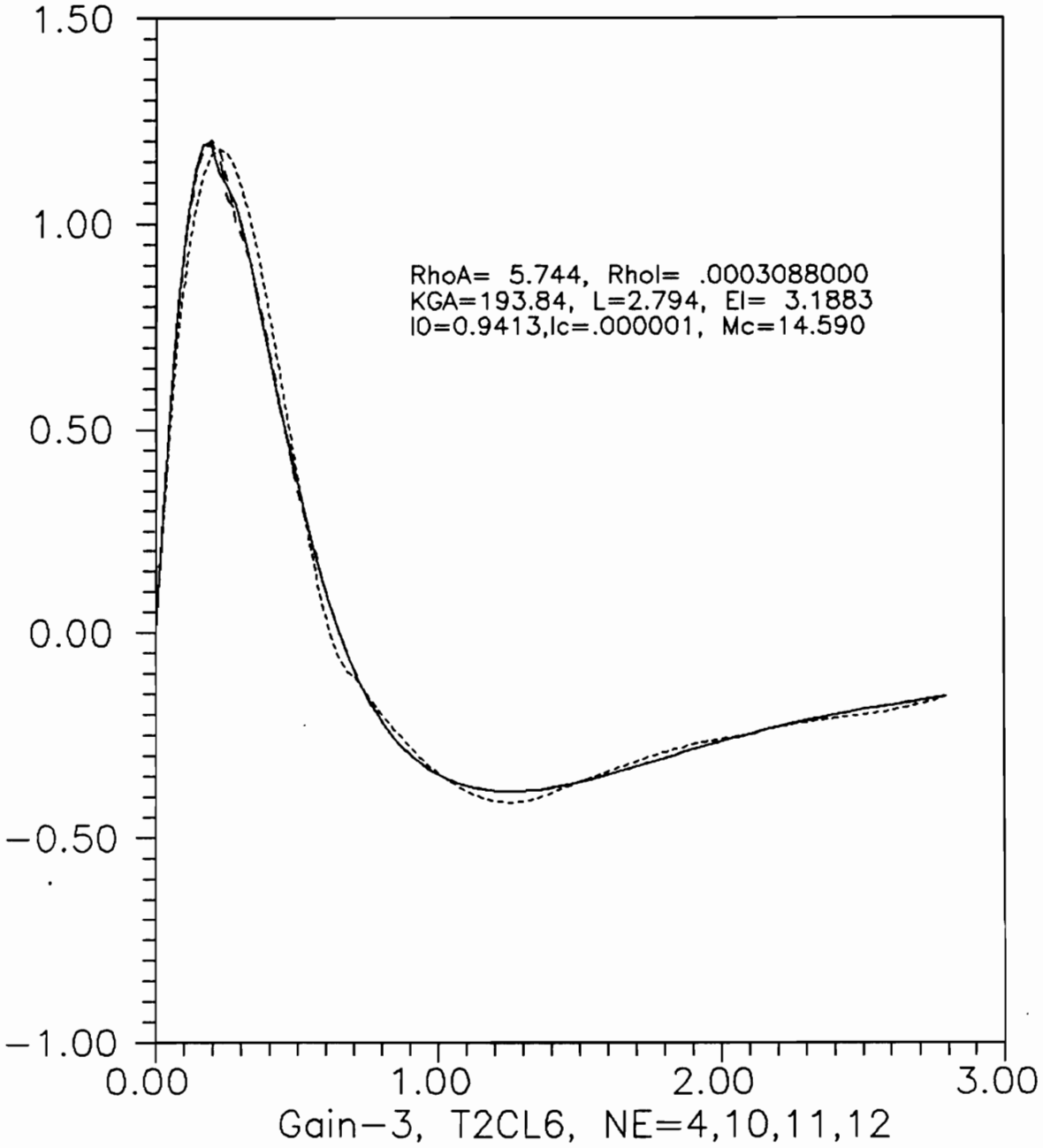

FIGURE 13. Functional Gain $K_4(x)$ vs x, T2CL6

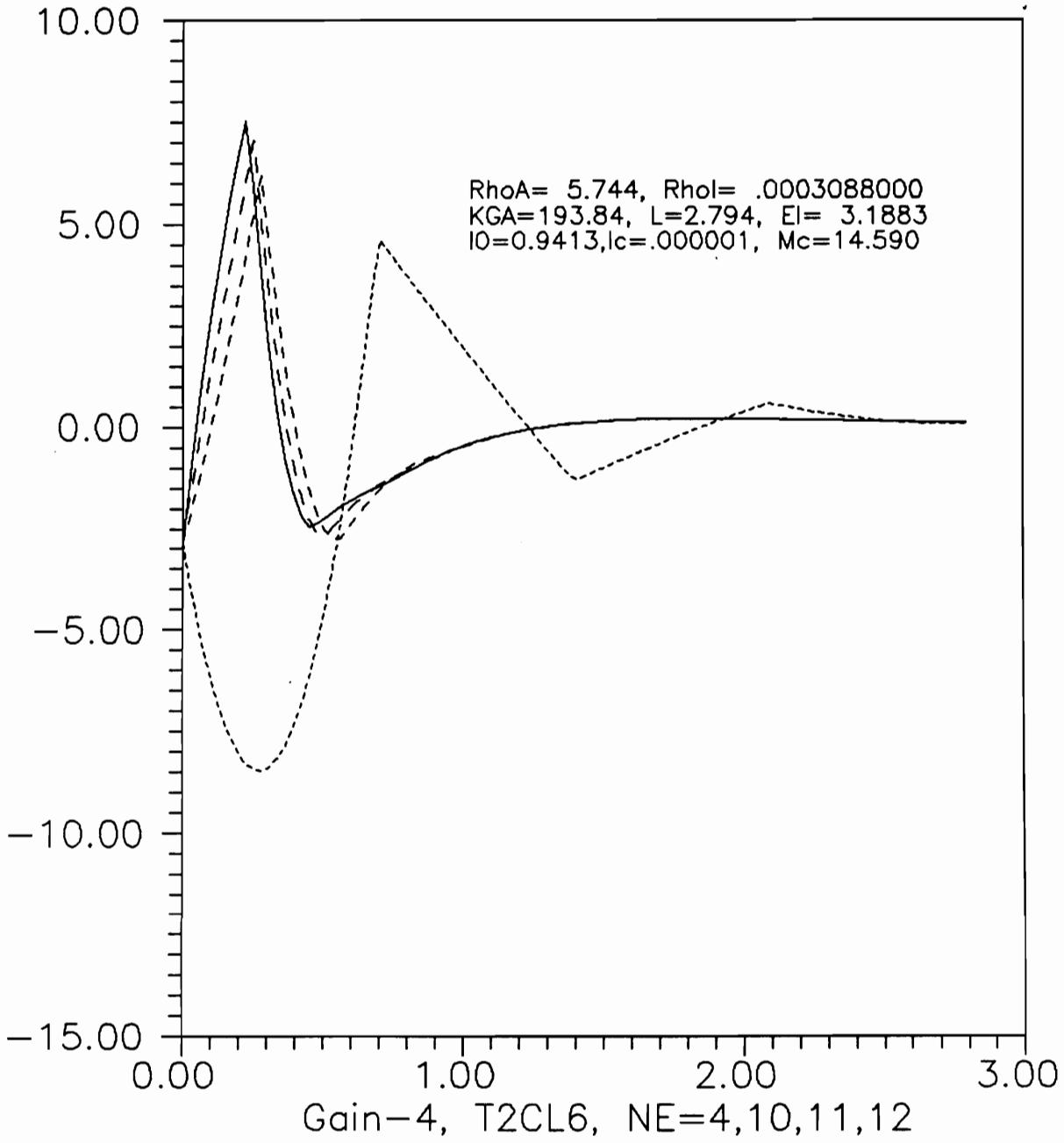

FIGURE 14. Functional Gain $K_5(x)$ vs x, T2CL6

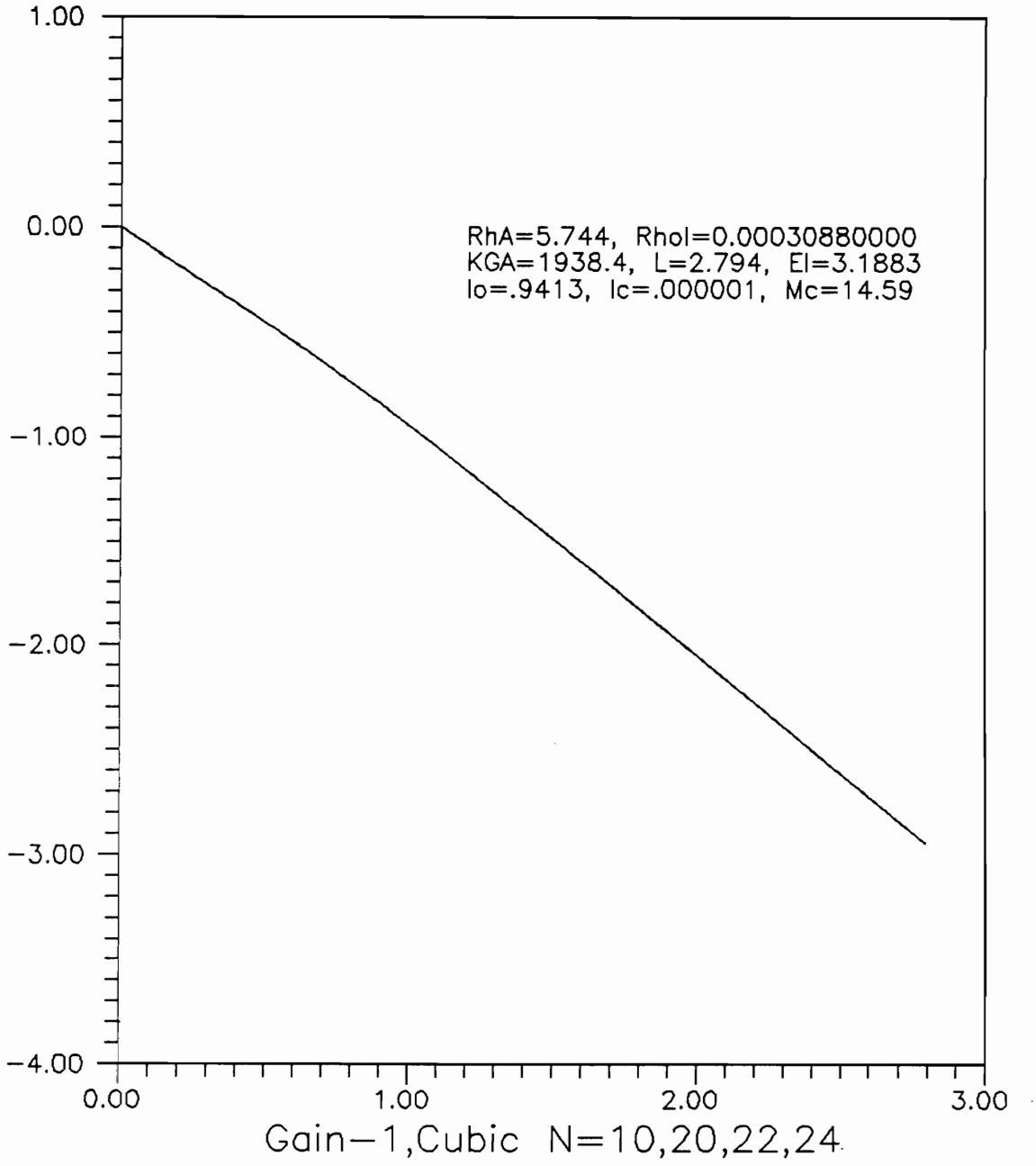

FIGURE 15. Functional Gain $\psi_f(x)$ vs x, Cubic

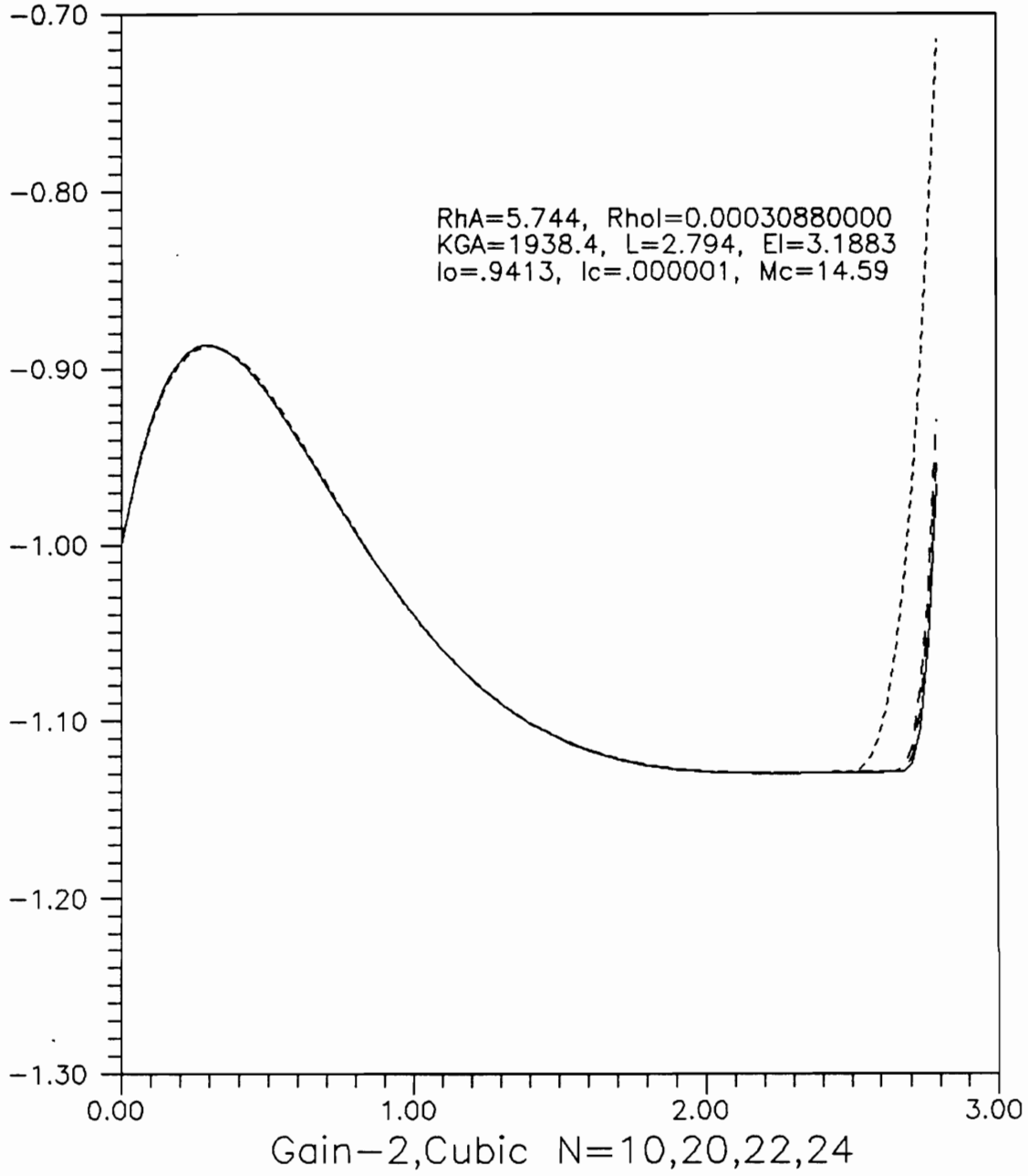

FIGURE 16. Functional Gain $\phi_f(x)$ vs x, Cubic

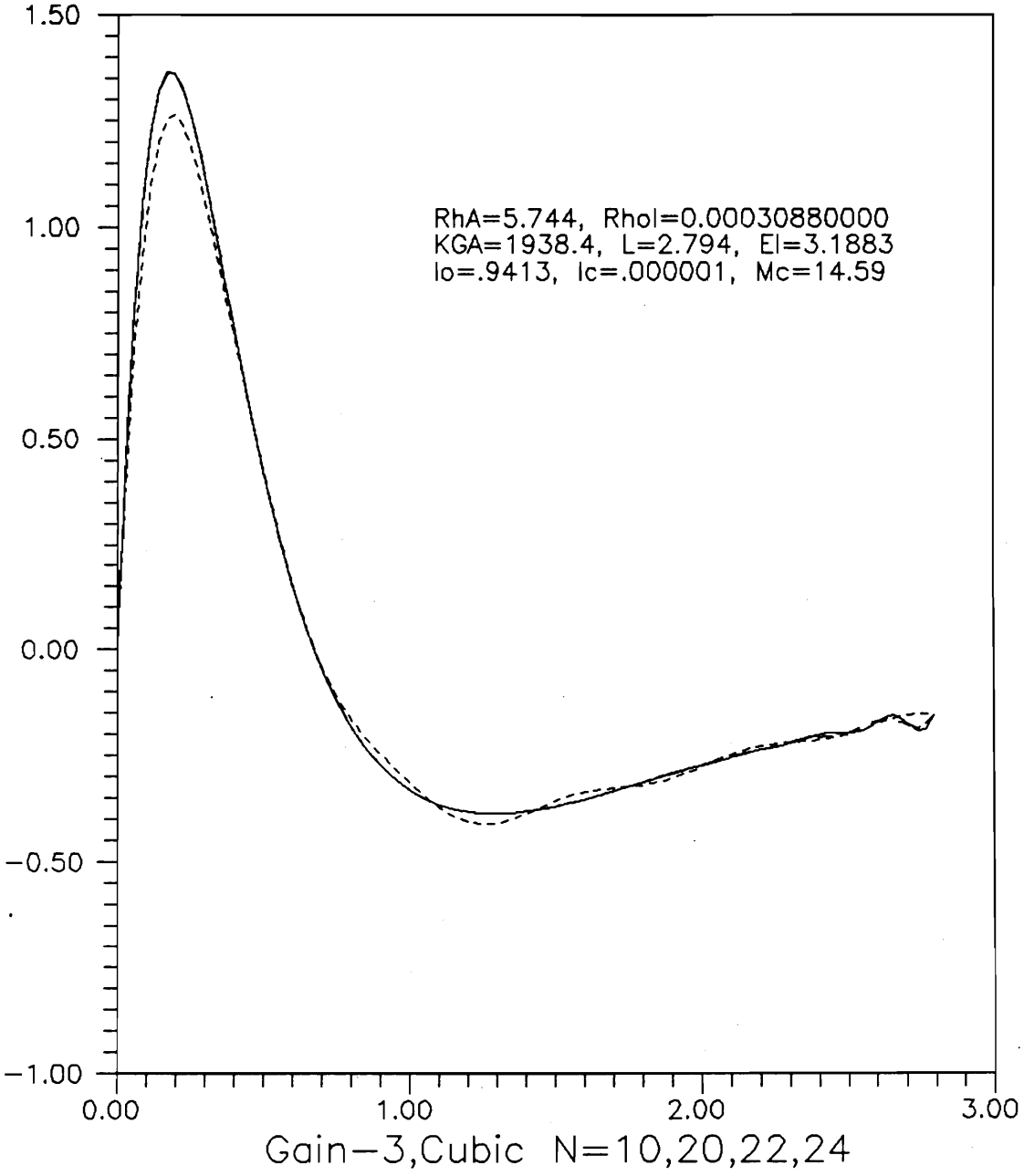

FIGURE 17. Functional Gain $K_4(x)$ vs x, Cubic

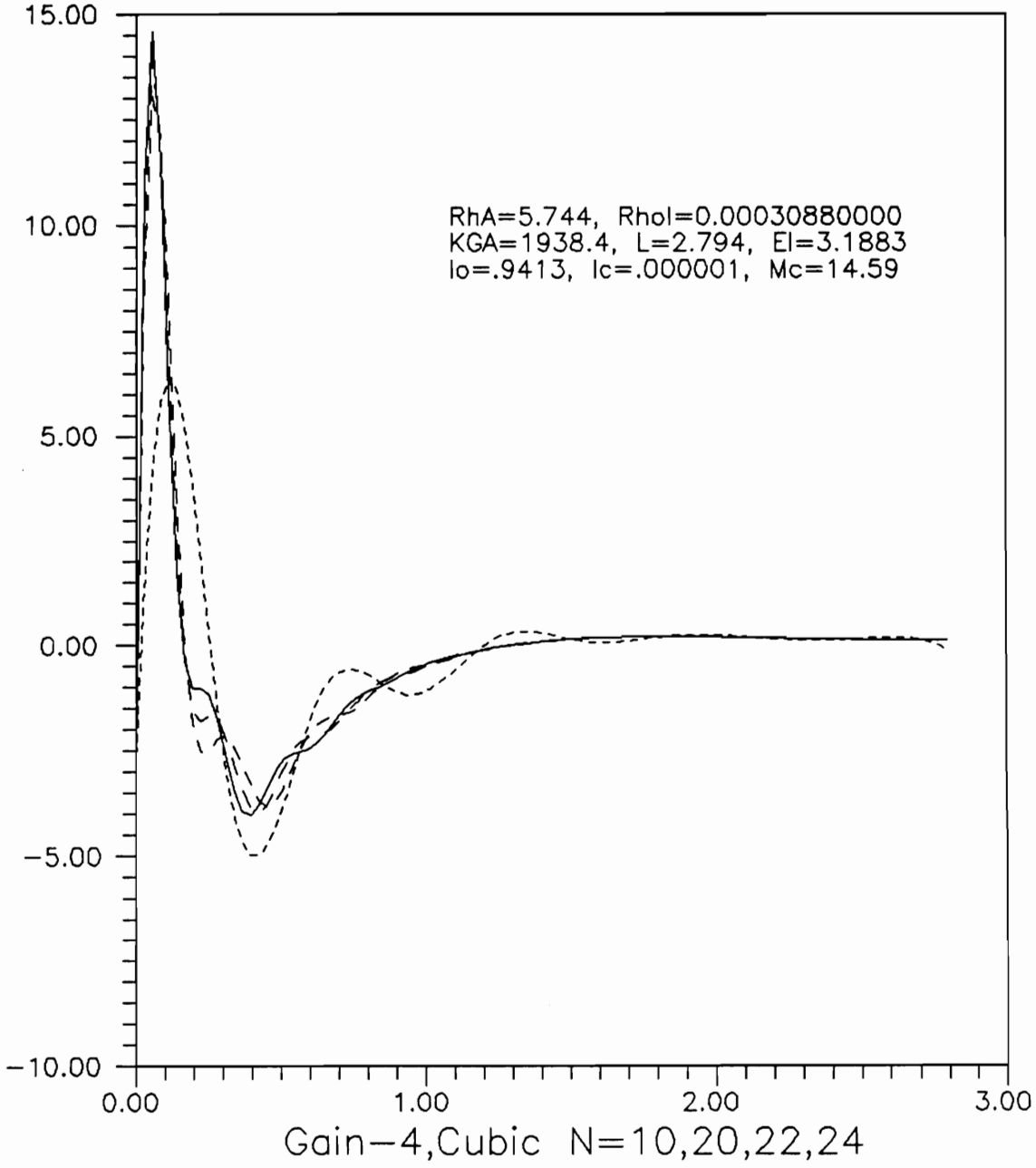

FIGURE 18. Functional Gain $K_5(x)$ vs x, Cubic

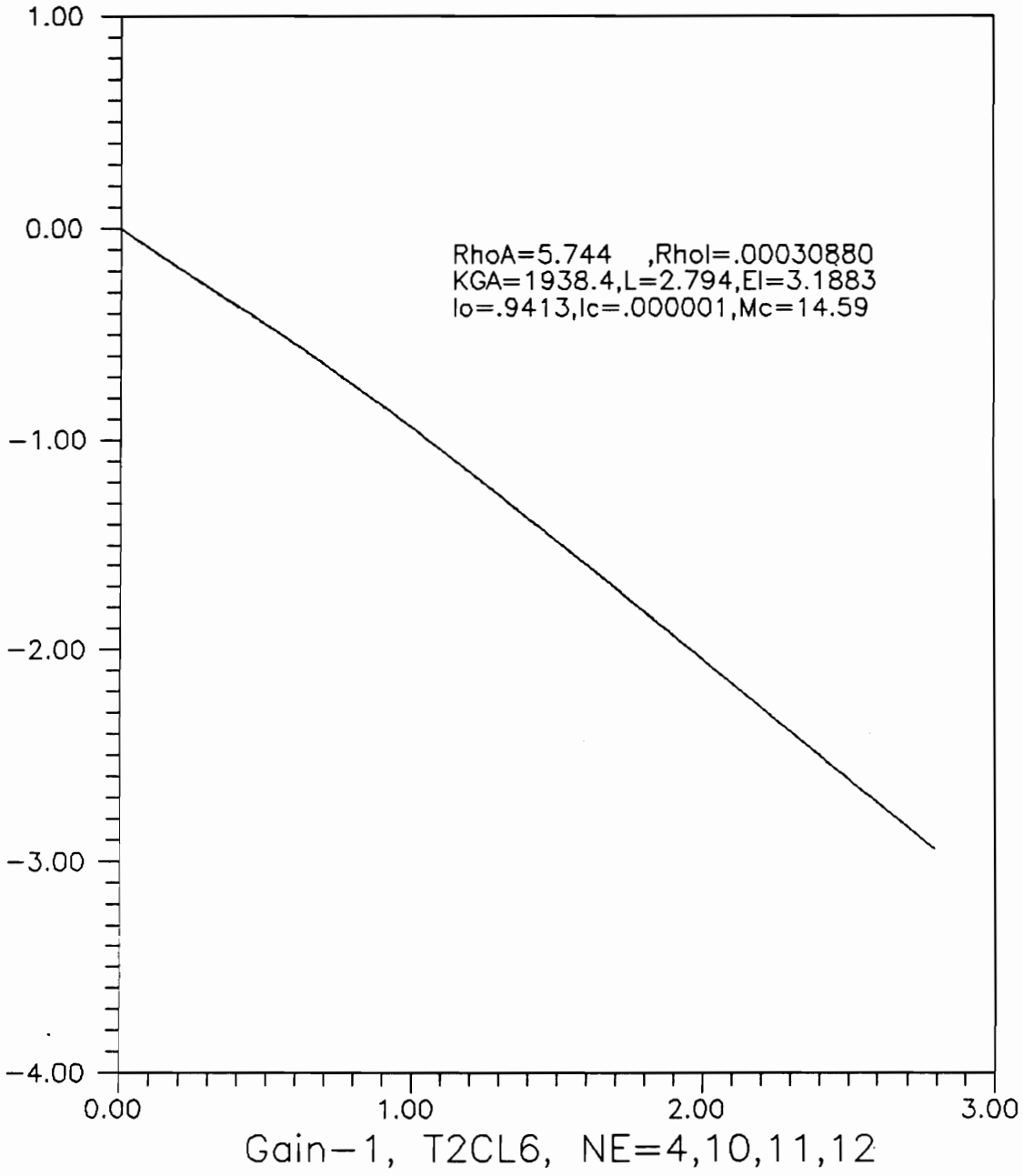

FIGURE 19. Functional Gain $\psi_f(x)$ vs x, T2CL6

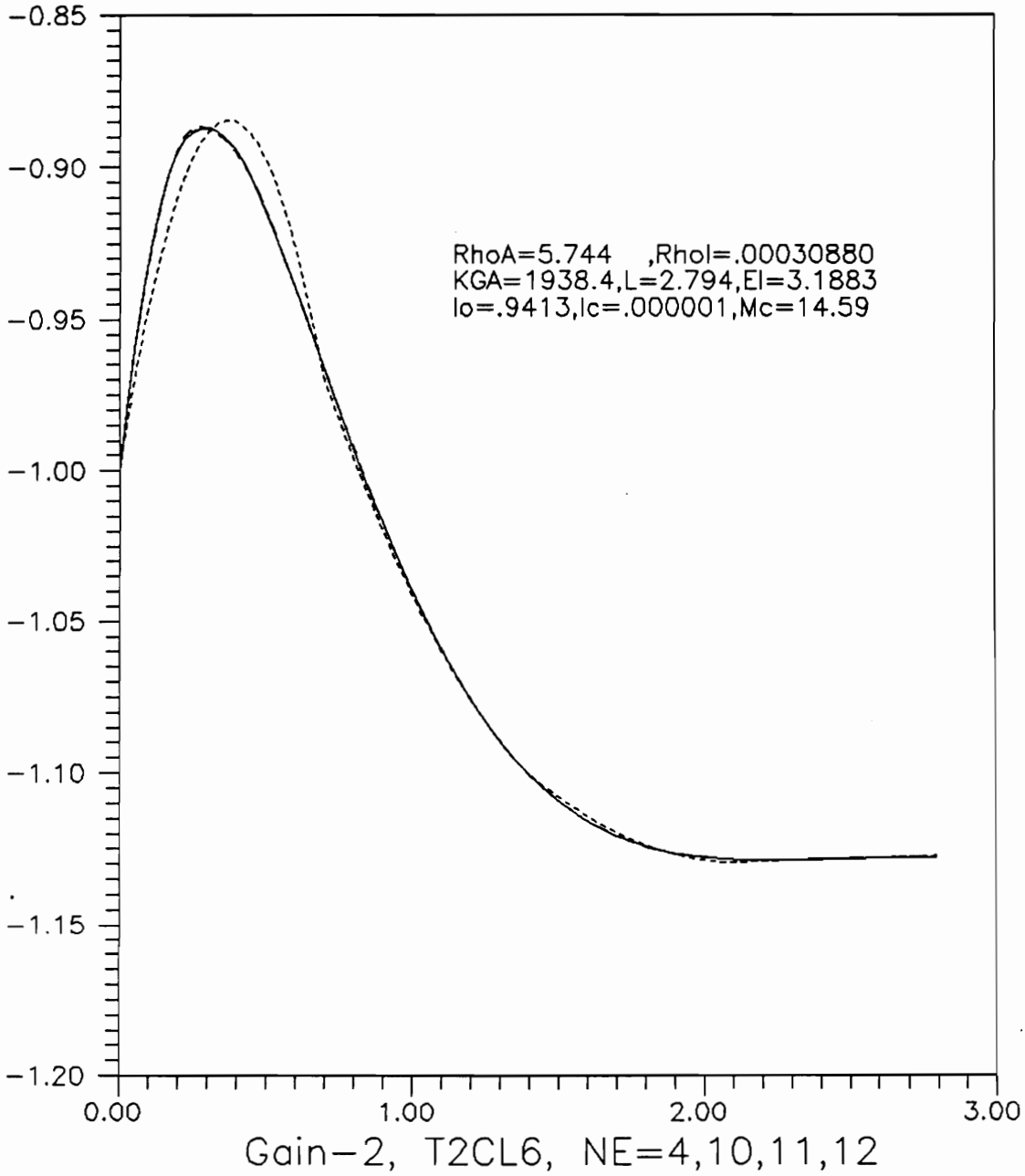

FIGURE 20. Functional Gain $\phi_f(x)$ vs x, T2CL6

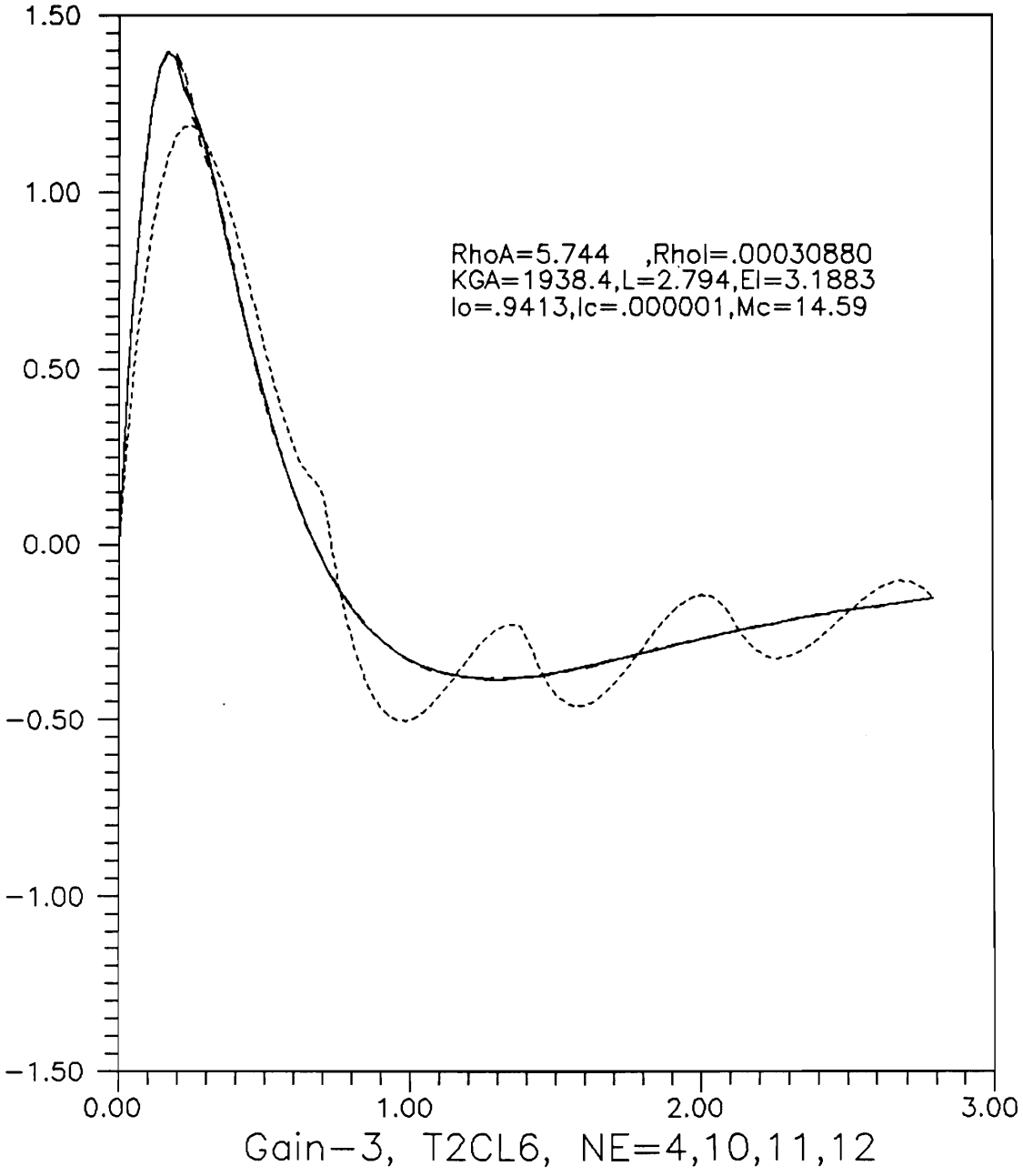

FIGURE 21. Functional Gain $K_4(x)$ vs x, T2CL6

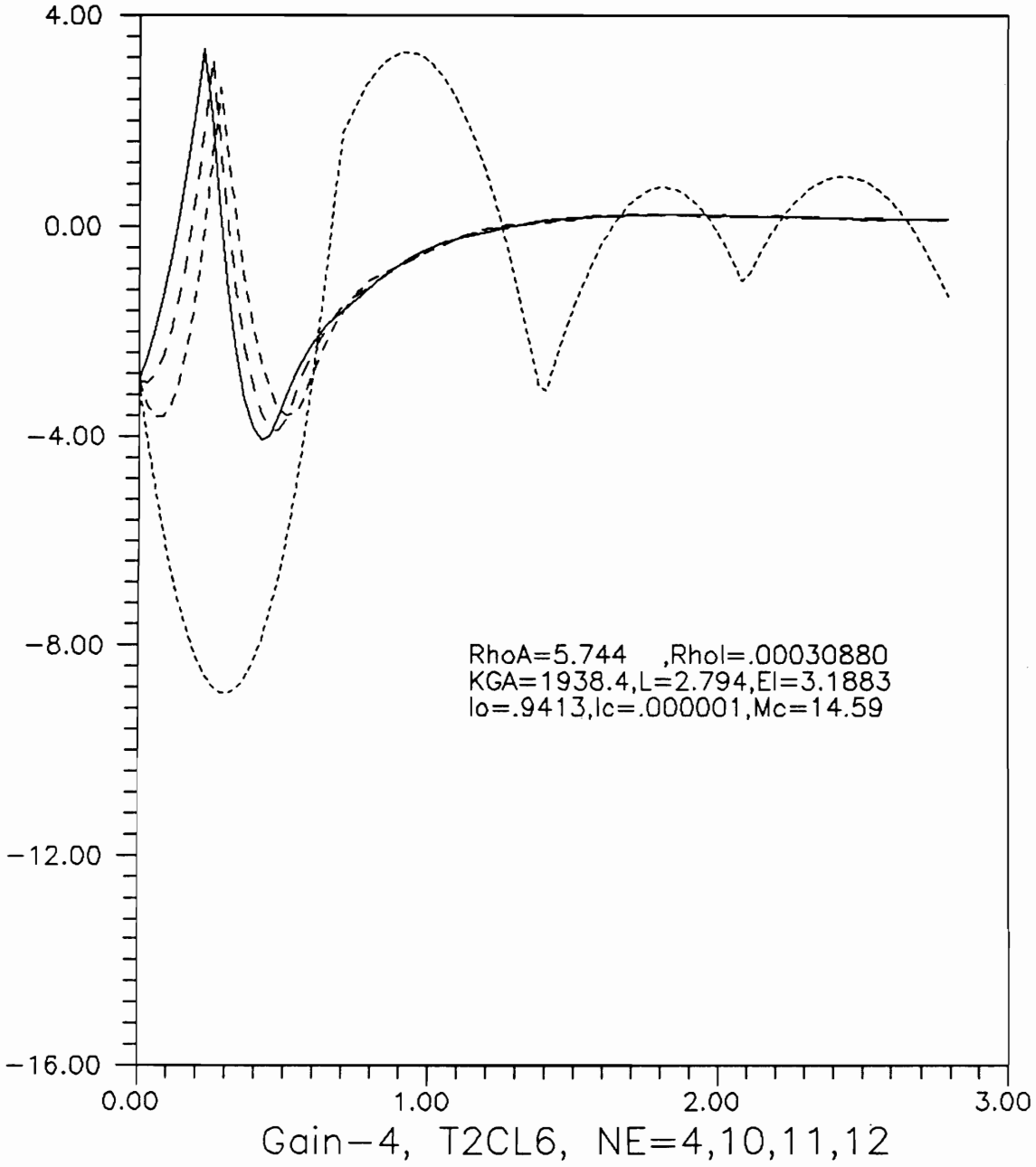

FIGURE 22. Functional Gain $K_5(x)$ vs x, T2CL6

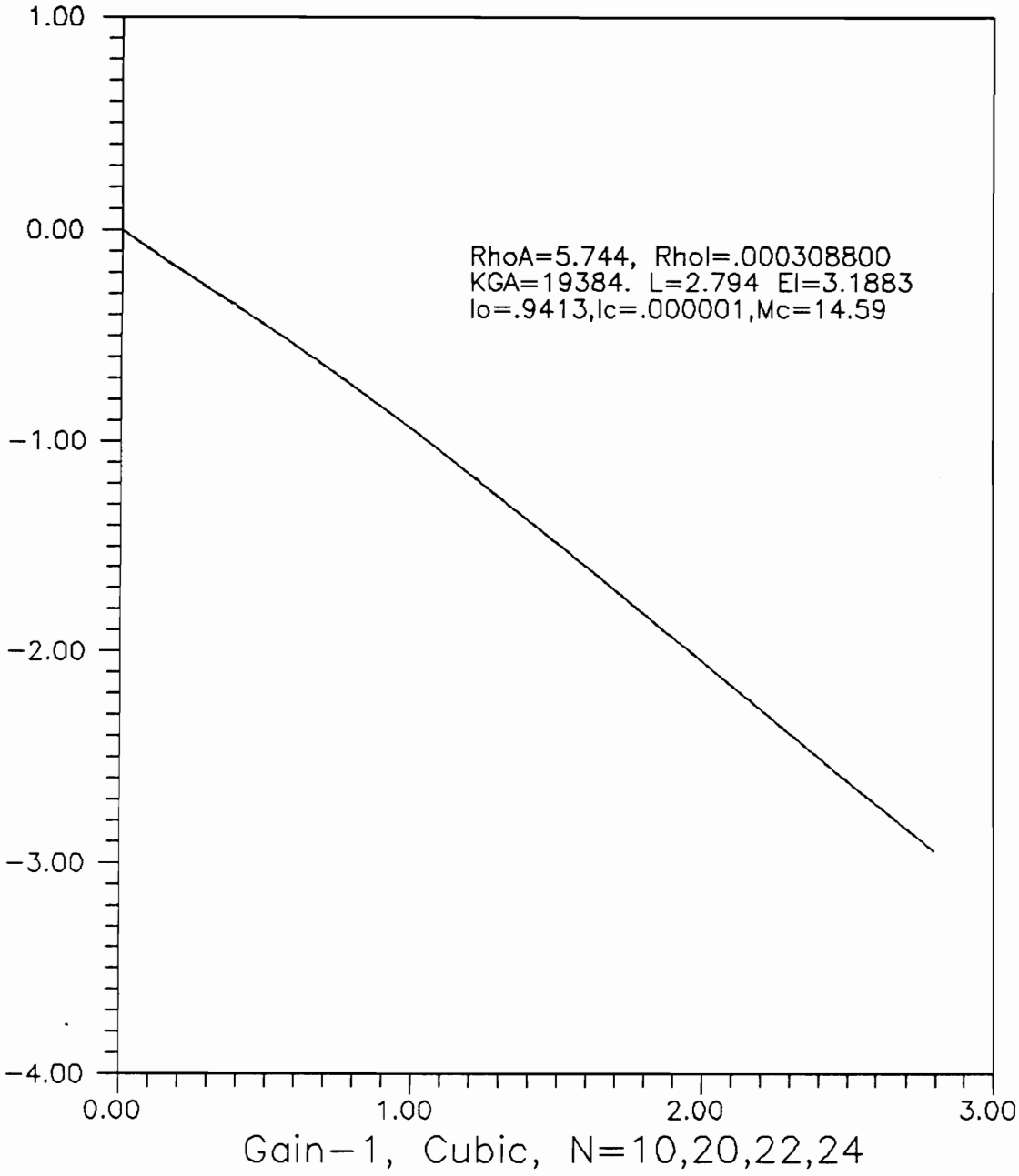

FIGURE 23. Functional Gain $\psi_f(x)$ vs x, Cubic

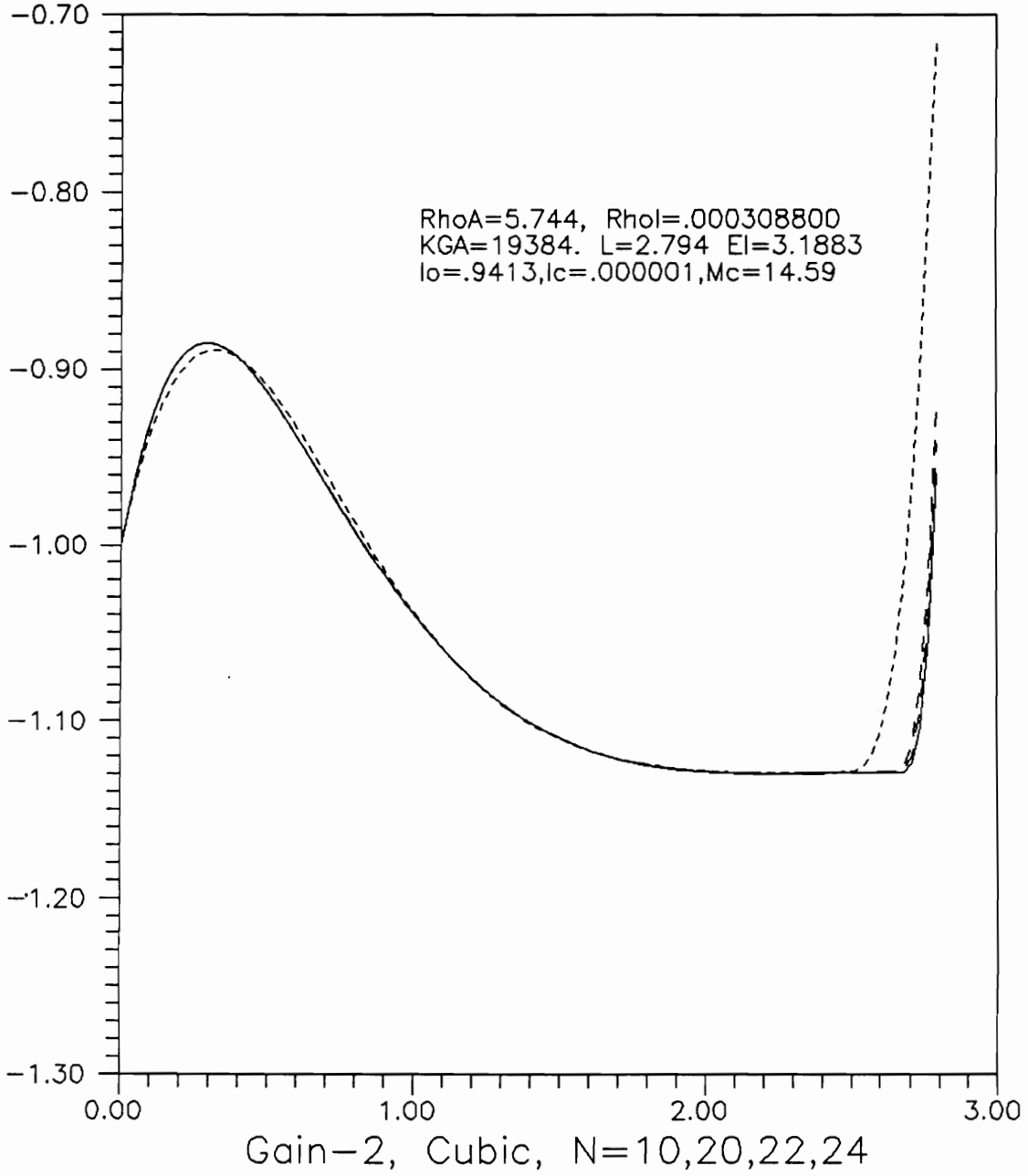

FIGURE 24. Functional Gain $\phi_f(x)$ vs x, Cubic

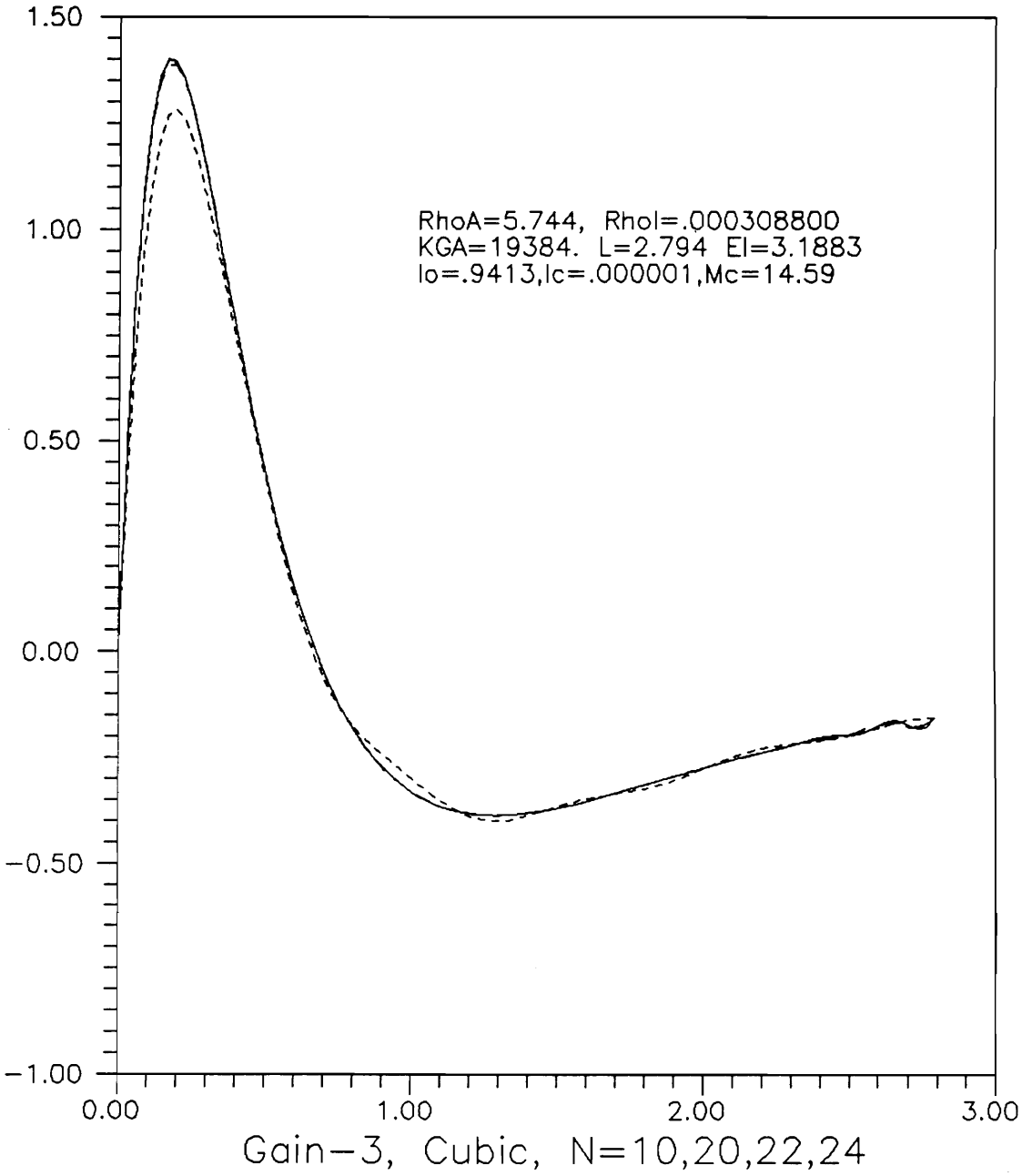

FIGURE 25. Functional Gain $K_4(x)$ vs x, Cubic

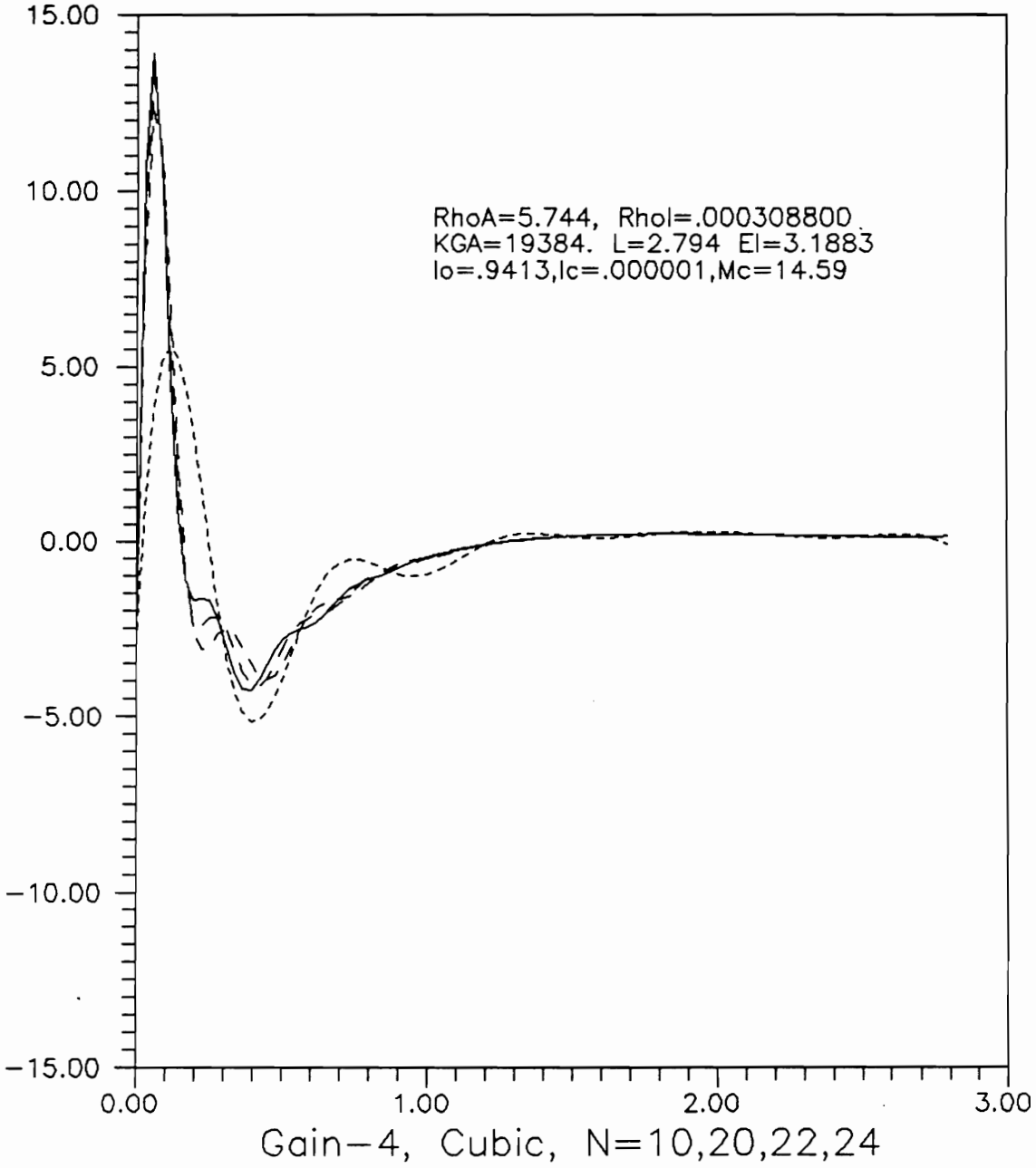

FIGURE 26. Functional Gain $K_5(x)$ vs x, Cubic

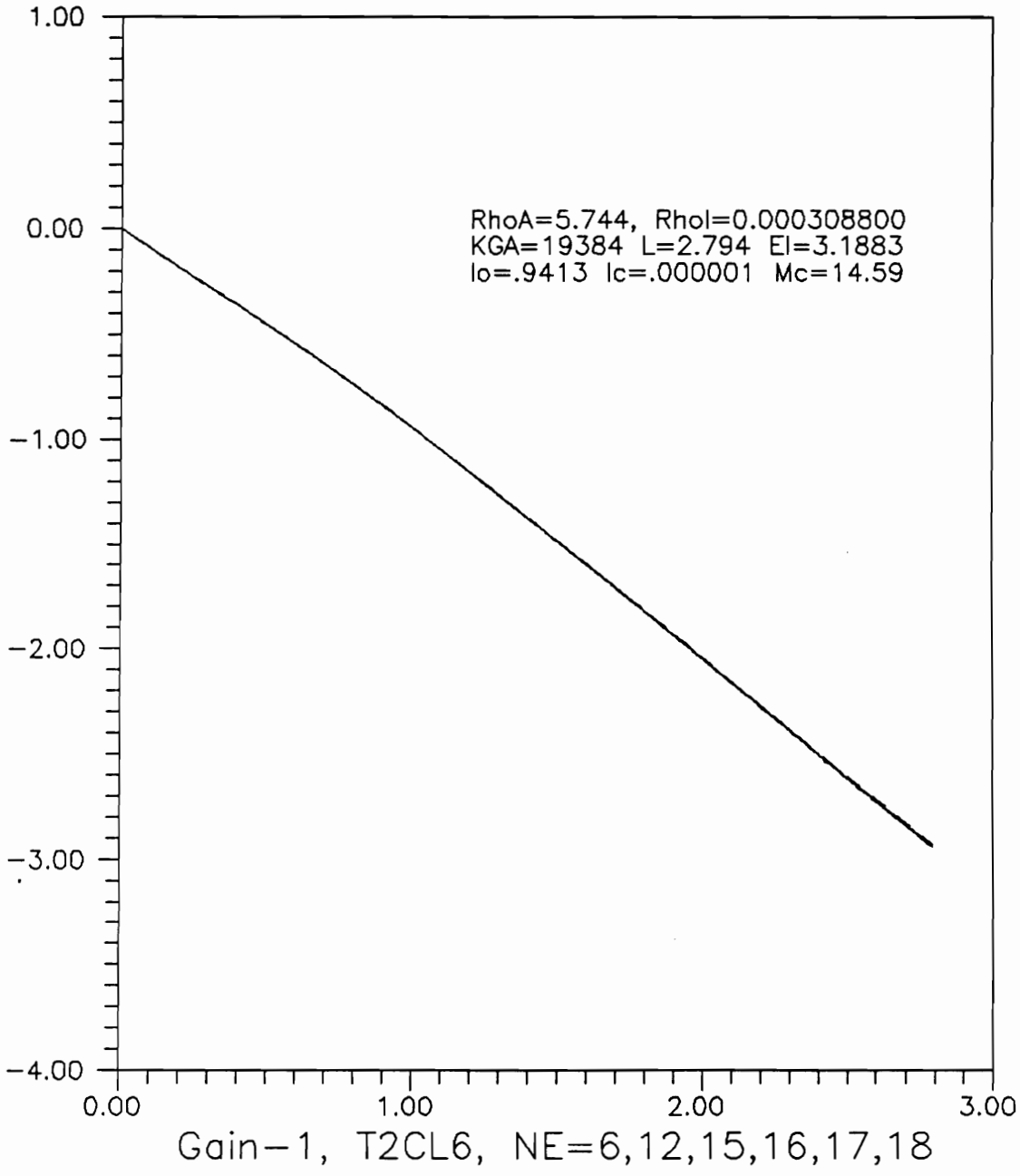

FIGURE 27. Functional Gain $\psi_f(x)$ vs x, T2CL6

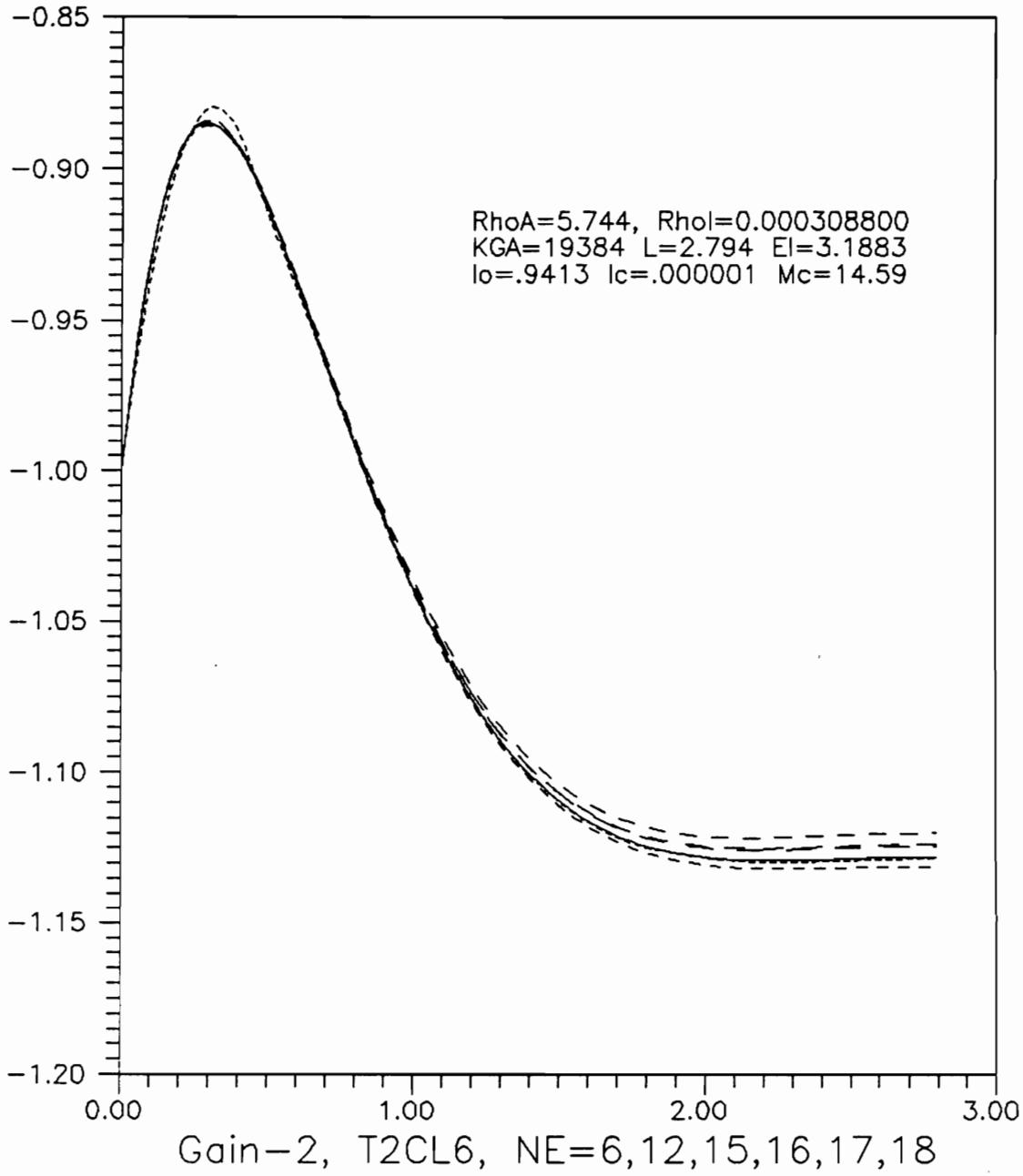

FIGURE 28. Functional Gain $\phi_f(x)$ vs x, T2CL6

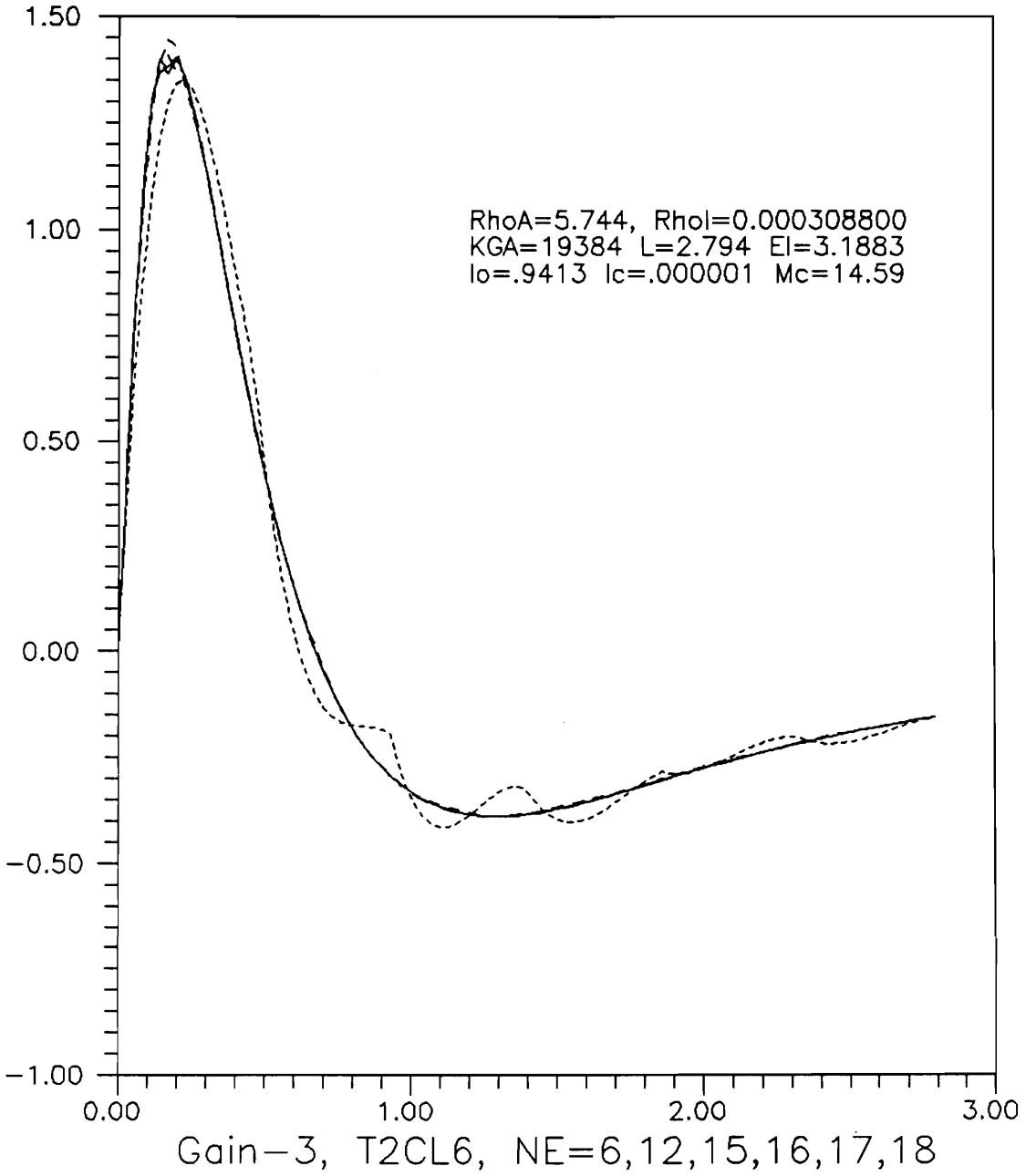

FIGURE 29. Functional Gain $K_4(x)$ vs x, T2CL6

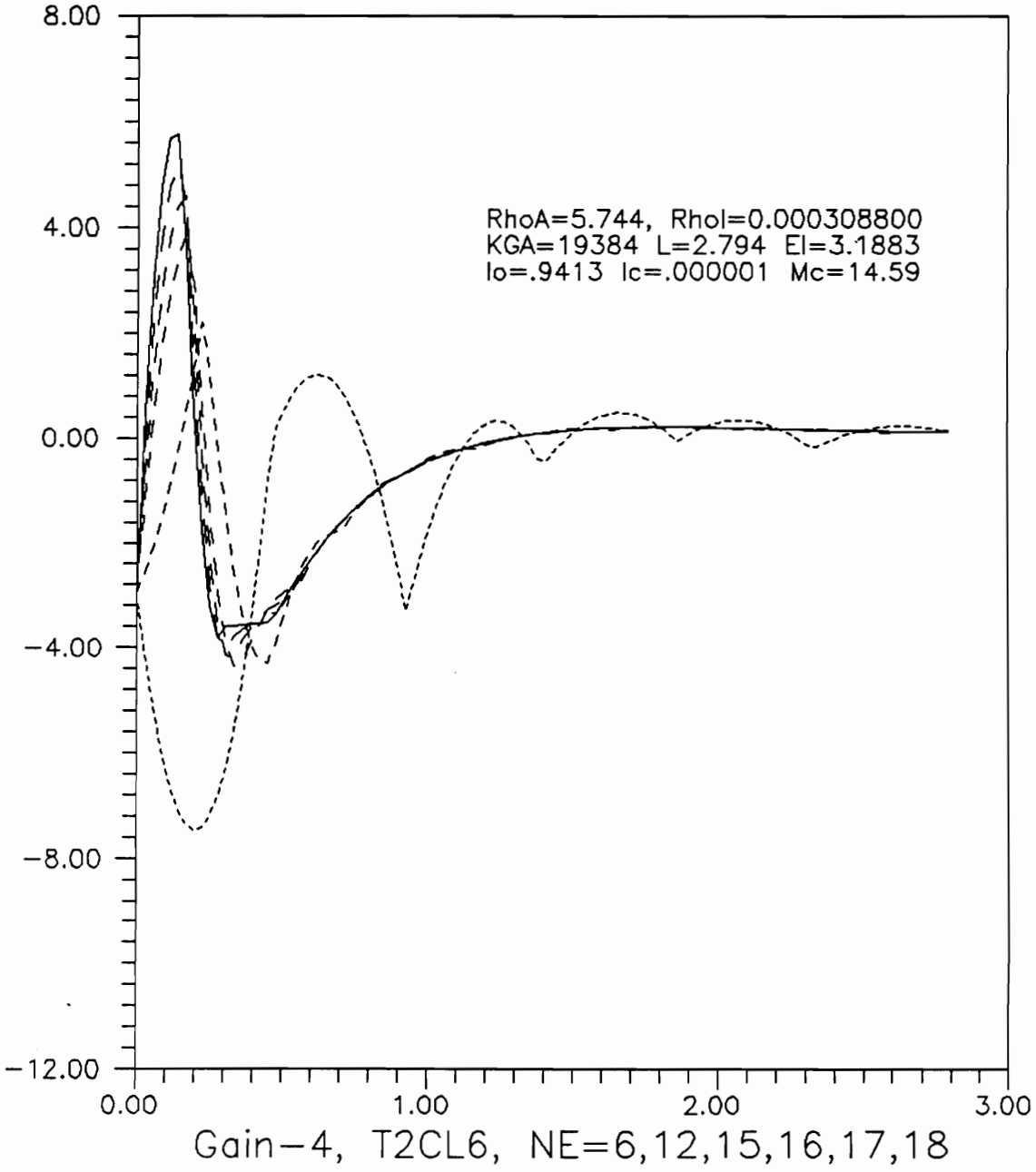

FIGURE 30. Functional Gain $K_5(x)$ vs x, T2CL6

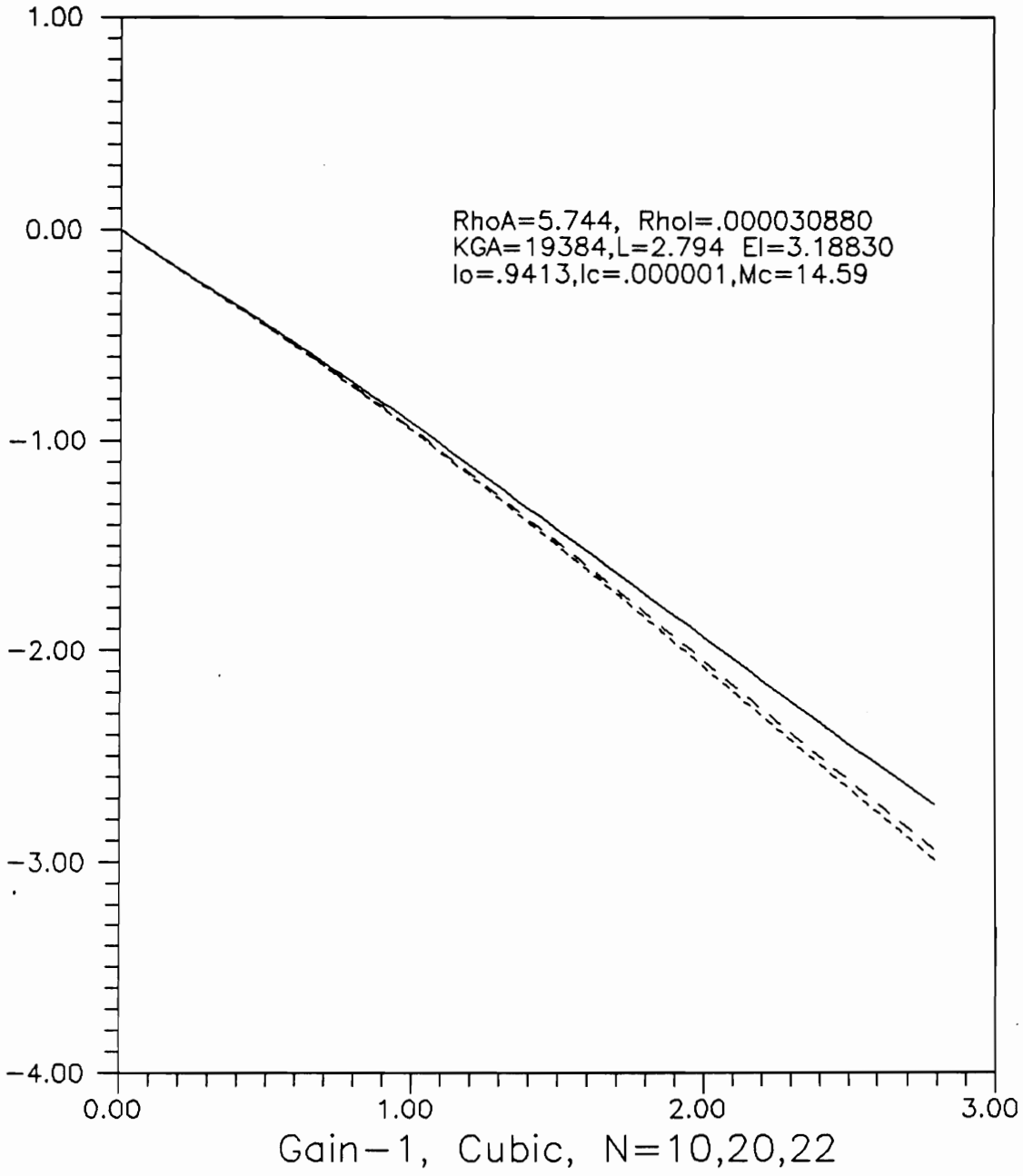

FIGURE 31. Functional Gain $\psi_f(x)$ vs x, Cubic

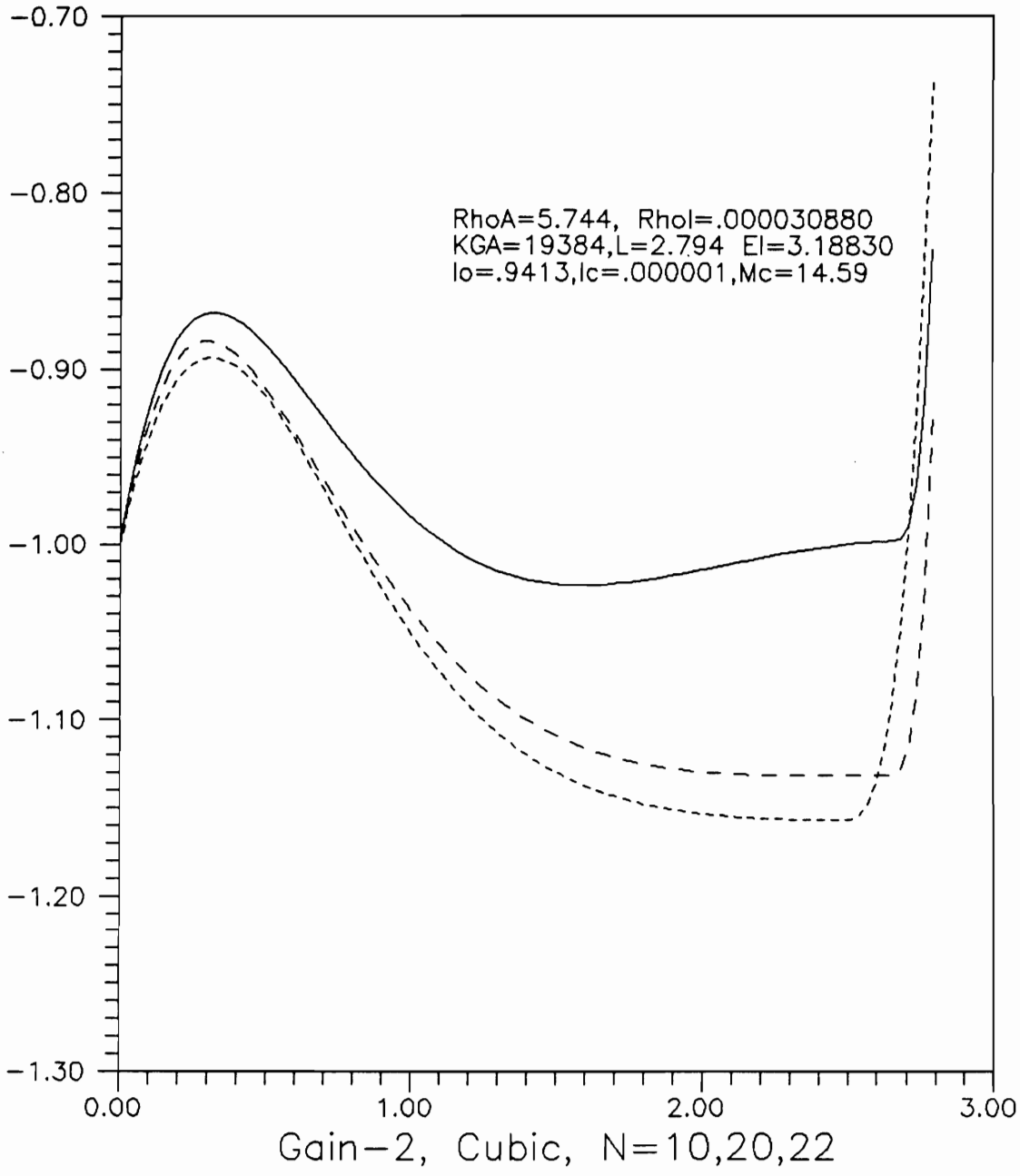

FIGURE 32. Functional Gain $\phi_f(x)$ vs x, Cubic

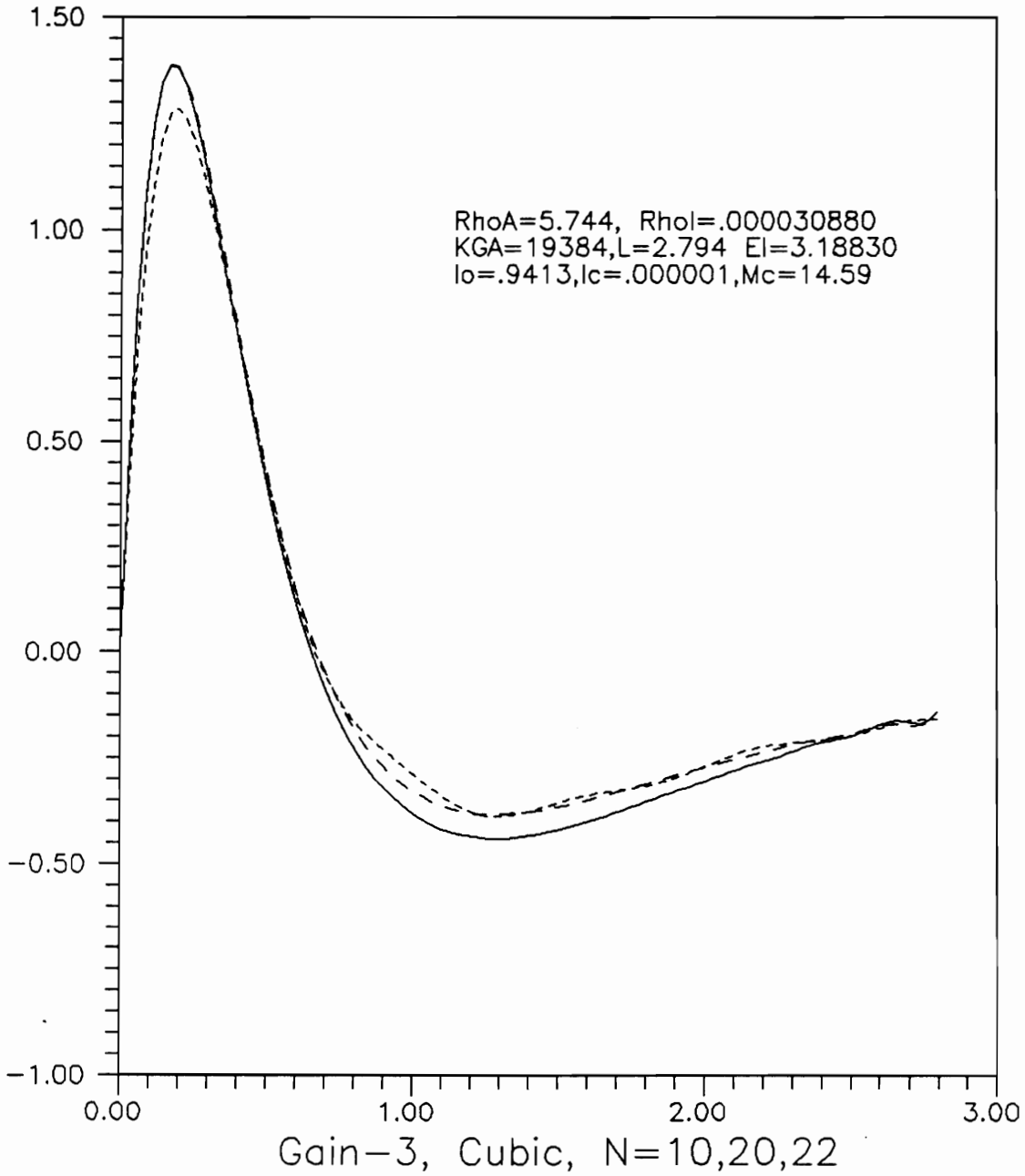

FIGURE 33. Functional Gain $K_4(x)$ vs x, Cubic

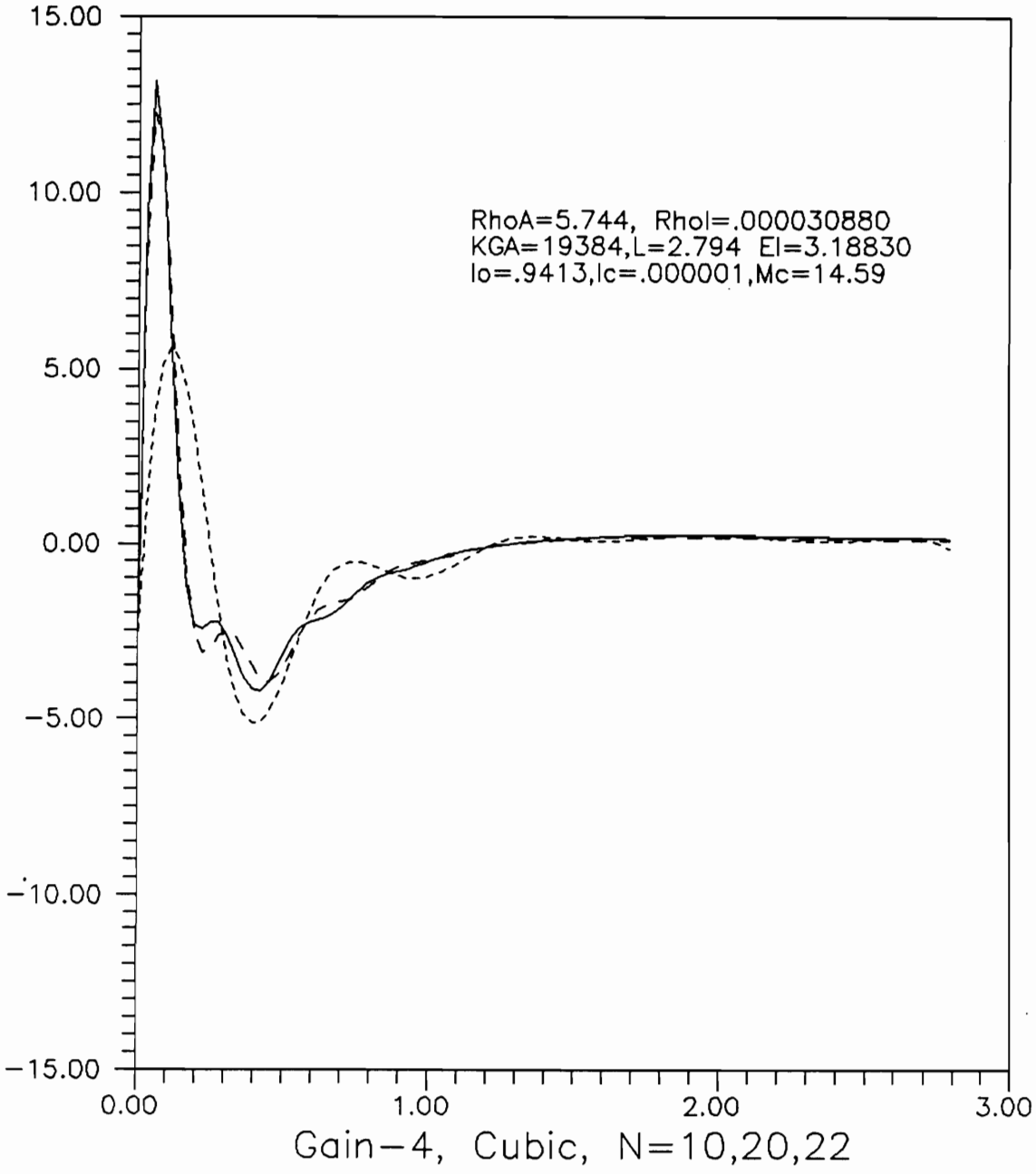

FIGURE 34. Functional Gain $K_5(x)$ vs x, Cubic

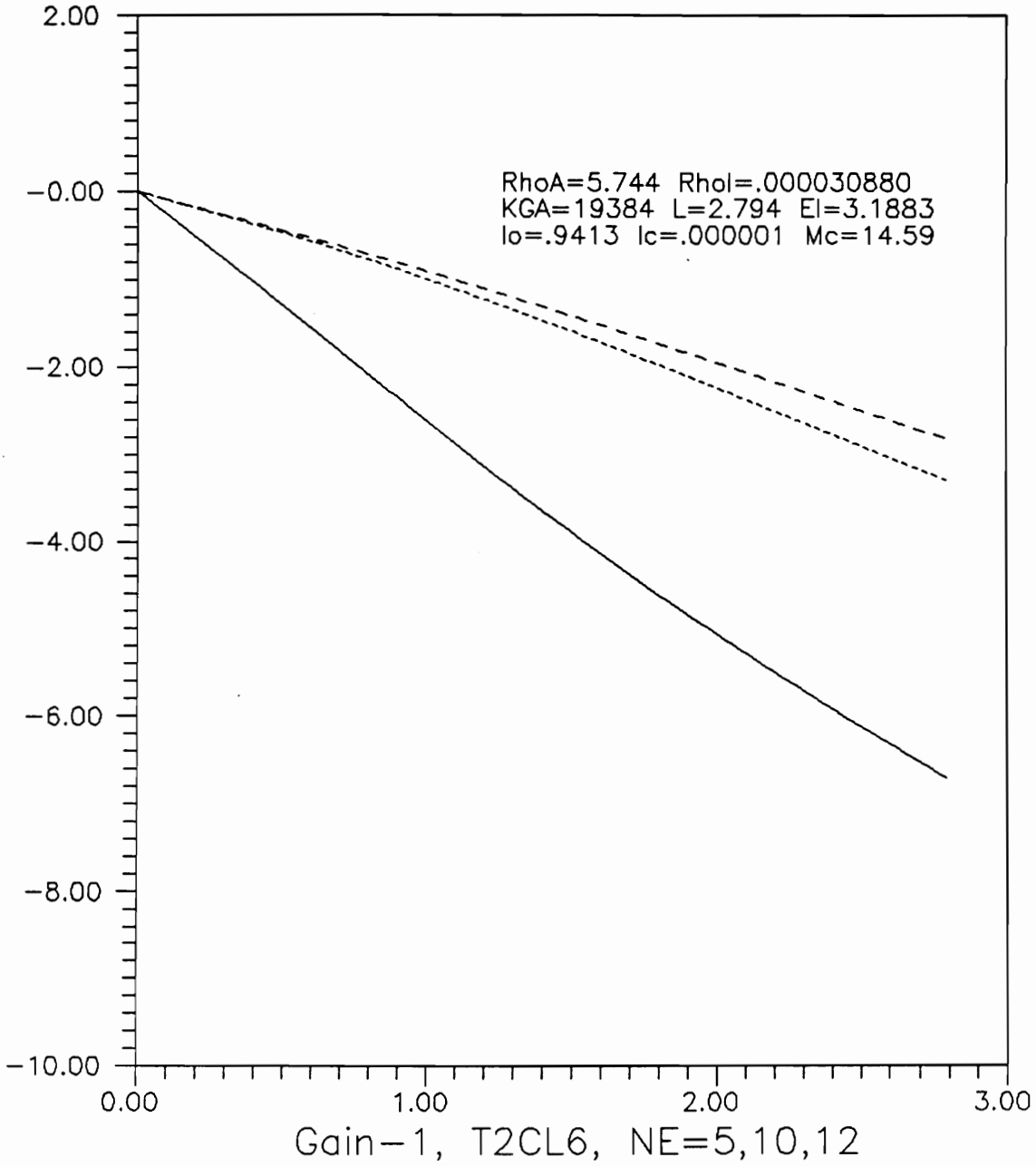

FIGURE 35. Functional Gain $\psi_f(x)$ vs x, T2CL6

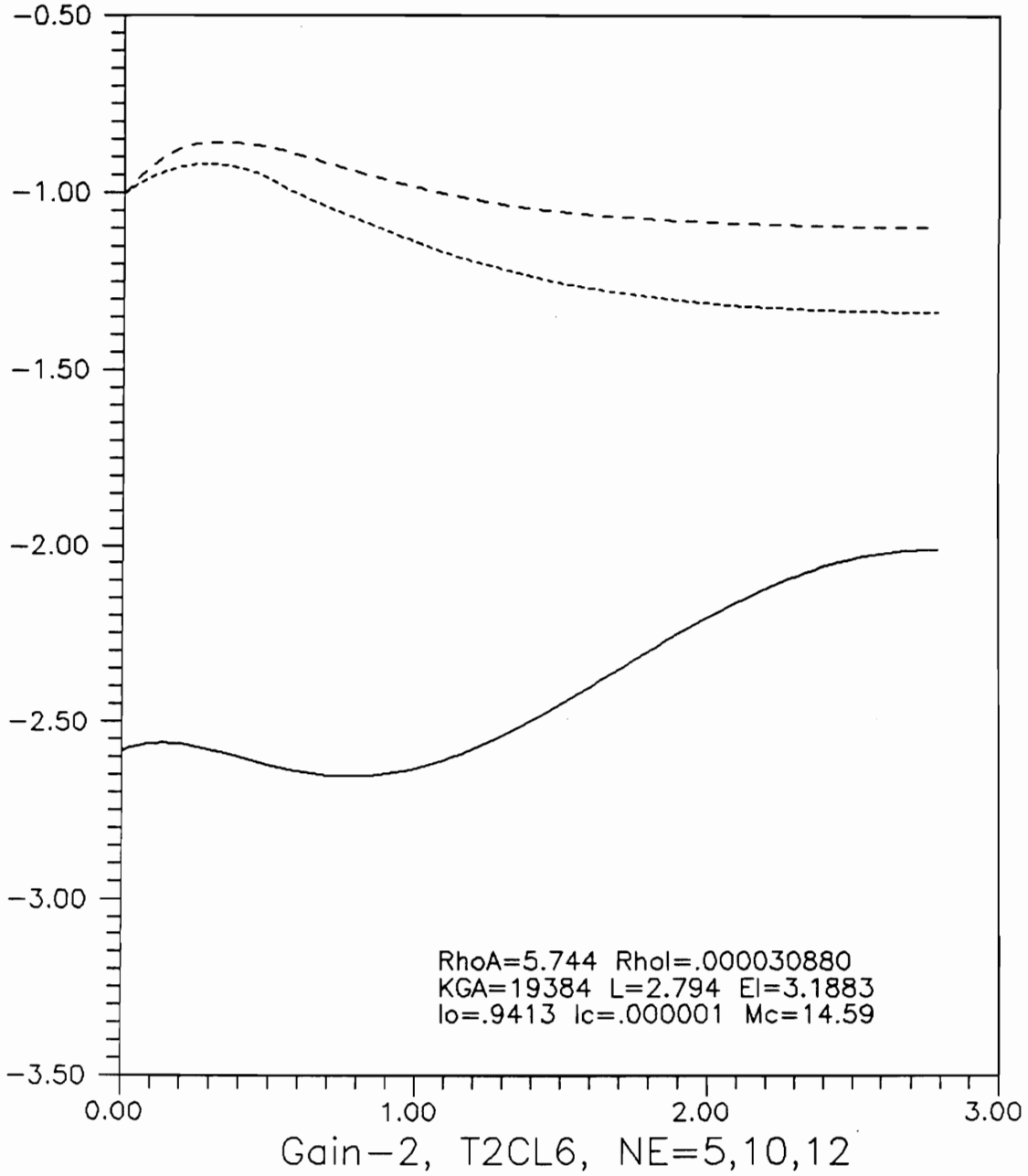

FIGURE 36. Functional Gain $\phi_f(x)$ vs x, T2CL6

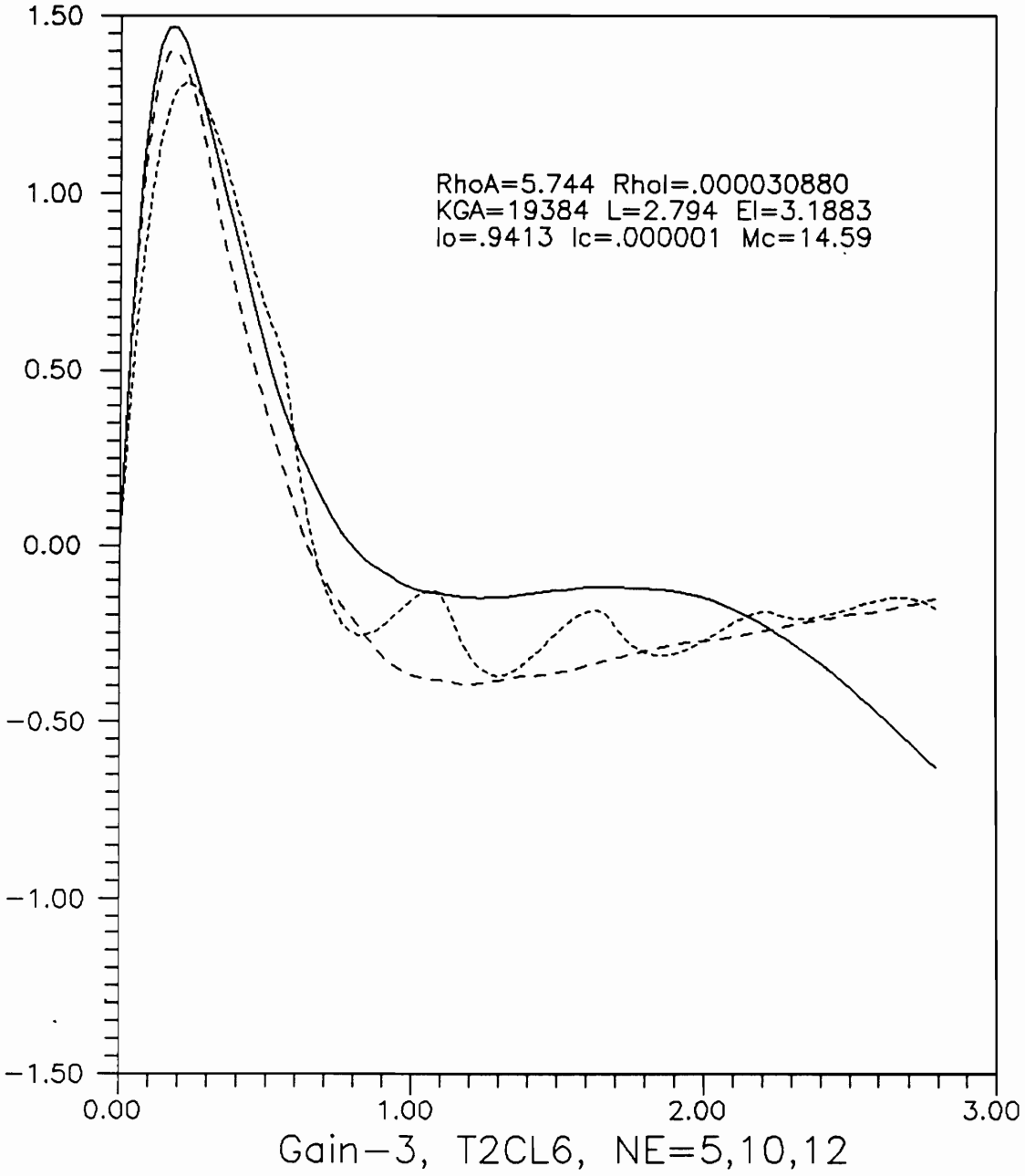

FIGURE 37. Functional Gain $K_4(x)$ vs x, T2CL6

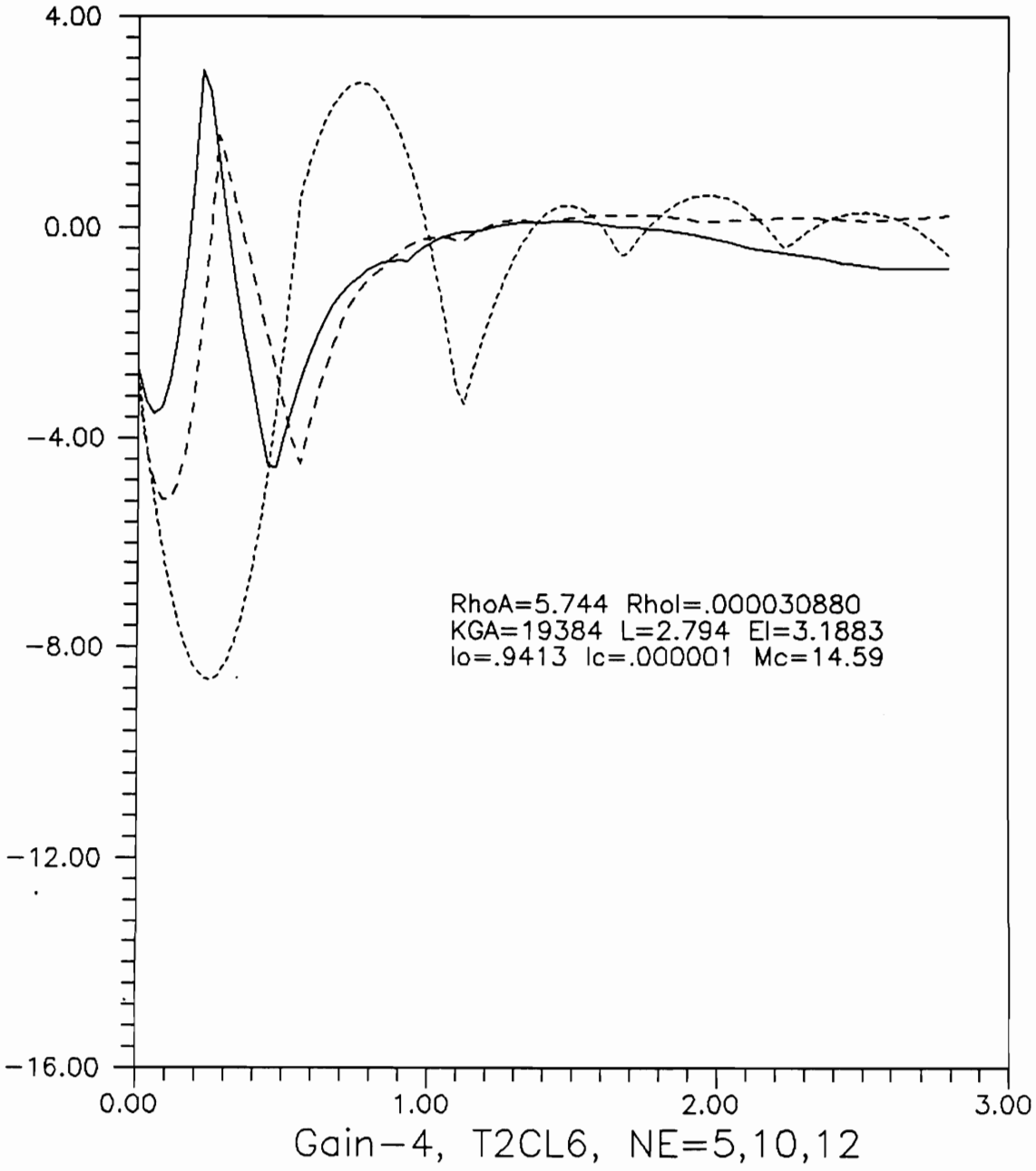

FIGURE 38. Functional Gain $K_5(x)$ vs x, T2CL6

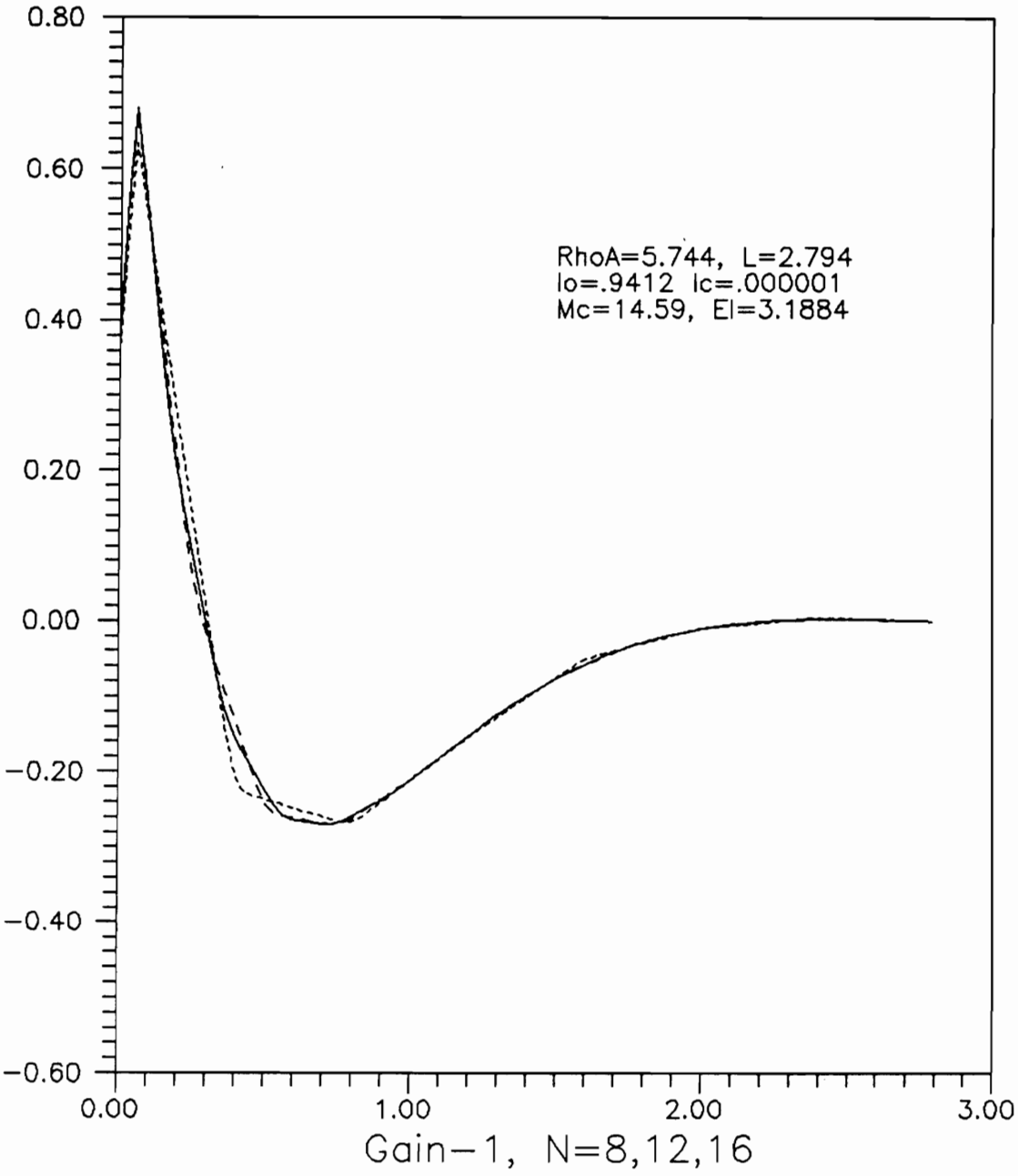

FIGURE 39. Functional Gain Bending, Euler-Bernoulli

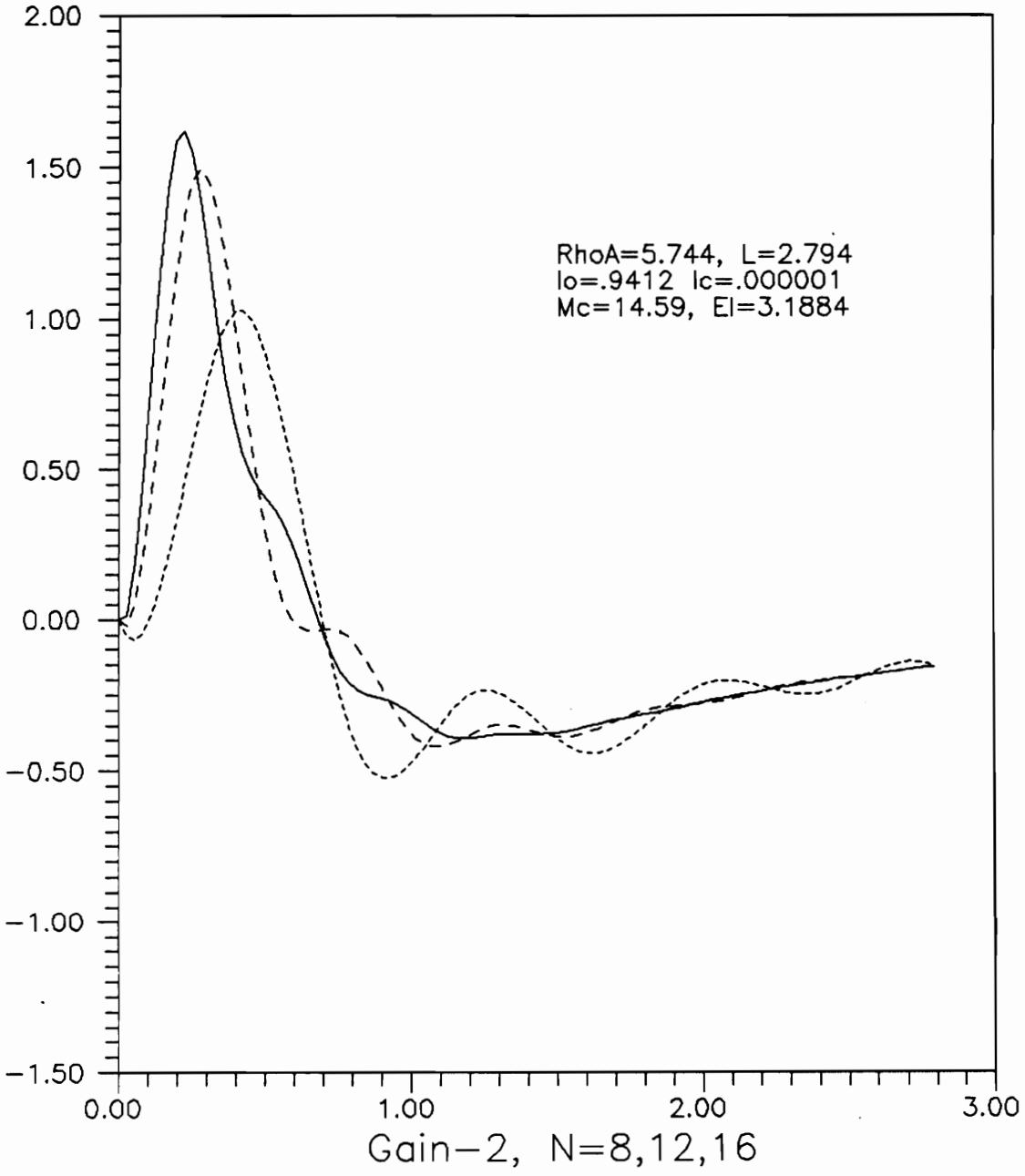

FIGURE 40. Functional Gain Velocity, Euler-Bernoulli

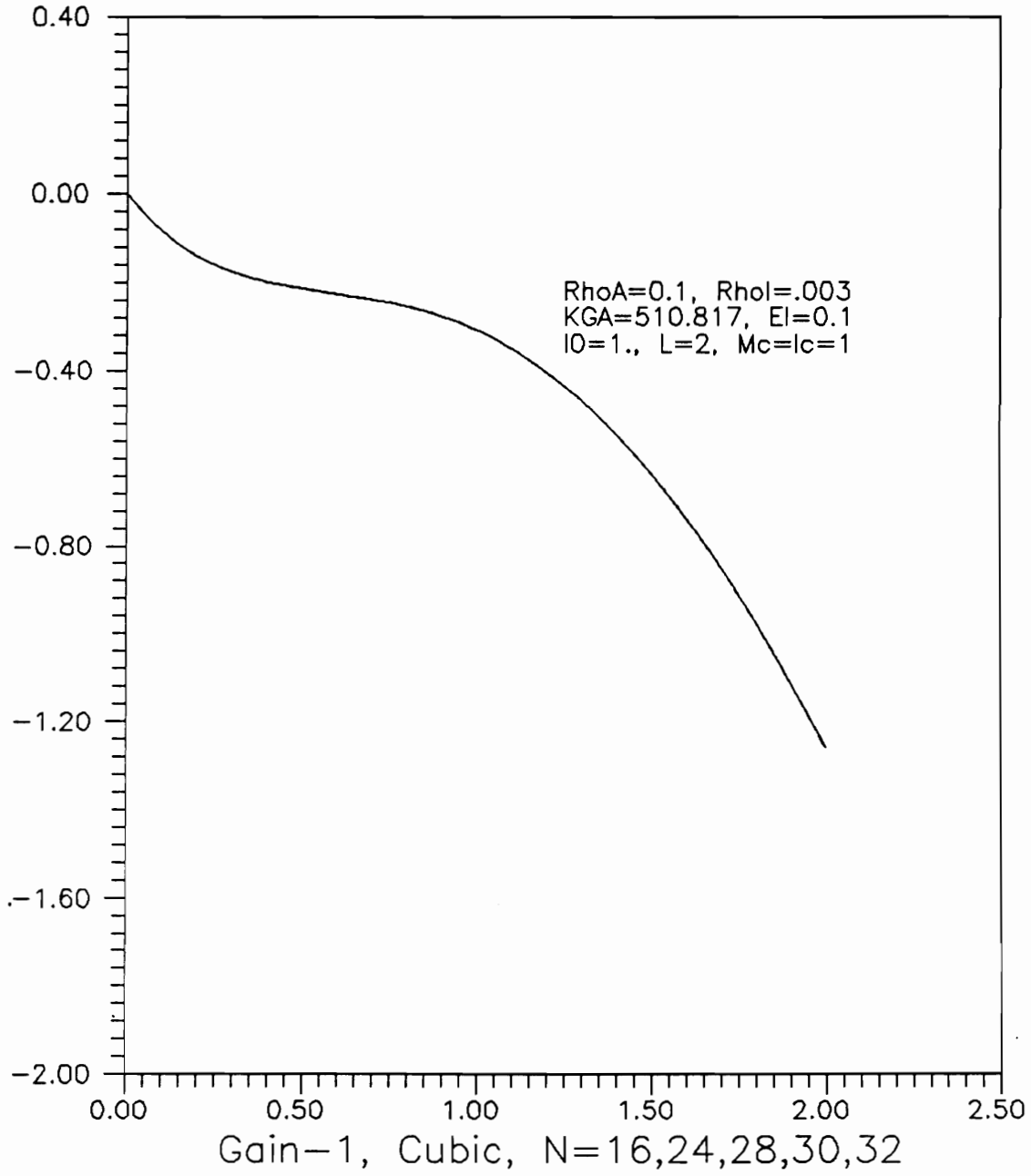

FIGURE 41. Functional Gain $\psi_f(x)$ vs x, Cubic

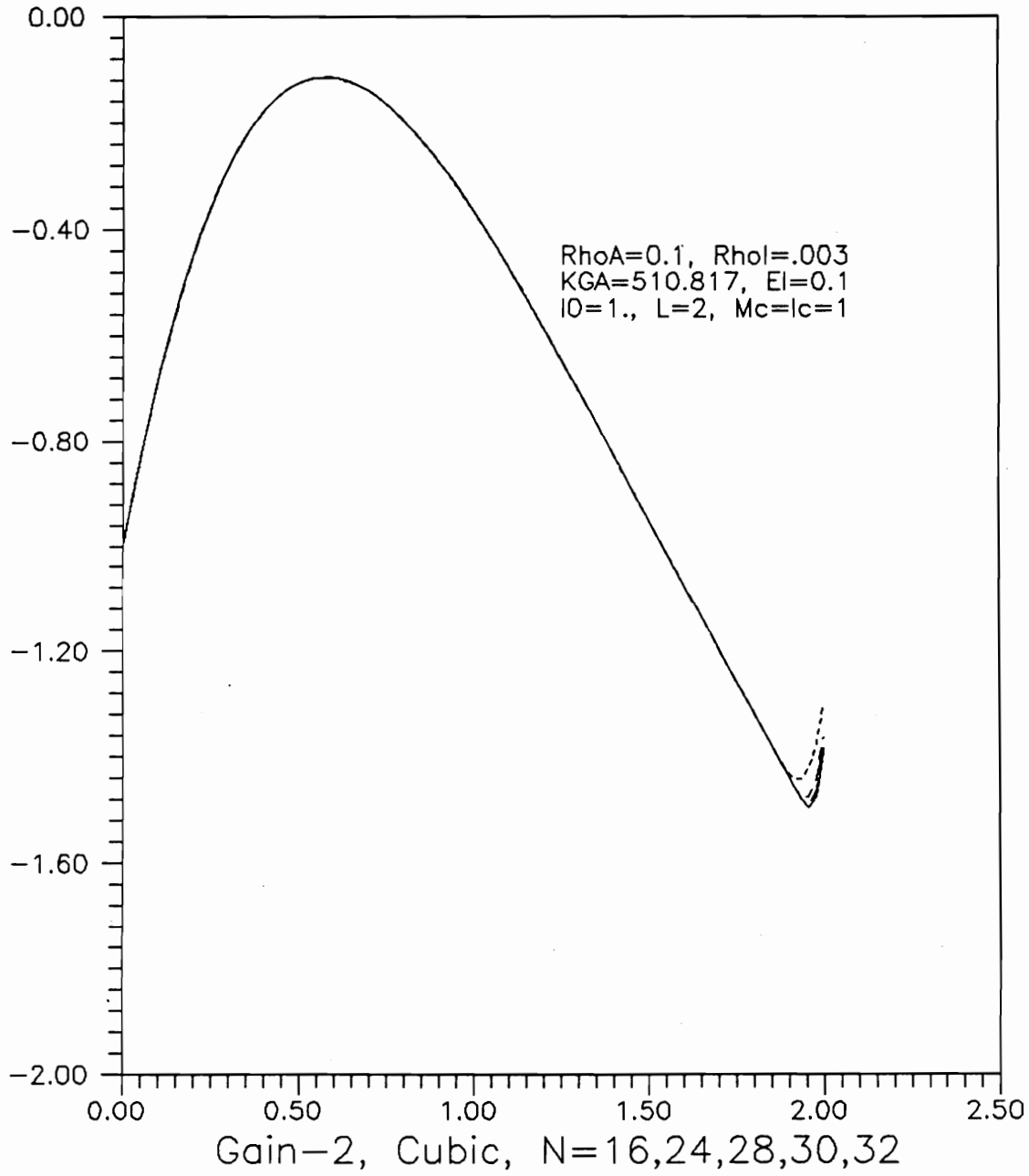

FIGURE 42. Functional Gain $\phi_f(x)$ vs x, Cubic

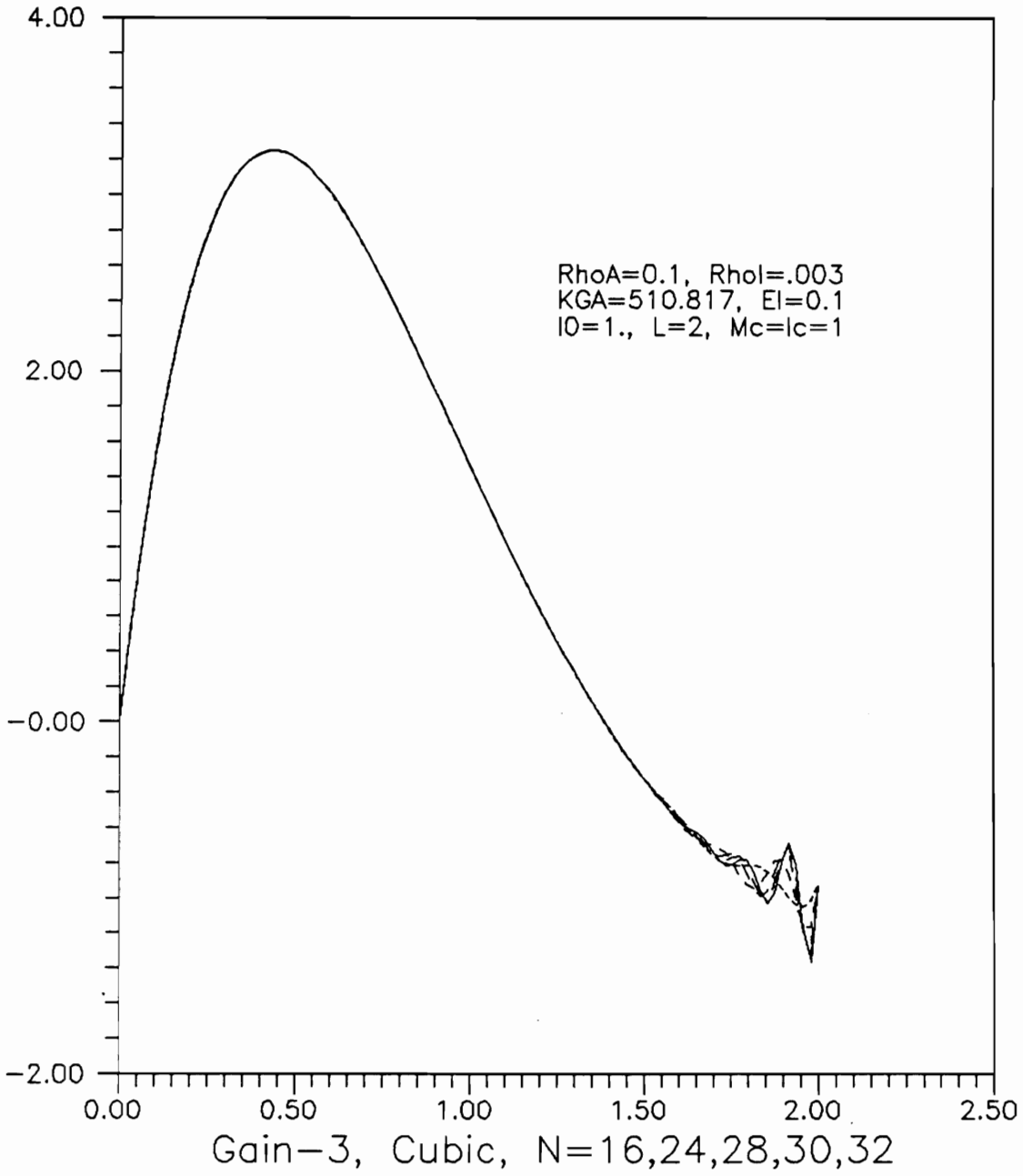

FIGURE 43. Functional Gain $K_4(x)$ vs x, Cubic

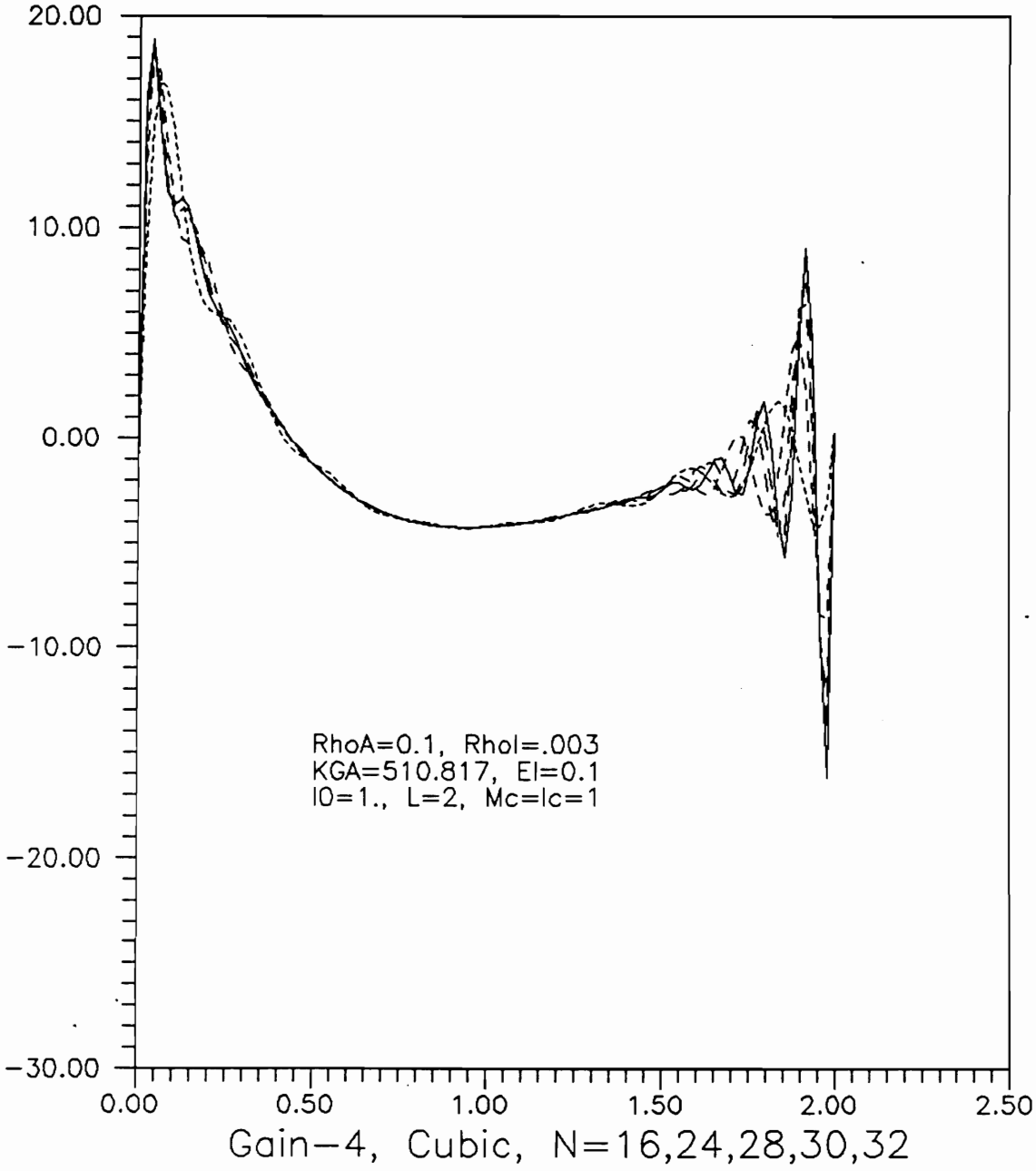

FIGURE 44. Functional Gain $K_5(x)$ vs x, Cubic

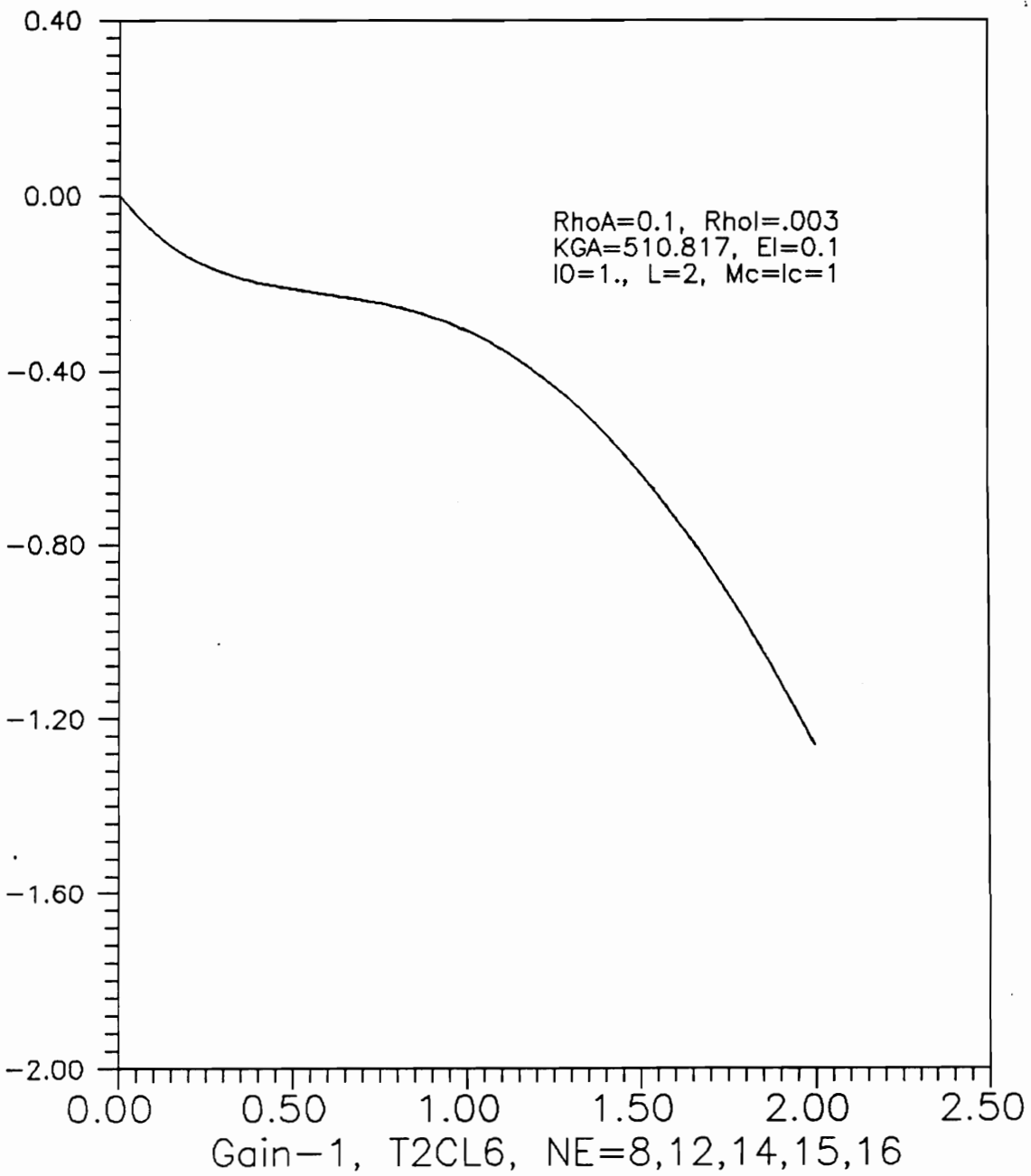

FIGURE 45. Functional Gain $\psi_f(x)$ vs x, T2CL6

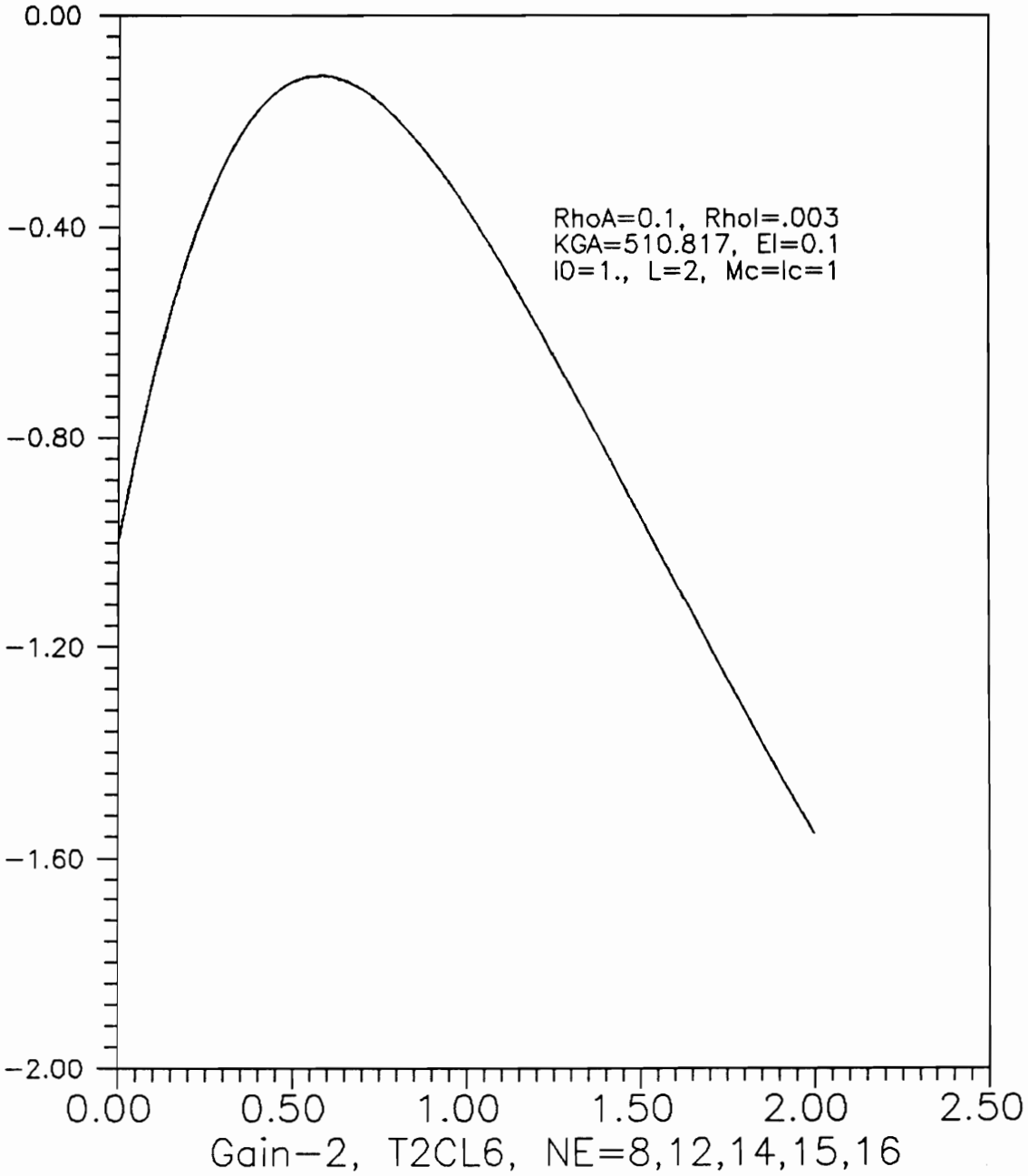

FIGURE 46. Functional Gain $\phi_f(x)$ vs x, T2CL6

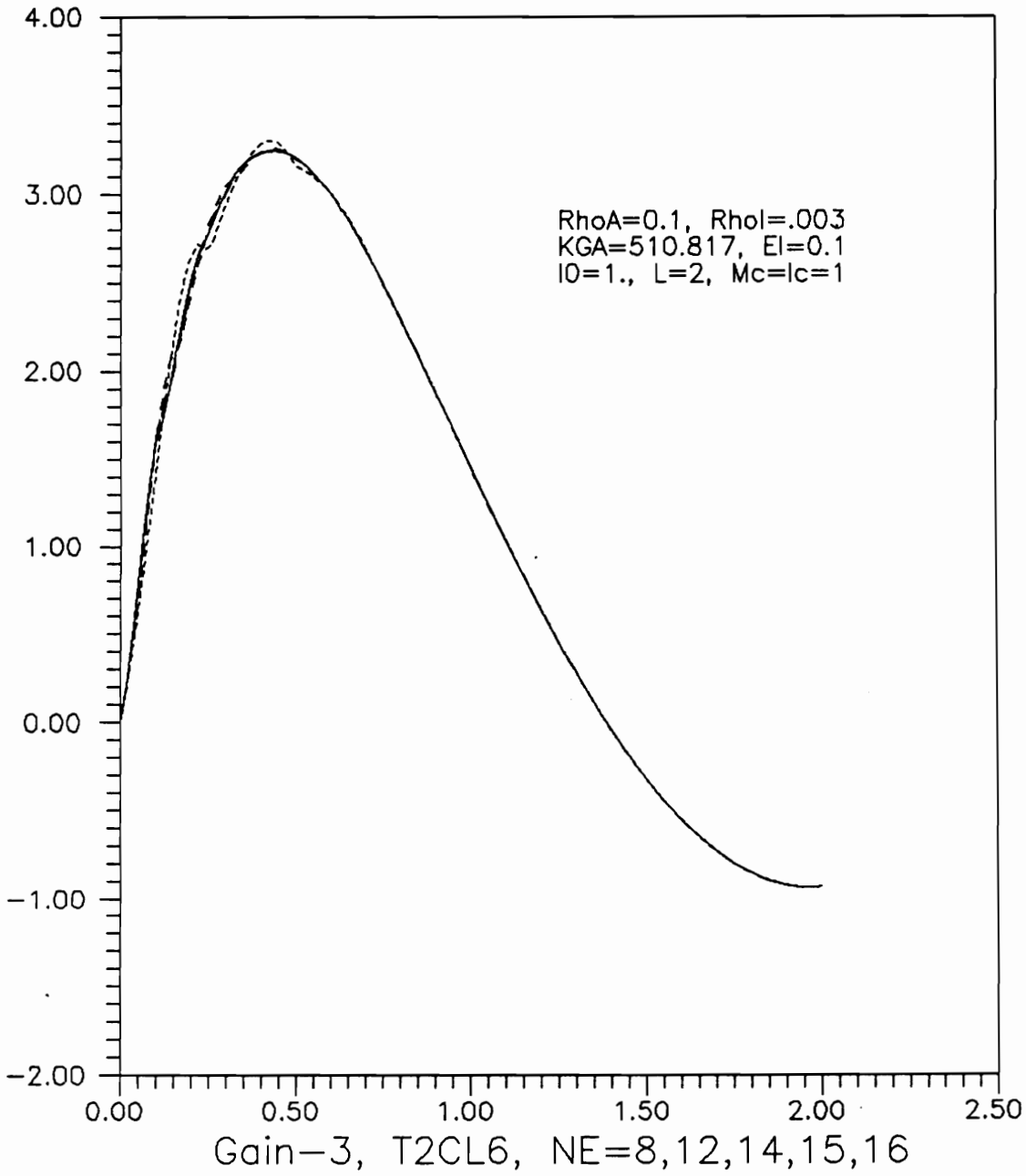

FIGURE 47. Functional Gain $K_4(x)$ vs x, T2CL6

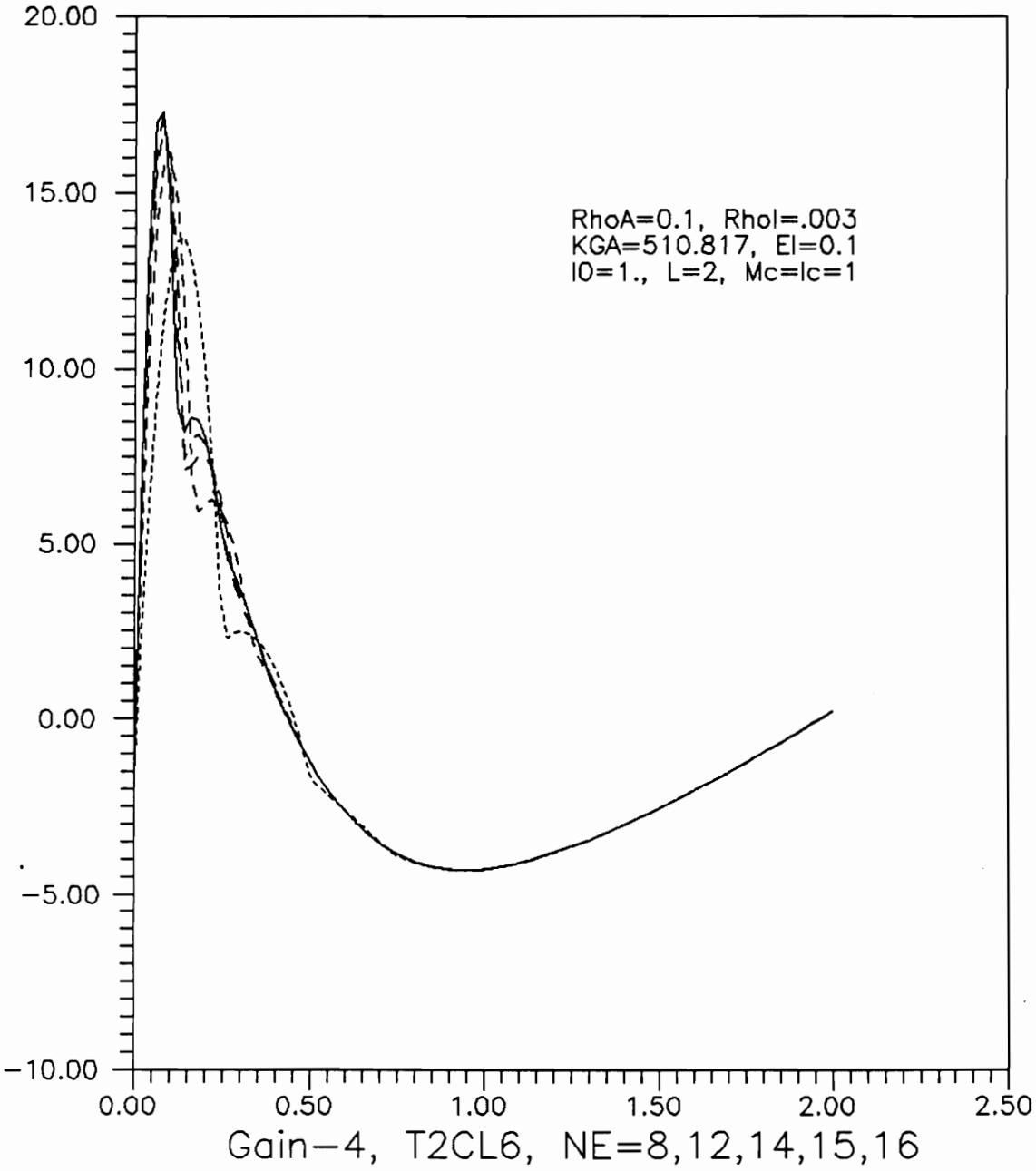

FIGURE 48. Functional Gain $K_5(x)$ vs x, T2CL6

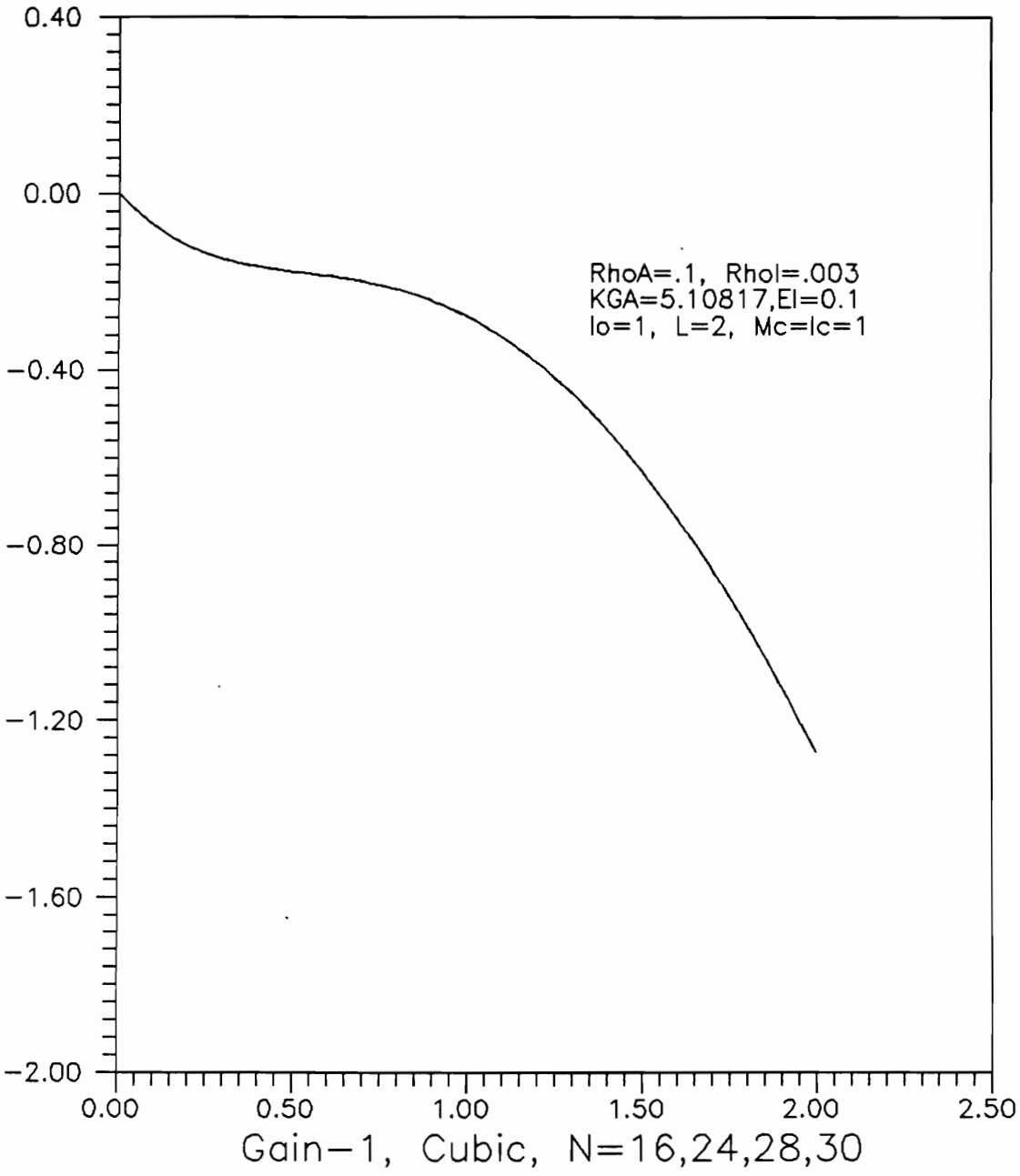

FIGURE 49. Functional Gain $\psi_f(x)$ vs x, Cubic

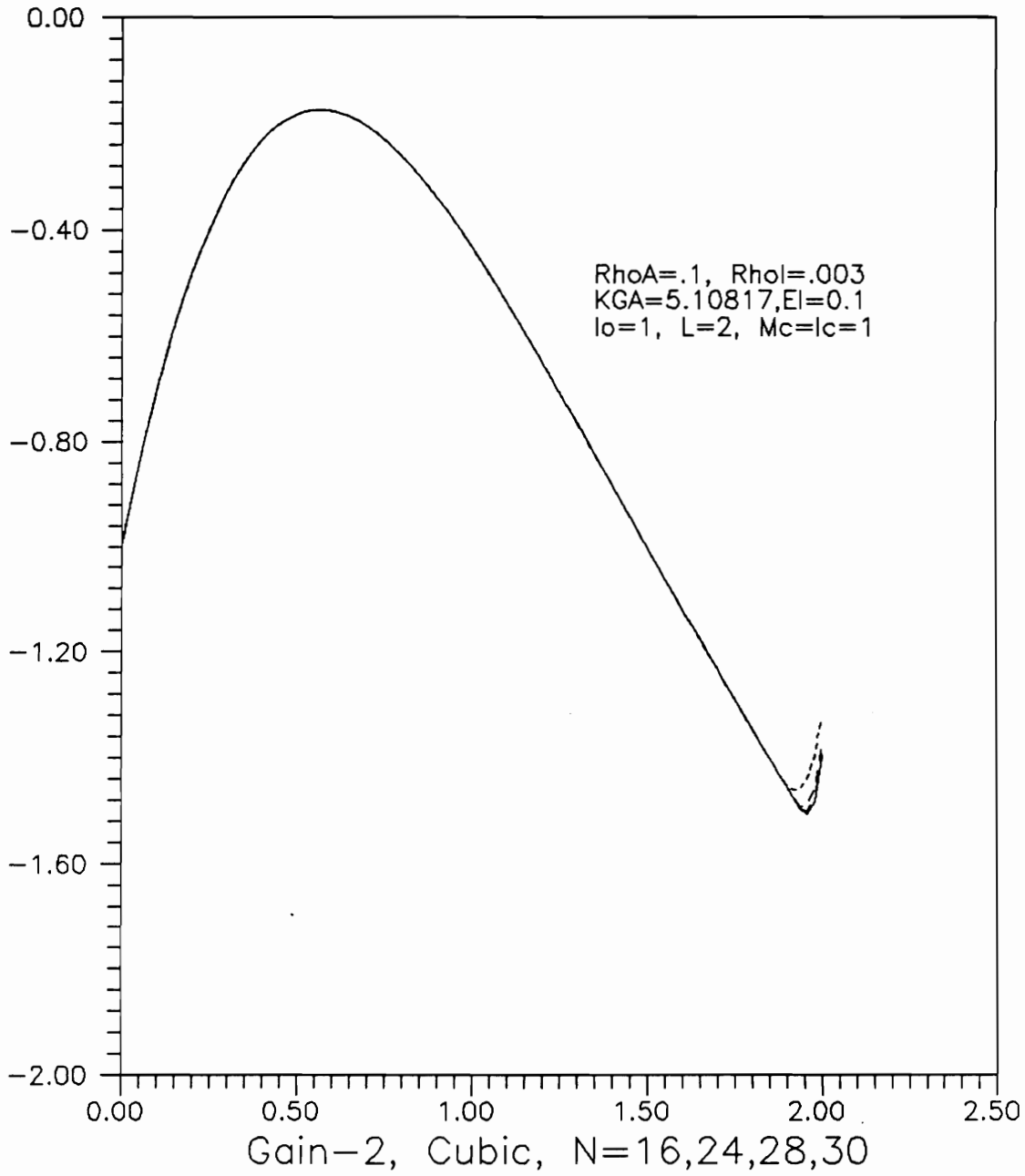

FIGURE 50. Functional Gain $\phi_f(x)$ vs x, Cubic

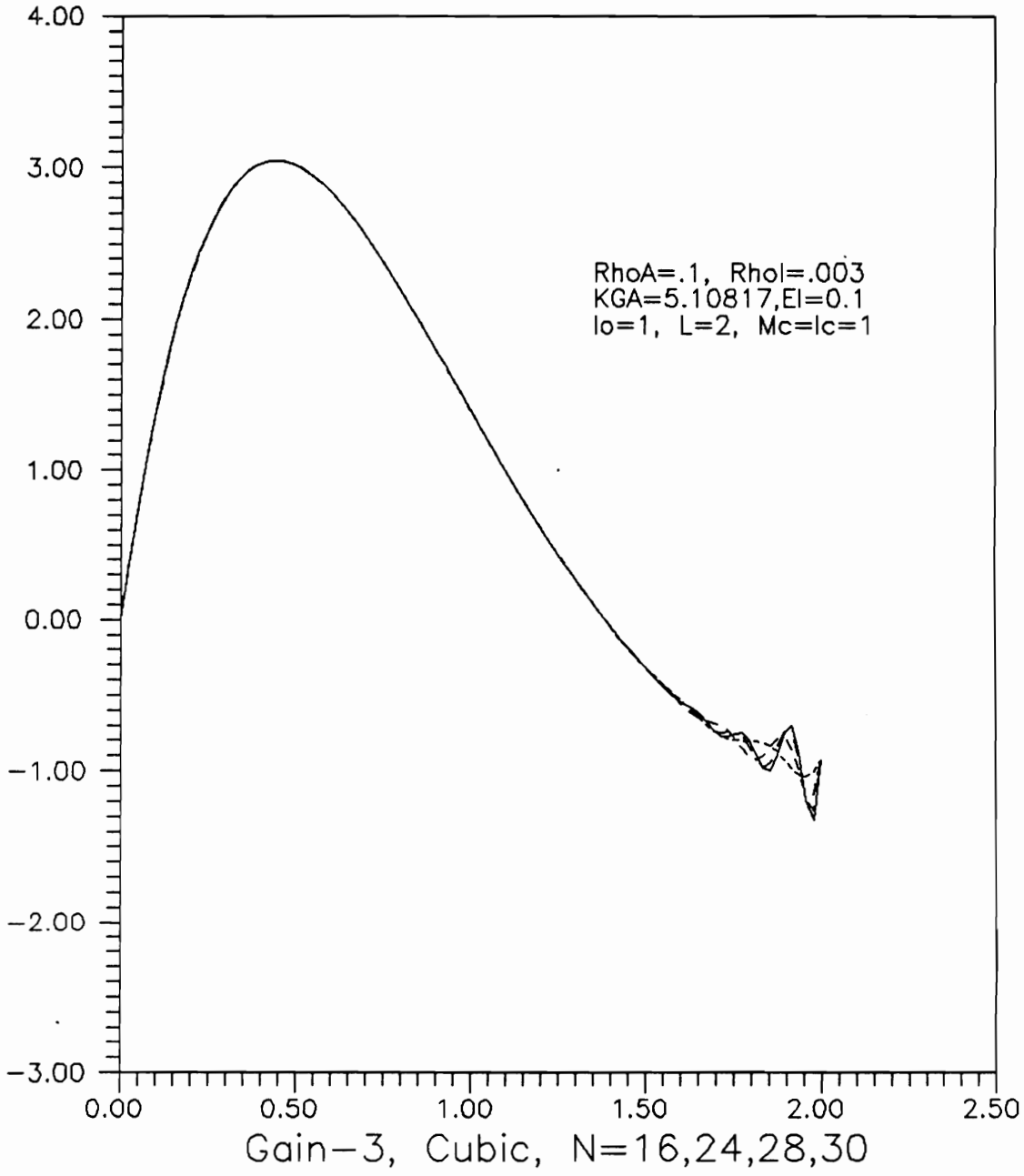

FIGURE 51. Functional Gain $K_4(x)$ vs x, Cubic

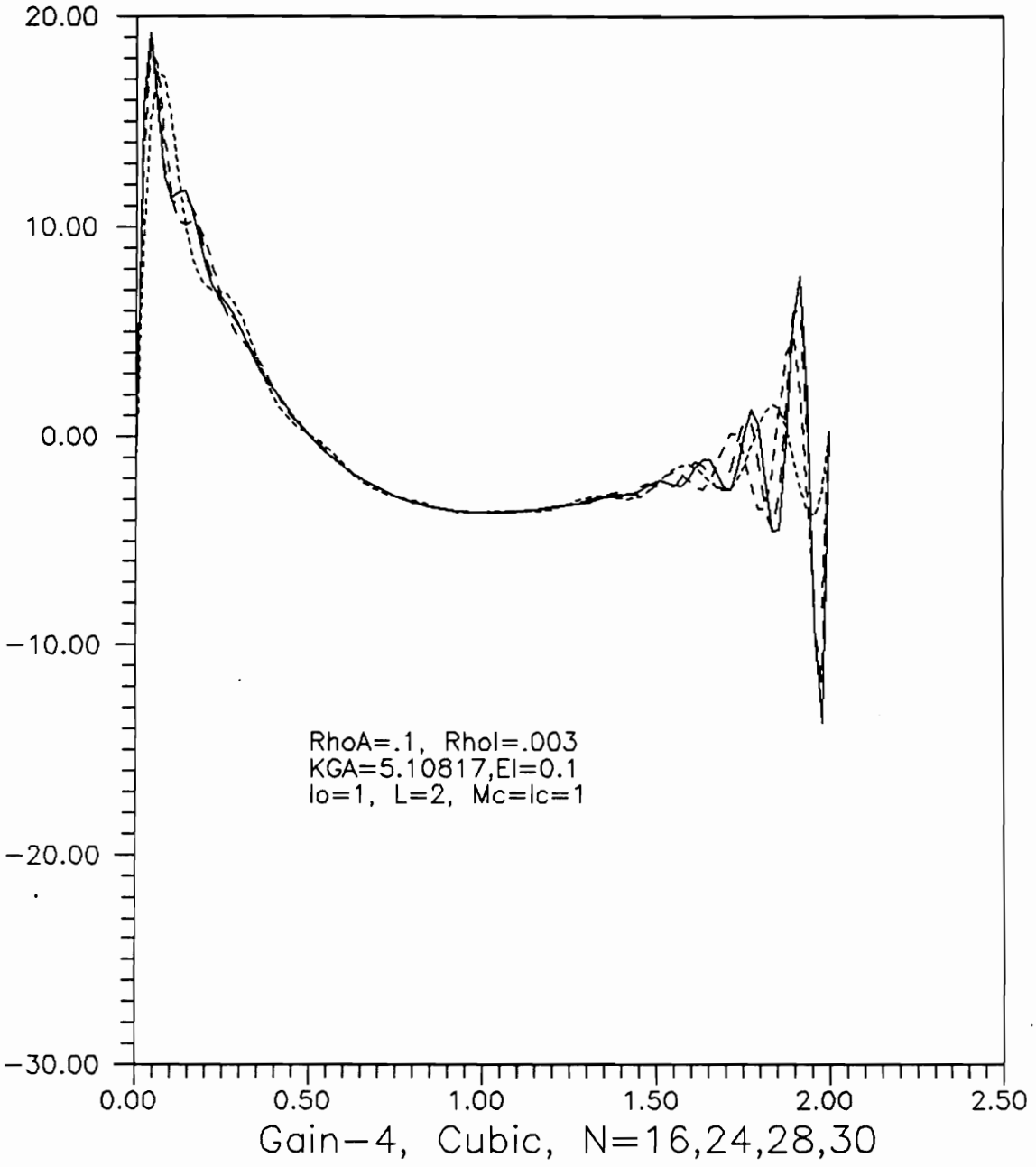

FIGURE 52. Functional Gain $K_5(x)$ vs x, Cubic

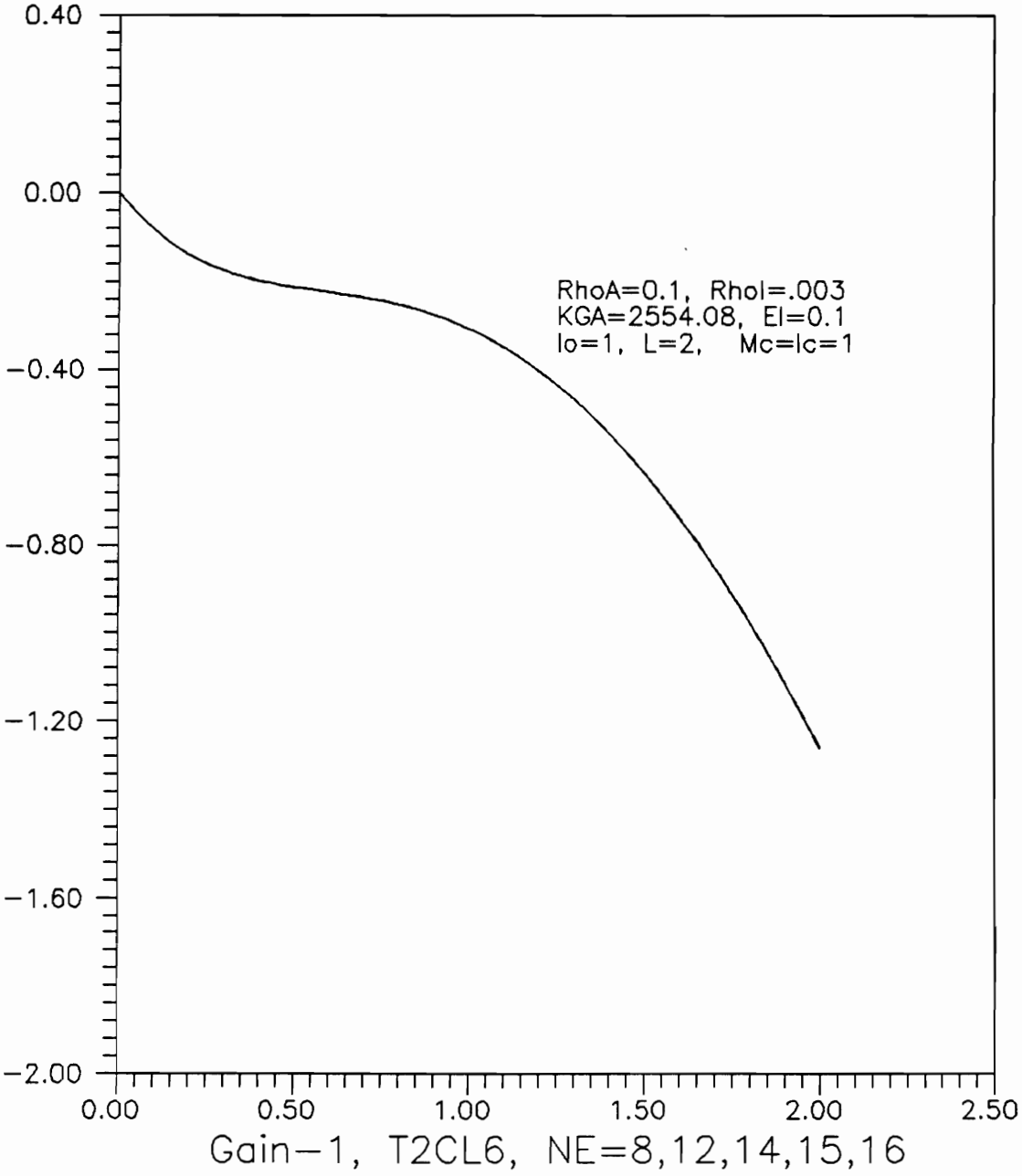

FIGURE 53. Functional Gain $\psi_f(x)$ vs x, T2CL6

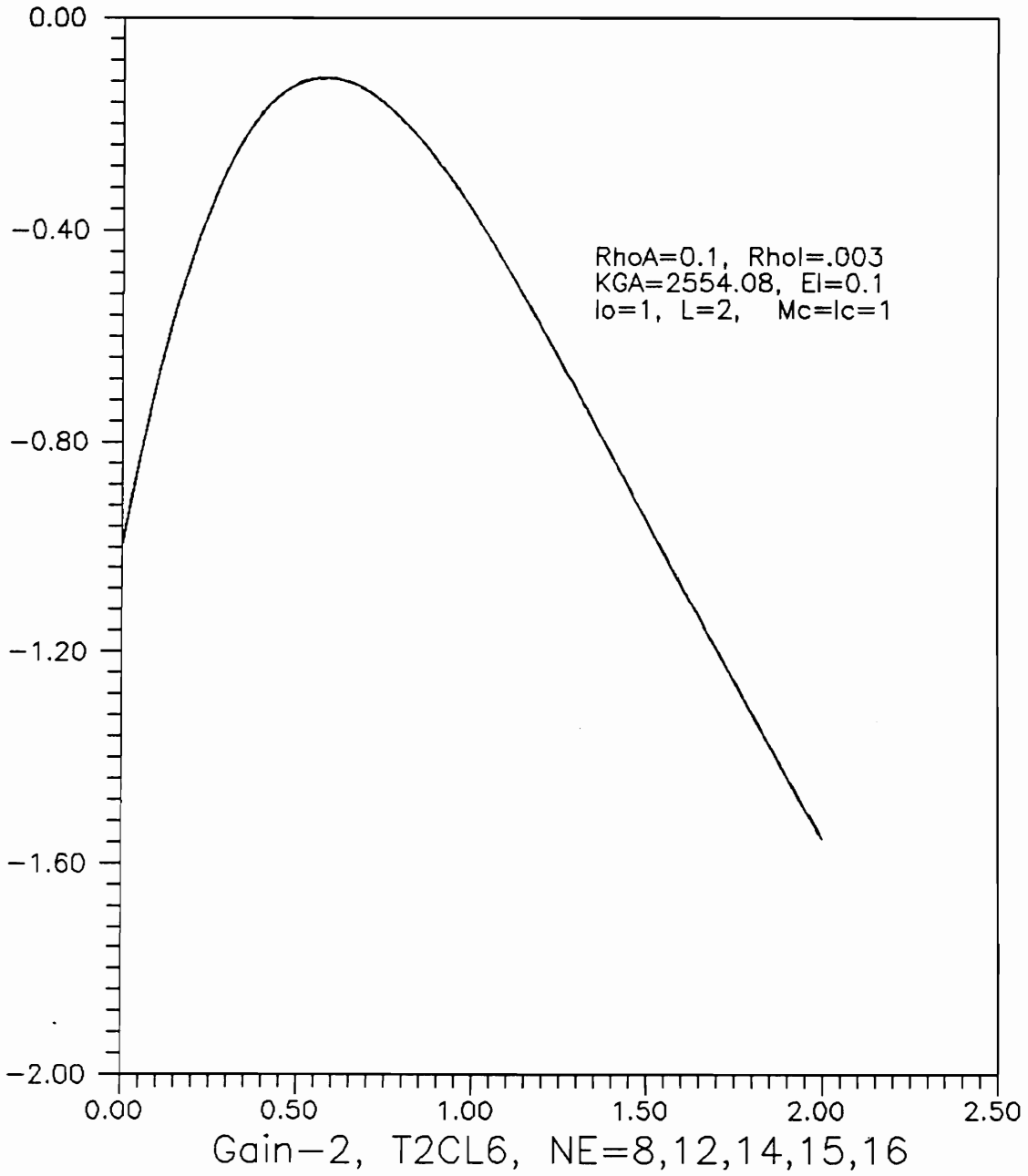

FIGURE 54. Functional Gain $\phi_f(x)$ vs x, T2CL6

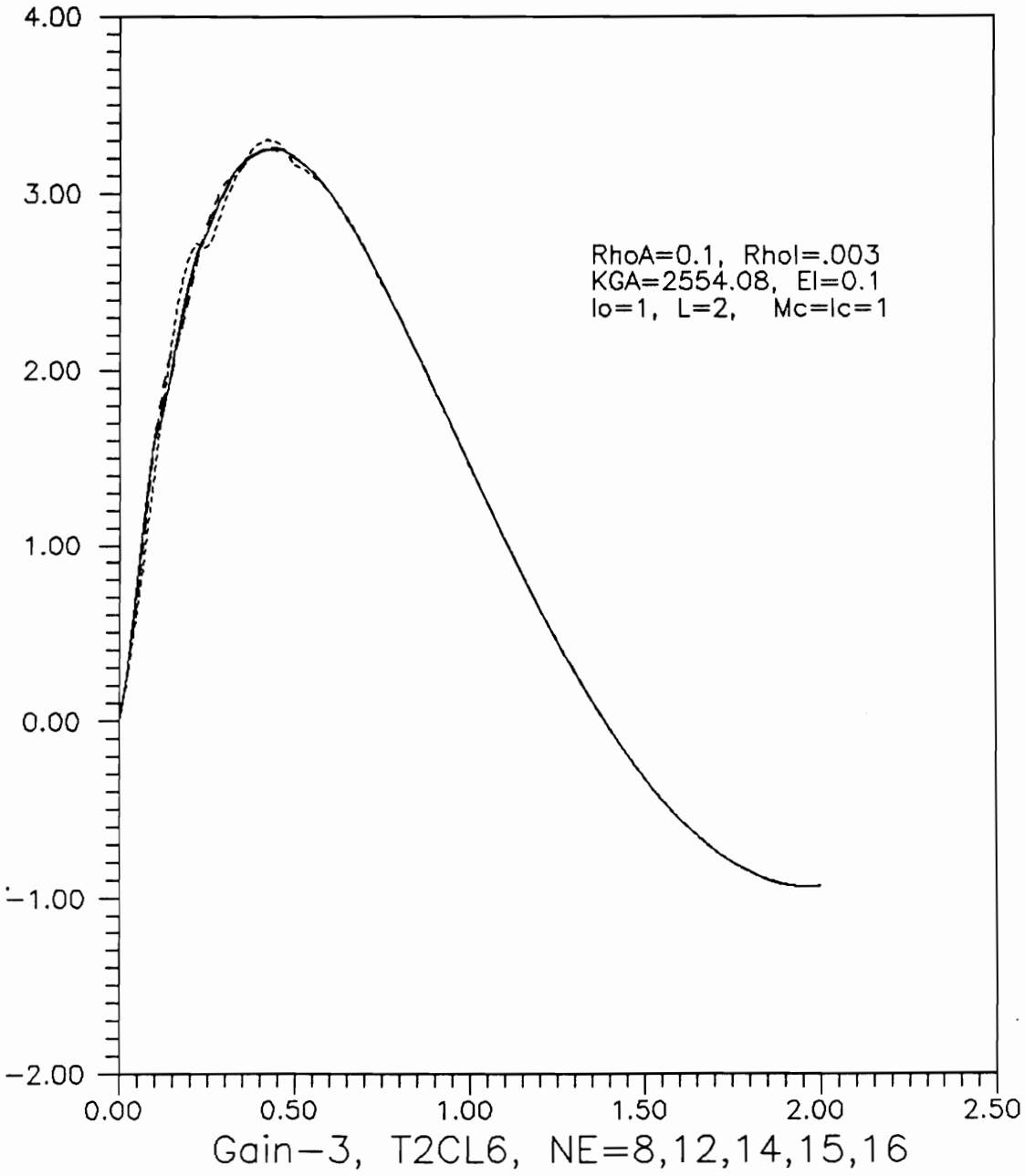

FIGURE 55. Functional Gain $K_4(x)$ vs x, T2CL6

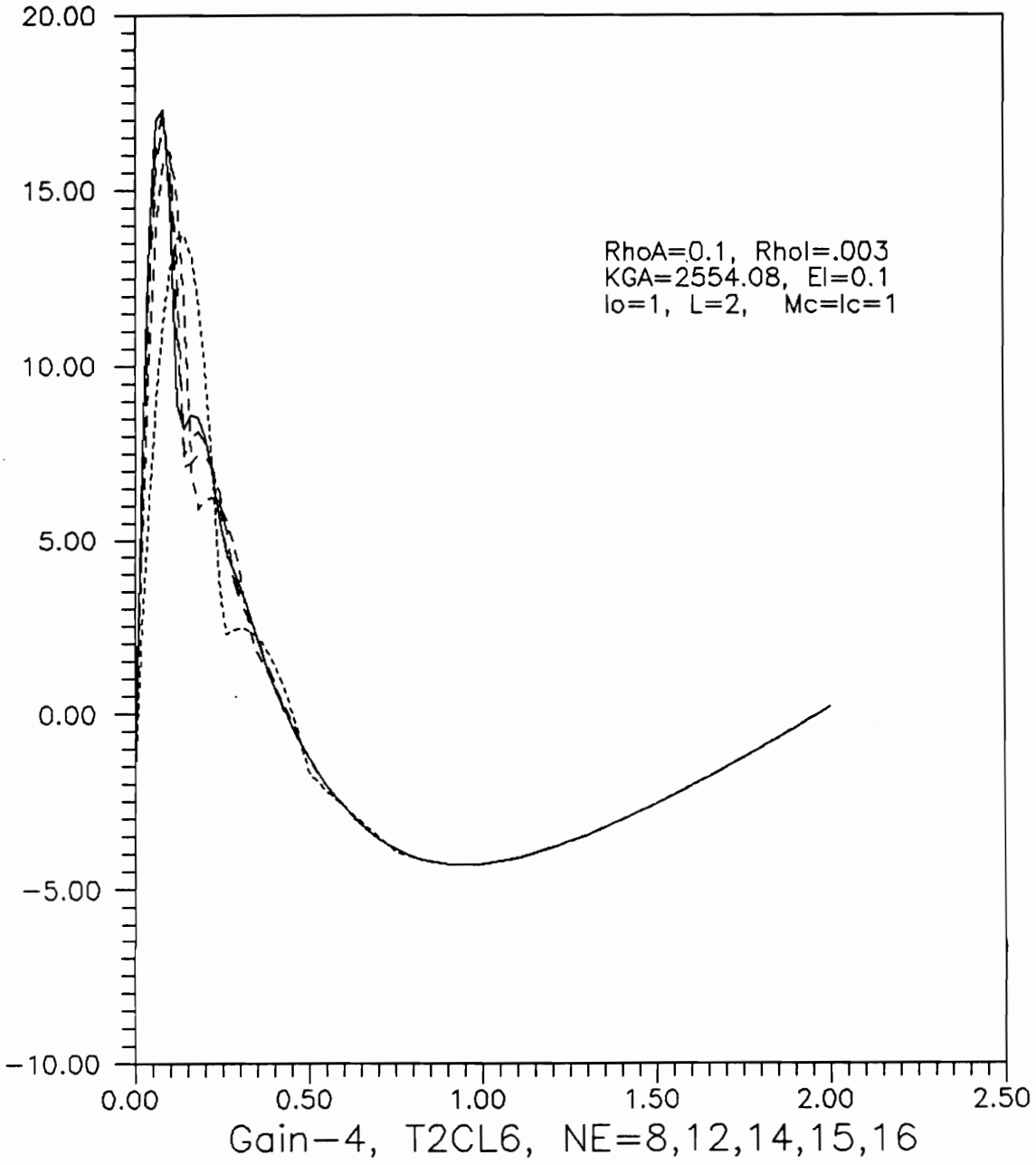

FIGURE 56. Functional Gain $K_5(x)$ vs x, T2CL6

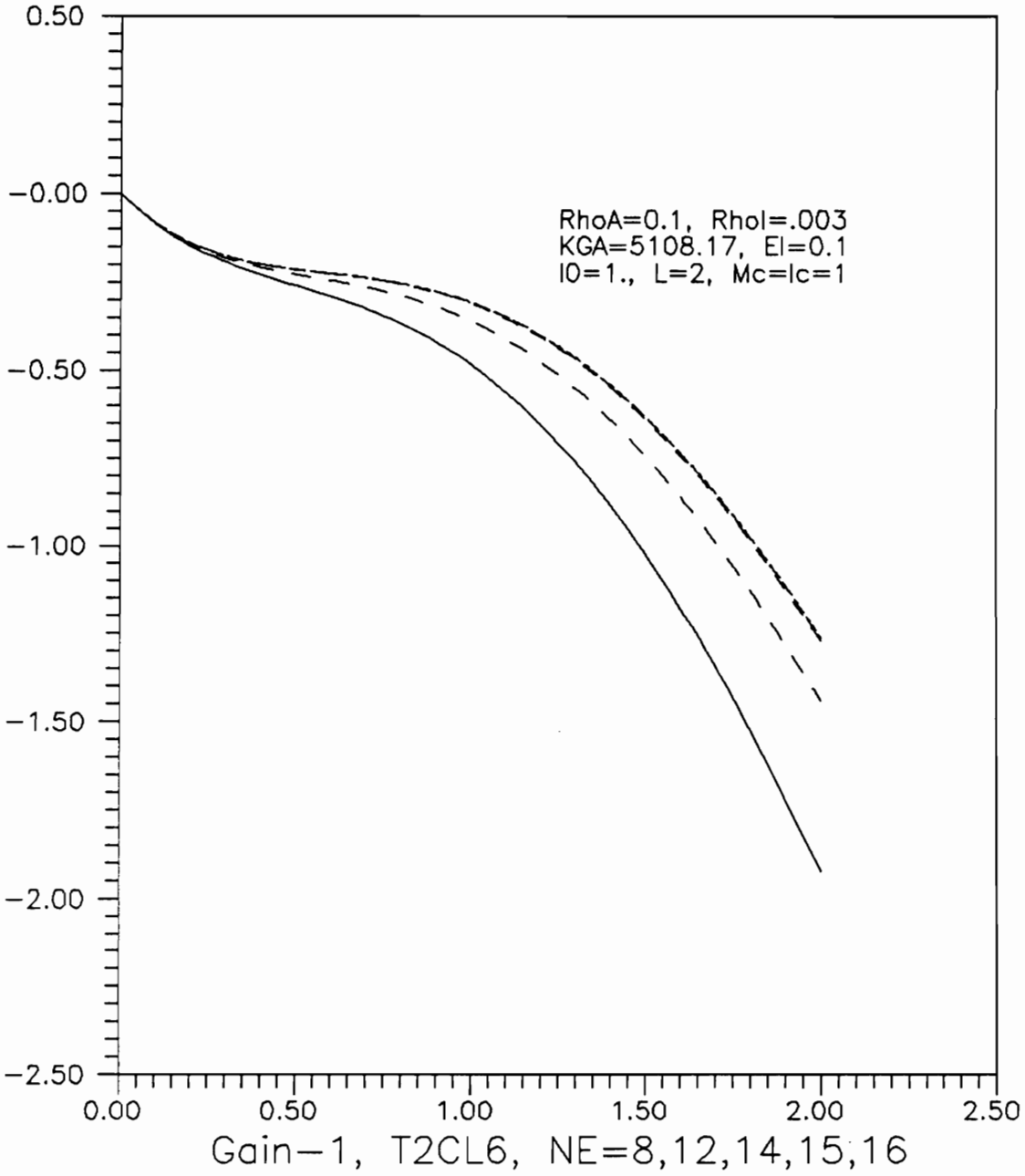

FIGURE 57. Functional Gain $\psi_f(x)$ vs x, T2CL6

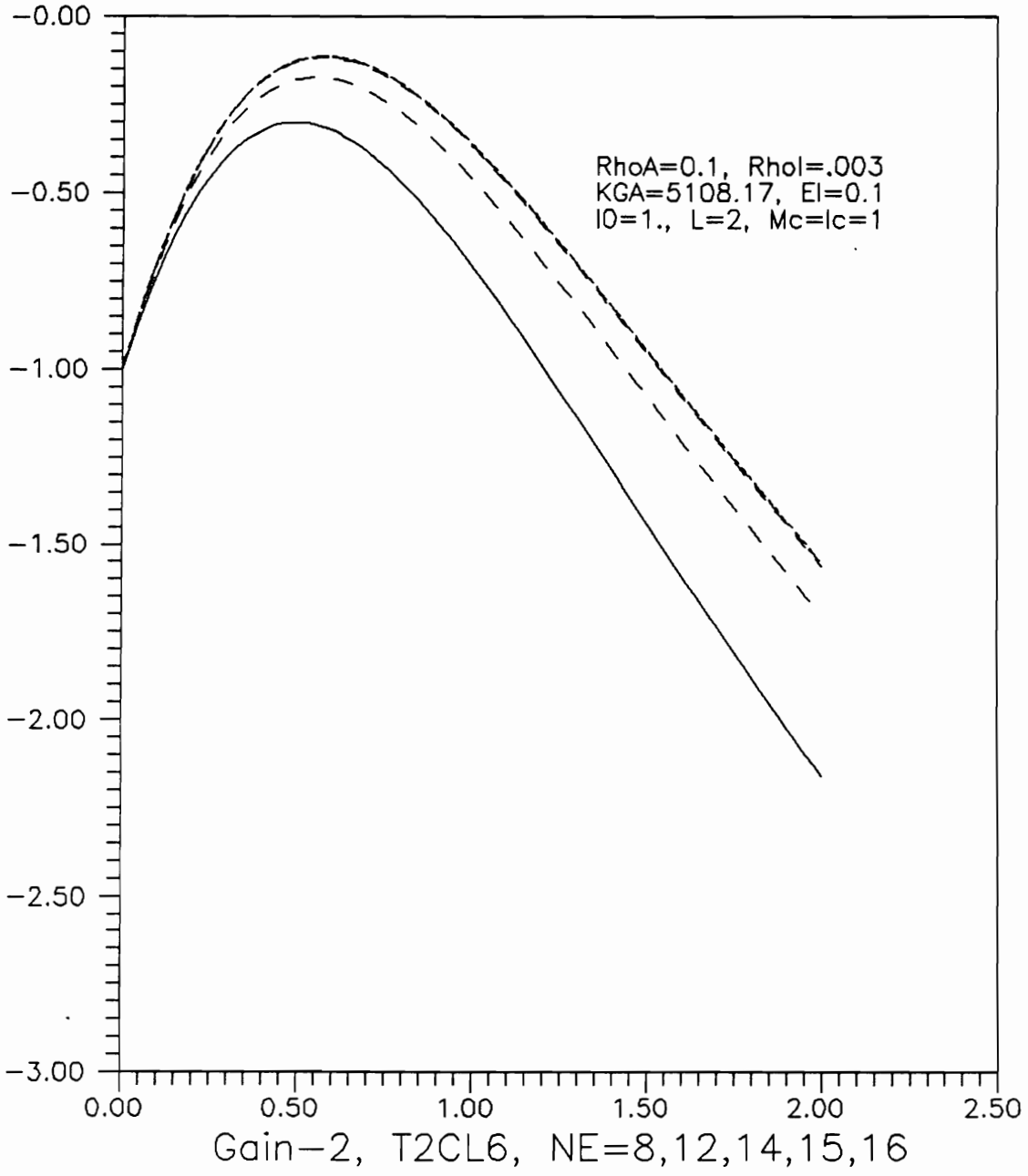

FIGURE 58. Functional Gain $\phi_f(x)$ vs x, T2CL6

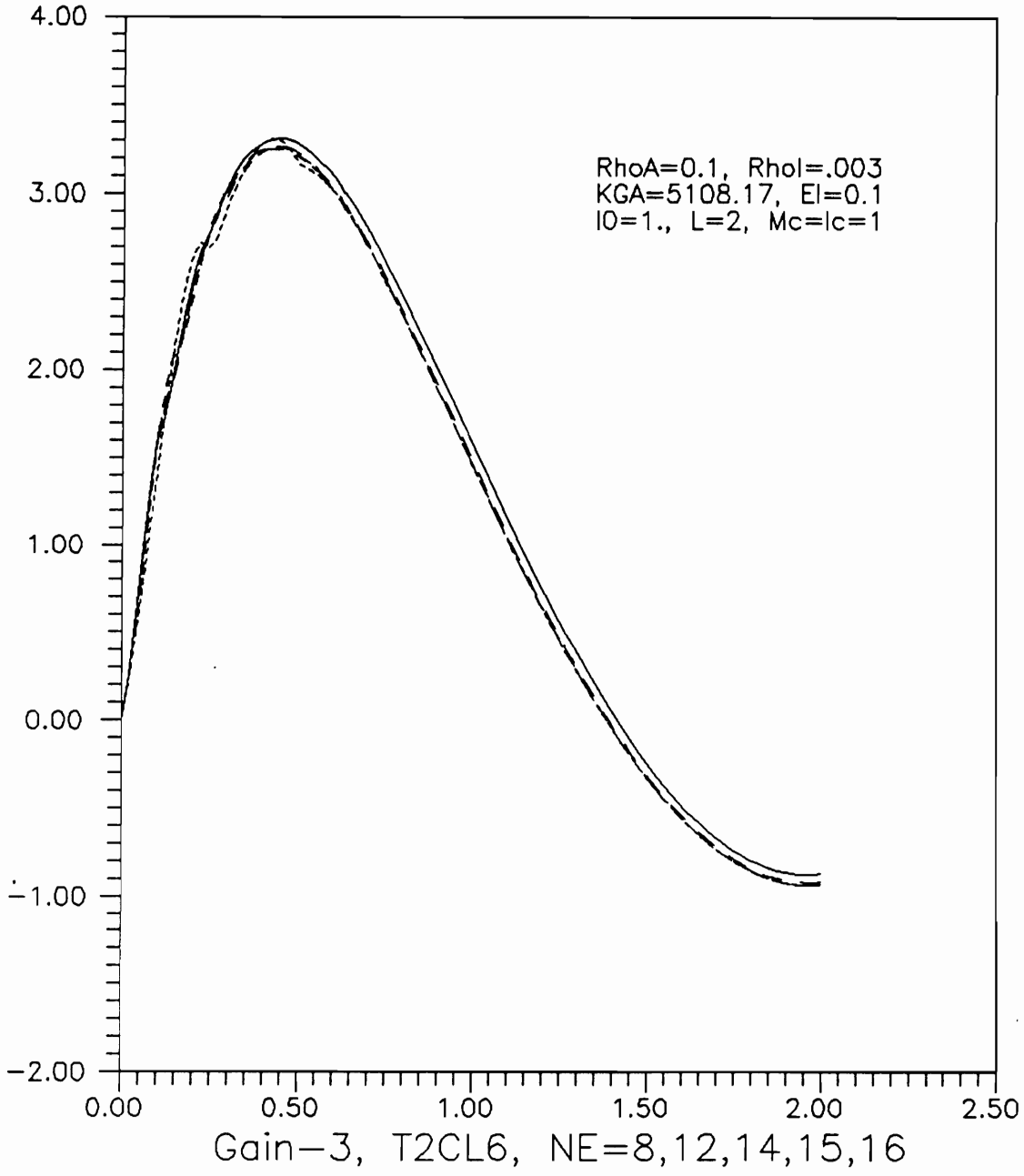

FIGURE 59. Functional Gain $K_4(x)$ vs x, T2CL6

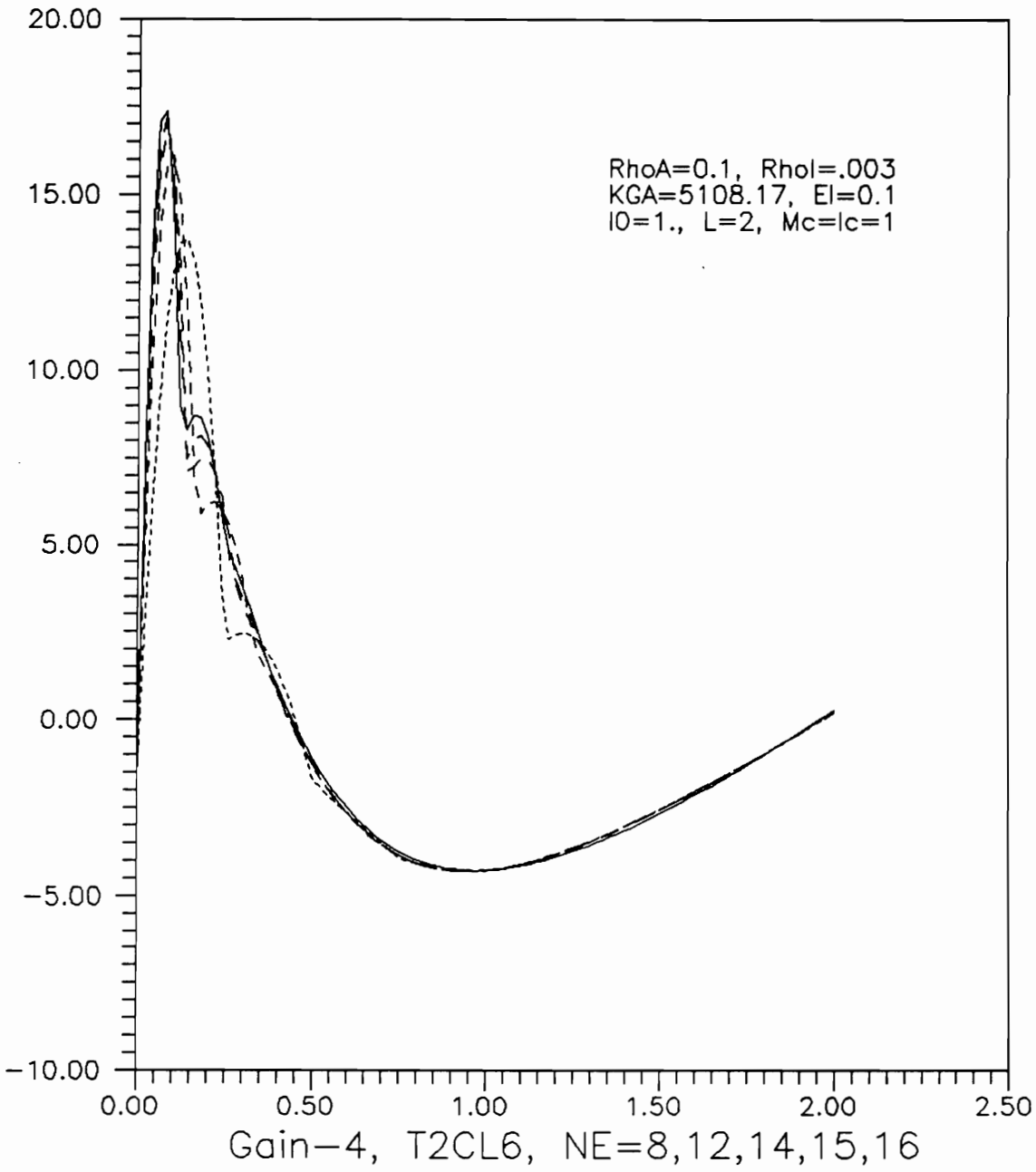

FIGURE 60. Functional Gain $K_5(x)$ vs x, T2CL6

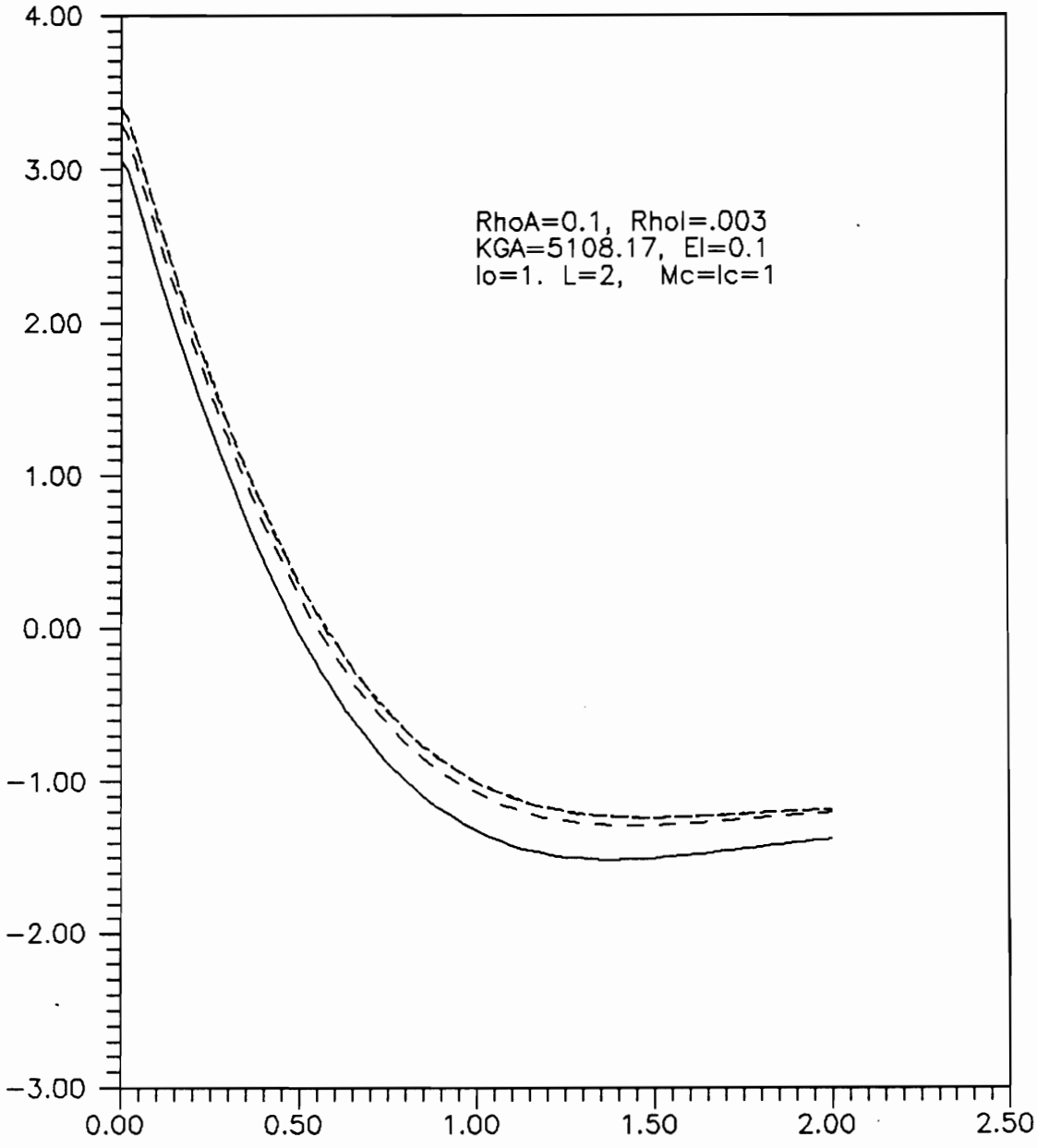

FIGURE 61. Functional Gain $K_3(x)$ vs x, T2CL6

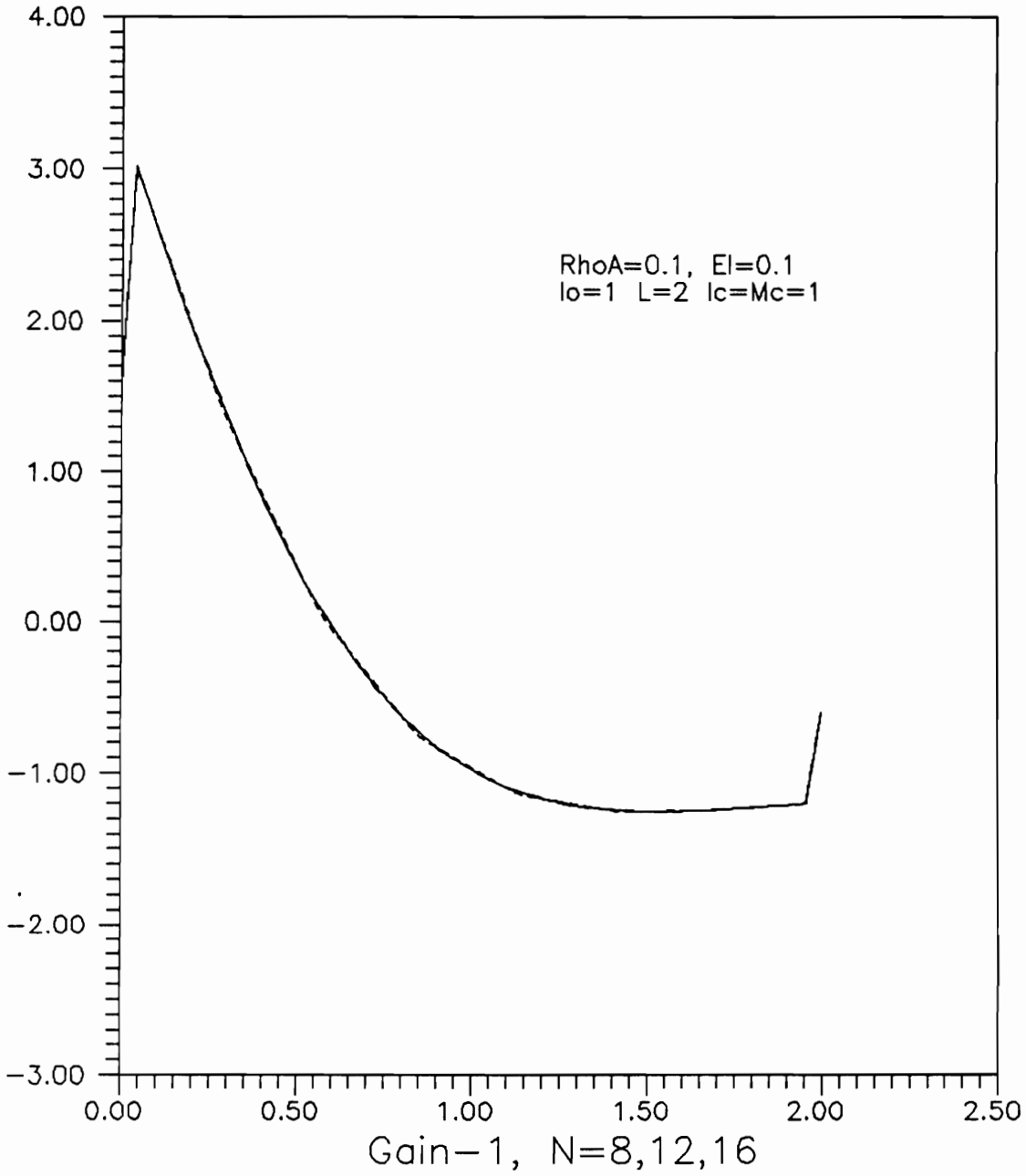

FIGURE 62. Functional Gain Bending, Euler-Bernoulli

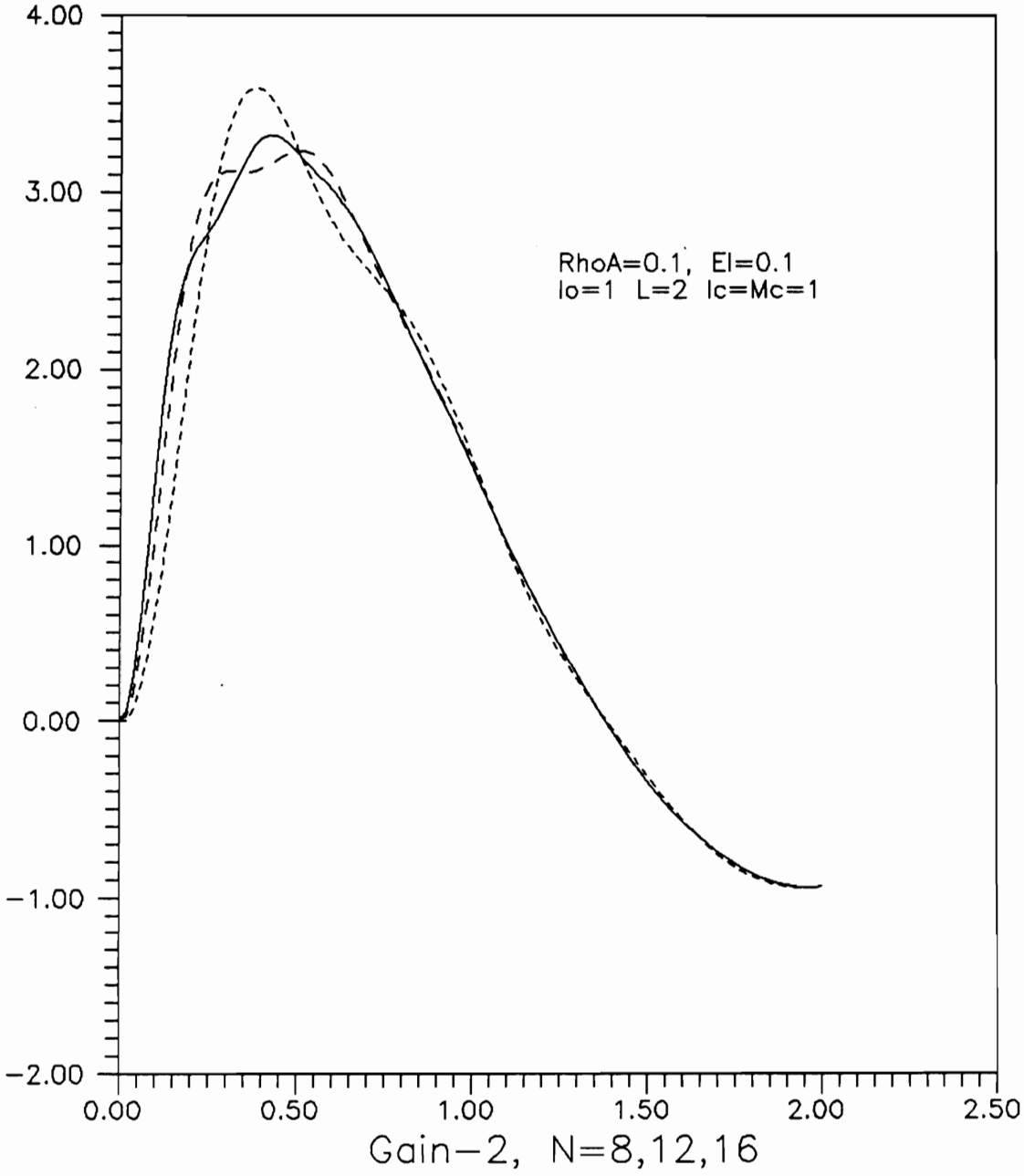

FIGURE 63. Functional Gain Velocity, Euler-Bernoulli

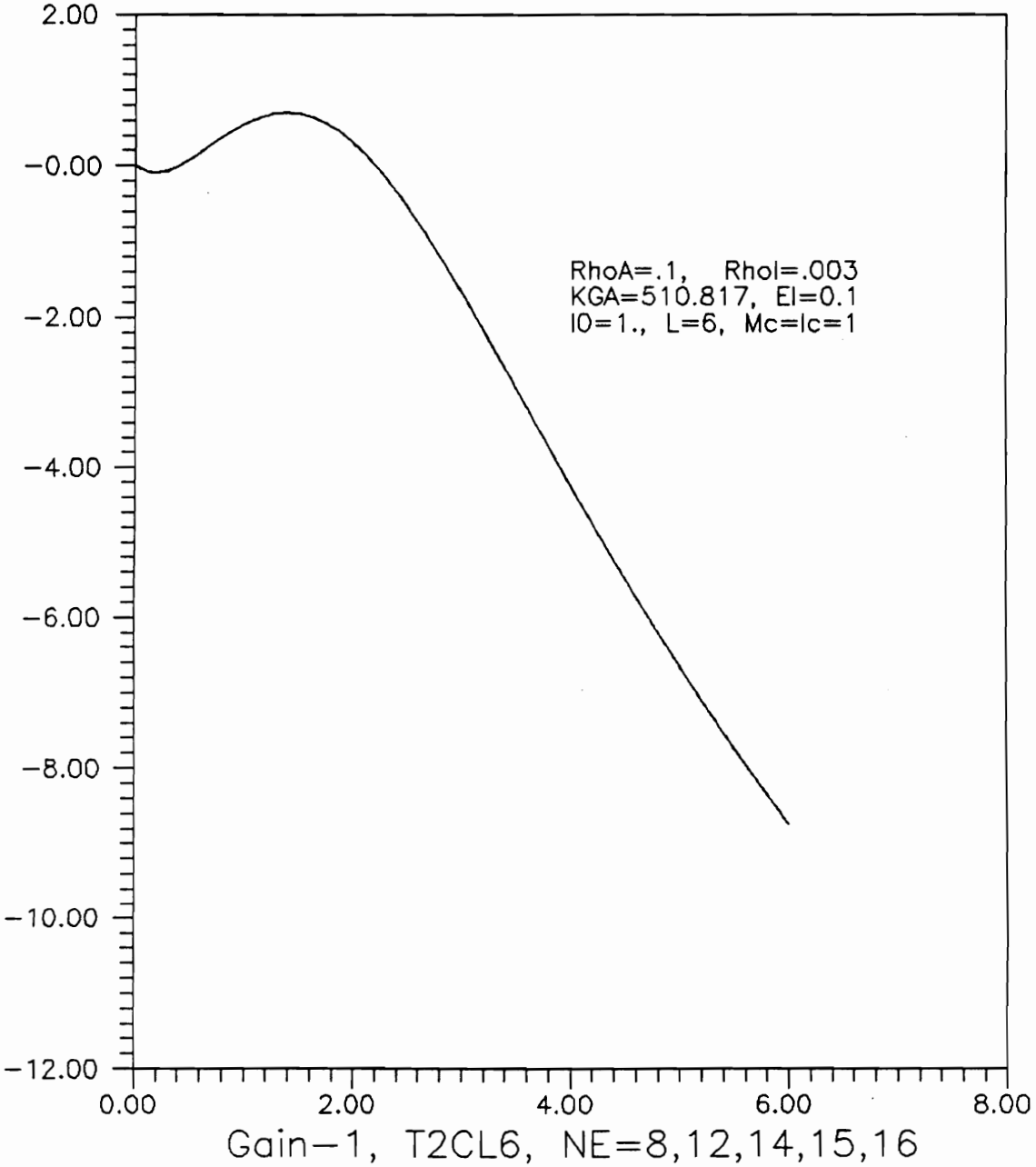

FIGURE 64. Functional Gain $\psi_f(x)$ vs x, T2CL6

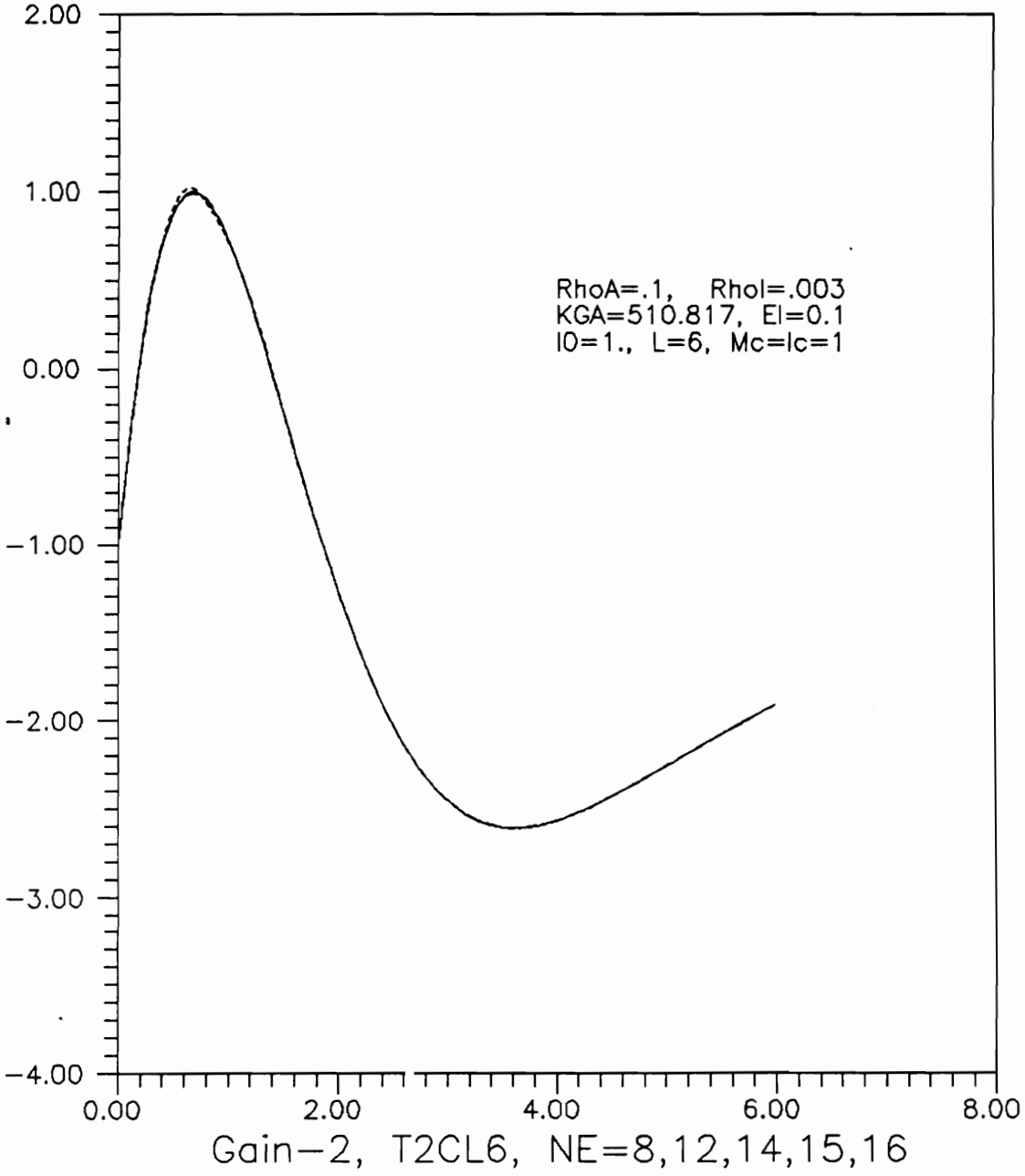

FIGURE 65. Functional Gain $\phi_f(x)$ vs x, T2CL6

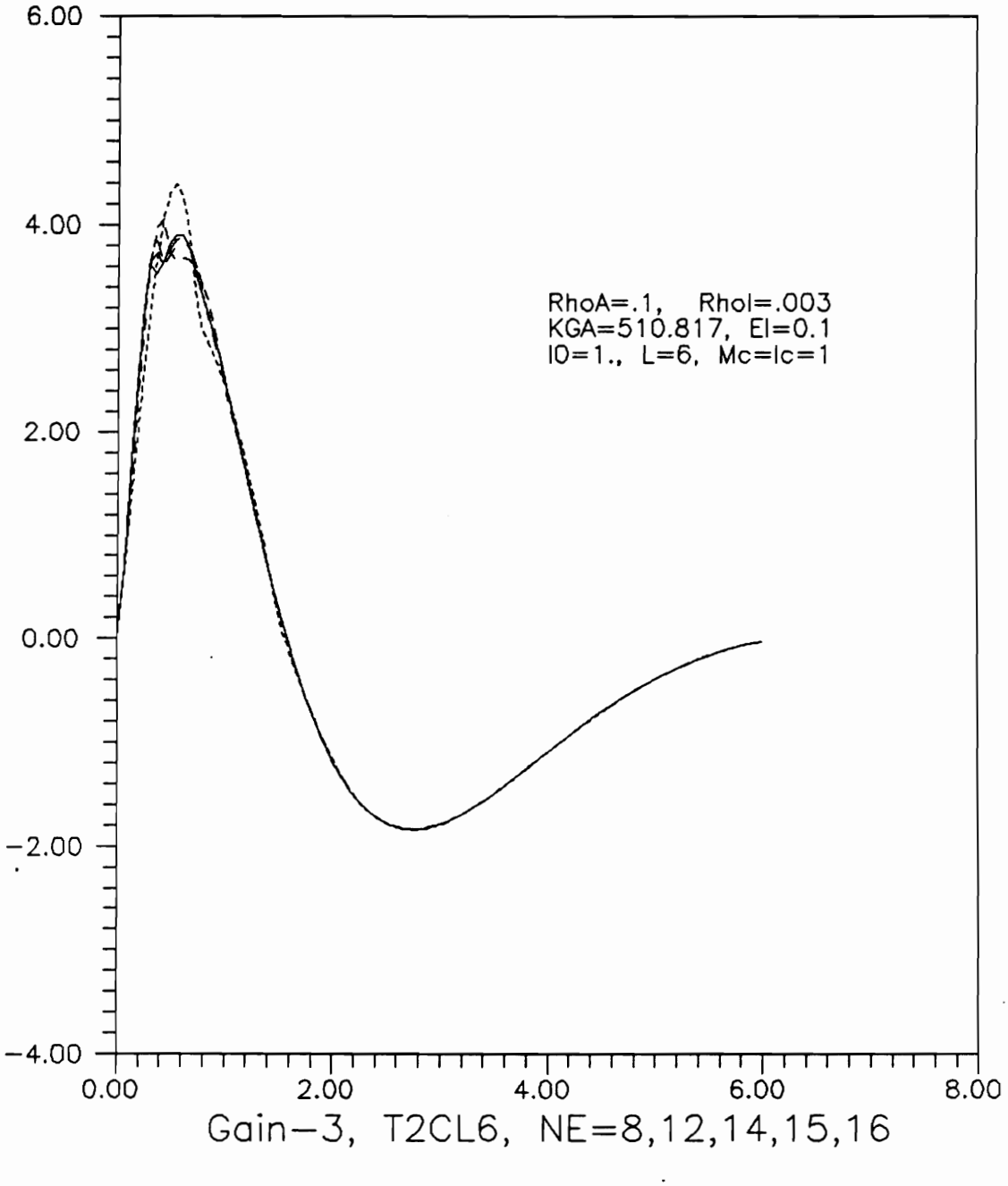

FIGURE 66. Functional Gain $K_4(x)$ vs x, T2CL6

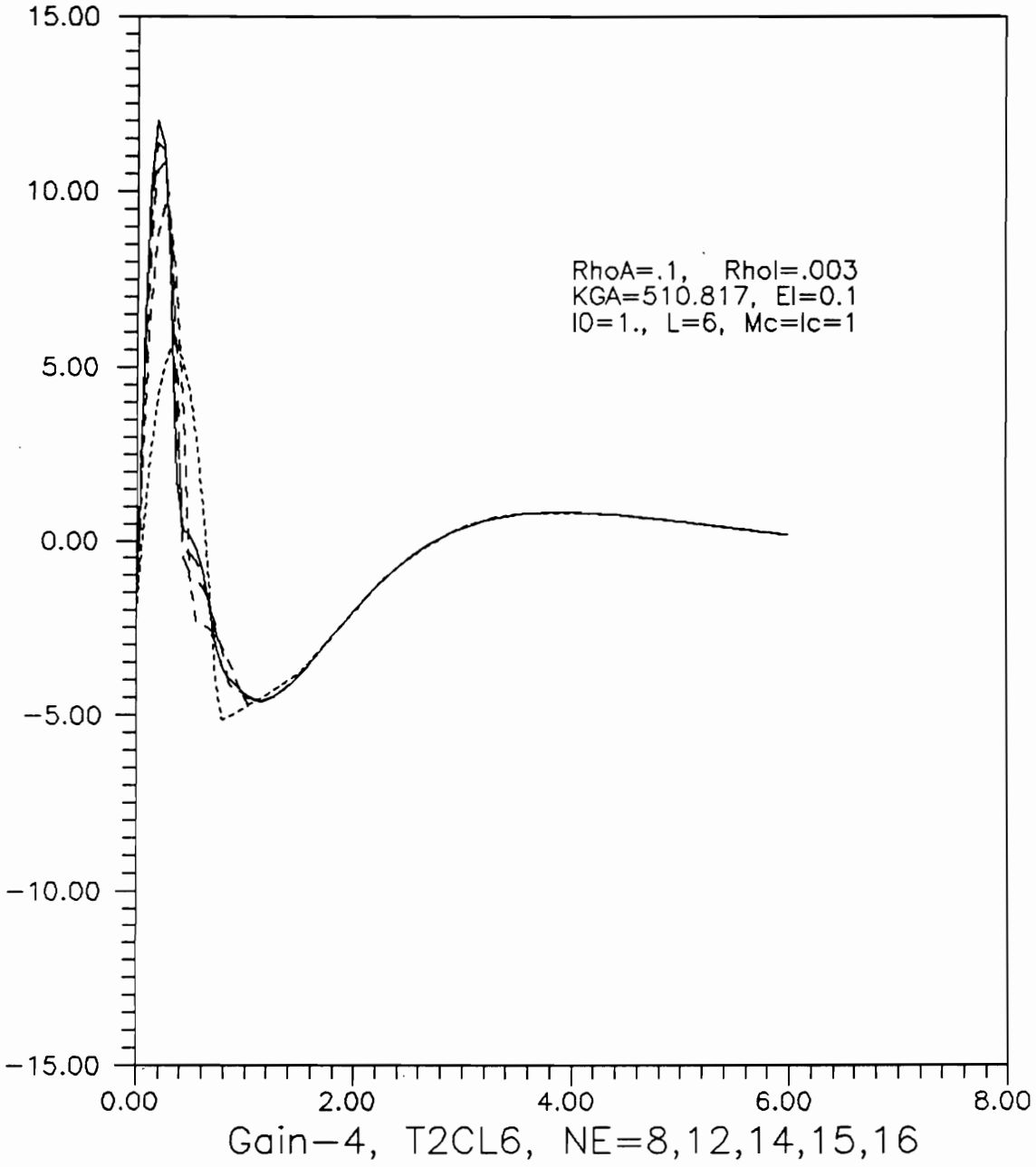

FIGURE 67. Functional Gain $K_5(x)$ vs x, T2CL6

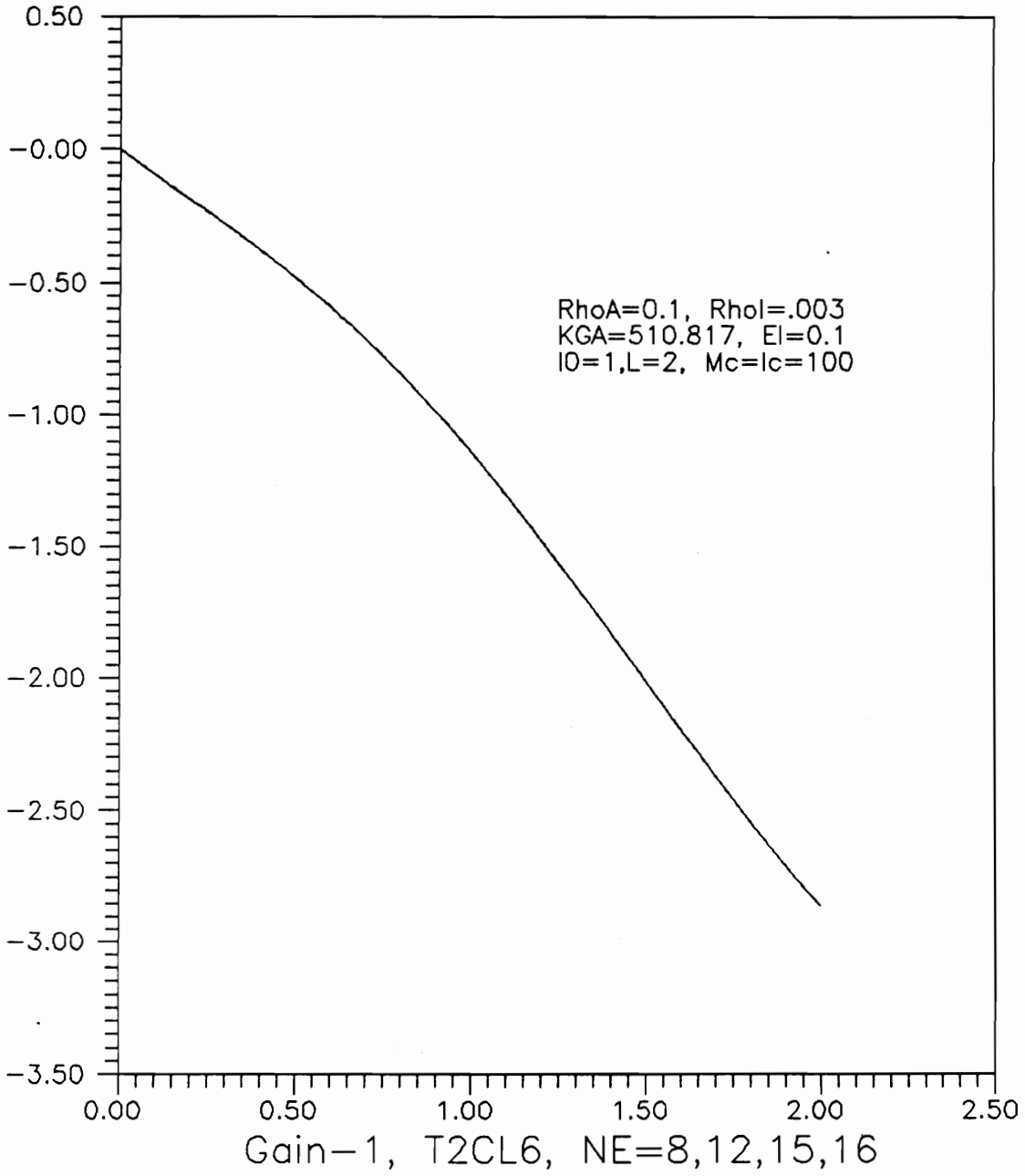

FIGURE 68. Functional Gain $\psi_f(x)$ vs x, T2CL6

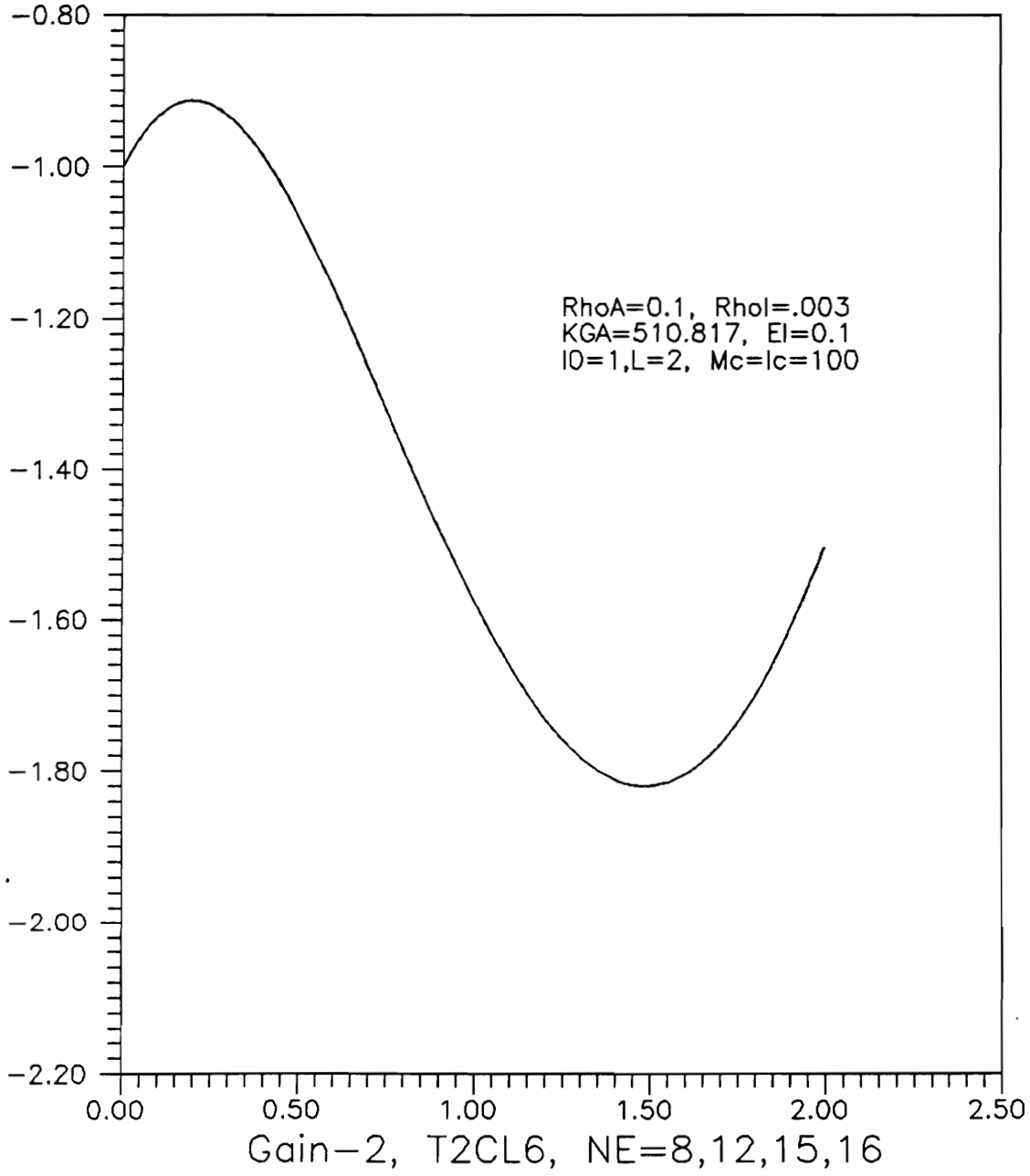

FIGURE 69. Functional Gain $\phi_f(x)$ vs x, T2CL6

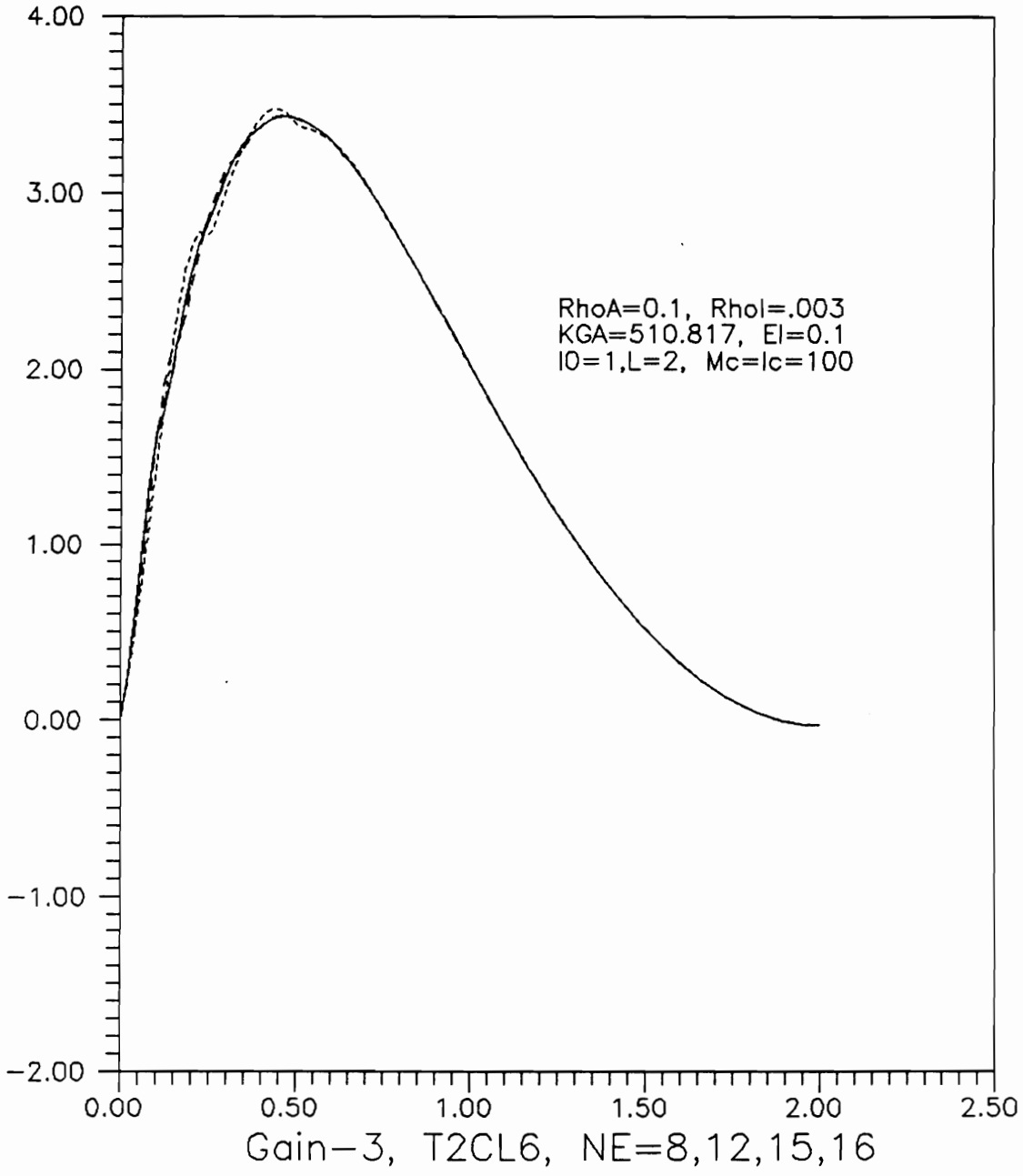

FIGURE 70. Functional Gain $K_4(x)$ vs x, T2CL6

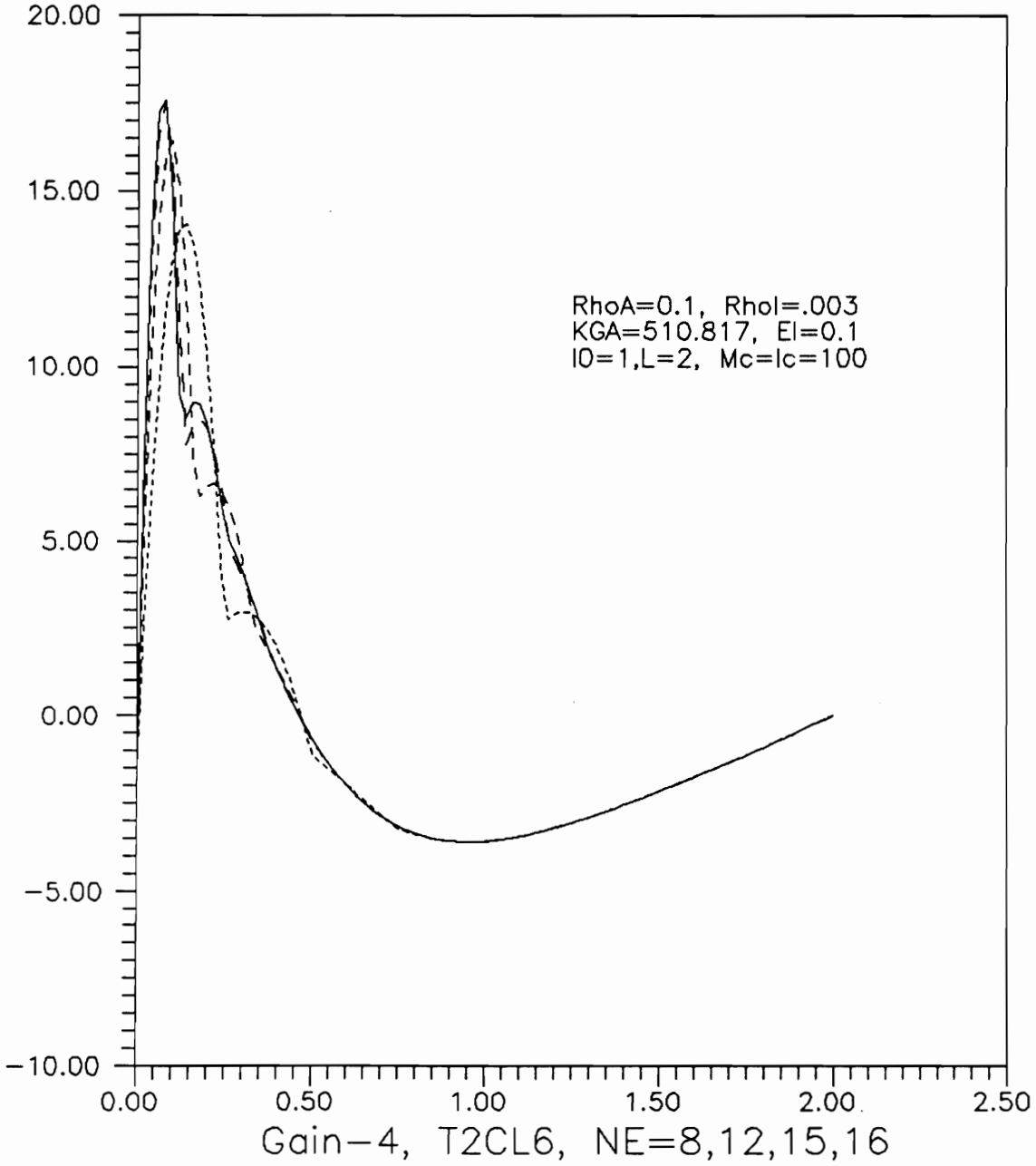

FIGURE 71. Functional Gain $K_5(x)$ vs x, T2CL6

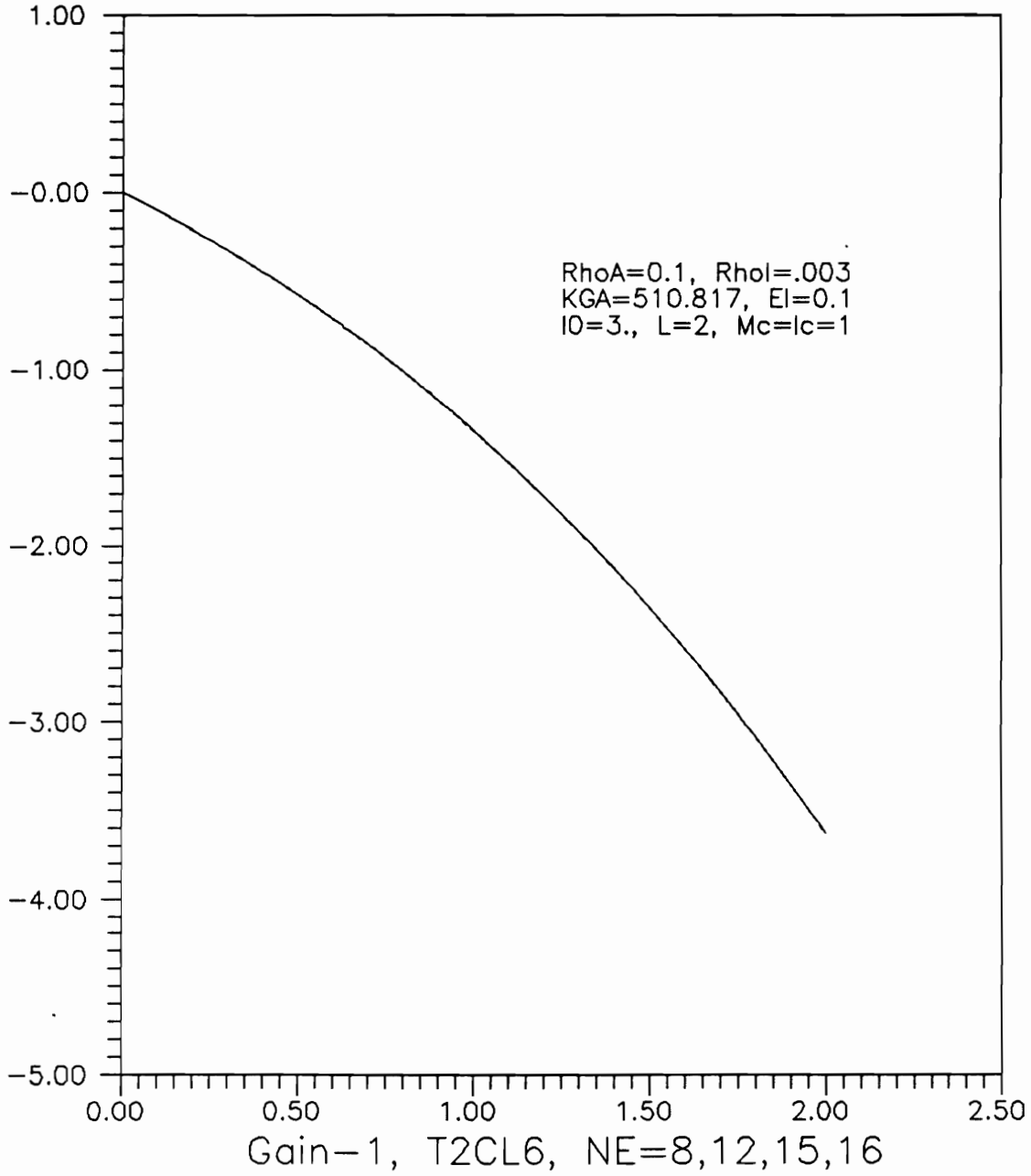

FIGURE 72. Functional Gain $\psi_f(x)$ vs x, T2CL6

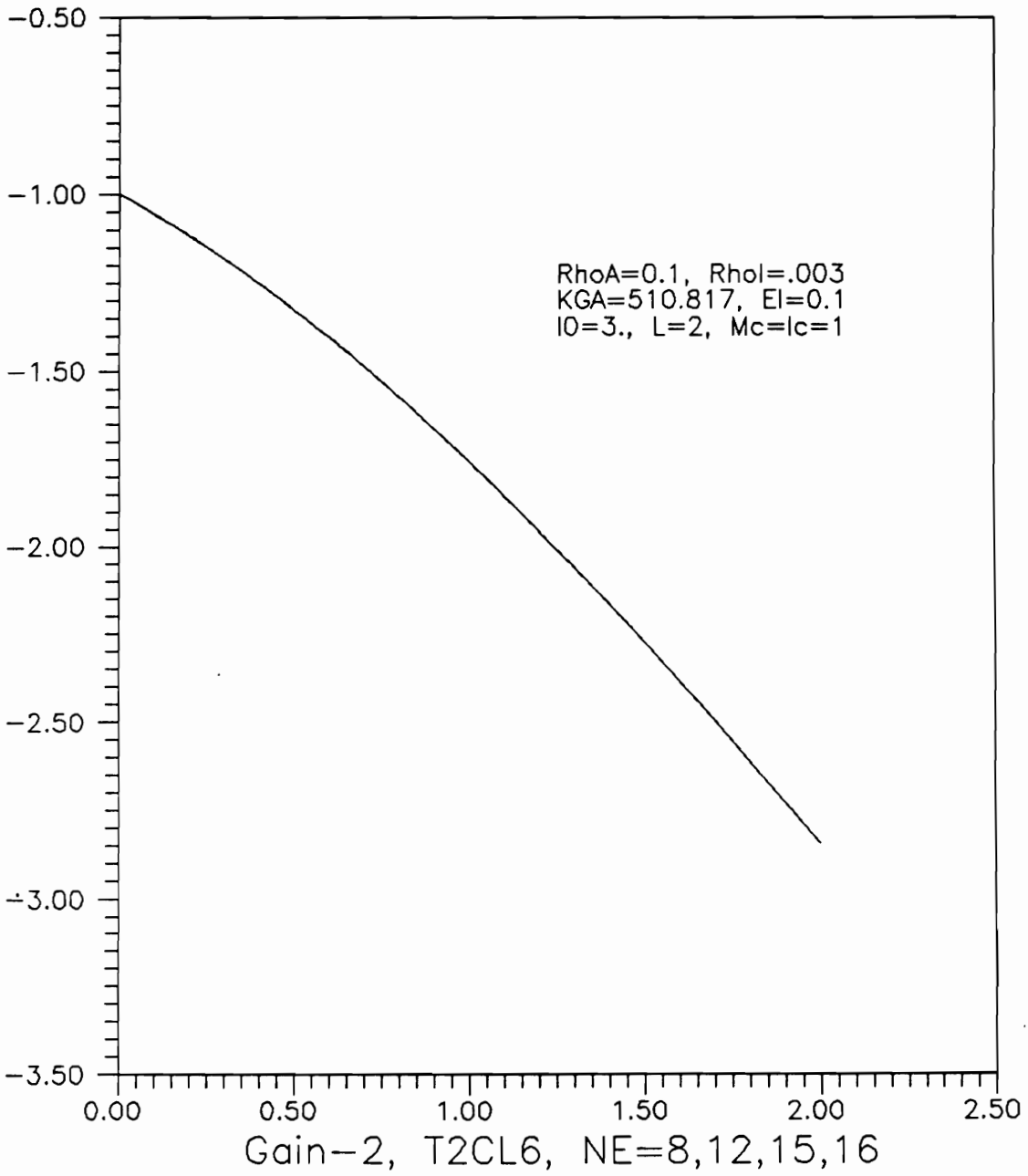

FIGURE 73. Functional Gain $\phi_f(x)$ vs x, T2CL6

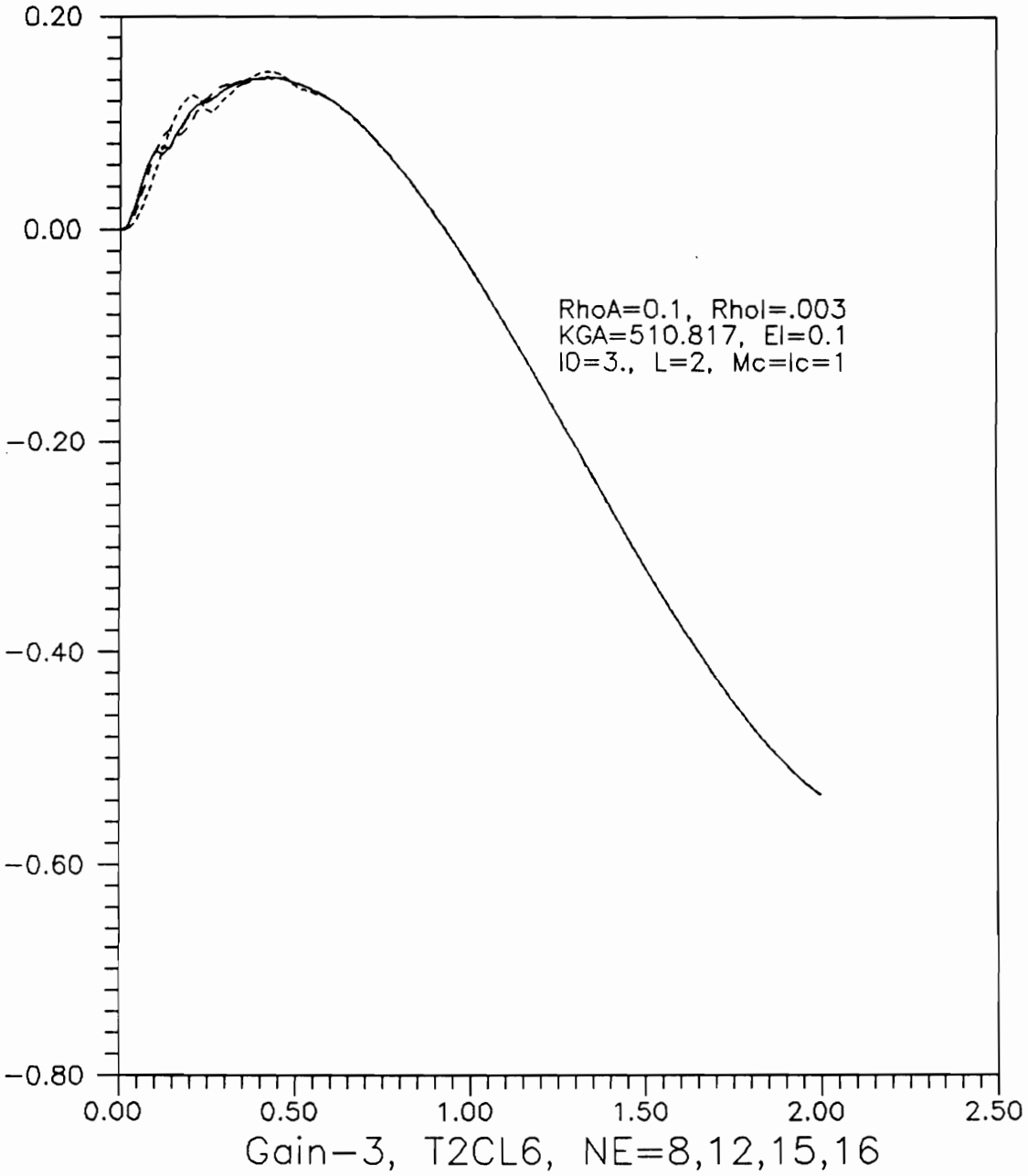

FIGURE 74. Functional Gain $K_4(x)$ vs x, T2CL6

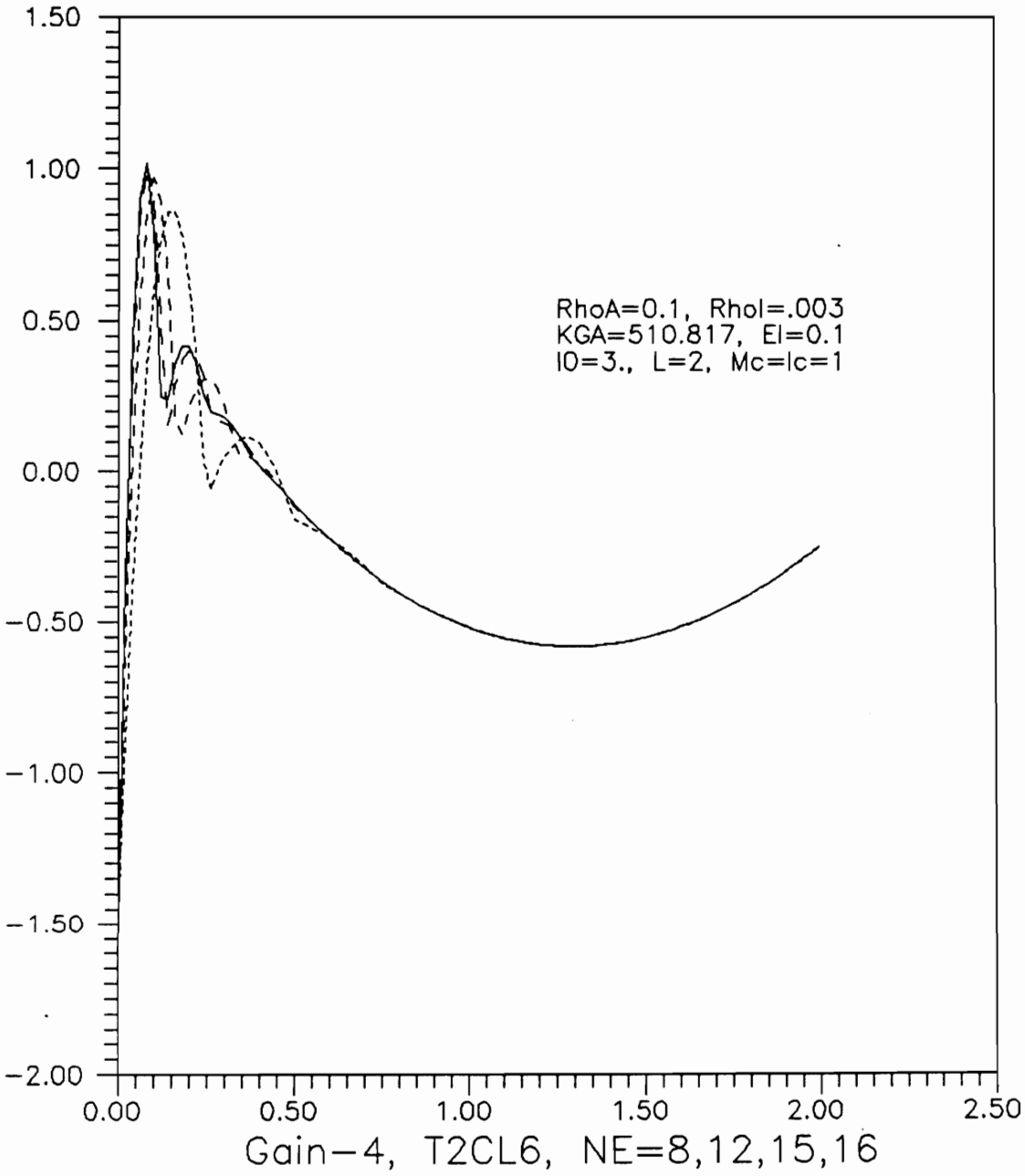

FIGURE 75. Functional Gain $K_5(x)$ vs x, T2CL6

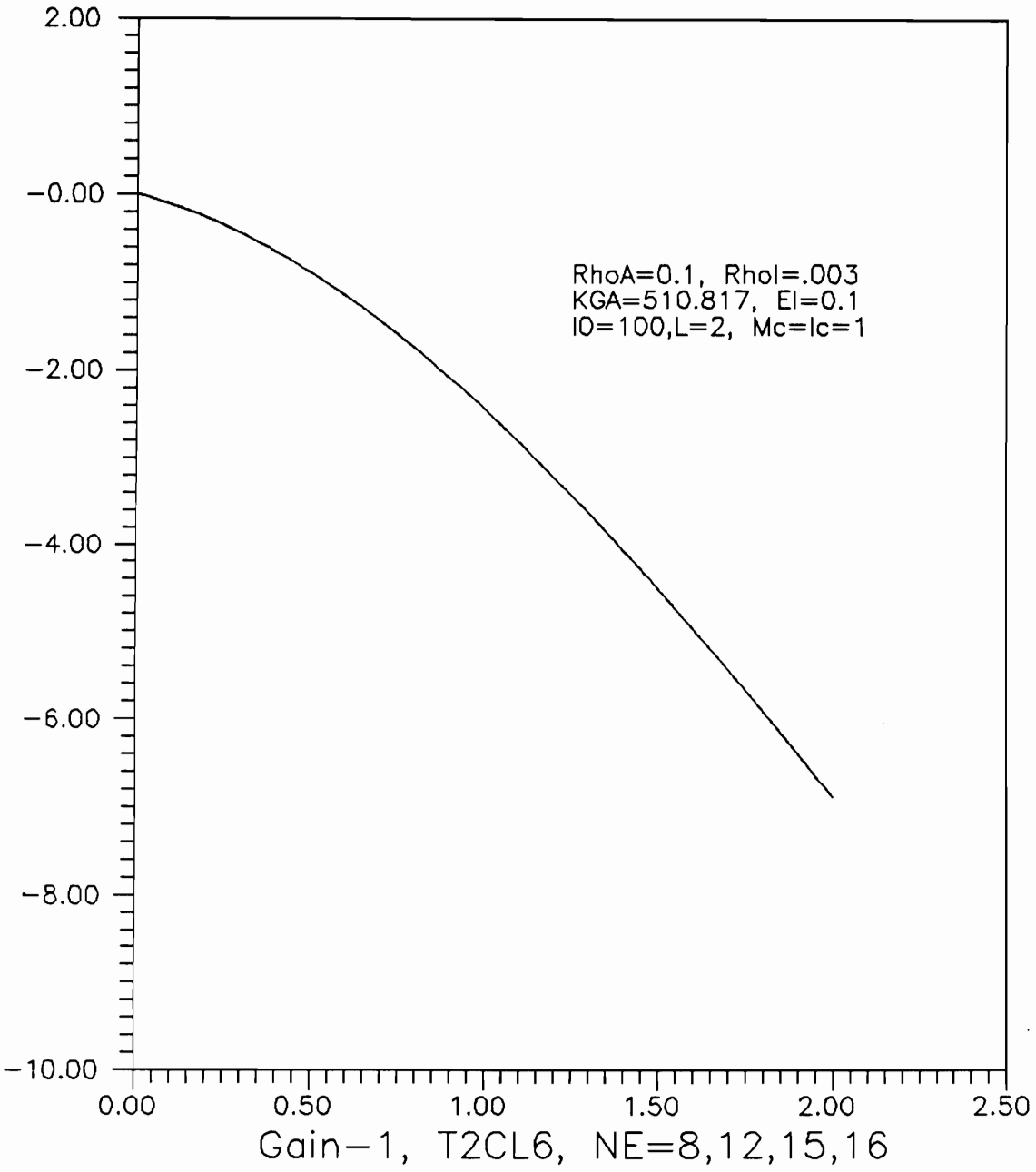

FIGURE 76. Functional Gain $\psi_f(x)$ vs x, T2CL6

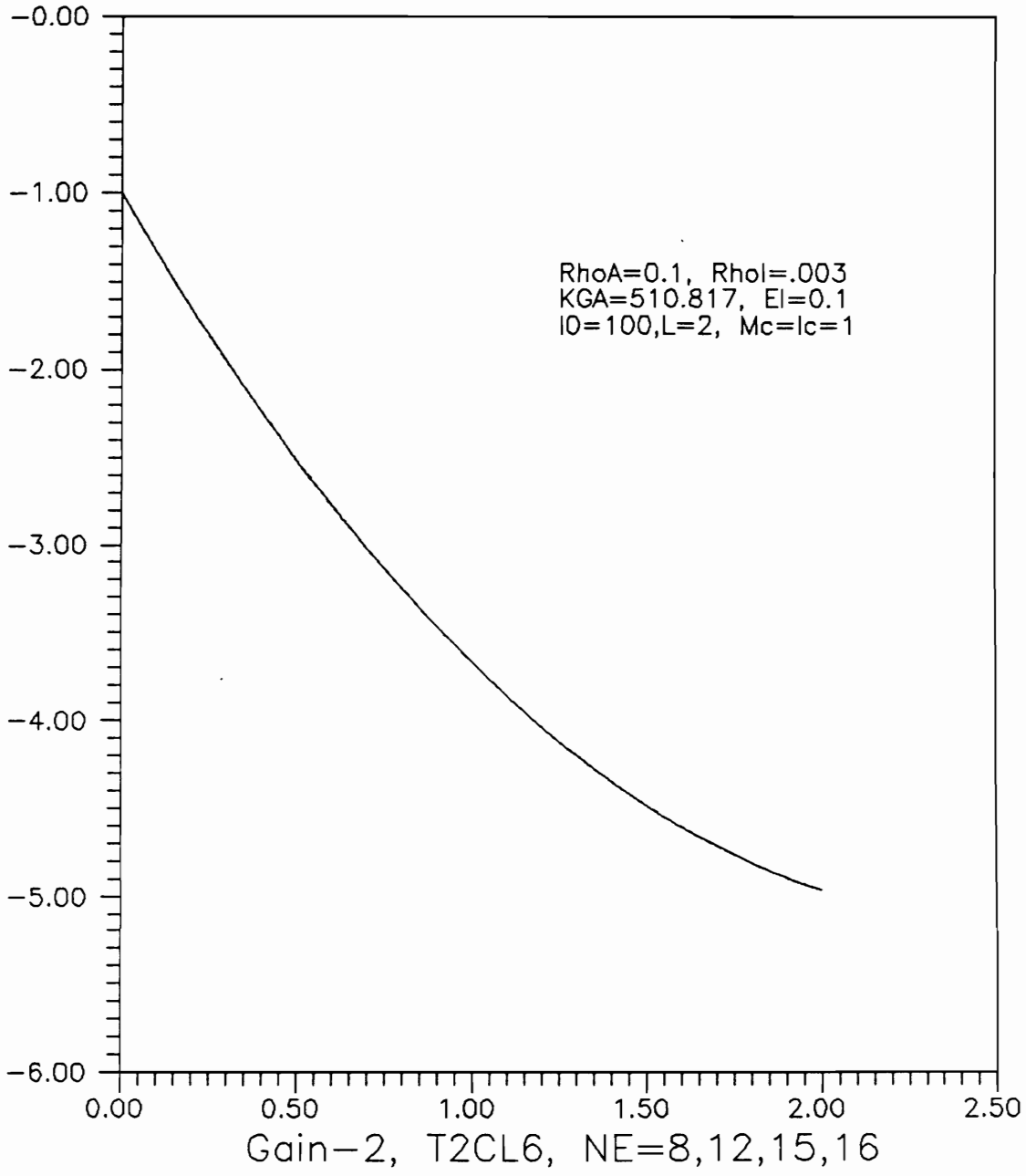

FIGURE 77. Functional Gain $\phi_f(x)$ vs x, T2CL6

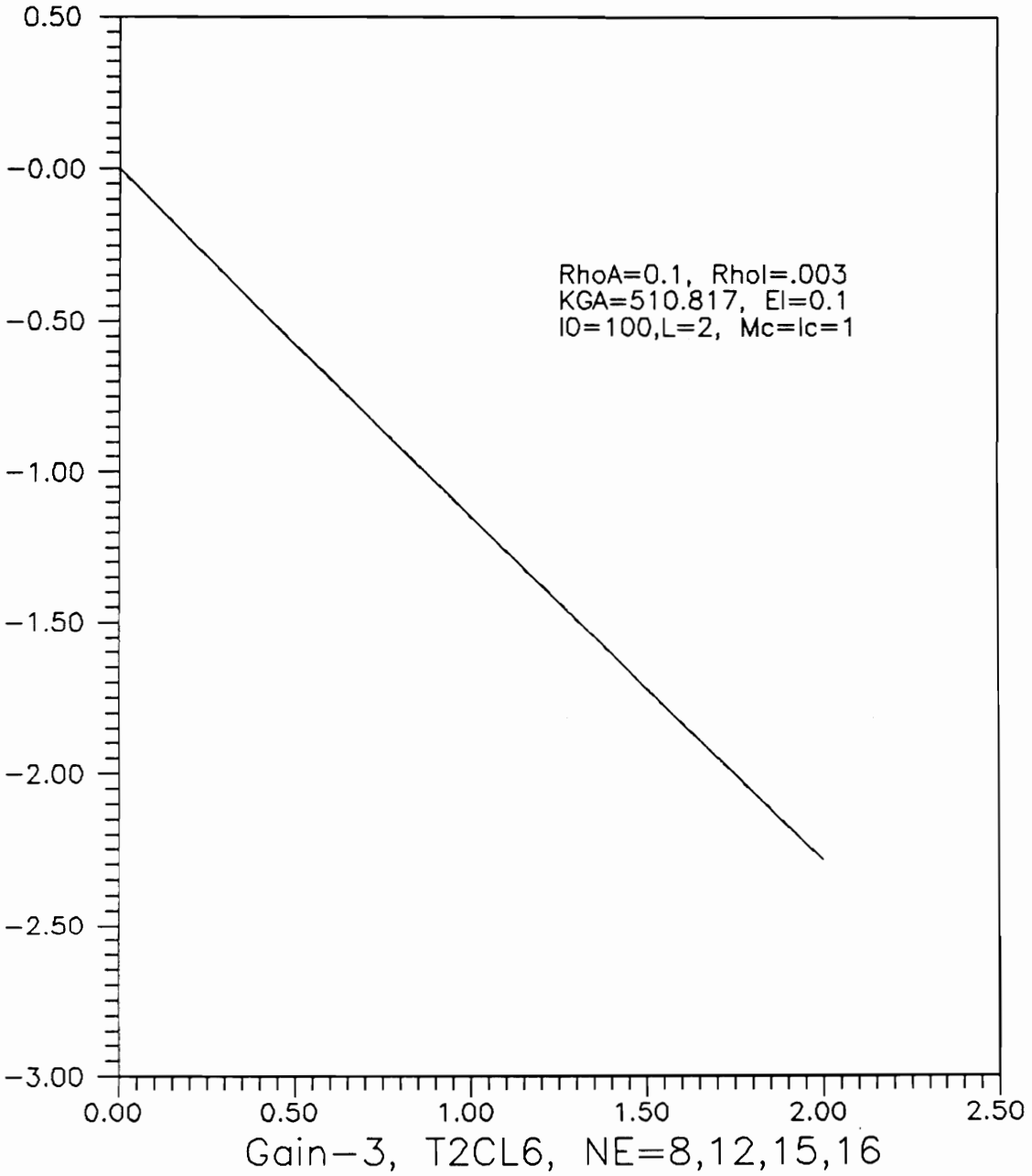

FIGURE 78. Functional Gain $K_4(x)$ vs x, T2CL6

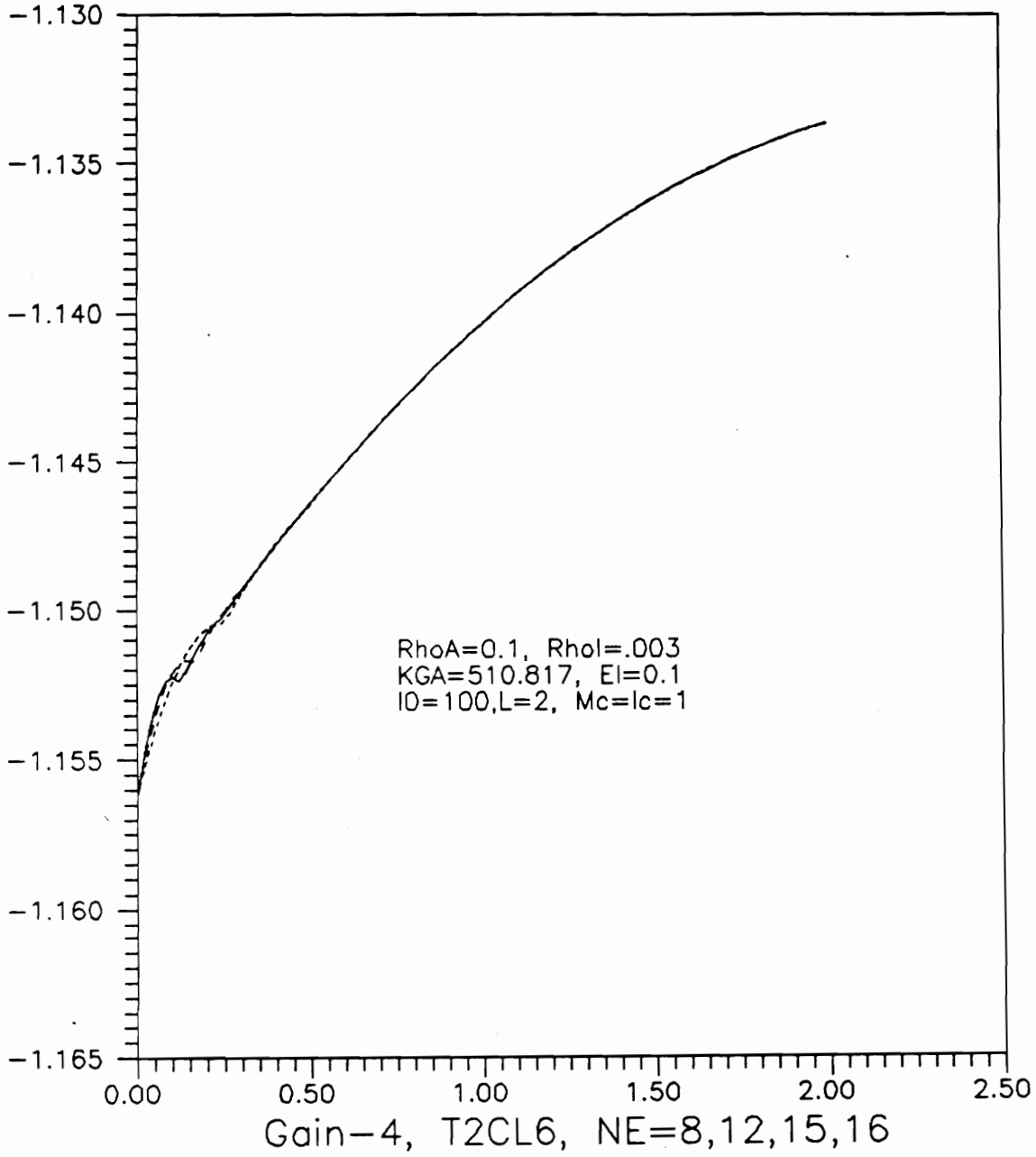

FIGURE 79. Functional Gain $K_5(x)$ vs x, T2CL6

REFERENCES

[1] Gibson, J. and Adamian A.,"Approximation theory for Linear Quadratic Gaussian Control of Flexible Structures." *SIAM J. of Control and Optimization*, Vol. 29, No. 1, (1991), page 1-37.

[2] Banks, H. T. and J. M. Crowley, "Parameter Estimation for Distributed Systems Arising in Elasticity", *LCDS Report No. 81-24* , (1981).

[3] Burns, J. A., E. M. Cliff, H. J. Kelley and F. H. Lutz, "Control of Flexible Structures", Optimization Incorporated, Blacksburg, Virginia, December 1988.

[4] Tessler, A. and S. B. Dong, "On a Hierarchy of Conforming Timoshenko Beam Elements", *Journal of Computers and Structures*, Vol. 14, No. 3-4, pp 335-344, 1981.

[5] Kato, T., *Perturbation of Linear OPerators.* Springer-Verlag, New York, 1981.

[6] Walker, J. A., *Dynamical Systems and Evolution Equations.* Plenum Press, New York, 1980.

[7] Wouk, A., *A Course of Applied Functional Analysis,* John-Wiley, New York, 1979.

[8] Weidmann, J., *Linear Operators in Hilbert Space.* Springer-Verlag, New York, 1980.

[9] Hille, E. and R. S. Phillips, *Functional Analysis and Semi-Groups.* Providence: AMS Colloquium Publications, Vol. 31, 1957.

[10] Pazy, A., *Semigroups of Linear operators and Applications to Partial Differential Equations,* Springer-Verlag, New York, 1983.

[11] Chen, G. and D. Russell, "A Mathematical Model for Linear Elastic Systems with Structural Damping", *Quat. Appl. Math.*, Vol. 39, pp 433-454, (1982).

[12] Phillips, R., "Dissipative Operators and Hyperbolic Systems of Partial Differential Equations", *Transactions of American Mathematical Society*, Vol. 90, pp 193-254, 1959.

[13] Hanson, S., "Frequency Proportional Damping Model for Euler- Bernoulli Beam", Ph.D. Thesis University of Madison-Wisconsin, Madison, 1988.

[14] El Jai, A. and A. J. Pritchard, *Sensors and Controls in the Analysis of Distributed Systems*, Ellis Norwood Limited, England, 1988.

[15] Banks, H. T., J. A. Burns and E. M. Cliff, "Parameter Estimation and Identification for Systems with Delays", *SIAM J. of Control and Optimization,* Vol. 19, No. 6, 1981.

[16] Kim, J., Private Communication.

[17] Banks, H. T. and Kunisch K., "The Linear Regulator Problem for Parabolic System", *SIAM J. of Control and Optimization,* Vol. 22, No. 5, 1984.

[18] Berdaguer, E. F., J. A. Burns, Peichl G. H. and R. S. Sanchez Pena, "A note on Computing System Radii for Galerkin Approximations of Elastic Systems", *29th IEEE Conference on Decision and Control,* pp 17-21, 1990.

[19] Lions, J. L. *Control of Distributed Singular Systems*, Gauthier-Villars, Paris,1983.

VITA

Mohsen Tadi was born on October 23, 1961 in Tehran, Iran. He graduated from Arvand Rood High School in Tehran, Iran in 1977. He received the B.S. degree in Mechanical Engineering from University of the District of Columbia in Washington D.C. in 1981, the M.S. in Mechanical Engineering from Catholic University of America in Washington D.C. in 1986 and the Ph.D. in Engineering Mechanics from Virginia Polytechnic Institute and State University in 1991. He is a member of SIAM.